The University of Nottingham

UNITED KINGDOM · CHINA · MALAYSIA

CONACYT

Consejo Nacional de Ciencia y Tecnología

Genetic analysis of physiological traits to increase grain partitioning in high biomass cultivars in wheat (*Triticum aestivum L.*)

Aleyda Aryadne Sierra-Gonzalez, B.Eng

Thesis submitted to
The University of Nottingham
for the degree of Doctor of Philosophy

Sutton Bonington Campus
School of Bioscience

September 2019

Abstract

Wheat (*Triticum* spp.) is the second most grown crop in the world, being used as a raw ingredient in different foods making this cereal an essential component of the global food security. FAO estimates that for 2050, the global population could reach between 9.3 to 10 billion people (Peña-Bautista et al., 2017). The current global rate of yield increase in wheat is approximately 1% per year (FAOSTAT, 2013); however, to meet predicted future demand and avoid price hikes, taking into consideration unpredictable climate, genetic gains in grain yield potential are required of 1.5% per year (Fischer & Edmeades, 2010). To achieve this, it is essential to expand current understanding of how physiological traits are associated with genetic gains in yield potential and to adopt phenotypic and genotypic approaches to increase crop productivity (Aisawi et al., 2015).

On this thesis the overall objective was to identify grain partitioning traits and genomic regions associated to maximize yield potential in high biomass elite backgrounds. With the use of a high biomass spring wheat association panel in NW Mexico (**High Biomass Association Panel: HIBAP**) and a doubled-haploid winter wheat population (**Savannah x Rialto DH: SxR DH**) in the UK. Field results over two seasons (Y15: 2015-15 & Y16: 2016-17) confirmed that spike partitioning index (SPI: spike dry matter / above-ground dry matter) at seven days after anthesis (GS65) and fruiting efficiency (FE: grain number / spike dry matter at GS65+7d) were positively associated with harvest index (HI: portion of biomass partitioned into grain) and grain number per m^2 (GN), which in turn (HI and GN) were linearly related to grain yield. Higher SPI and HI were correlated with a shorter length of stem internode 2 (internode below peduncle) and internode 3 and reduced dry-matter partitioning to stem internode 2 and internode 3. Detailed within spike dry-matter (DM) partitioning analysis at GS65+7d revealed that FE was associated with decreased awn DM partitioning and lower rachis DM partitioning with higher grain weight (GW) and grain yield (GY). Therefore, selecting for these traits would contribute to maximising SPI and FE and, thus, HI and GN.

Different molecular analysis were used within each experiment (panel/DH) depending on the sequencing data available. For the spring wheat high biomass association panel (**HiBAP**) using the 35K breeders' array it was possible to identify genetic regions for grain partitioning traits on chromosomes 1A, 2B, 5A, 6A, 6B and 7A. These regions allowed the identification of candidate genes for grain partitioning traits for validation in further studies. On the other hand, for the DH winter wheat population (**SxR DH**) stable quantitative trait loci (QTLs) related to spike fertility and internode lengths were found on 3A, 6A and 6D using a SNP map based on KASP assays which will be useful for further fine-mapping studies.

In order to test further that shortening internodes 2 and 3 (from terminal spikelet initiation to anthesis) enables more assimilates to be partitioned to the spike during stem elongation and

spikelet development (pre-anthesis stage) increasing HI an experiment was carried out where plant growth regulator (PGR: Moddus 250EC) was applied as soon as the second internode was at least one centimetre (GS31-2) in 12 genotypes of the HiBAP during one season (Y17: 2016-17). Results suggested that using the adequate concentration and timing of application of PGR is possible to reduce internode lengths but further study is needed in order to make definite conclusions on effects on HI.

Work contribution

All the work presented in this thesis is my own work with collaboration with CIMMYT, The University of Nottingham, Earlham Institute and The John Innes Centre.

Phenotypic measurements obtained during seasons 2015-16, 2016-17 on the HiBAP (High Biomass Association Panel) and 2017-18 on the HiBAP_PGR (High Biomass Association Panel Plant Growth Regulator) were done at NW Mexico at CIMMYT experimental station Norman Borlaug with the help of Physiology CIMMYT team (chapters 2, 4 and 6). For the Savannah x Rialto Doubled Haploid (SxR DH) population sown at The University of Nottingham during seasons 2015-16 and 2016-17 data was recorded with the help of John's Foulkes team (chapters 3 and 5).

For the molecular analysis, data was obtained from the Earlham Institute (EI) and The John Innes Centre (JIC). Results of the genome-wide analysis study (GWAS) on chapter 4 were part of the IWYP (International Wheat Yield Partnership) project N-IWYP700 in collaboration with the Earlham Institute. From this chapter, some of the methodology (DNA extraction, molecular marker generation, population structure, linkage disequilibrium) was developed by Anthony Hall's group. As a matter of fact, some of the marker-trait associations (MTAs) mentioned (grain yield, days to anthesis, harvest index, thousand-grain weight, spikes per m^2, grains per m^2, spikelets per spike, length spike and above-ground DM at physiological maturity) have already been reported by Molero et al. (2018). For chapter 5 where quantitative trait loci (QTL) analysis were done using the SxR DH phenotypic data the genetic map used was provided by The John Innes Centre (Luzie Wingen).

THANKS... :)

First, I want to acknowledge **CONACYT** (National Council of Science and Technology) for awarding me with a 48 months scholarship which allowed me to continue developing and preparing as a research scientist. At the same time, I'm very grateful that I had the opportunity of being a student at **The University of Nottingham** internationally recognised for its prestige and high-quality teaching and learning, providing exceptional student experience. At the same time, I am grateful to have been supervised by John Foulkes, thanks for the knowledge, wisdom and shared advice.

All my love and appreciation to **CIMMYT-MasAgro**, for supporting me with all my expenses and everything that I needed to run my field experiments in NW Mexico, in specific the Physiology team starting with my supervisors: Matthew Reynolds and Gemma Molero thanks for believing in me, for the patience and knowledge shared with me, also I want to thank Carolina Rivera-Amado, Francisco Pinera-Chavez, Jacinta Gimeno, Sivakumar Sukumaran, Francisco Pinto, Araceli Torres, Nayeli Quiche, Jazmin Rowalldez and the great "ingenieros & eventuales" team that assist me recording data in the field and in the laboratory.

Jayalath and Minuka, John Foulke's team, I'm grateful for your support and help for sampling and data collection while I had my foot immobilised.

I'm delighted that I got to collaborate with Anthony Hall and Ryan Joynson at the **Earlham Institute** and with Luzie Wingen at The **John Innes Centre**: Thanks for sharing

A big shout-out to my favourite persons in the world **MY FAMILY**, mom, dad and sister for all their love and support during my entire life. My super-duper supporting Mexican girls (**Martha & Gaby**). THANKS to my second family, **Caro Sansaloni** & **Cesar Petroli**, which encourage me to continue preparing myself as a researcher.

To all those persons that I have met during this AMAZING four years: **Crossfit girls** (Dannie, Laura & Tam), **Girls with Guns** (Celia, Hannah, Lauren, Caitlyn, Orla), **Crossfit Urban Outlaw** (Louise, Ash, Tom, Dan, Char, Mark, Chris, Paule, Penny, EVERYONE), but special YOOOOOU Mr. **Ricardo Cram**, Thanks for always been there pushing me to give my best and especially for all your patience and loveeeeeeeeee (and also for my customed Metcons 5s) <3!!!

Table of contents

Abstract ii
Work contribution iv
THANKS… :) v
Table of contents 1
List of figures 5
List of tables 7
List of abbreviations 10
Thesis structure 14
1. Literature review 16
1.1. Wheat global production 16
1.2. Wheat development, growth and morphology 17
1.3. Biomass production 21
1.3.1. Leaf and canopy photosynthesis 21
1.3.2. Spike fertility and fruiting efficiency 22
1.3.3. Harvest index 24
1.3.4. Optimising above-ground DM partitioning 25
1.3.5. Enhancing below ground partitioning 25
1.3.6. Source-sink balance 26
1.4. Wheat genome and its evolution 31
1.4.1. Genome-wide association study (GWAS) in wheat 33
1.4.2. Quantitative trait loci (QTL) in wheat 40
1.5. Wheat breeding and high-throughput phenotyping 43
Project objectives 44
2. Dry matter partitioning to enhance yield, grain number and harvest index in a high biomass spring wheat panel 45
2.1. Introduction 46
2.1.1. Dynamics of plant developmental stage 47
2.1.2. Grain number determination 47
2.2. Materials and methods 49
2.2.1. Plant material and experimental design 49
2.2.2. Crop measurements 50
2.2.3. Statistical analysis 51
2.3. Results 53
2.3.1. Physiological maturity, grain yield and yield components 55
2.3.3. Biomass, DM partitioning and stem internode lengths at GS65+7d 56
2.3.4. Internode DM partitioning 58
2.3.5. Spike morphological partitioning 60
2.3.6. Correlations between partitioning traits, grain number, harvest index and grain yield 61

2.3.7. Stepwise regression analysis 64
2.3.9. HiBAP genetic background 66
2.4. Discussion 66
2.4.1. Association between biomass, harvest index and grain yield 66
2.4.2. Pre-anthesis growth, partitioning and determination of GN 67
2.4.3. Spring wheat ideotype for optimised partitioning 69
2.4.4. Implications for plant breeding programs 70
2.5. Conclusions 71
2.6. Supplementary material 72
3. Enhancing dry matter partitioning to increase yield, grain number and harvest index in a doubled haploid winter wheat population 87
3.1. Introduction 88
3.1.1. Biomass and grain production 88
3.1.2. Enhancing pre-anthesis growth and grain number 90
3.2. Materials and methods 91
3.2.1. Plant material and experimental design 91
3.2.2. Crop measurements 92
3.2.3. Statistical analysis 94
3.3. Results 94
3.3.1. Crop development 96
3.3.2. Grain yield and yield components 96
3.3.3. Biomass, DM partitioning and stem internode lengths at GS65+7d 98
3.3.4. Internode DM partitioning 100
3.3.5. Spike component DM partitioning 102
3.3.6. Correlations between partitioning traits, grain number, harvest index and grain yield 103
3.3.7. Stepwise regression analysis 105
3.4. Discussion 106
3.4.1. Yield improvement in high biomass genotypes 106
3.4.2. Pre-anthesis growth, partitioning and determination of grain number 108
3.4.3. Winter wheat ideotype for optimized partitioning 109
3.4.4. Implications for plant breeding programs 110
3.5. Conclusions 111
3.6. Supplementary material 112
4. Genetic analysis of physiological traits to increase grain partitioning in a spring wheat high biomass association panel 119
4.1. Introduction 120

4.1.1. Physiological traits to increase grain partitioning 120
4.1.2. Genome-wide association analysis for grain partitioning traits 120
4.2. Materials and methods 122
4.2.1. Plant material and experimental design 122
4.2.2. DNA extraction and genotyping 122
4.2.3. High biomass spring wheat panel conformation 123
4.2.4. Marker-trait analysis 123
4.3. Results 124
4.3.1. Population structure, linkage disequilibrium and principal component analysis 124
4.3.2. Genome-wide association analysis 126
4.3.3. Candidate genes 131
4.4. Discussion 133
4.4.1. Genetic and phenotypic variation in the high biomass association panel 133
4.4.2. Marker-trait associations 135
4.4.3. Next steps: marker-trait validation 137
4.5. Conclusions 137
4.6. Supplementary material 138
5. Characterization of partitioning and yield-related QTL in a doubled haploid winter wheat population 149
5.1. Introduction 150
5.1.1. Physiological traits to increase grain partitioning 150
5.1.2. Quantitative trait loci for grain partitioning traits 151
5.2. Materials and methods 152
5.2.1. Plant material and experimental design 152
5.2.2. Construction of genetic linkage map 152
5.3. Results 154
5.3.1. QTL analysis 155
5.4. Discussion 164
5.4.1. Genetic and phenotypic variations among high biomass progeny 164
5.4.2. Detection of stable partitioning and grain yield QTLs 165
5.4.3. Implications of detected QTLs 167
5.5. Conclusions 167
5.6. Supplementary material 169
6. Optimising dry-matter partitioning using plant growth regulators in a high biomass spring wheat background 173
6.1. Introduction 174
6.1.1. Spike/stem dry-matter distribution 174

6.1.2. Plant growth regulators and their action 175
6.2. Materials and methods 176
6.2.1. Plant material and experimental design 176
6.2.2. Crop measurements 177
6.2.3. Statistical analysis 179
6.3. Results 179
6.3.1. Crop development and canopy temperature 184
6.3.2. GS29 and GS41 biomass DM partitioning 184
6.3.3. GS65+7d biomass DM partitioning and plant components lengths 186
6.3.4. Stem internode DM partitioning at GS65+7d 187
6.3.5. Spike morphological partitioning 187
6.3.6. Biomass, grain yield, yield components and DM partitioning at PM 188
6.3.7. Correlations between partitioning traits, grain number, harvest index and grain yield 189
6.4. Discussion 192
6.4.1. Enhance and effective timing for PGR 192
6.4.2. Plant growth regulators on yield potential crops 192
6.5. Conclusion 193
6.6. Supplementary material 194
7. General Discussion 198
7.1. Genetic variation for grain partitioning traits in high biomass wheat backgrounds 198
7.2. Partitioning traits to increase spike growth 200
7.3. High-throughput phenotyping and application of molecular markers for grain partitioning 201
7.4. Overall conclusions 202
7.5. Future work 204
7.5.1. Optimising partitioning during stem elongation and floret development 204
7.5.2. Genotyping platforms available worldwide 205
8. References 207

List of figures

Figure 1.1. Wheat growing locations and environment distribution worldwide.

Figure 1.2. Description of growth stages of a wheat plant.

Figure 1.3. Wheat development stages at field level: a) vegetative stage, b) reproductive stage (GS47: leaf-sheath opening), c) reproductive (GS65: anthesis), d) grain filling (GS87).

Figure 1.4. Wheat organ plant diagram.

Figure 1.5. Structures of the wheat inflorescence (spike or ear), spikelet and floret.

Figure 1.6. Summary of wheat genome evolution.

Figure 2.1. Stem internode partitioning (true stem & leaf sheath) at seven days after anthesis (GS65+7d).

Figure 2.2. Spike partitioning at seven days after anthesis (GS65+7d).

Figure 2.3. Linear regressions amongst traits measured at physiological maturity on the HIBAP.

Figure 2.4. Genetic ranges for 150 HiBAP genotypes for DM shoot-1 at GS65+7d (right) in spike (Spi), lamina (Lam) and stem (Ste) and spike and stem-internode lengths (left).

Figure 2.5. Linear regressions amongst the whole HIBAP (150 genotypes) between physiological traits measured at GS65+7d.

Figure 2.6. Linear regressions amongst HIBAP subset 1 genotypes between stem internode traits at GS65+7d.

Figure 3.1. Linear regressions amongst 94 SxR DH lines (parents were excluded from the linear regression analysis) between physiological maturity traits.

Figure 3.1. Measurement of morphological characteristics (stem internode, flag leaf and spike length), on SxR DH shoots collected at seven days after anthesis (GS65+7d).

Figure 3.2. Genetic ranges from SxR DH genotypes for DM per shoot-1 at GS65+7d (right) for spike (SPI), lamina (Lam) and stem (Ste) and spike and stem-internode lengths (left).

Figure 3.3. Linear regressions amongst the SxR DH population (parents were excluded from the linear regression analysis) between traits measured at GS65+7d.

Figure 3.4. Linear regressions (parents were excluded from the linear regression analysis) amongst 19 lines of the SxR DH population (subset 1) between stem-internode traits.

Figure 4.1. Significant (-log10<3) marker trait associations (MTAs) distribution among 148 genotypes by a) chromosome and b) genome.

Figure 4.2. HiBAP structure distribution of main two populations (by hierarchical clustering) between 148 genotypes using structure software.

Figure 4.3. HiBAP clusters based on PCA considering pedigree background: a) 2 main groups (elite and landrace-synthetic derivates) and b) 4 groups: elite, landrace-derivates, synthetic-derivates and synthetic+landrace-derivates.

Figure 4.4. GWAS for grain yield using naïve model (GLM1) model: a) Manhattan plot with two -log10 p-values cut-offs (blue/red line) plotted against the chromosomes position and b) QQ plot with -log10 transformed p-values.

Figure 4.5. GWAS for grain yield using naïve model + Q1-4 (GLM2) model: a) Manhattan plot with two -log10 p-values cut-offs (blue/red line) plotted against the chromosomes position and b) QQ plot with -log10 transformed p-values.

Figure 4.6. Chromosomal locations of SNPs (red lines), single MTAs (blue lines) and multi-trait MTAs (green lines) identified on the HiBAP based on cross-year means in Y16 and Y17.

Figure 5.1. SxR DH genetic map showing all the unique markers in each linkage group.

Figure 5.2. Linear regressions amongst 94 lines of SxR DH population (parents were excluded in the linear regression) between physiological maturity traits.

Figure 5.3. Genetic ranges from SxR DH genotypes for DM per shoot-1 at GS65+7d (right) for spike (SPI), lamina (Lam) and stem (Ste) and spike and stem-internode lengths (left).

Figure 5.4. Linear regressions amongst the SxR DH population (parents were excluded from the linear regression analysis) between traits measured at GS65+7d.

Figure 6.1. Gibberellin acid biosynthesis and points of inhibition by plant growth retardants.

Figure 6.2. Crop developmental stages for control and PGR treatment for 12 HiBAP genotypes from emergence to a) booting (DTB:GS41), b) seven days after anthesis (DTA: GS65+7d) and c) physiological maturity (DTM: PM).

Figure 6.3. Experiment development through stem elongation and booting stage.

Figure 6.4. DM stem and leaf-sheath (stem) and leaf lamina (leaves) partition (g shoot-1) among the 12 genotypes at a) control and b) PGR blocks at booting (GS41).

Figure 6.5. Partitioning of above-ground DM at GS65+7d among leaf lamina (LamPI), spike (SPI) and stem (StePI) on a) control and b) PGR blocks.

Figure 6.6. Genetic ranges for spike and stem-internode lengths on a) control and b) PGR plants.

Figure 6.7. Genetic variation among 12 HiBAP genotypes at PM in the control (ctrl) and PGR-treatment in a) grain yield (GY: 100% DM), b) Above-Ground DM (AGDM) and c) grains per m^2 (GN).

List of tables

Table 1.1. Summary of genetic variation in different types of wheat genotypes for a range of physiological traits related to grain yield potential.

Table 1.2. Summary of traits in different types of wheat genotypes for a range of different physiological traits associated with genomic regions (chr: chromosomes) and its phenotypic variation (PV) using next-generation sequencing technologies in GWAS studies.

Table 1.3. Summary of traits in different types of wheat genotypes for a range of different physiological traits associated with genomic regions (chr: chromosomes) and its phenotypic variation (PV) in QTL studies.

Table 2.1. Means for elite, landraces-derived (LD), synthetic-derived (SD) and synthetic+landrances-derived (S+LD) and phenotypic ranges, least significant differences (LSD*: P=0.05*), significance (p-values) and broad-sense heritability for 150 HiBAP genotypes at seven days after anthesis (GS65+7d) and physiological maturity (PM: GS87) between groups of genotypes and cross-year evaluation.

Table 2.2. Cross-year genetic ranges (Min: Minimum, Mean, Max: Maximum), broad-sense heritability (H^2), and significant values per genotype (G), year (Y) and environment x year (GxY) for detailed stem internode analysis for subset 1 for true-stem (TS) and leaf-sheath (LS) DM partitioning indices (PI) and specific weight (SW) at GS65+7d.

Table 2.3. Pearson's correlation coefficient among traits measured at GS65+7d and physiological maturity for 29 genotypes (subset 1) of the HiBAP.

Table 2.4. Cross-year genetic ranges (Min: Minimum, Mean, Max: Maximum), broad-sense heritability (H^2), and significant values per genotype (G), year (Y) and environment x year (GxY) for detailed stem internode analysis among 14 genotypes (subset 2) for spike morphology DM partitioning indices (PI) and specific weight (SW) at GS65+7d.

Table 2.5. Pearson's correlation coefficient among traits measured at GS65+7d, physiological maturity and spike morphological traits of 14 genotypes (subset 2) of the HiBAP.

Table 2.6. Pearson's phenotypic correlation coefficients between different traits measured at GS65+7d and physiological maturity among 150 HiBAP genotypes.

Table 2.7. HiBAP stepwise multiple linear regression analysis testing for grain yield (GY), harvest index (HI), spike partitioning index (SPI) and grain number (GN) as dependent variables against selected traits.

Table 3.1. Phenotypic ranges and means for DH lines, least significant differences (LSD, *P=0.05*), significance (p-values) and broad-sense heritability (H^2) for SxR DH population.

Table 3.2. Cross-year genetic ranges (Min: Minimum, Mean, Max: Maximum), broad-sense heritability (H^2), and significance values for 19 DH lines (subset 1) and parents (G), year (Y) and genotype x year (GxY) for true-stem (TS) and leaf-sheath (LS) DM partitioning indices (PI) and specific weight (SW).

Table 3.3. Pearson's correlation coefficient between traits measured at GS65+7d, physiological maturity and stem partitioning traits among 19 DH lines (subset 1) of the SxR DH population (parents were excluded from the correlation analysis).

Table 3.4. Cross-year genetic ranges (Min: Minimum, Mean, Max: Maximum), broad-sense heritability (H^2), and significance values for 12 DH lines (subset 2) and parents (G), year (Y) and genotype x year (GxY) for spike morphology DM partitioning indices (PI) and specific weight (SW).

Table 3.5. Pearson's correlation coefficient between traits measured at GS65+7d, physiological maturity and stem partitioning traits among 12 DH lines (subset 2) of the SxR DH population (parents were excluded from the correlation analysis).

Table 3.6. Pearson's phenotypic correlation coefficients between traits measured at GS65+7d and physiological maturity among the 94 SxR DH lines (parents were excluded from analysis).

Table 3.7. Stepwise multiple linear regression analysis testing GY, HI, SPI and GN as dependent variables different traits (parents were excluded from the analysis). Values presented are cross-year means (Y16 and Y17).

Table 4.1. Description of the implementation of different regression models used for the GWAS analysis.

Table 4.2. Phenotypic ranges and means, least significant differences (LSD: *P=0.05*), significance (p-values) and broad-sense heritability (H^2) for 150 HiBAP genotypes at seven days after anthesis (GS65+7d) and physiological maturity (PM: GS87).

Table 4.3. Pearson's phenotypic correlation coefficients between traits measured at GS65+7d and physiological maturity among 150 HiBAP genotypes.

Table 4.4. Summary of GWAS results obtained using a threshold of -log10 > 3 under different models.

Table 4.5. Summary of the marker-trait associations (MTAs) obtained on the HiBAP at GS65+7d and physiological maturity and their location at chromosome and genome level.

Table 4.6. List of potential genes identified on the MTAs scored on the HiBAP using KnetMiner.

Table 5.1. Marker number (M), map length (cM: centimorgans) and density in each chromosome and genome for the complete SxR DH genetic linkage map.

Table 5.2. Phenotypic ranges and means for 94 DH lines, least significant differences (LSD, *P=0.05*), significance (p-values) and broad-sense heritability (H^2) for SxR DH population.

Table 5.3. Pearson's phenotypic correlation coefficients between traits measured at GS65+7d and physiological maturity among the 94 SxR DH lines (parents were excluded from analysis).

Table 5.4. QTLs identified per chromosome (chr) with the specific location (cM) and its percentage of variation (PVE) for season 2015-16 (Y16) for 25 traits measured at GS65+7d and PM on 94 lines of the SxR DH population.

Table 5.5. QTLs identified per chromosome (chr) with the specific location (cM) and its percentage of variation (PVE) for season 2016-17 (Y17) for 25 traits measured at GS65+7d and PM on 94 lines of the SxR DH population.

Table 5.6. QTLs identified per chromosome (chr) with the specific location (cM) and its percentage of variation (PVE) for cross-year data (Y16 & Y17) on 25 traits measured at GS65+7d and PM on 64 lines of SxR DH population.

Table 5.7. Phenotypic ranges, significance (p-values) and broad-sense heritability (H^2) for 12 HiBAP genotypes for control and PGR treatments in Y18 (2017-18) for traits at stem elongation (GS29), booting (GS41), seven days after anthesis (GS65+7d) and physiological maturity (GS87).

Table 6.1. Phenotypic ranges, significance (p-values) and broad-sense heritability (H^2) for 12 HiBAP genotypes for control and PGR treatments in Y18 (2017-18) for stem internode traits measured at GS65+7d.

Table 6.2. Phenotypic ranges, significance (p-values) and broad-sense heritability (H^2) for 12 HiBAP genotypes for control and PGR treatments in Y18 (2017-18) for spike partitioning traits measured at GS65+7d.

Table 6.3. Phenotypic ranges, significance (p-values) and broad-sense heritability (H2) for 12 HiBAP genotypes for control and PGR treatments in Y18 (2017-18) for spike partitioning traits measured at GS65+7d.

Table 6.4. Pearson's phenotypic correlation coefficients between traits measured at GS65+7d and physiological maturity in the control among 12 HiBAP genotypes in 2017-18 (Y18).

Table 6.5. Pearson's phenotypic correlation coefficients between traits measured at GS65+7d and physiological maturity in the PGR-treatment among 12 HiBAP genotypes in 2017-18 (Y18).

List of abbreviations

%	Percentage
°C	Degree centigrade
ABA	Abscisic Acid
AGDM	Above-Ground Dry Matter
AM	Association Mapping
ANOVA	Analysis of Variance
ATP	Adenosine Triphosphate
Aw	Awn
BLUE	Best Linear Unbiased Estimator
BT	Booting
bp	Base pair
CGR	Crop dry matter accumulation
CIMMYT	International Maize and Wheat Improvement Center
chr	Chromosome
cM	centimorgan
cm	centimeter
DAE	Days after emergence
DM	Dry Matter
DNA	Deoxyribonucleic acid
Ds	Duration of spike growth
DTA	Days to anthesis
DTM	Days to maturity
DW	Dry Weight
FAO	Food and Agriculture Organization
FE	Fruiting Efficiency
Fs	Fraction of this dry matter partitioned to the spike averaged over the spike growth period
FW	Fresh Weight
g	grams
G	Genotype
GA	Green Area
GAI	Green Area Index
GLM	General Linear Model
Glu	Glume
GN	Grain Number
GS	Growth Stage
GS65	Anthesis (Zadok's growth scale)

GS65+7d	Seven days after anthesis (Zadok's growth scale)
GS87	Physiological Maturity (Zadok's growth scale)
GW	Grain Weight
GWAS	Genome-Wide Association Study
GY	Grain Yield
h	hours
H^2	Broad-sense heritability
ha	Hectare
HI	Harvest Index
HiBAP	High Biomass Association Panel
HTFP	High-Throughput Field Phenotyping
IAA	Acetic Acid
Int	Internode
Int4+	Internode 4 and rest
IWGSC	International Wheat Genome Sequencing
IWYP	International Wheat Yield Partnership
kg	Kilogram
L	Liter
Lam	Lamina
LamPI	Lamina Partitioning Index
LD	Linkage Disequilibrium
Le	Lemma
Ln	Length
LOD	Logarithm of Odds
LS	Leaf Sheath
m	meters
MAF	Minor Allele Frequency
Max	Maximum
MAS	Marker Assisted Selection
Mean	Average
mg	Milligrams
Min	Minimum
MJ	MegaJoule
MLM	Mixed Linear Model
mm	Millimeter
MTA	Marker Trait Association
N	Nitrogen
NADPH	Nicotinamide Adenine Dinucleotide Phosphate Oxidase
NGS	Next-Generation Sequencing

NIL	Near-Isogenic Lines
NW	New West
P(G)	Significance of the genotype
P(G×T)	Significance treatment × genotype
P(G×Y)	Significance of the genotype x environment;
P(T)	Significance per treatment
P(Y)	Significance of the year
Pa	Palea
PAR	Photosynthetically Active Radiation
PCA	Principal Component Analysis
Ppd	Photoperiod
PGR	Plant Growth Regulator
PH	Plant Height
PI	Partitioning Index
PM	Physiological Maturity
QTL	Quantitative Trait Loci
Ra	Rachis
Rht	Reduced Height
RIL	Recombinant Inbread Line
Rubisco	Ribulose-1,5-bisphosphate carboxylase/oxygenase
RUE	Radiation Use Efficiency
SDWa	Dry weight of spikes at anthesis
SE	Stem Elongation
SG	Stay Green
SNP	Single Nucleotide Polymorphism
SPI	Spike Partitioning Index
Spk	Spike
Spklspk	Spikelets per spike
StePI	Stem Partitioning Index
SW	Specific Weight
SxR DH	Savannah x Rialto Doubled Haploid
TGW	Thousand-Grain Weight
Tin	Tiller inhibition
t	Ton
TS	True Stem
UK	United Kingdom
Vrn	Vernalization
WSC	Water Soluble Carbohydrates
Yr	Year

Y16	Season from 2015 to 2016
Y17	Season from 2016 to 2017
Y18	Season from 2017 to 2018

Thesis structure

This project used a physiological approach in which trait characterisation for grain partitioning traits was done at field level as well a molecular approach aiming to understand the genetic basis of the traits using sequencing technology and bioinformatics tools. The format for this PhD thesis will be in a series of chapters written in the form of articles which will be submitted to journals. The thesis includes seven chapters with the first one dedicated to a literature review, three chapters will show results obtained in phenotyping physiological traits, two chapters will report novel findings of the genotype-wide association studies (GWAS) and quantitative trait loci (QTL) analysis and in the last chapter the key findings and future work will be discussed.

Chapter 1: Literature review

Introductory chapter incorporating a comprehensive summary of the concepts and terms studied during this PhD and including the structure and aims of the overall project.

Chapter 2: Dry matter partitioning to enhance yield, grain number and harvest index in a high biomass spring wheat panel

Results obtained from the phenotypic data collected at NW Mexico in 2015-16 (Y16) and 2016-17 (Y17) crop cycles on an association panel (HIBAP) of 150 spring wheat genotypes (landraces-derivates, synthetic-derivates and elite cultivars).

Chapter 3: Enhancing dry matter partitioning to increase yield, grain number and harvest index in a doubled haploid winter wheat population

Results obtained from phenotyping 94 winter wheat doubled-haploid Savannah x Rialto (SxR) lines and parents characterised by moderate/high biomass and high yield potential, in experiments sown in 2015-16 and 2016-17 in an unirrigated environment at The University of Nottingham.

Chapter 4: Genetic analysis of physiological traits to increased grain partitioning in a spring wheat high biomass association panel

A genome-wide association study (GWAS) was carried-out on 148 genotypes and 24 traits measured over two seasons (Y16 & Y17) at seven days after anthesis and physiological maturity.

Chapter 5: Characterization of partitioning and yield-related QTLs in a doubled haploid winter wheat population

A Quantitative Trait Loci (QTL) analysis using rQTL was implemented on 91 genotypes and 25 traits measured over two seasons (Y16 & Y17) at seven days after anthesis and physiological maturity trait.

Chapter 6: Optimizing dry-matter partitioning using plant growth regulators

Effects of shortening the stem with the use of a plant growth regulator (insensitivity to gibberellin acid-based) applied at GS31-2 on a subset of the HiBAP (12 genotypes) in one season (Y18: 2017-18) at NW Mexico.

Chapter 7: General discussion

Interpretations and analysis of the hypotheses and results will be discussed, and suggestions and predictions for future work research will be stated in this chapter.

1. Literature review

1.1. Wheat global production

In recent years modern plant breeding has started to utilise the wheat genetic diversity, which the material available in gene banks can offer. With the use of this powerful resource, scientists are able to cross elite cultivars with wider wheat germplasm (landraces and near wheat relatives) to increase yield potential under optimal environments and resource limitations (Araus et al., 2008; Tanksley 1997). Currently, the global land area is 13 billion ha[1], of which 12% is used for agricultural purposes (Figure 1.1) (Asseng et al., 2019; FAO, 2011). Facing instability with climate change (temperature increases, fluctuations in the amount of water-rainfall available), urbanisation, soil degradation and resistance to herbicides and fungicides, the expectation of supplying yield increases demanded for food security is uncertain. For 2025, grain production will need to increase to 891 million tonnes per year, 2.4% per year, to satisfy global demand (Mitchell & Sheehy, 2018; Ray et al., 2013; Xu et al., 2017).

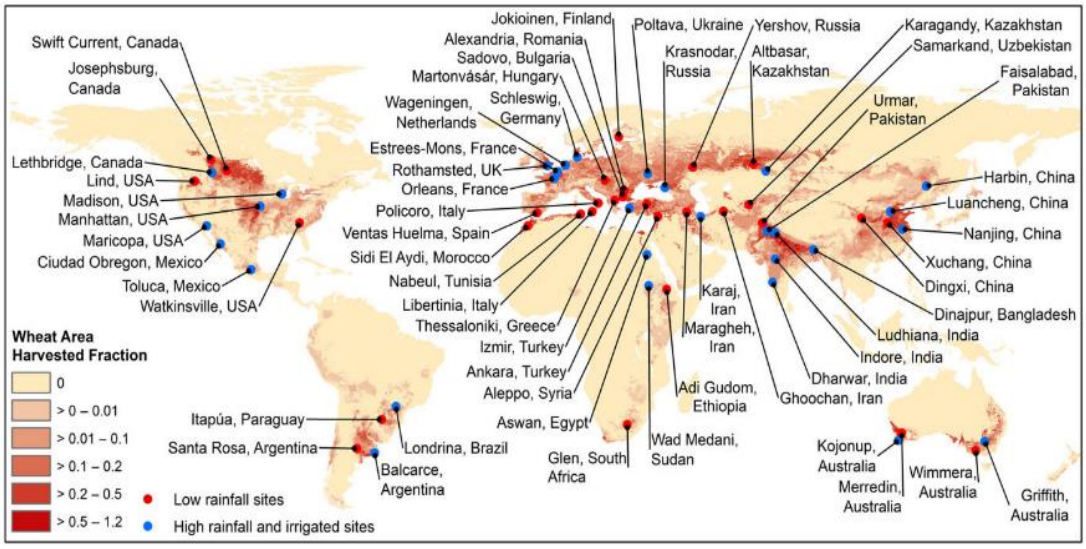


Figure 1.1. Wheat growing locations and environment distribution worldwide (FAO, 2011).

Wheat, spring or winter (vernalization required) types, is an essential crop of the global food grown on more than 240 million ha[1] with bread wheat (*Triticum aestivum L.*) and durum wheat (*Triticum turgidum L.*) being the two most sown species. Bread wheat was first domesticated 10,000 years ago as part of the Neolithic Revolution where civilisation combined their hunter-gatherer lifestyle with the establishment of agriculture. With the establishment of agronomy practices, it started to become essential to adapt wild species to be efficient in assimilating resources for grain yield production.

In the early part of the last century wheat plants were characterised as tall, tillering with weak stems which led them to lodge making them challenging to harvest and resulting in reduced yield potential (Khush, 2001). During the Green Revolution, a tremendous impact on food

production, socio-economic conditions and environmental sustainability brought an increase in wheat yield potential (Fischer, 2014). The incorporation of better agronomic practices was combined with improved genetic resources with the introduction of *Rht* (reduced height) genes which resulted in varieties with increased spike fertility, grain number per m^2 (GN), harvest index (HI: grain dry-matter/above-ground dry matter) and grain yield (Ehdaie et al., 2006, Furbank et al., 2015, Hedden, 2003). Compared to landraces and old cultivars, these genotypes have a strong-short stem (~21% height reduction) able to support heavier spikes as the amount of assimilates available to the spike during the stem elongation and floret survival phase increased.

Some reports have suggested that following the Green Revolution wheat productivity gains have continued but at a slower rate in the last 30 to 40 years (Aisawi et al., 2015; Lopes et al., 2015). However, in some regions genetic yield progress has become stagnant (Brisson et al., 2010; Ray et al., 2012). Therefore, it is important to improve our understanding of the physiological basis of yield, identifying new physiological avenues in order to increase the rate of genetic (Sanchez-Garcia et al., 2012).

1.2. Wheat development, growth and morphology

A crop will display changes in its morphology and function from the emergence of the first leaf until grain ripening. Wheat growth and development can be divided into three general growth stages (Figure 1.2, 1.3) (Chen et al., 2010; Reynolds et al., 2009; et al., 2012; Zadoks et al., 1974):

- ***Vegetative (emergence to stem elongation: [Zadoks' scale: GS10 - GS30)*:**

During this stage, changes at canopy level will be perceived starting with the emergence of first leaves 15 to 20 days after the crop was sown; at this stage, the photosynthetic activity will begin. Potential tillers will appear continuing and floral differentiation will occur (double ridge) (Kirby 1988).

- ***Reproductive (stem elongation to anthesis: [Zadoks' scale: GS31 - GS61]):***

Spikelet primordia will begin (subapical meristematic activity is at a low level) until the apex become reproductive (where meristematic dome will produce cells which will end as part of the flower). At this point, stem growth becomes competitive with the developing spikes. Florets within spikelets go through seven developmental stages (Barber et al., 2015; Guo & Schnurbusch, 2015):

i) Terminal spikelet: completion of spikelet initiation. The floret apex, surrounded by the carpel, develops into the ovule. A single egg (megaspore) mother cell is formed from one archesporial cell in each ovule and undergoes meiosis. Each anther contains many archesporial cells, each forming four pollen mother cells which each undergo meiosis while the anthers are green and apparently about 1 mm long.

ii) White anther: lemmas of florets F1 and F2 completely enclose stamens and other structures.

iii) Green anther: glumes cover all but the tips of florets.

iv) Yellow anther: glumes are fully formed, and the lemmas of the first three florets are visible.

v) Tipping: first awns visible, depending on the type of wheat.

vi) Heading: 50% of spikes visible.

vii) Anthesis: 50% of spikes with anthers, at this point a percentage of the florets may die between the onset of stem extension and booting limiting the number of grains per unit area (GN) (González et al., 2011). The proportion of above-ground dry matter (AGDM) partitioned to reproductive growth at anthesis is reflected in the spike partitioning index (SPI: spike dry matter / AGDM at anthesis) and the efficiency of spike growth is reflected in the ratio of grain number to spike dry weight defined as fruiting efficiency (FE: grains gram^{-1}) (Foulkes et al., 2011).

- *Grain filling (anthesis to physiological maturity: [Zadoks' scale: GS61 - GS91]):*

The last phase is where fertilisation and grain growth occurs, pre-stored assimilates are remobilised to the grains which reach their maximum dry weight at maturity (Asseng et al., 2017). Grain filling follows a sigmoidal pattern; slow endosperm cell division phase, a linear rapid grain growth phase and finally a passive grain growth phase as ripening occurs (Sofield et al., 1977; Xie et al., 2016).

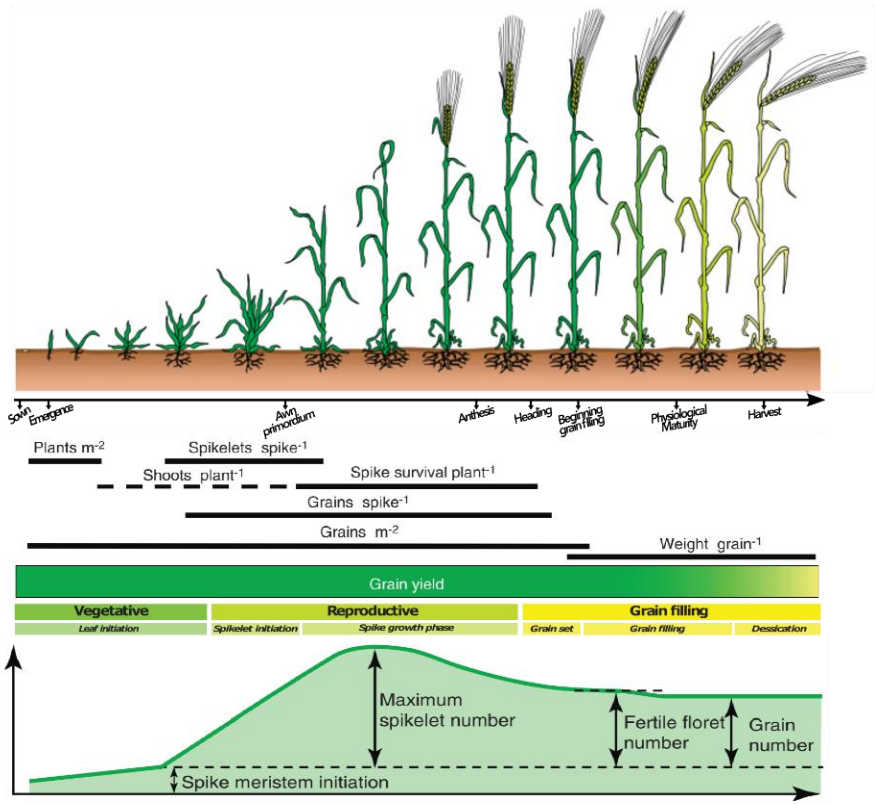


Figure 1.2. Description of growth stages of a wheat plant (adapted from: Sreenivasulu & Schnurbusch, 2012).



Figure 1.3. Wheat development stages at field level: a) vegetative stage, b) reproductive stage (GS47: leaf-sheath opening), c) reproductive (GS65: anthesis), d) grain filling (GS87).

A wheat plant is divided into four main components (Figure 1.4): spike, stem, leaf and roots, each part is involved in the determination of grain yield.

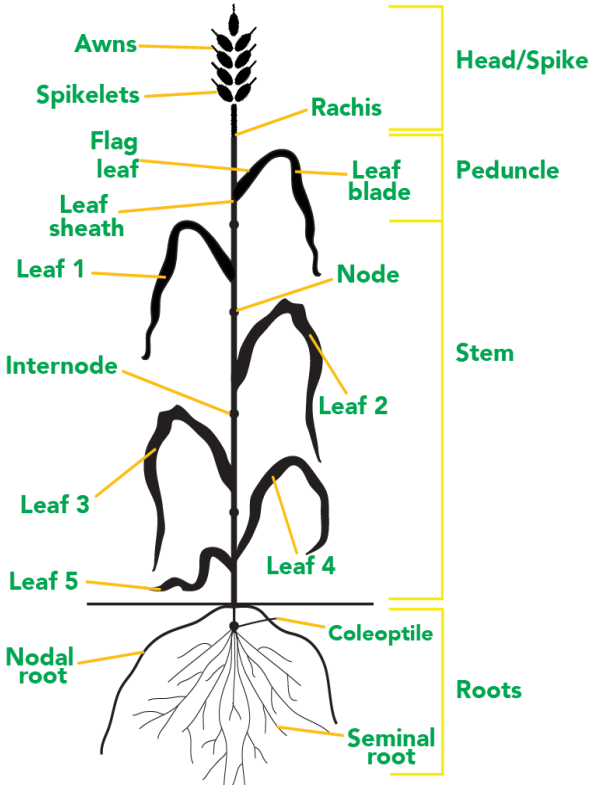


Figure 1.4. Wheat organ plant diagram.

The ear or spike (Figure 1.5) is formed by two rows of spikelets arranged on opposite sides of the central rachis. Spikelets are comprised of a rachilla containing approximately 10 to 12 florets enclosed by a lemma and a palea. The florets contain a carpel consisting of the ovary with the feathery stigmas, and three stamens bearing the pollen sacs or anthers (Anderson & Garlinge 2000; Rasmussen & Minteer 2014). Depending on the genotype some spikes will develop awns which are filiform and sclerophyllous prolongations of the lemmas which can contribute more than 50% of net photosynthesis (Maydup et al., 2014). According to the position, grains differ in their weight where distal grains are lighter compared to the basal

grains which, in turn, are lighter than central grains (Calderini & Ortiz-Monasterio 2003; Lawlor & Paul 2014).

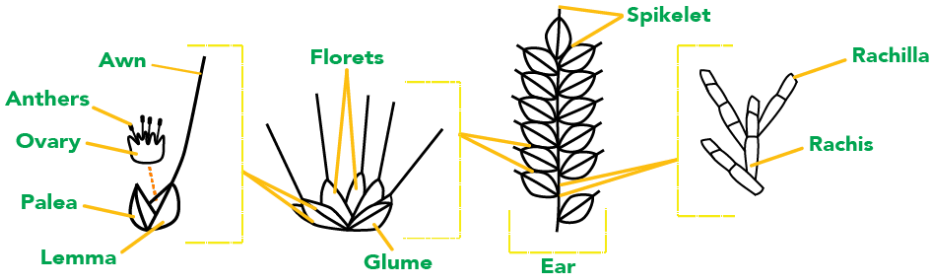


Figure 1.5. Structures of the wheat inflorescence (spike or ear), spikelet and floret (adapted from Anderson & Carlton, 2000).

Leaves consist of two sections: the sheath which is the basal part that wraps around the stem and the lamina often described as the blade. The expanded portion of the leaf produces carbohydrates through photosynthesis which can be often be limited (high light) by the amount and activity of the rubisco (Ribulose-1,5-bisphosphate carboxylase/oxygenase) enzyme which is responsible for catalysing the photosynthetic assimilation of carbon dioxide into organic compounds (Carmo-Silva et al., 2015). The first process involves light capture to produce two types of energy molecules: ATP (Adenosine Triphosphate) and NADPH (Nicotinamide Adenine Dinucleotide Phosphate Oxidase). Then these molecules will be used on the dark phase, also known as the Calvin cycle, where carbon dioxide is converted into carbohydrates. Products (carbohydrates) generated on the leaves will subsequently be translocated to the spike (Krenzer et al., 1995; Rasmussen & Minteer 2014).

The stem is made up of the peduncle, nodes, and internodes acting as a significant temporary store of carbohydrates, which can be used after anthesis to contribute to grain growth (Borrell et al., 1989). Currently, the optimum height for a wheat plant is between 70 to 100 cm (Rebetzke et al., 2012). Below this threshold, it is hard to achieve high grain yield because of poor radiation distribution within the canopy and consequent reductions in radiation-use efficiency (RUE) (Araus et al., 2008).

Plant roots are fundamental for soil resource capture and assimilation (Eshel & Beeckman, 2013). In wheat, a fibrous root system is present in which two types of roots can be found: seminal and nodal or adventitious roots. Seminal roots constitute 14% of the entire root system; three to six seminal roots usually emerge from the seed (Lynch & Brown, 2012). On the other hand, nodal roots which derive from the nodes of the shoot apex which grow mostly in the upper soil layers, and their number depend mainly on the plant tillering ability. The number of nodal roots and shoots are thus positively correlated, conferring adaptability of the plant to the environment in which it is growing (Hockett 1986; Reynolds et al., 2002).

1.3. Biomass production

Grain yield is related to the above-ground dry matter production per unit area (AGDM) depending on the capacity that the plant has to accumulate biomass (Giunta et al., 2009) and the ratio between AGDM and yield (HI: Harvest Index) (Slafer et al., 1990) (Equation 1.1):

$$\text{Grain Yield (g m}^{-2}\text{)} = \text{Above-Ground Dry Matter (g m}^{-2}\text{)} \times \text{HI} \quad [1.1]$$

Grain yield can be partitioned into three components: (i) dry matter produced after anthesis and translocated directly to the grain, (ii) dry matter produced before anthesis and remobilized to the grain during grain filling (contributing 3 to 50% of the grain dry matter at maturity), and (iii) dry matter produced after anthesis but stored temporarily in vegetative organs before being remobilized to the grain (Pheloung & Siddique 1991). Competition and/or optimisation of assimilates between organs can impact grain partitioning. Therefore, it is necessary to identify traits that impact directly on grain partitioning to improve breeding programs (Richards 2000).

1.3.1. Leaf and canopy photosynthesis

A plant can grow using assimilates produced during photosynthesis (Sharma-Natu & Ghildiyal, 2005). Biomass production will start when the first leaf emerges above ground and continues until physiological maturity. The accumulation will rely on the amount of interception of photosynthetically active radiation (PAR) by the green canopy surface area per unit ground area, i.e. green area index (GAI) (Murchie & Reynolds, 2012). The arrangement of leaves (spatial structure and the total surface area) in a plant plays an important role in determining the radiation-use efficiency (RUE: AGDM per unit radiation interception) which affects crop productivity and the amount of biomass produced (Tripathi et al., 2018). Using various crops (pea, faba bean, durum wheat and triticale) Giunta et al. (2009), reported that longer growing cycles would allow the plant to intercept more PAR resulting in an increase of biomass.

Leaves are the main source organs to assimilate carbon dioxide and sunlight (Wu et al., 2014). In wheat, leaves can be classified as sun leaves which tend to be small, with thick cell walls, low water content, and higher specific leaf weight (SLW: leaf dry matter (DM)/leaf area) which intercept radiation from the sun. Shaded leaves exhibit a higher water content, but their photosynthetic capacity is less compared to the top leaves (Araujo et al., 2008; Devasenapathy 2008; Eaton-Rye et al., 2011; Rhizopoulou et al., 1991). If leaves are roughly horizontal, the uppermost layer will intercept most of the light at midday while about 10% may penetrate to the next layer and 1% to the layer below that. A better arrangement for these conditions would be for the upper layer to intercept a smaller fraction of the light, reducing light saturation of photosynthesis and allowing more light to reach the lower layer; as a consequence, erect leaves should increase canopy photosynthesis (Long et al., 2006).

The green surface of a plant, chloroplast level, is the primary interface between atmosphere and crop, exchanging energy, water and carbon with the atmosphere (Duveiller et al., 2011;

Rinaldi & Garofalo, 2012). Leaf stomatal conductance determines the interchange of carbon dioxide and water vapour through the stomata (Motzo et al., 2013; Wang et al., 2009). This is often the rate-limiting step (Rubisco: Ribulose-1,5-bisphosphate carboxylase/oxygenase) in photosynthesis at the top of the canopy in field-grown crops (Carmo-Silva et al., 2015). To have efficient water use and high photosynthesis rate, more stomas are located on the abaxial surface (presence of veins) than the adaxial (smooth surface). Guard cells open the stoma to permit the entrance of carbon dioxide for carbon fixation, close them to prevent loss of water vapour and regulate gas interchange between the intercellular spaces within the plant tissue and the surrounding environment (Blatt, 2000; Hetherington, 2001; Sharma-Natu & Ghildiyal, 2005).

After plant emergence leaves initially act as a sink for organic carbon, nitrogen (N), and other nutrients (Thomas & Ougham, 2014). During grain filling senescence occurs and the photosynthetic apparatus within chloroplasts disassembles causing photosynthetic activity to decrease (Verlag et al., 2002). The last leaf to senesce is the flag leaf which contributes about 30 to 50% of the carbon assimilates for grain filling (Zhang et al., 2006). This process involves the breakdown of plastids, mitochondria, vacuoles and nuclei, leading to ultimate cell death and subsequently turning senescing leaves yellow (Kusabaet et al., 2002). The delayed timing of leaf senescence, defined as stay-green (SG), has been frequently attributed to significant yield gains, specifically under abiotic stress conditions (Luche et al., 2015). Using advanced lines and a recombinant inbred line (RIL) population derived from a cross between Seri and Babax, Lopes and Reynolds (2012) reported that SG was correlated with grain yield under heat stress which could be attributed either to the interaction of hormones (high cytokinin levels and/or low ethylene) or higher nitrogen assimilation. SG behaviour can be divided into four types (Thomas & Howarth, 2000):

i. Type A is where the senescence starts late but then proceeds at a normal rate, this happens when a correlation exists between net carbon output and chlorophyll content.
ii. Type B differs from A by initiating senescence on schedule but then senescing at a slower rate, but both type A and B are functional.
iii. When chlorophyll is retained but without photosynthesis activity this behaviour is considered as type C.
iv. Similar to C, but in D is related to more colour retention, both types C and D are non-functional stay-green type.

1.3.2. Spike fertility and fruiting efficiency

Spike photosynthesis can contribute significantly to grain yield, ranging from 20 to 40% of mature grain dry mass depending on cultivar and growing conditions (Ding et al., 2018; Maydup et al., 2012). Around 20 days before anthesis a floral degradation process is initiated, determining the number of fertile florets produced based on the amount of assimilates

available during the latter stages of stem extension (Bancal, 2009; Fischer, 1984). This floret abortion occurs at a time when assimilate competition between plant organs is high, due to the coincidence of source-limited crop growth (rapid spike growth and stem elongation) and interplant competition (González et al., 2011). Spike fertility is also affected through the fruiting efficiency (FE) defined as the number of grains per unit spike weight (grain number g^{-1}) at anthesis reflecting the ability with which dry-matter (DM) allocated to the spike is utilised (Slafer et al., 2015).

After the introduction of *Rht* (Reduced height) genes into wheat genotypes, more assimilates were available for spike growth explaining the genetic progress in grain yield, heavier spikes with more fertile floret (Flintham, 1997). The quantity of assimilates partitioned by the crop to the spike will affect the survival of initiated florets and subsequently, spike partitioning index (SPI: spike DM / above-ground DM at anthesis) and the number of grains m^{-2} (Foulkes et al., 2011). Since enhanced grain number per spike is associated with a higher yield, increasing spikelet number per spike will potentially boost grain number per spike and therefore grain yield (Philipp et al., 2018). Using Recombinant Inbred Lines (RIL) with contrasting SPI Alonso et al. (2018b) concluded that the selection of lines with high SPI should increase GN and grain yield, even considering a potential trade-off with grain weight.

Wheat grains m^{-2} (GN) can be described as the product of spike dry weight at the beginning of grain filling (SDWa) and the number of grains per unit spike DM as an indicator of spike fertility (IRRI 1983; Lázaro & Abbate 2012) (Equation 1.2):

$$\text{GN (grains m}^{-2}\text{)} = \text{SDW (g m}^{-2}\text{)} \times \text{FE (grains g}^{-1}\text{)} \quad [1.2]$$

By allocating more assimilates to distal florets by reducing the demand of basal florets, an improvement in grains per unit area was demonstrated using shading and photoperiod treatments (González et al. 2011a). However, a trade-off of increased fertile florets per spike could be at the reduction of grain weight, as the size of the carpels and/or ovaries could be affected (González et al. 2011b). Using two contrasting modern durum wheat genotypes Ferrante et al. (2015) reported that Donduro had lower FE than Vitron associated with heavier grains in central and apical spikelets. Similarly to Terrile et al. (2017) results suggested that genotypes with higher FE (Baguette Premium "B11" and Baguette 19 "B19") produced more GN, but grain weight (GW) decreased. Therefore, increasing GN via higher FE may result in yield improvement, but special attention is required due to possible negative associations between GW and spike DM, as grain weight potential is related to the size of the ovaries. Therefore, increasing GN via higher FE may result in a small yield improvement if final grain weight is decreased due to a concomitant reduction in potential grain weight (Ferrante et al., 2012; González et al., 2014).

Manipulating the level of hormones, such as indole acetic acid (IAA: auxin) in charge of cell elongation and cell division, gibberellin acid (GA_3) which can stimulate rapid stem and root

growth, abscisic acid (ABA) acting as growth inhibitor, and zeatin (cytokinin) which promotes growth of lateral buds, in florets at specific stages in the regulation of floret development could be a strategy to consider to increase GN (Wang et al., 2001). Grain development is divided into endosperm cell division and differentiation during early embryogenesis, cell expansion and rapid dry weight gain, and cell and embryo maturation (Wang et al., 2006). In rice, it was found that the lack of gibberellin and kinetin hormones in the spikelets of the basal branches of the panicle caused sterility or degeneration (Patel & Mohapatra, 1992). In wheat, the concentration of total soluble sugar and sucrose in the spike was increased by the application of zeatin (Wang et al., 2001) in contrast to the results found with GA_3 where fertile number of grain increased but the final grain set decreased. Furthermore, in rice Ashikari (2005) showed that grain number1a *(GN1A)*, responsible for the regulation of cytokinin oxidase/dehydrogenase (OsCKX2), enhanced grain number (~21%) by accumulating cytokinin in inflorescence meristems.

1.3.3. Harvest index

Grain yields of wheat have historically increased through plant breeding due to higher GN and harvest index (HI: grain DM / above-ground DM) (Foulkes et al., 2011). For wheat, there is a hypothetical limit for HI of approximately 0.62 (Austin, 1980), but Foulkes et al. (2011) estimated that further gains to 0.64 could be achieved by a 10% grain in AGDM at harvest and increasing the ratio of chaff to grain to 175 mg chaff $grain^{-1}$. The study of Austin et al. (1989) on UK cultivars introduced from 1908 to 1986 showed HI to be positively associated with yield progress, with only a slight, non-significant increase in AGDM at harvest. Studying UK winter wheat cultivars released from 1972 to 1995, Shearman et al. (2005) suggested that genetic gains of later cultivars (introduced since 1985) occurred due to increases in both harvest AGDM and HI. More recently, Sanchez-Garcia et al. (2012) compared 26 wheat genotypes, widely grown in Spain during the 20th century, across eight environments and concluded that from the early 1970s with the introduction of semi-dwarf germplasm from CIMMYT and some French cultivars HI increased up to 0.45. Studying CIMMYT spring wheat cultivars released from 1966 to 2009 Aisawi et al. (2015) reported HI values ranging from 0.41 to 0.47 were at higher HI (~0.45) grain yield was decreased. Average values of HI across European countries have been around 0.49 in crops with late maturity associated with a long grain filling period (Rose et al., 2017). Semenov et al. (2014) predicted, using the Sirius wheat model, that average HI among 10 Europe sites could reach 0.56, 15% higher than current values. Using 26 CIMMYT elite spring wheat genotypes Rivera-Amado et al. (2019) reported variation in HI from 0.46 to 0.53 and concluded that HI was correlated with SPI and FE, suggesting that if more assimilates are available to the spike during the critical stem elongation-floret survival phase higher indices could be achieved. With 34 spring durum wheat genotypes with different flowering time, Ammar et al. (2017) confirmed the importance of regulating phenological stages, a more extended vegetative stage and increased biomass accumulation might not be translated into

higher yield due to high temperatures and solar radiation during grain filling.

1.3.4. Optimising above-ground DM partitioning

Dry matter (DM) partitioning is the result of coordinated metabolic processes which affects the distribution and flow of assimilates from source organs via a transport path to the sink organs (Marcelis, 1996). In modern wheat cultivars, variation in grain yield is predominantly explained by GN under favourable conditions and partly related to the amount of assimilates partitioned to the spike before flowering (García et al., 2014). Increasing the number of grains per unit area, by reducing the competition between the spike and other plant organs during stem elongation, could boost GN and yield potential (Satorre & Slafer, 1999).

The stem is a significant temporary store of carbohydrate and is divided into phytomers (Figure 1.3), which consist of a leaf node and an associated section of stem (internode) (Sanchez et al., 2012). Internodes are the hollow parts of stems, mainly surrounded by leaf sheath, situated between nodes and in a wheat plant the presence of 4 to 6 internodes is possible depending on the genotype. The growth of stem internodes, which is useful to predict developmental stages, starts with a vigorous extension and occurs in sequence; when the extension of an internode is half-completed the internode above will begin to extend (Lupton, 2014; Schnyder, 1993; Weightman et al., 1997). For 26 CIMMYT spring wheat cultivars Rivera-Amado et al. (2019) showed that reduced partitioning to the stem internode 2 (top-down, internode below peduncle), ranging from 15.8 to 23.3 cm, and internode 3, ranging from 9.5 to 16.5 cm, increased SPI and spike DM per unit area seven days after anthesis.

Carbohydrates stored, mainly as fructans, in the stem both before and after flowering can be remobilised, contributing directly to grain growth (Borrell et al., 1989). Remobilised reserves (non-structural dry matter) from the stem can provide between 5 to 50% of the final grain weight, depending on the allocation of assimilate efficiency from stem to the spike (Slewinski 2012; Wardlaw & Willenbrink 1994). The amount of accumulated and remobilised stem reserves can be estimated either by monitoring the changes in stem dry weight or directly by measuring stem water-soluble carbohydrates (WSC) content during the grain-filling period. Stem carbohydrate reserves were estimated to contribute from 10 to 62% of the final grain weight in wheat under normal conditions and as much as 40–100% depending on the severity of the environmental conditions (Ehdaie et al., 2008). Using five spring wheat cultivars and one winter wheat cultivar, Zhang et al. (2012) showed that high post-anthesis DM accumulation and high stem WSC at anthesis were highly correlated with HI, and the sink size was the factor limiting whether the plant can convert those assimilates into grains.

1.3.5. Enhancing below ground partitioning

Roots are the hidden organ critical for plant growth (Herder et al., 2010) which acquire water and nutrients from the soil and provide anchorage with phenotype while varying from 0.08 to 0.17 for the total DM partitioning to roots at harvest (Foulkes et al., 2011). Two types

of roots can be distinguished; seminal roots which will grow directly from the seed providing support, whereas nodal (crown or adventitious) arise from the stem basal nodes and begin to extend when tillering starts (Xie et al., 2017).

A mature wheat plant typically produces about six seminal root axes and 10 to 15 crown root axes which can spread 30-90 cm laterally from the stem and grow to a maximum depth of 1 to 2 m. Extension of both seminal and nodal roots usually continues to flowering when they will start to senesce (Slack et al., 2018; York et al., 2018). The size of the root system is determined by the total root biomass and cumulative length (Figueroa-Bustos et al., 2018). A more deep root system is beneficial for genotypes sown under non-optimal conditions, and canopy temperature can provide an estimate of genetic potential for deep roots (Pinto & Reynolds, 2015). Lopes & Reynolds (2010) using a random selection of progeny derived from a Seri/Babax cross concluded that genetic variation in roots DM between 60 to 120 cm soil depth as associated with superior adaptation to drought and more water extraction. Results from a F_5 RIL progeny cross from two winter wheat (Forno and Oberkulmer) showed that higher yields, and increased GN, were associated with a larger root system; however, the total root length and seminal root number had negative effects on TGW (Xie et al., 2017).

1.3.6. Source-sink balance

Source-sink association can be defined as relationships between plant parts in which one part serves as the producer of materials (source) translocated to other plant parts where materials accumulate or are consumed (sink). The type of limitation (source, sink or co-limited) will rely on environmental factors such as temperature, light, humidity, carbon dioxide concentration as well as soil quality (Chang & Zhu, 2017).

There is a debate in the literature on the extent to which grain yield under favourable conditions is sink-limited, i.e. limited by the capacity of the grains to store assimilate (Slafer & Savin, 1994). Using a RIL of 146 genotypes Alonso et al. (2018a) suggested that sink limitation of modern wheat genotypes is due to genetic improvement, as sink is improved the source for grain filling decreases relatively. During grain filling pre-stored assimilates are remobilised to the grains, which act as a backup when the current photosynthetic source is limiting grain growth (Blum et al., 1994).

The yield of cultivars could also be limited by the source photosynthetic capacity, i.e. demand for assimilates outstrips maximal photosynthetic capacity (Jaikumar et al., 2014). Source-sink manipulation treatments such as shading and/or defoliation of the shoot have been done to determine the source-sink balance by the analysis of photosynthesis in organs remaining. Maydup et al. (2010) using genotypes with contrasting spike morphology (BioINTA 3000 and Klein Escudo), on which a defoliation treatment was applied at anthesis (GS65), showed that defoliation reduced total grain weight per ear around 25%, therefore implying source limitation. Grain growth co-limitation could also be present where a partial effect of low source

availability-high sink capacity restricts grain growth (Jaikumar et al., 2014). Using a doubled-haploid spring wheat population for which parents were characterised as high grain number and high thousand-grain weight, Bustos et al. (2013) concluded that there is a possibility to integrate both traits as a result of more spike DM accumulated after anthesis and also higher RUE after anthesis.

For modern wheat genetic variation its key for source-sink traits (Table 1.1), however but some recent reports (Borrill et al, 2015; Ferrante et al., 2012; Reynolds et al., 2017) have stated that yield under optimal conditions is explained mainly through grain number partitioning of photo-assimilates to the spike at anthesis which is not optimal, making grain growth sink-limited (Chang & Zhu, 2017).

Table 1.1. Summary of genetic variation in different types of wheat genotypes for a range of physiological traits related to grain yield potential.

Type of wheat	Germplasm	Environment	Trait(s)	Mechanism	Reference
Durum	Well adapted to different regions of Spain Checks High yield potential Drought tolerance	Field: contrasting conditions (individual plants and dense sown	N/A	Individual plant yield-related to plant height, tillers per plant and green leaf area (GS65+7d) Dense: Nitrogen uptake, HI and specific leaf weight (GS65+7d)	Pedró et al., 2012
Winter and spring	Wheat varieties with a geographically broad (northern China WW 'wheat-producing area', Southern China WW and SW) sample released from 1920 to 2014	Records from regional testing data	Plant height stable from 1990 Yield and its components (GN, SM2, TGW)	Winter wheat GN and TGW increased on modern varieties, while spike number per area did not change Decrease in variation, narrowing genetic bases resulting in a plateau	Qin et al., 2015
Spring	Genotypes containing the alien translocation 7DL.7Ag	Field: NW Mexico, yield potential conditions	Radiation-use efficiency = leaf photosynthesis	Grain yield (grains per spike), AGDM and HI increased	Reynolds et al., 2005
Winter and spring	Presence of *Rht-B1b or Rht-D1b* on SW and *Rht-B1b or Rht-D1b* + *Vrn* on WW	Field: Western Australia	Proportions of DM leaf (15%), stem (66%), and spike (19%)	Grain yield averaged among three years 431 g m^{-2} resulting in low HI values (~0.37)	Zhang et al., 2012

Type of wheat	Germplasm	Environment	Trait(s)	Mechanism	Reference
N/A	Landraces grow before 1940 Old wheat (mid-1940) Derived semi-dwarf (1970) Modern cultivars (released 20th century)	Field: four representative regions in Spain	AGDM unchanged	Yield gains were due to increases in HI, from 0.24 in landraces to 0.48 in modern cultivars	Sanchez-Garcia et al., 2012
Winter and spring	DH cross between large spike spring and Rialto	Field: NW Mexico, yield potential conditions	Number of shoots (presence of *Tin1* gene) Plant height (*Rht-B1b* and/or *Rht-B1a* + *Tin1*)	Decreased spikes m^{-2} (5.7%), increased grains m^{-2} (+6.6%), grains $spike^{-1}$ (+13.9%) and grains $spikelet^{-1}$ (+11.3%) Reduced height (-23%), increased grain yield (+20.4%)	Gaju et al., 2014
Winter	Genotypes developed between 1950 to 2005	Field: China, rainfed + different nitrogen treatments	Nitrogen (N) fertilisation rates	Plant height, leaf area, and grain yield increased as modern cultivars were more responsive to high N	Tian et al., 2011
Winter, spring and durum	Diverse (Landraces, semi-dwarf bread and durum wheat	Field: water treatment (well-watered and drought)	Water treatments	Shorter development cycle, less WSC and grain yield on drought environment. This treatment accelerated stem reserves mobilisation into grains (10 days earlier)	Ehdaie et al., 2008

Type of wheat	Germplasm	Environment	Trait(s)	Mechanism	Reference
Durum	Wide range of genetic variability of well-adapted commercial genotypes and CIMMYT/ICARDA breeding program	Field: southern Spain, rainfed and irrigated conditions	Growing conditions	All yield components (GY: 67% ha^{-1} and 80% $plant^{-1}$) higher under irrigated conditions GY under rainfed conditions was related mainly to the increase in the number of spikes per square meter	Elhani et al., 2007
Durum	Modern and well-adapted genotypes	Outdoors large microcrops and field: Spain; rainfed and irrigated conditions		Variation affected by the growing condition; GY was related to AGDM and GN. Greater crop AGDM resulted in the greater dry weight of the spikes at anthesis resulting in more grains	Ferrante et al., 2012
Spring	Best adapted to the region		DM assimilate partitioning to the spike	More DM allocated to their inflorescences tended to increase GN, but proportionally lower FE. Inflorescence dry weight explained large differences in GN	Garcia et al., 2019
Durum	Landraces and modern cultivars	Field: East (EM) and West Mediterranean (WM) Basin	Growing conditions (water available before and after anthesis)	EM showed more spikes per unit area, while WM were taller plants, more days required to get to anthesis, shorter grain filling period, and heavier grains	Roselló et al., 2019

1.4. Wheat genome and its evolution

In the last few years, modern plant breeding has started to utilise the genetic diversity gene banks can offer. With the use of this powerful resource, scientists can cross elite cultivars with more extensive wheat germplasm, such as landraces (75% more variation than the derived domestic crop), wheat relatives, synthetic wheat and wheat with mutations and translocations. This has resulted in new varieties suitable for growing with environmental limitations and with increased yield potential (Araus et al., 2008; Warburton et al., 2006).

For the selection of desirable characteristics, breeders conventionally use classic Mendelian genetics and wait "n" generations/years to have the trait fixed to obtain a pure line. With the use of sequencing and bioinformatics technologies, it is possible to improve the efficiency of breeding programs by using marker-assisted selection (MAS), which consists of the mapping and tagging of a specific genome sequence that is linked with a particular desired trait(s). This type of selection has allowed breeders and geneticists to accelerate plant breeding by recognising and evaluating the interaction that a gene/allele has with the expression of a trait (phenotype). The generation of saturated maps enables the genetic dissection of the trait by a quantitative trait loci (QTL) analysis (Landjeva et al., 2007; Nelson et al., 1995; Sa 2009).

The widespread breeding of wheat varieties adapted to different agro-ecological zones and climate change has brought the exchange of diversity distributed within gene pools between wild species, landraces and local cultivars based on evolutionary distances and success rate of crossing (Hoisington et al., 1999; Müller et al., 2018). In wheat, the primary gene pool is represented by *T. Aestivium L.* germplasm that shares a common genome, but that has become isolated from mainstream gene pools such as landraces, including polyploidy Triticum species that have genomes homologous with *T. aestivium* subsp aestivum and the diploid donors of the A and D genomes. For the introduction of disease resistance as well as drought-adaptive traits the secondary gene pool is used, which comprises closely related genomes that can be utilised through interspecific hybridisation, and includes the development of so-called synthetic wheat. The tertiary gene pool (no homologous genome) includes related genera of grasses from which transfer of genes requires special techniques such as the generation of amphidiploid (Pratap 2014; Rauf et al., 2015; Reynolds et al., 2009).

In recent decades plant breeding has introduced important characteristics into modern cultivars that allow them to withstand abiotic stresses, efficiently capture light for assimilate production and resist shattering of the spike at maturity (non-brittle rachis) and loss of seed dormancy (Denison, 2015; Gustafson et al. 2009; Shewry, 2009; Vergauwen & De Smet, 2017). Bread wheat (*T. aestivum* L.: 2n = 6x = 42) originated by hybridization between cultivated tetraploid emmer (*T. dicoccum*, AABB; 2n = 4x = 28) and diploid goat grass (*Ae. tauschii*, DD; 2n = 2x = 14) (Jia et al., 2018; Wang et al., 2015; Figure 1.6).

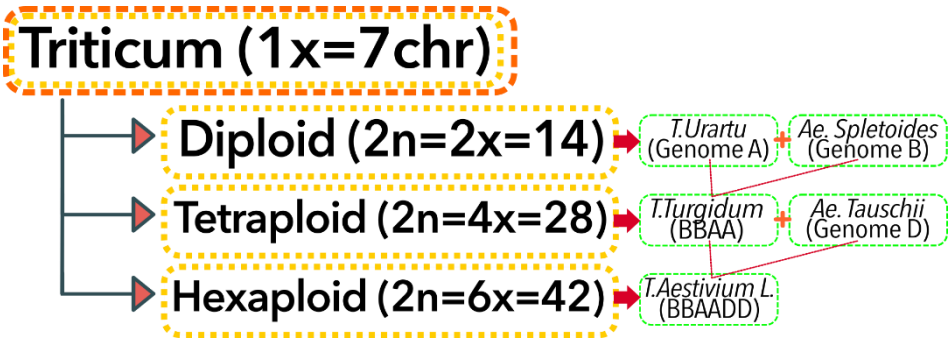


Figure 1.6. Summary of wheat genome evolution.

This genome arrangement has resulted in extensive stretches of repetitive DNA (>80%) containing multiple highly-homologous sequences but also transposable elements (IWGSC, 2018; Wang et al., 2015). Recently, an annotated reference sequence of the Chinese spring wheat variety has been analysed (94% of genome coverage containing 107,891 high-confidence gene models) to identify the distribution and genomic context of coding and noncoding elements across the A, B, and D subgenomes on the 21 chromosomes (IWGSC, 2018).

Wheat grain yield and its components are controlled by numerous genes with additive or epistatic effects and genotype by environment interactions due to complex genetic interactions (Rustgi et al., 2013; Zhang et al., 2010). Conventional breeding in the last century has grown dramatically, pushing genetic gains in wheat to a near-linear increase of approximately 1% in potential grain yield yearly (Xu et al., 2017). Most crop-breeding programs rely on phenotypic evaluations of the plant or crop measured following high-throughput methodologies (Ghanem et al., 2015). Using this approach a new variety needs around 5-10 years to be released making it potentially not suitable at the time of release due to environmental, nutrient, climate and population changes (Semenov & Halford, 2009).

Associations among genetic polymorphism and phenotypic differences have been of significant interest since Mendel stated that internal factors are passed from one generation to the next (Korte & Farlow, 2013). The detection and application of marker-trait associations (MTA) in wheat breeding programs has allowed breeders to accelerate plant breeding by recognising and evaluating the interaction that a specific genome region has in the expression of a trait (phenotype) (Landjeva et al., 2007; Nelson et al., 1995; Sa 2009). Evaluation of the purity/identity of cultivars, mapping of QTLs, controlled crossing (diversity and parental selection), gene introgression/pyramiding and selection of traits with quantitative inheritance are just a few examples of how this technology can assist (Leonova, 2013). Genome-wide association studies (GWAS) and QTL mapping, are two approaches that enable identifying genetic loci associated with phenotypic variation among a panel/population by using statistical models. The type of analysis selected will depend on the genetic architecture, type of

sequencing used to generate the markers, number of individuals and the goal of the analysis, making this a cost-time effective technology.

1.4.1. Genome-wide association study (GWAS) in wheat

GWAS has been used in the last decade to evaluate the association between high-density markers and phenotypic data of interest by exploiting linkage disequilibrium and population structure and familial relatedness (Chen et al., 2017). Factors such as sample size, genome coverage and statistical methods must be considered when running this type of analysis. Large sample sizes are needed to achieve enough statistical power in order to detect polymorphisms of small effect that underlie complex traits (Zhang et al., 2010). Depth of sequencing data will either lead to the detection of additional associations or improve the significance of existing associations, as low coverage could lead to insufficient linkage (Pasam et al., 2012). Because of the large number of tests (statistical methods), significance criteria must be stringent to avoid false positives, which may cause systematic biases (Hong & Park, 2012).

This type of molecular analysis is a cost-effective and powerful study that allows detecting the presence of genetic loci through marker-trait associations (MTAs). Polymorphic alleles in the individual are identified through genotyping sequencing techniques, which allows to align reads to a reference genome (if there is one available) and detect any base change, an SNP (Single Nucleotide Polymorphism) (Gao et al., 2016; Ogihara et al., 2015). Correct identification of SNPs is fundamental, missing data and a significant degree of homogeneity (MAF: Minor Allele Frequency) between a marker and the trait under study can result in inadequate power to infer a statistically significant relationship (Reed et al., 2015). Removing SNPs for which MAF is less than 1 to 5% is recommended before anchoring markers to a reference genome. Mapping consists of putting markers in order, indicating the relative genetic distances between them, and grouping them, depending on their pairwise combinations, into linkage groups (Jones et al., 1997). Linkage and association mapping have improved in the last decade through better marker density and coverage. Linkage mapping (LM) identifies regions associated with a particular phenotypic trait with large support intervals because of limited recombination; alternately, association mapping (AM) relies on both wider genetic diversity and accumulated historical recombinations (Milner et al., 2016).

Hexaploid bread wheat has different rates of gene flow in the three diploid genomes. While diversity levels are similar in the A and B genomes, in the D genome it is significantly reduced, showing the highest level of linkage disequilibrium (LD) (Chao et al., 2010). LD can be quantified as the square of the correlation coefficient between the two loci (generated during the segregation process) (Clarke et al., 2011; Flint-Garcia et al., 2003). In simple terms, if a marker is in linkage disequilibrium with a genetic variant which causes a change in the phenotype, there will be differences in the average phenotype between marker genotype classes (Bush & Moore, 2012; Hamblin et al., 2011). High LD in a population often facilitates

marker-trait detection with a reduced number of markers required, whereas low LD usually implies that high mapping resolution can be achieved, provided that enough markers are available in the target chromosome region (Zhang et al., 2010).

Implementation of population structure is required to minimise false discoveries which may be caused due to geographical origins, local adaptation, breeding history and unequal relatedness among genotypes (Sorrells & Yu, 2009; Yu et al., 2006). Population structure creates genome-wide linkage disequilibrium between unlinked loci. When the allele frequencies between sub-populations of a species are significantly different, due to factors such as genetic drift, domestication or background selection, genetic loci that do not have any effect on the trait may demonstrate statistical significance for their co-segregations with a trait of interest (Ersoz et al., 2007). Population stratification was initially addressed using general linear model (GLM)-based methods such as structured association, genomic control and family-based tests of association. This type of method finds the ordinary least squares solution fitting markers as fixed effects (Bradbury et al., 2007).

The introduction of mixed linear models (MLM) has more recently been demonstrated as an improved method that enables multiple levels of relatedness among individuals to be found through the use of population genetics (Q matrix) and relative kinship (K matrix: average relationship between individuals) as covariates eliminating spurious associations (Yu et al., 2006). On the other hand, principal component analysis (PCA) is a covariate used in genetic diversity analysis as a fast and effective way to study population structure based on genetic correlations among individuals (Wang et al., 2009). This type of matrix summarises variation observed across all markers into a smaller number of underlying component variables. In this scenario, each principal component will describe the population membership or the ancestry of each individual (Zhu et al., 2008).

The last and most critical element in the GWAS analysis is the analytic method to identify the genetic associations in an unbiased fashion. A range of models can be tested, including main effects, interactions, nested effects and covariates (Bradbury et al., 2007). Some traits are underpinned by a small number of loci with large size effects (a simple genetic architecture) while other traits have more complex architectures as they could be controlled by rare variants causing a substantial effect on the phenotype. Therefore, the causative variants may be clustered in one or a small number of genes, or across many genes (polygenetic) (Korte & Farlow, 2013). A logarithm of odds (LOD) score reports the statistical likelihood that two markers will be inherited together (as observed in the experiment) compared to random chance and is used to order markers correctly along a chromosome (O'Rourke, 2014).

Nowadays, identifying MTAs through GWAS on wheat is still a challenging area as the genetic basis of some of the traits are controlled by multiple genes and highly influenced by the environment. Most of the literature that exists is disease-resistance related such as spotch

blotch, leaf rust and Septoria tritici. As new bioinformatic tools become available, access to a complete reference wheat genome sequence and the generation of larger sets of molecular markers are now allowing the identification of superior alleles that underlie complex traits such as grain yield, grain number, AGDM, crop development, length-related (Table 1.2).

Table 1.2. Summary of traits in different types of wheat genotypes for a range of different physiological traits associated with genomic regions (chr: chromosomes) and its phenotypic variation (PV) using next-generation sequencing technologies in GWAS studies.

Strategy	Type of wheat	Environment	Genotype	Trait type	Chr	Trait	% PV	Reference
Disease and pest resistance	Leaf rust AM spring wheat panel (381 genotypes)	Field: Crookston, MN and St. Paul, MN	Illumina iSelect 90K SNP array	Seedling resistance and field resistance (leaf rust)	5A 5D 1B, 1D, 2A, 4A, 5B, 6B & 7B	Anthesis day Rust resistance Seedling resistance	24–34%	Liangliang et al., 2016
	Landrace spring wheat AM panel (528 genotypes)	Growth chambers	Illumina iSelect 9K wheat beadchip assay	Leaf spot diseases	1A, 2B, 3A, 5A, 5D & 6B 1B, 5A, 5B, 6B & 7B 2D, 3A & 5B 3B, 6B & 7B	Bacterial leaf streak Spot blotch Stagonospora nodorum Septoria tritici blotch	1.9–7.6% 1.0–6.5% 0.1–5.8% 0.01–14.5%	Gurung et al., 2014
	National Small Grains Collection (1596 winter wheat & 1556 spring wheat)	Glasshouse: Stillwater, OK	Illumina iSelect 90K SNP array + DaRT markers	Leaf rust resistance	1B, 1D, 2D, 4A, 4B, 5B & 7A	Leaf rust resistance	1.36–8.35%	Li et al., 2016
Physiological traits	Soft red winter wheat 239 genotypes)	Field: Arkansas and Oklahoma, USA	Illumina 9K iSelect	Yield-related traits	1B, 2D, 5B, 6A, 6B, 7B & 7D 2A, 2B, 3B, 7B & 7D 1A, 2A, 3A, 6A & 7D 1A, 2A, 2B, 4A, 6A, 6B, 6D, 7A, 7B & 7D 2A, 3A, 4D, 6A, 7A & 7B 1A, 5B, 7A, 7B & 7D 2A, 3A, 5B & 7A 2B, 6A, 6B, 7A & 7D	Heading day Maturity day Spikes m^{-2} Thousand-grain weight Flag leaf stay green Grains m^{-2} Grain weight Grain yield	N/A	Lozada et al., 2017

Type of wheat	Environment	Genotype	Trait type	Chr	Trait	% PV	Reference
Bread wheat cultivars (163 genotypes) under different environments	Field: Yellow and Huai Valley of China	Illumina iSelect 90K SNP array	Yield-related traits	5B, 6A, 6B & 7A 2A, 2B, 3A, 3B, 3D, 4A, 5A, 5B, 6A & 7B 1B, 2B, 3B, 6A, 6B & 6D 3B, 5B, 6A, 6B, 6D & 7D 1A, 2B, 2D, 3A, 3D, 4D, 6B, 7B & 7D 1A, 1B, 2B, 3A, 3D, 4D, 6B, 7B & 7D 1B, 2A, 2B, 2D, 4B, 4D & 6D 1B, 2A, 2D, 3A, 4B, 7A & 7D	Thousand grain weight Grain size Spike length Grain weight per spike Grain # per spike Spikelets # per spike Plant height Peduncle length	15.7–31.6% 20.9–42.2% 4.4–21.0% 13.0–22.6% 5.4–20.2% 15.5–33.7% 35.8–63.6% 26.5–49.9%	Sun et al., 2017
Heat-stress elite and landraces spring wheat (130 genotypes)	Field: NW Mexico + Glasshouse: Lancaster, UK		Ethylene for spike development	1A, 1B, 1D, 3B, 5B & 7B 2A, 2B, 3A, 3B, 3D, 4B, 5A, 5B, 6A, 6B, 7A & 7B	Spike ethylene production Spike dry weight	5.7–10.5% 6.8–14.9%	Valluru et al. 2017
Recombinant Inbred Line Population ($F_{8:9}$) cross from Shannong 01-35 winter wheat (137 genotypes)	Field: Beijing and and Hebei province	SSR + DaRT + 90K iSelect wheat chip	Spike traits	1B, 4B, 5B & 6A 4B, 5A, 6B & 7B 3A, 4B & 5A 2D, 4B, 5A & 6A 4B, 5A & 6A 1A, 3A, 4B,6B & 6D	Grain weight Spike length Grain # per spike Fertile spikelet per spike Total spike # per spike Spikelet density	6.0–36.3% 5.0–25.4% 8.7–37.7% 6.4–29.2% 9.8–16.3% 4.3–10.2%	Liu et al., 2018

Type of wheat	Environment	Genotype	Trait type	Chr	Trait	% PV	Reference
High Biomass Association Spring Wheat Panel (150 genotypes)	Field: NW Mexico	Illumina iSelect 90K SNP array	RUE and yield-related traits	5A, 6A & 7A	Grain yield	7–17%	Molero et al., 2019
				1A, 2B, 3B & 5A	Plants m^{-2}		
				2B & 6B	Stems E+40d m^{-2}		
				1A, 2D, 3A & 6B	Stems InBoo m^{-2}		
				2B, 3A, 3D, 5B & 6B	Days Eme to booting		
				2B, 3A & 3D	Days Eme to anthesis		
				2A & 6A	Harvest index		
				2D & 6D	Thousand grain weight		
				2B, 3B, 5A, 6D & 7B	Grains m^{-2}		
				1A, 2B, 3B, 5B, 6B & 7B	Spikes m^{-2}		
				1A, 2B, 3D, 4B & 7A	Spikelets per spike		
				5A, 5B & 7A	Length spike		
				1B & 3B	BM Eme +40d		
				2A, 4B & 7A	BM InBoo		
Spring wheat panel: commercial prospective, Europe and CIMMYT (194 genotypes)	Field: different regions of Kazakhstan		Plant growth stages and yield parameters	2A, 4B, 5A, 5B, 6B, 6D & 7A	Days to booting	N/A	Turuspekov et al., 2017
				1B, 2A, 2B, 5A, 5B, 5D, 6A, 6B, 7A & 7D	Days to heading time		
				1B, 2B, 3A, 6A & 7D	Days to maturity		
				1A, 1B, 1D, 2B, 3B, 4B, 5B, 5D, 6A, 6B & 7A	# of fertile spikes		
				1A, 3B, 5B & 6A	# of grains per spike		
				1A, 1B, 2A, 2B, 2D, 3B, 4A, 4B, 5B, 6B & 7D	Plant height		
				1A, 1B, 1D, 2D, 4B, 4B, 5A, 5D & 7D	Peduncle length		
				1A, 2D, 4B, 5D & 6B	Spike length		
				1D, 3A, 3B, 4B, 5B & 5D	Thousand-grain weight		
				1A, 1B, 3A, 4B, 5A, 5D & 7B	Grain yield		

Type of wheat	Environment		Trait type	Chr	Trait	% PV	Reference
Canadian spring wheat panel resistance to *Ptr* toxins under different environments (81 genotypes)	Field: different regions of Canada		Agronomic traits and grain protein content	1B, 3B & 5A	Days to heading	15.5–17.8%	Chen et al., 2017
				1B & 2B	Days to maturity	15.4–19.4%	
				4B, 5B & 7A	Plant height	17.2–26.1%	
				1B & 4A	Grain protein	4.5–4.8%	
				2A, 2B, 3A, 5B, 6B & 7A	Grain yield	8.5–16.1%	
Elite facultative winter wheat (120 genotypes)	Field: rain-fed in Syria	DaRTseq	Yield, yield-related and quality	2D, 3B, 4A, 5A & 6B	Grain yield	9.0–17%	Tadesse et al., 2015
				3A, 3B & 5B	Days to heading	15.4–19.4%	
				2B, 4B & 6B	Plant height	15.4–19.4%	
				1A & 7B	Thousand-grain weight	11–13%	

1.4.2. Quantitative trait loci (QTL) in wheat

This type of analysis will depend on the difference between phenotypic means for marker parental alleles indicating if that region, few/many loci with large/minor effects, is/are linked to a QTL controlling the trait which sometimes may be affected by genotype-by-sex, genotype-by-environment, and epistatic interactions (Abdollahi Mandoulakani et al., 2017; Miles & Wayne, 2008). In wheat most of the genetic analysis and marker development to date has been undertaken on qualitative traits: e.g. disease resistances fusarium, rust, powdery mildew (Ali et al., 2018; Liu et al., 2018) and grain protein quality traits (Jiang et al., 2018; Kumar et al., 2018) but results for a few yield potential QTLs have already been published in wheat (Guan et al., 2018; Kato et al., 2000; Kuchel et al., 2007).

Physiological traits mostly are affected by complex networks interacting and being influenced by environmental factors resulting in a continuous range of variation as the result of the impact of different genetic loci: quantitative trait loci (QTL) (Chen, 2013). However, the detection depends on the allelic differences which may occur in structural or regulatory genes producing much smaller effects (Kearsey, 1998). This type of analysis requires a bi-parental mapping population that shows segregation for a specific trait depending on the difference between phenotypic means and marker alleles indicating if that region is linked to a QTL controlling the trait (Table 1.3) (Abdollahi Mandoulakani et al., 2017; Miles & Wayne, 2008).

Four methods for detecting QTLs can be used (Sehgal et al. 2016):

i. Where phenotypic means of each marker class are compared, the farther the QTL from a marker, the less likely it is to be detected statistically due to crossover events between the marker and the gene (single-marker analysis).
ii. Test a model for the presence of a QTL at several positions between two mapped marker loci (interval mapping by maximum likelihood).
iii. Regression on coded marker genotypes except that when phenotypes are regressed on QTL genotypes since they are unknown, they are replaced by probabilities estimated from the nearest flanking markers (interval mapping by regression).
iv. Variance from other QTLs accounted by including partial regression coefficients from markers 'cofactors' in other regions of the genome (composite interval mapping).

For grain yield and its component traits: grain number, spikes per unit area, grain weight, spikelets per spike and 1000-grain weight several QTLs have been reported (Table 1.3), although it is essential to consider that some of them are less environmentally sensitive and have higher heritabilities. However, it has been demonstrated that correlated, yield component traits often have QTL mapping at similar locations (Kato et al., 2000).

Table 1.3. Summary of traits in different types of wheat genotypes for a range of different physiological traits associated with genomic regions (chr: chromosomes) and its phenotypic variation (PV) in QTL studies.

Type of wheat	Environment	Chr	Trait	% PV	Reference
Hexaploid DH wheat cross Chinese Spring x SQ1 (a high abscisic acid-expressing breeding line)	Field: UK, Serbia, Kazakhstan, & Spain	1D, 5A, 7A & 7B		12–21.6%	Quarrie et al., 2005
		4A		20%	
RIL Dharwar Dry (drought tolerant) x Sitta	Field: NW Mexico + irrigation; different soil moisture regimes				Kirigwi et al., 2007
CIMMYT DH population Weebill x Bacanora	Field: Mexico, Argentina, Chile and UK	1A & 7B		11.2–22.7%	Griffiths et al., 2015
Spring DH population: RAC875 (stable GY) x Kukri (reduce GY)	Field: irrigation	3B	Grain yield	22%	Bennett et al., 2012
Trident/Molineux DH cross (182 lines)	Field	1B, 4D & 7D		N/A	Kuchel et al., 2007
118 RIL Spring (Cappelle-Desprez 5A x *Triticum spelta* 5A) genotypes	Field	5A		21–23%	Kato et al., 2000
95 recombinant inbred chromosome lines (RICLs): Cheyenne (CNN) x CN(WI3A)	Field + Glasshouse	3A & 7D		23%	Rustgi et al., 2013

Type of wheat	Environment	Chr	Trait	% PV	Reference
194 F_7 RIL Renan x RécitNal (more productive)	Field	2B, 5B, 7A & 7D	Thousand grain weight	20%	Groos et al., 2003
Near isogenic lines (NILs) winter Spark 9 Rialto (SR) genotypes	Field	1D	Earliness *per se*	N/A	Zikhali et al., 2014
204 RIL $F_{2:4}$ Jingdong 8 x Aikang58	Field: Limited and full irrigation	4D & 6A	Plant height	61.3–80.2%	Li et al., 2015
203 Spring DH ND3338 x JD6	Field	1B, 2D, 3A, 4B, 4D, 5A, 6A, 6D, 7A & 7B		0.12–46.0%	Guan et al., 2018
BC_4, BC_5F_2: 492 x Banks; Spring NIL and DH: Fukuho- komugiand x 380	Green house	1A	Tiller production	N/A	Spielmeyer & Richards 2004
RIL: Opata 85 x synthetic hexaploid wheat W-7984	Field	6A		N/A	Li et al., 2002
203 Spring DH ND3338 x JD6	Field	4A, 4B & 4D	Spikes per plant	2.98–18.5%	Guan et al., 2018
371 RIL ($F_{11:12}$) CN18 x T1208	Field: Chengdu Plains, China	4D	Spike formation rate per unit area	18.4–24.5%	Hu et al., 2017

1.5. Wheat breeding and high-throughput phenotyping

High-throughput field phenotyping (HTFP) is an ambitious technology which enables the characterisation of thousands of lines remotely in an accurate, non-destructive, cost and time-efficient way (Rebetzke et al., 2018). Remote-sensing is an aerial technology, using unmanned aerial vehicles such as drones with numerous sensors to automatically collect large amounts of data with the advantage of high operational efficiency, non-invasiveness, and low cost (Wang et al., 2018). Evaluating canopy surface area and plant height Yue et al. (2017) created a model to predict AGDM in winter wheat. Using canopy radiative transfer theory, based on the green area index, Duveiller et al. (2011) suggested that it is possible to predict crop growth. Similarly, Olanrewaju et al. (2019) predicted crop growth using spectral vegetation indices and percentage ground cover.

At glasshouse level, using a total of 320 Australian bread wheat varieties Golzarian et al. (2011) reported a method for accurate estimation of plant shoot dry weight, substituting conventional destructive biomass measurement with two dimensional images (one top view and two side view sat a 90° horizontal rotation). Other studies have been reported (Fernandez-Gallego et al., 2018; Summerer et al., 2019; Sun et al., 2019; Walter et al., 2018) suggesting that HTFP is an approach that could mitigate bottlenecks especially when using hundreds or even thousands of genotypes (core collections, association panels, etc) (Mir et al., 2019). However, there are still some challenges, such as daily environmental variations, creating a training database, processing of data using the right model assessment and computational time, that need to addressed to make this technology reliable, and cost-time effective.

The possibility of integrating HTFP and GWAS has the potential to provide insights into fundamental biological processes, revolutionise the rate of trait discovery and vastly improve phenotypic predictions resulting in accelerated genetic gain compared to standard phenotypic selection (Crain et al., 2018). Using a rice-core germplasm panel with an automatic phenotyping platform (RAP) and a yield traits scorer Yang et al. (2014) reported the manual and automated measurements for 13 traditional traits such as: plant height (PH), tiller number, green leaf area, FW shoot, DW shoot, etc as well as plant compactness (density and architecture) and grain-projected area (grain size evaluation). For the GWAS analysis, the loci detected (~141 associations) were consistent with RAP and manual measurements, but RAP provided a relatively more complete representation. Using 117 temperate and 135 tropical maize inbred lines Wang et al. (2018) measured plant height at four growth stages using aerial vehicles. Results showed that data recorded manually was highly correlated with data obtained using the drones. A total of 68 unique QTLs were identified, of which 24 QTLs (35%) had been identified in previous studies. The application of these high-throughput, automated phenotyping systems can significantly increase throughput and accuracy, thus allowing for the discovery of novel phenotypes. More importantly, the traits discovered using high-throughput

platforms can identify known genes/markers as well as new loci, providing increased capacity for gene identification and marker-assisted selection (Wolters et al., 2019).

Project objectives

The overall aim of the project is to determine the physiological basis of traits related to grain partitioning and their genetic regulation using a high biomass spring wheat panel and a doubled-haploid winter wheat population. The use of this type of germplasm will allow us to understand novel variation by screening different resources from the World Wheat Collection and John Innes Centre.

The specific objectives of the present thesis were to:

- Understand interactions and association of different physiological processes determining yield potential and harvest index using a spring wheat High Biomass Association Panel (HiBAP) and a winter wheat doubled-haploid Savannah x Rialto population (SxR DH).
- Quantify the physiological basis of genetic variation in traits at crucial growth stages in order to increase spike fertility (SPI: spike partitioning index), fruiting efficiency (FE), grain number per unit area (GN) and harvest index (HI).
- Physiologically dissect selected grain partitioning traits for yield potential (stem internode lengths, and spike DM partitioning) in subsets of genotypes to identify determinants of SPI and HI to propose better breeding strategies.
- Perform genome-wide association study (GWAS) analysis using a Wheat Breeders' Array to identify genetic regions that could explain phenotype variations in grain partitioning traits in the spring wheat panel (HiBAP) and identify candidate genes for grain partitioning traits.
- Identify quantitative trait loci (QTL) using an assembly map conformed of single sequence repeat (SSR) and SNPs in the doubled-haploid S×R population to understand the genetic basis of the grain partitioning traits.
- Quantify the effects of shortening internode length by trinexapac-ethyl used as a plant growth regulator (PGR) on spike partitioning, GN, HI and grain yield and interactions with genotype.

2. Dry matter partitioning to enhance yield, grain number and harvest index in a high biomass spring wheat panel

Breeding to raise yield potential through enhancing photosynthesis will have limited impact unless harvest index (HI: proportion of final above-ground biomass as grain yield) is maintained or ideally increased. Boosting grain dry matter (DM) partitioning will require increased translation of assimilates to sink organs to enhance spike growth. A high biomass spring wheat panel of 150 genotypes encompassing elite, landrace- and synthetic-derived lines was grown under yield potential conditions in two seasons. Results showed that the incorporation of landrace- and synthetic derived backgrounds into elite lines resulted in higher expression of final above-ground biomass, and leaf lamina and stem DM partitioning at anthesis. However, no grain yield advantage was observed over elite lines, due to decreased HI and lower grain number per unit area (GN).

Positive linear associations were found among spike fertility-related traits - HI, fruiting efficiency (FE: grains per unit of spike DM at anthesis) and GN - which were in turn related positively to grain yield (GY). Stem internode lengths were negatively associated with spike partitioning index (SPI: ratio of spike DM to total above-ground DM at anthesis) and HI, suggesting a competition for assimilates between the spike and stem middle internodes during pre-anthesis. Within spike DM partitioning analysis (glume, lemma, palea, rachis, awn) showed decreased DM partitioning to non-grain spike structures was associated with greater FE, thousand-grain weight (TGW) and GY.

While the use of exotic material can enhance biomass, special attention needs to be paid in the selection for novel DM partitioning traits that maximize HI and GN coming from the elite genepool. The selection for DM partitioning traits in wheat breeding and the combination with sources expressing high biomass can potentially allow breeders to maximize grain assimilation that will deliver higher yields.

**This chapter will be submitted to a high impact journal, where authors contributed equally to the work presented.

Aleyda Sierra-Gonzalez[ab], Gemma Molero[b], Carolina Rivera-Amado[b], Md Ali Babar[c], Matthew Reynolds[b] and John Foulkes[a]

[a]*Division of Plant and Crop Sciences, School of Biosciences, University of Nottingham, Leicestershire, LE12 5RD, UK*

[b]*CIMMYT International Maize and Wheat Improvement Center (CIMMYT), Km. 45, Carretera Mexico, El Batan, Texcoco, Mexico*

[c] *Agronomy Dept., University of Florida, Gainesville, FL, United States of America*

2.1. Introduction

Cereals form a fundamental part of the human diet, with wheat being the most widely grown crop worldwide (Gustafson et al., 2009; Shewry, 2009). The FAO has predicted that by 2050 the global population will increase 34% and, as a result, wheat production will need to be augmented to satisfy global food demand (FAO, 2017). Therefore, it is necessary to accelerate genetic gains in yield to ensure food security in future decades (Sanchez-Garcia et al., 2012) while considering the challenges that climate change is bringing. To achieve this, crop scientists and breeders need to understand better the physiological and genetic basis of biomass production and grain partitioning.

Biomass formation occurs mainly during stem-elongation and grain filling, both phases playing essential roles in the formation of grain yield (Asseng et al., 2017; Zhang et al., 2016). Yields have increased in breeding programs by identifying and applying selectable traits maximizing its production directly related to biological yield (above-ground dry matter), and the proportion of biomass partitioned to the grain (HI: Harvest Index) (González et al., 2011; Slafer et al., 1990). During the Green Revolution, the introduction of semidwarf (*Rht*: Reduced Height) genes into wheat cultivars raised grain gains associated with more fertile florets per spike as a consequence of increased assimilate partitioning to the spike during the pre-anthesis period (Hedden, 2003; Khush, 2001). After this period, breeding programs started to incorporate different genetic background to make strategic crosses allowing yield potential to increase, but at a slower rate (Aisawi et al., 2015; Lopes et al., 2015) but in some regions, the progress has become stagnant (Brisson et al., 2010; Ray et al., 2012).

Studies on the physiological basis of genetic growth in grain yield in sets of historical wheat cultivars (grown under optimal conditions) released before 2000 shown that grain number and harvest index were correlated positively with grain yield, but no similar relation was found between above-ground DM at harvest and grain yield (Foulkes et al., 2007; Rivera-Amado et al., 2019). The study of Austin et al. (1990) on UK winter wheat cultivars introduced from 1908 to 1986 showed HI to be associated positively with yield progress, with only a slight, non-significant increase in above-ground DM at harvest. More recently, Lo Valvo et al. (2017) using seventeen commercial wheat bread in Argentina showed that changes in grain yield were mostly explained by increases in harvest index, but not associated with above-ground DM at harvest.

Some recent studies have shown genetic improvement in biomass; using a traditional and a contemporary cultivar under different Mediterranean environments and treatments Ferrante et al. (2017) found that yield was closely related to AGDM at harvest but not to HI. Similarly, in a set of 12 CIMMYT semi-dwarf spring wheat released from 1966 to 2009 increases in above-ground DM contributed to higher yield associated with heavier grains rather than higher grain number, were a negative relationship between harvest index and above-ground DM (Aisawi et al., 2015) was recorded. For harvest index there is a theoretical upper limit of ~0.64 (Austin

et al., 1980); presently in spring wheat rarely exceeds 0.50 suggesting that there is still scope for further improvement, which could drive yield potential increases in high biomass genotypes by achieving an optimum source-sink ratio (Asseng et al., 2017).

2.1.1. Dynamics of plant developmental stage

The decrease of plant height due to the introduction of *Rht* genes increased the proportion of above-ground DM allocated to the spike reducing the competition between the growing spikes and stems enhancing spike partitioning and growth (Sanchez-Garcia et al., 2012; Zhou et al., 2007). In a recent study using a high yield potential CIMMYT wheat panel of 26 cultivars Rivera-Amado (2019) reported that seven days after anthesis (GS65+7d) stem partitioning index (StePI) (true stem and leaf sheath) had a genetic range between 0.48 to 0.65 and was negatively correlated with spike partitioning index (SPI) which ranged between 0.20 to 0.27; leaf-lamina partitioning index (LamPI) ranged from 0.18 to 0.23.

For ten bread and a durum wheat cultivars evaluated under well-watered conditions, Ehdaie et al. (2006) reported that the stem DM per shoot at harvest was 1523 mg with 376 mg in the peduncle, 397 mg in the penultimate internode and 750 mg in the lower internodes weights that were reduced by 30-37% in drought conditions. Examining CIMMYT spring wheat semi-dwarf cultivars released from 1966 to 1998, Aisawi et al. (2015) showed that at seven days after anthesis lamPI ranged from 0.21 to 0.22, SPI from 0.21 to 0.28 and stePI from 0.52 to 0.57, these two components being negatively associated.

Post-Green Revolution studies on sets of historic cultivars showed increases in grain yields were associated with increased grain number per unit area (Sadras & Denison, 2009; Xie et al., 2016). Grain yield is frequently reported as the outcome of different numerical components allowing this complex component to be studied in a detailed: i) spikes per unit area, ii) grain number per unit area, and iii) thousand-grain weight (TGW) (Pask et al., 2012). Grain number of wheat is determined mainly by anthesis and under optimal conditions, genetic variation in grain yield is far more strongly related to GN than to average grain weight (Duan et al., 2018; Ferrante et al., 2017; González-Navarro et al., 2015).

2.1.2. Grain number determination

There are several physiological determinants of grain number per unit area (Alonso et al., 2018; Pedró et al., 2012), including the spike dry weight at anthesis (as floret survival is related to pre-anthesis spike growth) (Martino et al., 2015). This is determined by the duration of rapid spike-growth period, crop growth rate during the spike growth period, and the spike DM partitioning which is explained by the Fischer (2011) model (Equation 2.1):

$$SDW_a = D_s \times CGR \times Fs \qquad [2.1]$$

where SDW_a is the dry weight of spikes at anthesis (per unit area basis); D_s is the duration of spike growth; CGR (crop growth rate) is crop dry matter accumulation (per unit area per day)

and F_s is the fraction of this dry matter partitioned to the spike averaged over the spike growth period.

Under optimal conditions (water, nutrients and radiation level), Abbate et al. (1997) and Duan et al. 2018 stated that during the spike growth period genetic variation in grains per m^2 is determined by the DM of spikes at anthesis. These was similarly showed on a winter wheat population in China, found that variation in both spike and non-spike organs showed a significantly positive relationship with grain number from booting to anthesis.

After accounting for above-ground biomass, grain number can be increased via two physiological avenues: the proportion of AGDM partitioned to the spike: SPI (spike partitioning index: spike DM/AGDM at anthesis) or the ratio of grains to spike DM at anthesis, known as the fruiting efficiency (FE: grains g^{-1}) (Slafer et al. 2015). The FE is an indicator of spike fertility reflecting the efficiency with which assimilate allocated to the juvenile spike growing before anthesis is converted into grains (Alonso et al., 2018; González et al., 2011; IRRI, 1983; Lázaro & Abbate, 2012; Slafer et al., 2015) (Equation 2.2):

$$GN = AGDM \times SPI \times FE \qquad [2.2]$$

where GN is the number of grain (per unit area basis); AGDM is the above-ground DM (per unit area); SPI is the ratio between the spike DM and the AGDM and FE is the number of grains per unit spike DM at anthesis.

Using a bi-parental population of 146 recombinant inbred spring wheat lines, Alonso et al. (2018) reported a strong positive association between fruiting efficiency and grains per m^2 as well as with grain yield. On the other hand, using nine elite cultivars with different nitrogen treatments Elía et al. (2016) found that genetic variation in grain number was positively associated with the spike DM at anthesis, but there was no relationship with fruiting efficiency. It has been suggested that allowing more distal florets to become fertile florets or allocating more assimilates to florets by reducing the assimilate demand of the floret for maintaining its normal development could increase fruiting efficiency as well grain number, as this trait is determined mainly by the pre-anthesis floret survival within spikelets (González et al., 2011). Generally, each spikelet produces up to ten florets, but fewer than five (only those closest to rachis), and the remaining could die just before anthesis (Ferrante et al., 2012; Xie et al., 2016). If florets constitutively demand less assimilates for normal development, the proximal florets would leave more resources available for distal florets, which would maintain their growth and development for longer. This possible avenue for raising fruiting efficiency could, however, reduce grain weight due to a reduction in the size of the carpels of fertile florets, as grain weight potential is related to the size of the ovaries (Ferrante et al., 2015). Some studies have reported a negative trade-off between fruiting efficiency and grain weight (Elía et al., 2016; Terrile et al., 2017). Across a wide range of environments for two cultivars, Anzar and Soissons, Ferrante et al. (2017) reported that yield variation was due to fruiting efficiency concluding that

this trait could be a useful breeding trait if it does not bring about a potential trade-off with grain weight.

In this chapter the aim was to identify grain partitioning traits to increase grain number per unit area, HI and grain yield using a high biomass spring wheat association panel (HIBAP) with different genetic background grown under high yield potential conditions. Field experiments were carried out over two seasons in NW Mexico under fully irrigated conditions evaluating biomass and DM partitioning traits at seven days after anthesis (GS65+7d) and physiological maturity (PM: GS87) where associations among traits measured were quantified.

Chapter hypotheses:

- Genetic variation in grain number is determined by (i) percentage of dry-matter partitioned to the spike and/or (ii) grains per unit spike dry matter at anthesis.
- Spike partitioning index and harvest index are related to internode length and dry-matter partitioning internodes (peduncle true-stem and internode 2 true-stem) near the spike rather than those close to the ground.
- Fruiting efficiency is related to the dry-matter variation found within spike organs (palea, lemma, glume, rachis and awn).
- Incorporation of different pedigree backgrounds increases genetic variation in biomass and grain partitioning traits.

2.2. Materials and methods

2.2.1. Plant material and experimental design

The experiments were carried out over two seasons (Y16: 2015-16 and Y17: 2016-17) under high yield potential conditions using an alpha-lattice design with four replicates (Figure S2.1 & 2) at the Norman E. Borlaug experimental station near Ciudad Obregon, Sonora, Mexico (27°N, 110°W and 38 m above the sea level). A CIMMYT spring bread wheat High Biomass Association Panel (**HiBAP**) was used comprising 150 genotypes, including landrace-derivates, synthetic-derivatives, and landrace + synthetic-derivatives and elite cultivars (Table S2.1). This panel was grown in raised beds (2 beds per plot each 0.8 m x 4 m) with four (Y16) and two (Y17) rows per bed (Figure S2.4) using a seed rate of 102 kg ha^{-1}. The sowing dates were 24 November 2015 (on dry soil) and 23 November 2016 (on irrigated soil). Fifty percent plant emergence occurred on 7 December 2015 and 30 November 2016 for Y16 and Y17, respectively (Figure S2.3). Irrigation was supplied through the whole cycle using a gravity-based system, with the first application shortly after (Y16) or before (Y17) sowing and then every three-four weeks. In each season, herbicides (two applications) for broad-leaved weeds, fungicides (two applications) and insecticides (two applications) were applied to minimize the effects of weeds, diseases and pests (Table S2.2). In each season an application of fertilizer nitrogen (50 kg N ha^{-1}) as urea was applied during land preparation, followed by an application of triple super phosphate (50 kg P ha^{-1}) at sowing. A second and third N application (50, 150

kg N ha^{-1}, respectively) as urea was applied at the same time that the experiment was irrigated (first and second irrigations).

Weather means for temperature, accumulated rainfall and solar radiation were calculated for both seasons during booting (GS41-GS49), anthesis (GS59-GS69) and grain filling (GS71-GS91) stages (Table S2.3). Meteorological data were obtained from a weather station located within 1 km of the experiments (lat: 27.4°, long: -109.9°, altitude: 38 m).

2.2.2. Crop measurements

Sampling and crop development

Samples were collected seven days after anthesis (GS65+7d) and at physiological maturity (PM, shoots with yellow-green peduncle, GS87) (Zadoks et al., 1974). The stages were taken as when 50% of the fertile shoots in the plot had reached the stage (Pask et al., 2012).

Biomass and DM partitioning at GS65+7d

At GS65+7d in two replicates (150 genotypes), sampling was carried out in a quadrat of 0.8 x 0.5 m (at least 50 cm from ends of plots); where shoots were cut at ground level, and the fresh weight (FW) of the total sample was recorded. From the sample collected from the field 12 fertile shoots (spike fully emerged) were randomly selected for plant dry-matter partitioning analysis (PI: Partitioning Index, ratio between component DM and above-ground DM) which was done by separating each plant component into (i) spike, ii) leaf lamina and iii) stem (true stem+leaf sheath). The material for each plant component was dried for 48 h at 70°C and dry weight was recorded. Additionally, the lengths of each stem internode: i) peduncle, ii) internode 2 (phytomer below peduncle) and iii) internode 3 were recorded with a ruler.

For 29 genotypes (subset1; Table S2.1) selected to be representative of genetic variation in spike DM partitioning in the panel the 12 shoots sampled at GS65+7d were further separated into true-stem (TS) and leaf sheath (LS) for each internode (Figure 2.1): peduncle (ped), internode 2 (int2), internode 3 (int3) and internode 4 and below (int4+). The dry weights were recorded for each component after oven drying at 70°C for 48 h.



Figure 2.1. Stem internode partitioning (true stem & leaf sheath) at seven days after anthesis (GS65+7d): 1) stem dry samples, 2) stem internode segments, 3) leaf sheath from each stem, 4) true-stem from each stem, 5) internode 4+ segments (true stem & leaf sheath was not separated for this segment).

Finally, for 14 of the 29 genotypes (subset2; Table S2.1), the 12 spikes sampled at GS65+7d were dissected into i) glume, ii) lemma, iii) palea, iv) rachis and v) awn (Figure 2.2). The different spike components were bulked for the 12 spikes and weighed separately after drying at 70ºC for 48 h. For every internode and the rachis, specific weight (SW: linear density, phytomere and/or rachis DM per unit length) was calculated at this stage.

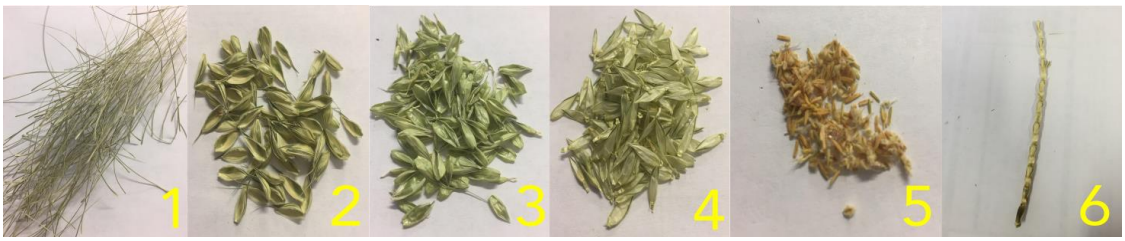


Figure 2.2. Spike partitioning at seven days after anthesis (GS65+7d): 1) awns, 2) glume, 3) lemma, 4) palea, 5) grains and anthers (this organs were not considered on the analysis), 6) rachis.

Plant and spike length measurements at post-anthesis

Plant height, spike length, and awns length were measured in two replicates at the beginning of the grain-filling period on five representative shoots per plot. Plant height was measured from the soil surface level (avoiding wells or uneven ground) to the tip of the spike and spike length from the spike collar to the tip of the spike (awns were excluded in both measurements) and awns from the initiation of the awn to the end of the awn.

Physiological maturity growth analysis, grain yield and yield components

At physiological maturity (PM) 50 randomly selected fertile shoots were cut at ground level in two replicates and separated into the spike and stem (true stem + leaf sheath). Dry weight for each plant organ was recorded after drying for 48 h at 70ºC. Spikes from this sampling were threshed to collected grains and chaff. After sampling each plot for yield components, the whole experiment (four replicates) was machine-harvested in a plot area of ~3-4 m^{-2}, after harvesting grain sample was collected to determined the weight of 200 grains using the image analysis system SeedCounter (SeedCountSC5000 Image Analyser, New Jersy) and the weight recorded after drying for 48 h at 70ºC. From the data obtained spikes m^{-2} (SM2), grains m^{-2} (GN), HI, final AGDM per unit area and fruiting efficiency (FE) were calculated (Table S2.4).

2.2.3. Statistical analysis

Statistical analysis (adjusted means, ANOVA, regression analysis and heritability) of phenotypic data was carried out using an alpha-lattice design using the program MetaR, Windows R code-based platform program (Alvarado et al., 2018). For the combined analyses (cross-year means), the heritability was calculated as (Equation 2.3):

$$h^2 = \frac{\sigma^2 g}{\frac{(\sigma^2 g + \sigma^2 ge)}{nlocs + \sigma^2 e}(nlocs)(nreps)} \quad [2.3]$$

where σg^2 and σe^2 are the genotype and error variance components, respectively, nreps is the number of replicates, σge^2 is the genotype × environment interaction variance component and

nlocs is the number of locations in the analysis (Vargas et al., 2013). For each trait, ANOVA and BLUEs were calculated for genotypes considering genotype as a fixed effect and replicates as a random effect. Combined analysis of variance across experiments (cross-year) was done considering genotypes and years as fixed effects.

GenStat 17th edition (VSN International) was used for calculating the Pearson's correlation coefficients, linear/non-linear regressions and stepwise multiple linear regressions between traits using the BLUEs obtained with MetaR. For the stepwise multilinear regression analysis, the variable selected to be explained was the dependent variable, and the variables tested in the model acted as independent variables.

Student T-tests were employed using the data collected (plot data) from both seasons for the 150 genotypes of the HiBAP using a SAS code provided by CIMMYT run on the SAS statistical package University Edition (SAS).

2.3. Results

Considering the field data from the different genetic backgrounds that made-up the HiBAP during two seasons (Y16: 2015-16 and Y17: 2016-17), significant genetic variation was found for grain partitioning related traits (Table S2.5). Similarly, for the subsets of lines where detailed stem internode (Table S2.6) and spike morphology (Table S2.7) DM partitioning traits were measured, most of them showed genetic variation. Cross-year analysis reported significant phenotypic variation, where the genotypic effect (G) was significant for most of the traits in the combined analysis while the significance of year (Y) or G × Y was variable among traits measured (Table 2.1).

Interesting associations were found within different traits measured seven days after anthesis (GS65+7d) and at physiological maturity (GS87) which will be relevant for the proposal of new breeding strategies to improve assimilation of DM to improve yield potential.

Table 2.1. Means for elite, landraces-derived (LD), synthetic-derived (SD) and synthetic+landrances-derived (S+LD) and phenotypic ranges, least significant differences (LSD: *P=0.05*), significance (*p-values*) and broad-sense heritability for 150 HiBAP genotypes at seven days after anthesis (GS65+7d) and physiological maturity (PM: GS87) between groups of genotypes and cross-year evaluation. Values represent means of Y16 and Y17.

			Y16 and Y17														
	Traits	Units	Elite		LD		SD		S+LD		Whole panel: 150 genotypes						
											H^2	Min	Max	LSD	*P(G)*	*P(Y)*	*P(G×Y)*
Anthesis + 7days (GS65+7d)	DTA	DAE	76	B	79	A	76	B	76	B	0.87	68	85	3	***	***	***
	$AGDM_{A+7}$∞	g m^{-2}	856	B	891	A	867	AB	872	AB	0.60	701	1005	129	***	***	*
	LamPI		0.21	B	0.22	A	0.21	B	0.21	B	0.68	0.17	0.26	0.03	***	**	ns
	SPI∞		0.27	A	0.26	B	0.26	B	0.27	B	0.75	0.21	0.32	0.03	***	ns	*
	StePI		0.52	B	0.52	B	0.53	A	0.52	B	0.76	0.46	0.57	0.03	***	*	***
	$DMSpk_{A+7}$	g m^{-2}	258.4	A	259.8	A	254.9	A	251.7	A	0.48	171.4	320.7	57.8	**	ns	ns
	FE∞	grains g^{-1}	51.5	A	46.0	B	49.0	A	44.5	B	0.73	41.5	84.2	14.0	***	ns	*
Physiological maturity (GS87)	DTM	DAE	115	B	117	A	114	C	114	C	0.85	105	124	3	***	***	***
	$AGDM_{PM}$	g m^{-2}	1346	B	1394	A	1358	AB	1389	A	0.51	1105	1642	206	***	**	***
	GY	g m^{-2}	597	A	592	A	594	A	593	A	0.60	485	705	71	***	ns	***
	TGW	g	42.6	C	45.7	B	45.6	B	48.2	A	0.94	30.0	53.8	2.92	***	***	***
	HI		0.47	A	0.45	C	0.46	B	0.46	B	0.80	0.40	0.53	0.04	***	ns	*
	GN∞	grains m^{-2}	14077	A	13118	B	13096	B	12320	C	0.83	10382	16669	16727	*	ns	***
	SM2	spikes m^{-2}	307.6	A	287.7	B	301.5	A	283.5	B	0.86	234	411	46	***	**	ns

A+7: Seven days after anthesis; **PM:** Physiological Maturity; **DTA:** Days from emergence to seven days after anthesis; **AGDM:** Above-ground DM; **LamPI:** Lamina Partitioning Index; **SPI:** Spike Partitioning Index; **StePI:** Stem Partitioning Index; **DMSpk:** DM Spike per unit area; **DTM:** Days from emergence to physiological maturity; **FE:** Fruiting Efficiency; **GY:** Grain Yield; **TGW:** Thousand Grain Weight; **HI:** Harvest Index; **GN:** Grain Number; **SM2:** Spikes per unit area

P(G): Significance of the genotype; ***P(Y):*** Significance of the year; ***P(G×Y):*** Significance of the genotype x environment; **H^2:** Broad sense heritability (cross-year analysis) **P<0.05; **P<0.01; ***P<0.001; ns: non-significant*

∞ cross-year (Y16 and Y17) adjusted means using DTA as covariate; Means followed by the same letter are not significantly different (*P<0.05*) according to pairwise t tests

2.3.1. Physiological maturity, grain yield and yield components

Averaging over seasons grain yield (GY) ranged amongst genotypes from 485 to 705 g m^{-2} (*P<0.001*). Genetic variation for above-ground DM ($AGDM_{PM}$) varied overall from 1105 to 1642 g m^{-2} (*P<0.001*) and harvest index (HI) from 0.40 to 0.53 (*P<0.001*). Thousand-grain weight (TGW) and grain number (GN) did not differ between seasons ranging amongst genotypes from 30.0 to 53.8 g (*P<0.001*) and from 10,382 to 16,669 m^{-2} (*P<0.001*), respectively. All the above traits showed a significant genotype (G) x year (Y) interaction in the combined analysis and high heritabilities were obtained for most of the traits (H^2>0.5-0.7; Table 2.3)

Positive linear relationships were observed amongst genotypes between grain yield and each of $AGDM_{PM}$ (*P*<0.001; Figure 2.a) and HI (*P<0.001*; Figure 2.b). Grain yield also showed positive associations with both GN (*P<0.001*; Figure 2.d) and TGW (*P<0.001*; Figure 2.c); and there was a strong negative association between GN and TGW (*P<0.001*; Figure 2.e). Grains per unit area was also negatively associated with plant height (*P<0.01*; Figure 2.f).

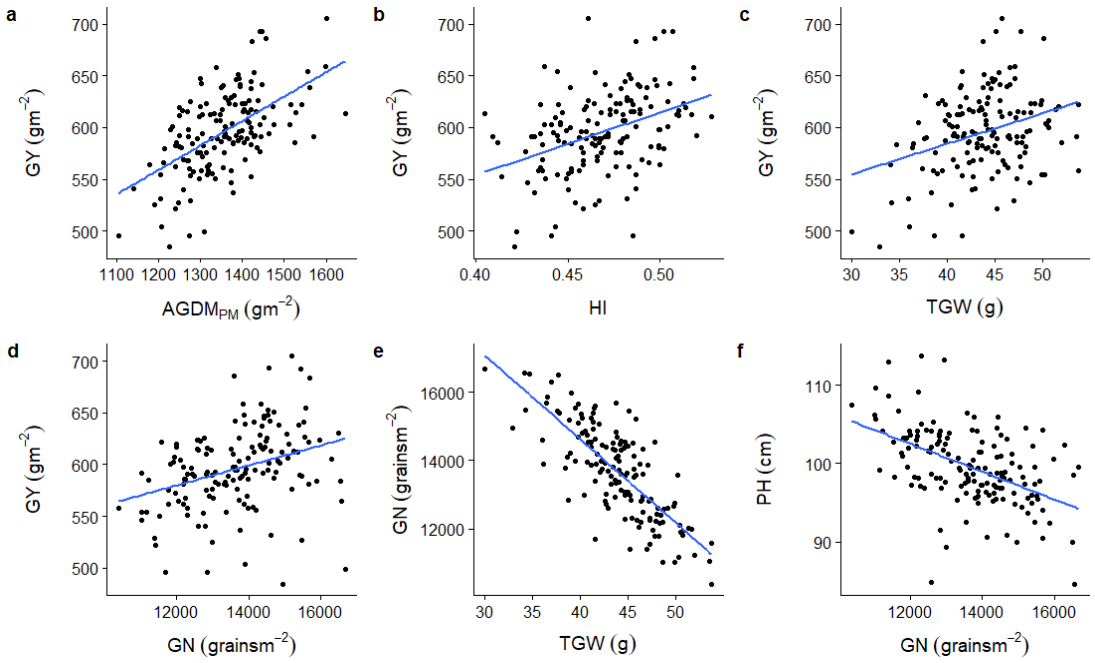


Figure 2.3. Linear regressions amongst traits measured at physiological maturity on the HIBAP:
a) Grain yield (GY) (100% DM) on Above-Ground DM at physiological maturity ($AGDM_{PM}$): y=0.24x+276.1, R^2=0.31***
b) GY on Harvest Index (HI): y=607.0x+311.1, R^2=*0.16****
c) GY on Thousand Grain Weight (TGW): y=2.93x+466.6, R^2=*0.10****
d) GY on grains per unit area (GN): y=0.02x+412.9, R^2=0.45***
e) GN on TGW: y=-244.6x+24412, R^2=0.61***
f) Plant height (PH) on GN: y=0.002x+123.9, R^2=0.21***
**P<0.05; **P<0.01; ***P<0.001; ns: non-significant*
Values presented are cross-year means (Y16 and Y17)

2.3.3. Biomass, DM partitioning and stem internode lengths at GS65+7d

Above-ground dry matter ($AGDM_{A+7}$) at GS65+7d for the two seasons varied from 702 to 1006 g m^{-2} (*P<0.001*), spike DM perunit area ($DMSpk_{A+7}$) from 171.4 to 320.7 g m^{-2} (*P<0.01*) while fruiting efficiency at GS65+7d (FE) ranged from 41.5 to 84.2 grains g^{-1} (*P<0.001;* Table 2.1). For the plant organ DM components, the stem (true stem+leaf sheath) accounted for the highest proportion of $AGDM_{A+7}$ ranging amongst genotypes from 0.46-0.57 (*P<0.001*); then the spike from 0.21-0.32 (*P<0.001*) and the leaf lamina from 0.17-0.26 (*P<0.001*; Table 2.1). For stem internode lengths, the peduncle was the longest, followed by internode 2 (LnInt2) and internode 3 (LnInt3) (Figure 2.4).

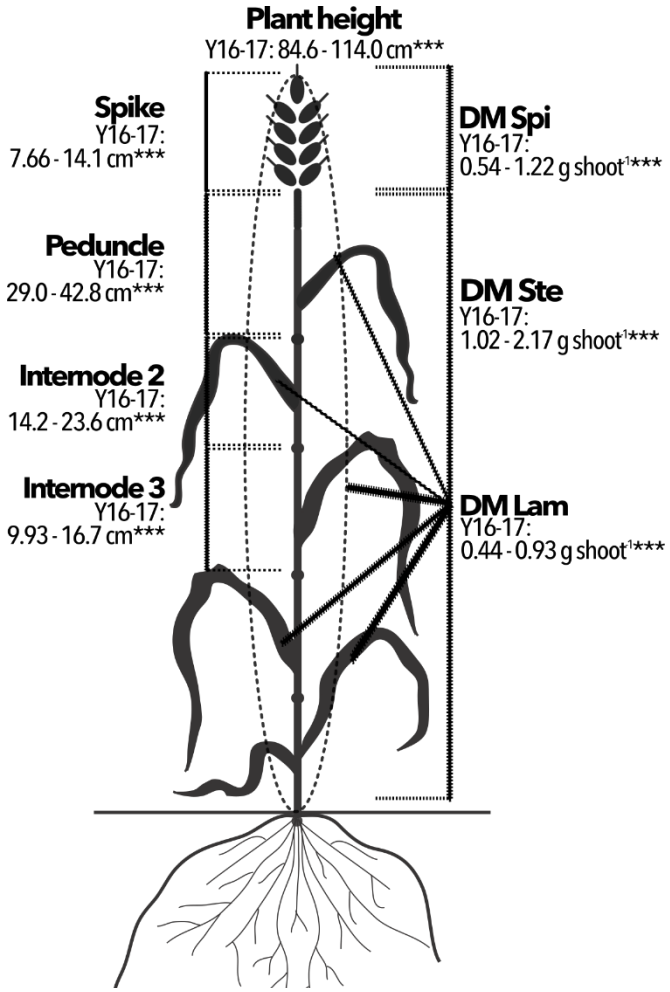


Figure 2.4. Genetic ranges for 150 HiBAP genotypes for DM $shoot^{-1}$ at GS65+7d (right) in spike (Spi), lamina (Lam) and stem (Ste) and spike and stem-internode lengths (left).
**P<0.05; **P<0.01; ***P<0.001; ns: non-significant*
Values presented are cross-year means (Y16 and Y17).

The lengths of each segment of the stem i) peduncle (ped), ii) internode 2 (int2), and iii) internode 3 (int3) were negatively associated with spike partitioning index (SPI) (Figure 2.5a), but positively with stem partitioning index (StePI) (Figure 2.5b). For lamina partitioning index (LamPI) a weak negative relation was recorded just with internode 2 length, but not with the other two internodes (Figure 2.5c). Same associations were found with $DMSpk_{A+7}$ where just a slightly negative association was found with int2 length (Figure 2.5d).

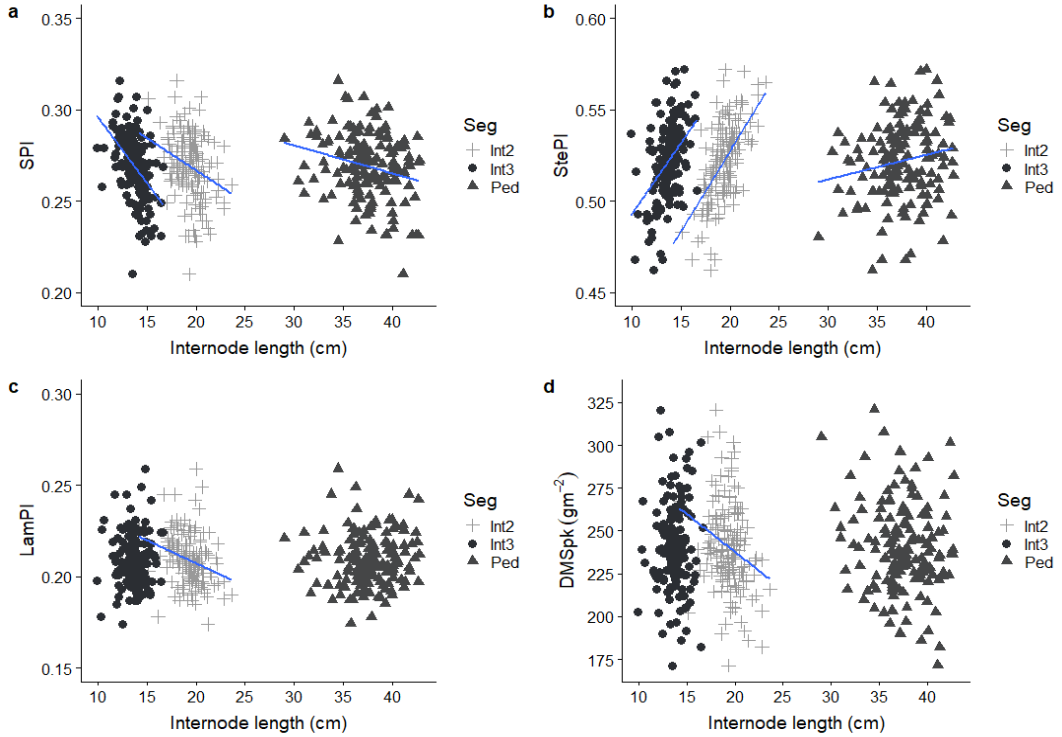


Figure 2.5. Linear regressions amongst the whole HIBAP (150 genotypes) between physiological traits measured at GS65+7d:
a) Spike partitioning index (SPI) on peduncle length (LnPed): y=-0.002x+0.33, R^2=*0.05***; Internode 2 length (LnInt2): y=-0.003x+0.33, R^2=*0.07****; Internode 3 length (LnInt3): y=-0.007x+0.37, R^2=*0.20****
b) Stem partitioning index (StePI) on LnPed: y=0.001x+0.47, R^2=*0.03**; LnInt2: y=0.009x+0.35, R^2=*0.35****; LnInt3: y=0.008x+0.42, R^2=*0.18****
c) Lamina partitioning index (LamPI) on LnPed: y=-0.002x+0.20, R^2=*0.002ns*; LnInt2: y=-0.003x+0.26, R^2=*0.07***; LnInt3: y=0.0002x+0.21, R^2=*0.0002ns*
d) DM Spike at GS65+7d on LnPed: y=-1.29+288.9, R^2=*0.02ns*; LnInt2: y=-4.40x+325.6, R^2=*0.07***; LnInt3: y=0.82x+229.2, R^2=*0.001ns*
**P*<0.05; ***P*<0.01; ****P*<0.001; *ns: non-significant*
Values presented are cross-year means (Y16 and Y17)

2.3.4. Internode DM partitioning

Genetic variation was recorded for detailed stem partitioning traits at GS65+7d on 29 genotypes (subset 1) in which the true-stem (TS) accumulated more DM than the leaf sheath (LS) (0.87 vs 0.45 total g shoot^{-1}, for Ped, Int2 and Int3 combined) and at the same time internodes closer to the spike accumulated more DM than those below (Table 2.2). Internode length and the amount of DM per unit length accumulated will influence internode DW (SW: specific weight, g cm^{-1}); true-stem specific weight (TSSW) was decreased in upper compared to lower internodes (Table 2.2).

Table 2.2. Cross-year genetic ranges (Min: Minimum, Mean, Max: Maximum), broad-sense heritability (H^2), and significant values per genotype (G), year (Y) and environment x year (GxY) for detailed stem internode analysis for subset 1 for true-stem (TS) and leaf-sheath (LS) DM partitioning indices (PI) and specific weight (SW) at GS65+7d. Values presented are cross-year means (Y16 and Y17).

Traits	Units	H^2	Min	Mean	Max	*P(G)*	*P(Y)*	*P(G×Y)*
PedTSPI		0.70	0.06	0.12	0.15	***	**	*
Int2TSPI		0.77	0.05	0.09	0.12	***	ns	ns
Int3TSPI		0.70	0.05	0.07	0.09	***	**	*
PedLSPI		0.65	0.05	0.08	0.11	***	ns	ns
Int2LSPI		0.18	0.03	0.04	0.05	ns	ns	ns
Int3LSPI		0.25	0.02	0.03	0.04	ns	ns	*
Int4+PI		0.79	0.05	0.09	0.12	***	*	ns
PedTSSW		0.64	0.005	0.009	0.013	***	*	ns
Int2TSSW	g cm^{-1}	0.81	0.009	0.014	0.20	***	*	ns
Int3TSSW		0.83	0.011	0.017	0.023	***	ns	ns

Ped: Peduncle; **Int2:** Internode 2; **Int3:** Internode 3; **Int4+:** Internode 4+; **TS:** True-stem; **LS:** Leaf-sheath; **DW:** Dry weight; **PI:** Partitioning index; **SW:** Specific weight

*P<0.05; **P<0.01; ***P<0.001; *ns: non-significant*

There was a positive linear relationship between TS internode length and TS DM g per shoot^1 stronger on int3 than int2 (Figure 2.6a), the same scenario recorded when associating the accumulation of DM over specific weight, but a positive link was found on the peduncle (Figure 2.6b). On the other hand, when SW was related to the length of each phytomer int3 and ped were positively related (Figure 2.6c).

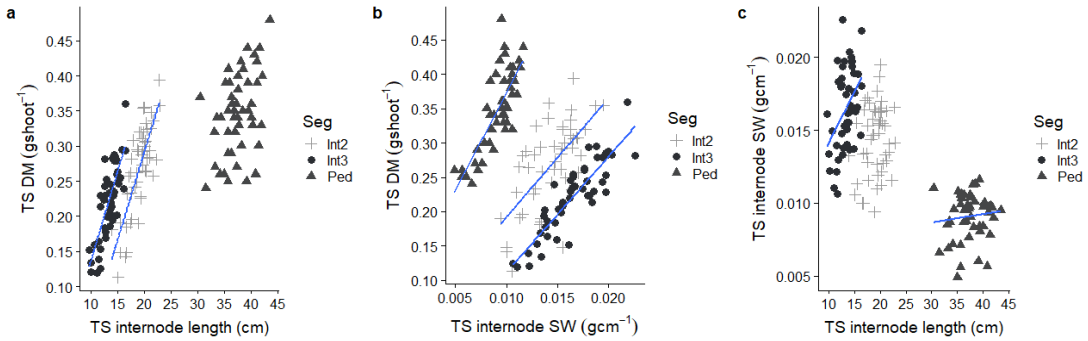


Figure 2.6. Linear regressions amongst HIBAP subset 1 genotypes between stem internode traits at GS65+7d:
Seg: Ped: Peduncle, Int2: Internode 2, Int3: Internode 3 and Int4+: Internode 4:
A) True Stem (TS) DM (g shoot^{-1}) on TS internode length (cm): Ped: y=0.001x+0.31, R^2=*0.01*ns; Int2: y=0.02x+0.01, R^2=*0.31****; Int3: y=0.03x+0.15, R^2=*0.72****
B) TS DM (g shoot^{1}) on TS internode specific weight (SW: g cm^{-1}): Ped: y=27.8x+0.09, R^2=*0.68****; Int2: y=21.0x+0.02, R^2=*0.83****; Int3: y=18.6x+0.08, R^2=*0.84****
C) TS internode SW (g cm^{-1}) on TS internode length (cm): Ped: y=0.0002x+0.02, R^2=*0.25***; Int2: y= 0.0003x+0.009, R^2=*0.03ns*; Int3: y=0.0009x+0.004, R^2=*0.31***
**P*<0.05; ***P*<0.01; ****P*<0.001
Values presented are cross-year means (Y16 and Y17)

The correlations between stem-internode traits, grain yield, harvest index, yield components, spike partitioning index and spike DM per unit area ($DMSpk_{A+7}$) at GS65+7d are shown in Table 2.3 (Figure S2.5). Spike partitioning index (SPI) showed a negative association with int3TSPI (*P<0.001*), int2TSPI (*P<0.001*), int4+PI (*P<0.001*) and all the LS phytomers been stronger on internode 4+ compared to internode 2. For harvest index (HI) positive associations were found between pedTSPI (*P<0.001*), int2TSPI (*P<0.10*) and int2LSPI (*P<0.10*) compared with int3TSPI (*P<0.001*), pedLSPI (*P<0.10*) and int4+PI (*P<0.001*) traits that showed a negative association. On the other hand, for grain yield (GY) most of the phytomers TS and SW were positively associated been int2TSPI and int3TSPI internode segments that showed stronger associations; contrasting results recorded on grain number (GN) as this two stem PI were negatively related. Spikes per unit area (SM2) was positively correlated with pedTSPI (*P<0.001*) and int2TSPI (*P<0.10*) but negatively with int4+PI (*P<0.001*), int2TSPI (*P<0.10*), all of the LSPI and TSSW.

Table 2.3. Pearson's correlation coefficient among traits measured at GS65+7d and physiological maturity for 29 genotypes (subset 1) of the HiBAP. Values presented are cross-year means (Y16 and Y17).

Trait	Correlation (r)					
	SPI	**HI**	**GY**	**GN**	**DMSpk$_{A+7}$**	**SM2**
PedTSPI	0.08	0.24***	0.10	0.13	-0.31***	0.47***
Int2TSPI	-0.37***	0.13†	0.29***	-0.16*	-0.24***	0.13†
Int3TSPI	-0.70***	-0.27***	0.22**	-0.44***	-0.19*	-0.26***
PedLSPI	-0.30***	-0.15†	0.05	-0.03	-0.40***	0
Int2LSPI	-0.16*	0.13†	0.21**	-0.09	-0.21**	-0.18*
Int3LSPI	-0.44***	0.01	0.02	-0.22**	-0.24***	-0.32***
Int4+PI	-0.49***	-0.31***	0.12†	-0.41***	-0.21**	-0.59***
PedTSSW	0.14	-0.02	0.39*	0.07	0.61	-0.54***
Int2TSSW	0.04	-0.03	0.28†	-0.26	0.43	-0.72*
Int3TSSW	-0.13	-0.18	0.18	-0.39*	0.27	-0.72†

Ped: Peduncle; **Int2**: Internode 2; **Int3**: Internode 3; **Int4+**: Rest of internodes; **TS**: True stem; **LS**: Leaf sheath; **SW**: Specific Weight; **SPI**: Spike Partitioning Index; **HI**: Harvest Index; **GY**: Grain Yield (100% DM); **DMSpk$_{A+7}$**: Spike DM per unit area at GS65+7d; **SM2**: Spikes per unit area

*†P<0.10; *P<0.05; **P<0.01; ***P<0.001*

2.3.5. Spike morphological partitioning

Spike morphological partitioning was studied in detail in a subset of 14 genotypes (subset 2). DM distribution among the spike components increased from lemma (Le) > awns (Aw) > glume (Glu) > rachis (Ra) > palea (Pa). Significant genetic variation was found for most spike morphological partitioning indices except for paPI trait that did not show any type of variation, for gluPI and raPI a GxY was found (Table 2.4).

Table 2.4. Cross-year genetic ranges (Min: Minimum, Mean, Max: Maximum), broad-sense heritability (H^2), and significant values per genotype (G), year (Y) and environment x year (GxY) for detailed stem internode analysis among 14 genotypes (subset 2) for spike morphology DM partitioning indices (PI) and specific weight (SW) at GS65+7d. Values presented are cross-year means (Y16 and Y17).

Traits	H^2	Min	Mean	Max	*P(G)*	P(Y)	*P(G×Y)*
GluPI	0.76	0.17	0.20	0.23	*	ns	**
PaPI	0.07	0.09	0.11	0.12	ns	ns	ns
LePI	0.91	0.26	0.29	0.31	***	*	*
AwPI	0.94	0.20	0.24	0.30	***	ns	ns
RaPI	0.95	0.13	0.15	0.18	***	ns	*
RaSW (g cm^{-1})	0.71	0.008	0.010	0.011	ns	ns	ns

Glu: Gluma; **Le:** Lemma; **Pa:** Palea; **Ra:** Rachis; **Aw:** Awns; **DW:** Dry weight; **PI:** Partitioning Index; **SW:** Specific weight

**P*<0.05; ***P*<0.01; ****P*<0.001; *ns: non-significant*

The correlations between spike morphology traits, grain yield (GY), harvest index (HI), yield components, spike partitioning index (SPI) and DM spike per unit area ($DMSpk_{A+7}$) at GS65+7d are shown in Table 2.5 (Figure S2.6). For SPI, three spike organs were negative associated (*P<0.10*), LePI and RaSW), compared to awPI organ that was positive associated (*P<0.10*). In the case of FE, lePI was the only trait positive-related (*P<0.10*) as awPI was negative associated (*P<0.10*); in instance awPI was positive associated with the DM of spike at GS65+7d (*P<0.10*) and lePI was negative related (*P<0.05*). For raPI was the only part of the spike positive correlated with grain yield (*P<0.05*), where raPI (*P<0.05*) and raSW (*P<0.01*) were positively linked with grain weight compared to awPI organ which was negative associated (*P<0.10*). Regarding grain number raSW was the only organ which showed a negative relation among it (P<0.05). There was no association between any of the spike morphological PIs and HI.

Table 2.5. Pearson's correlation coefficient among traits measured at GS65+7d, physiological maturity and spike morphological traits of 14 genotypes (subset 2) of the HiBAP. Values presented are cross-year means (Y16 and Y17).

Traits	Correlations (r)						
	SPI	**FE**	**GN**	**HI**	**GY**	**TGW**	**$DMSpk_{A+7}$**
GluPI	-0.50†	0.22	-0.29	-0.05	-0.12	0.16	-0.34
PaPI	0.24	-0.04	0.02	0.15	-0.11	-0.11	-0.11
LePI	-0.49†	0.41†	-0.15	0.18	-0.17	0.03	-0.53*
AwPI	0.49†	-0.31†	0.30	-0.18	-0.13	-0.39†	0.43†
RaPI	-0.07	-0.28	-0.14	0.20	0.55*	0.58*	0.10
RaSW	-0.45†	-0.17	-0.40†	0.18	0.34	0.67**	-0.16

Glu: Glume; **Pa:** Palea; **Le:** Lemma; **Aw:** Awns; **Ra:** Rachis; **PI:** Partitioning Index; **SPI:** Spike Partitioning Index; **FE:** Fruiting Efficiency; **GN:** Grain Number; **HI:** Harvest Index; **GY:** Grain Yield; **TGW:** Thousand Grain Weight; **$DMSpk_{A+7}$:** Spike DM per unit area

$^{\dagger}P<0.10$; $^{*}P<0.05$; $^{**}P<0.01$; $^{***}P<0.001$

2.3.6. Correlations between partitioning traits, grain number, harvest index and grain yield

A strong negative linear relationship was found between StePI and SPI (*P<0.001*) and spike DM per unit area ($DMSpk_{A+7}$) (*P<0.001*); SPI was also positively associated with harvest index (HI: *P<0.01*) and grain number (GN: *P*<0.001). On the other hand, HI was strong negative relation was observed between above-ground DM (AGDM: *P<0.001*; both stages), but positive with fruiting efficiency (FE: *P<0.001*), SPI (*P<0.001*) and length of internode 2 (LnInt2: *P<0.05*); however, neither SPI or $DMSpk_{A+7}$ were associated with grain yield. Grains per unit area was negatively related to thousand-grain weight (TGW: *P<0.001*) and stem partitioning index (StePI: *P<0.001*), similar to the association found among internode lengths (*P<0.001*). The lack of an association between SPI and HI may have related, in part, to effects of plant height which showed a positive association with above-ground at physiological maturity ($AGDM_{PM}$:*P<0.001*)

and with AGDM at seven days after anthesis ($AGDM_{A+7}$: *P<0.05*), but a negative association with SPI (*P*<0.001). For FE this trait showed a strong negative association with $DMSpk_{A+7}$ (*P<0.001*), TGW (*P<0.001*) and with $AGDM_{A+7}$ (*P<0.001*) but a positive association with GN (*P<0.001*) and GY (*P*<0.01; Table 2.6).

Table 2.6. Pearson's phenotypic correlation coefficients between different traits measured at GS65+7d and physiological maturity among 150 HiBAP genotypes. Values presented are cross-year means (Y16 and Y17).

Traits	GN	HI	TGW	GY	$AGDM_{PM}$	SPI	StePI	FE	PH	$AGDM_{A+7}$	LamPI	$DMSpk_{A+7}$	LnInt2	LnInt3	LnPed
GN	-														
HI	0.27***	-													
TGW	-0.76***	-0.05	-												
GY	0.39***	0.37***	0.28***	-											
$AGDM_{PM}$	-0.01	-0.50***	0.34***	0.47***	-										
SPI	0.23**	0.21**	-0.38***	-0.20*	-0.34***	-									
StePI	-0.21**	-0.02	0.37***	0.21**	0.24***	-0.77***	-								
FE	0.65***	0.29***	-0.40***	0.39***	-0.02	-0.25***	0.20**	-							
PH	-0.48***	-0.40***	0.51***	0.00	0.40***	-0.54***	0.46*	-0.27***	-						
$AGDM_{A+7}$	0.08	-0.26***	-0.04	0.06	0.27***	-0.11	0.00	-0.48***	0.20**	-					
LamPI	0.00	-0.26***	-0.03	-0.04	0.11	-0.24***	-0.43***	0.06	0.06	0.17*	-				
$DMSpk_{A+7}$	0.12	-0.12	-0.14†	-0.03	0.10	0.44***	-0.41***	-0.43***	-0.07	0.52***	0.00	-			
LnInt2	-0.27***	0.18*	0.33***	0.09	-0.06	-0.50***	0.62***	-0.01	0.36***	0.07	-0.24***	-0.24***	-		
LnInt3	-0.36***	-0.23**	0.33***	-0.08	0.17*	-0.49***	0.43***	-0.23***	0.63***	0.28***	0.04	0.04	0.51***	-	
LnPed	-0.44***	-0.28***	0.39***	-0.09	0.21**	-0.23***	0.18*	-0.24***	0.60***	-0.04	0.05	-0.15†	0.01	0.05	-

A+7: Anthesis + 7 days; **PM:** Physiological Maturity; **GN:** Grain Number; **HI:** Harvest Index; **TGW:** Thousand Grain Weight; **GY:** Grain Yield; **AGDM:** Above-Ground Dry Matter; **SPI:** Spike Partitioning Index; **StePI:** Stem Partitioning Index; **FE:** Fruiting Efficiency; **PH:** Plant Height; **LamPI:** Lamina Paritioning Index; **DMSpk:** Dry Matter Spikes per unit area; **LnInt2:** Length internode 2; **LnInt3:** Length internode 3; **LnPed:** Length peduncle

*†P<0.10; *P<0.05; **P<0.01; ***P<0.001*

Values presented are cross-year means (Y16 and Y17)

2.3.7. Stepwise regression analysis

The associations between GY, HI, SPI and GN (as the dependent variable) and selected physiological variables between all 150 lines from the stepwise linear regression model are shown in Table 2.7. For GY, 30.7% of the variation was accounted by AGDM at physiological maturity as a single trait, adding HI and FE increased the variation accounted for 87.2%. As a single trait, plant height explained most phenotypic variation in HI (16%) than stem internode 2 (27.5%), SM2, FE, and SPI (42.2%) increased the phenotypic variation accounted. For SPI, StePI explained most of the variation (38.9%) as a single trait; this increased when LamPI was added to the model (93%). Fruiting efficiency was the most important trait explaining (46.1%) of phenotypic variation for GN adding SPI and $AGDM_{A+7}$ increased the variation accounted for (88%).

For the 29 genotypes of subset 1, multiple linear regression was carried out for the same traits used as dependent variables for the 150 genotypes (Table 2.7). For GY, AGDM at PM, int2TSPI and $AGDM_{A+7}$ explained most of the variation (59.6%). For HI, int2TSPI explained 30.1% phenotypic variation and adding other traits did not improve the model. Spike partitioning index variation was explained through the LnInt2, int2TSPI, pedTSSW and $AGDM_{PM}$ (58.8%). In the case of GN, SM2, pedTSSW and int3TSSW explained 55.1% of the phenotypic variation.

Table 2.7. HiBAP stepwise multiple linear regression analysis testing for grain yield (GY), harvest index (HI), spike partitioning index (SPI) and grain number (GN) as dependent variables against selected traits.

Traits	Variables selected	R	Prob	Variables tested in model
	Whole panel: 150 genotypes			
GY	$AGDM_{PM}$	30.7	*<0.001*	$AGDM_{A+7}$, $AGDM_{PM}$, DTA, DTM, $DMSpk_{A+7}$, FE, PH, HI, LnInt2, LnInt3, LnPed, SPI, StePI, LamPI
	$AGDM_{PM}$, HI	86.0	*<0.001*	
	$AGDM_{PM}$, HI, FE	87.2	*<0.001*	
HI	PH	16.0	*<0.001*	PH, LnPed, LnInt2, LnInt3, SM2, SPI, FE, $AGDM_{A+7}$
	PH, LnInt2	27.5	*<0.001*	
	PH, LnInt2, SM2	33.0	*<0.001*	
	PH, LnInt2, SM2, SPI	36.8	*<0.001*	
	PH, LnInt2, SM2, SPI, FE	42.2	*<0.001*	
SPI	PH	25.1	*<0.001*	GN, SM2, FE, HI, PH
	PH, FE	38.7	*<0.001*	
	PH, FE, GN	49.7	*<0.001*	
GN	FE	46.1	*<0.001*	PH, LnPed, LnInt2, LnInt3, SM2, SPI, FE, $AGDM_{A+7}$
	FE, SPI	62.6	*<0.001*	
	FE, SPI, $AGDM_{A+7}$	88.0	*<0.001*	
	Subset 1: 29 genotypes			
GY	$AGDM_{PM}$	45.8	*<0.001*	Int2TSPI, Int3TSPI, PedTSPI, PedTSSW, Int2TSSW, Int3TSSW, LnInt2, LnInt3, LnPed, $AGDM_{PM}$, $AGDM_{A+7}$
	$AGDM_{PM}$, Int2TSPI	54.7	*<0.01*	
	$AGDM_{PM}$, Int2TSPI, $AGDM_{A+7}$	59.6	*<0.05*	
HI	Int2TSPI	30.1	*<0.001*	
SPI	LnInt2	11.7	*<0.001*	LnPed, LnInt2, LnInt3, PedTSPI, Int2TSPI, PedTSSW, Int2TSSW, Int3TSSW, Int3TSPI, SM2, $AGDM_{A+7}$ $AGDM_{PM}$
	LnInt2, Int2TSPI	39.1	*<0.001*	
	LnInt2, Int2TSPI, PedTSSW	47.1	*<0.01*	
	LnInt2, Int2TSPI, PedTSSW, $AGDM_{PM}$	58.8	*<0.01*	
GN	SM2	30.0	*<0.001*	
	SM2, PedTSSW	53.3	*<0.01*	
	SM2, PedTSSW, Int3TSSW	55.1	*<0.05*	

R: Variation explained (%); **Prob:** Probability; **A+7:** Seven days after anthesis; **PM:** Physiological Maturity; **DTA:** Days from emergence to seven days after anthesis; **AGDM:** Above-ground DM; **LamPI:** Lamina Partitioning Index; **SPI:** Spike Partitioning Index; **StePI:** Stem Partitioning Index; **DMSpk:** DM Spike per unit area; **DTM:** Days from emergence to physiological maturity; **TGW:** Thousand Grain Weight; **Ped:** Peduncle; **Int2:** Internode 2; **Int3:** Internode 3; **TS:** True-Stem; **PI:** Partitioning Index; **SW:** Specific Weight

2.3.9. HiBAP genetic background

Considering the breeding history and pedigree of the current panel, the 150 HiBAP bread wheat genotypes can be divided into four main groups: 99 elite genotypes (i.e. progeny of crosses between elite cultivars or advanced lines) of which three genotypes were durum wheat derivatives and 14 genotypes possed the rye introgression 7DL.7EL, another second group was formed by 11 landrace-derived genotypes, a third group was formed by 26 genotypes having a primary synthetic-derived background and a fourth group of 14 genotypes was made up of genotypes with a synthetic+landrace (s+l) pedigree (Molero et al., 2019).

At GS65+7d, landrace-derived lines accumulated 5% more AGDM than each of the three other groups, at the same time higher LamPI and late DTA (3 days) were observed for this group. On the other hand, elite lines were more efficient at partitioning assimilate to the spike with high SPI (0.27) compared to the other three groups (0.26). The synthetic-derived group was characterized by high StePI (0.53) compared to elite, landraces-derived and synthetic+landrace-derived groups (0.52). On the other hand, FE was 10% higher in the elite group than the landrace-derived or the synthetic+landrace derived group (Table S2.7).

For the stem-internode length, plant height, and spike length large significant differences were found between the four groups; the landrace-derived lines (103.3 cm) were taller than the elite cultivars (98.5 cm; Table S2.7). Peduncle length of the landrace-derived, and synthetic+landrace-derived groups was longer compared to the synthetic-derived (+3%) and elite groups (+5%). For stem internode 2 small differences were recorded among groups with synthetic-derived (19.5 cm), elite (19.3 cm) and s+l-derived (19.4 cm) lines with longer internode 2 compared to landraces-derived (19 cm). For internode 3, again small differences existed with s+l-derived (14.1 cm) and landrace-derived (14 cm) genotypes slightly longer compared to synthetic-derived genotypes (13.8 cm; Table S2.7).

At physiological maturity, there was no significant difference amongst the four groups in grain yield. The elite group had higher HI (0.47) compared to the synthetic-derived, and synthetic+landrace-derived group (0.46) and the landrace-derived group (0.45). Above-ground DM was lower in the elite group (1,346 g m^{-2}) than the other three groups (1,371 to 1,394 g m^{-2}). Variation was also recorded among grain number per unit area and TGW at elite genotypes as reported by Molero et al. (2019).

2.4. Discussion

2.4.1. Association between biomass, harvest index and grain yield

Genetic yield improvement has historically been achieved as the result of more above-ground dry matter (DM) partitioned to the grains (Aisawi et al., 2015; Ferrante et al., 2017; Pennacchi & Carmo-Silva, 2018). However, recently within CIMMYT semi-dwarf spring wheat cultivars there is evidence biomass has increased rather than harvest index (HI) which showed no progress since the mid-1980s in cultivars released from 1966 to 2009 (Aisawi et al., 2015).

Grain yield in the HiBAP was strongly correlated and better explained by above-ground DM at physiological maturity ($AGDM_{PM}$) than HI. However, a trade-off was found between $AGDM_{PM}$ and HI indicating a requirement to identify lines achieving higher biomass, while maintaining or ideally increasing HI (Duan et al., 2018; Foulkes et al., 2007; Giunta et al., 2009).

Increased grain partitioning could be as a result of more grains per ear as a result of more fertile florets per ear, through increasing assimilate partitioning to the spike during the pre-flowering period (González et al., 2011). The trade-off found among grain number (GN) and grain weight (GW) in the present study could be due to the contribution of extra grains at more distal position in the spike of small potential size (Acreche et al., 2008); associated with the competition that exists for assimilates during the grain growth stage (Duan et al., 2018; Ferrante et al., 2015, Slafer & Savin, 1994).

The present experiments were sown under a raised bed system (plot size 0.8 x 4.0 m) using a seed rate of 102 kg ha^{-1}, with plots having a relatively large gap between the beds (row spacing of 24 cm). This planting system may favour taller genotypes able to close the gaps between the raised beds quicker, enabling earlier canopy closure increasing light interception and biomass. The positive relation between $AGDM_{PM}$ and plant height in the HiBAP may partly be explained by this behaviour. Thus taller plants had lower HI as a result of the investment of more assimilate in the stem, but higher biomass associated overall with a higher yield. On *Rht* near-isogenic lines (NILs) lines, Addisu et al. (2010) reported that semi-dwarfism was associated with increased HI but decreased $AGDM_{PM}$.

As stated above within the CIMMYT semi-dwarf lines in this panel there was a strong negative association between $AGDM_{PM}$ and HI, something that Aisawi et al. (2015) also reported in CIMMYT spring wheat cultivars released from 1966 to 2009. The idea that HI is decreasing or at least stagnant with plant breeding coincides with results in this panel and with results published recently in spring wheat under high yield potential conditions (Dai et al., 2016; Piñera-Chavez et al., 2016; Reynolds et al., 2017; Rose et al., 2017). One avenue to increase HI in high biomass backgrounds may be to improve the fruiting efficiency, which represents the efficiency with which DM allocated to the spike is converted to grains (Sonder et al., 2017), and which showed a strong positive associations in this panel with grain number, harvest index and yield.

2.4.2. Pre-anthesis growth, partitioning and determination of GN

As expected, biomass at seven days after anthesis (GS65+7d) was positively associated with GN since grain number is fixed in the pre-anthesis period (Foulkes et al., 2011). González et al. (2011) and García et al. (2014) also found a positive correlation between grain number per unit area and fruiting efficiency (FE) when testing the performance of modern cultivars (spring and winter wheat lines, under yield potential conditions). Genetic variation in GN in the HiBAP was also partly due to the positive association with spike partitioning index (SPI).

However, there was a negative relation between GN and grain weight (GW), which may be partly explained by the trade-off between FE and grain weight. Additional grains through improved floret survival will compete for more for assimilate during grain filling and may be located in more distal floret positions with lower potential grain weight (Slafer et al. 2015), agreeing with Terrile et al. (2017) finding where FE increased GW decreased limiting yield increments when GN is boost via higher FE.

The physiological model applied to analyse GN in this panel is based on three traits: (i) AGDM at GS65+7d, (ii) SPI and (ii) FE (Fischer, 1985; González et al., 2014). Results showed that FE seemed the most important trait to increase GN and FE was also associated with HI and yield. In various studies using spring wheat FE was also found to be strongly associated with genetic variation in GN (Bustos et al., 2013; Elía et al., 2016; Ferrante et al., 2015). The use of FE in breeding programs will require high heritability, genetic variation within adapted high-yielding modern cultivars and a lack of trade-off with other yield components (Elía et al., 2016) such as spike DM m^{-2}, grain weight and DM per spike. Within the HiBAP, spike DM per unit area and SPI were negatively associated with FE as was reported for two high FE cultivars by Terrile et al. (2017) suggesting that the increases in FE may be associated with lower spike dry matter. However, Ferrante et al. (2012) reported using different durum wheat lines grains m^{-2} was positively associated with spike DM at anthesis, indicating no trade-off with FE. It can be speculated that in the high HiBAP the trade-off between SPI and FE related to either: (i) plants not able to allocate enough resources to the florets, (ii) excessive investment in non-rachis components (DW chaff) (González et al., 2011), (iii) presence of large ovaries leading to heavy grains (trade-off between FE vs thousand-grain weight), (iv) spike DW measurement timing which was done 7 days after anthesis when initial growth of grains had accrued, leading to underestimated values of FE (Elía et al. 2016) or (v) limited assimilate supply to distal florets due to restricted vascular connections within the rachilla.

In the subset of 14 genotypes, the amount of DM partitioned to the glume, lemma and rachis presented a negative association with SPI suggesting that this organs compete for assimilates during spike development. On the other hand, for fruiting efficiency results indicated that decreased awns PI (positively associated with SPI) and increased lemma PI were associated with higher fruiting efficiency values. Decreased allocation of assimilates to awns may increase FE since this represents a saving of spike dry matter with potentially relatively little impact on grain number since awns do not have an essential structural role in supporting grains in spikelets. The mechanisms basis for the association between lemma PI and FE is less clear; is possible that this was not a causal effect but an indirect effect of the strong negative association between awnsPI and lemma PI. Although rachis PI was not associated with FE, it showed a positive association with TGW and GY from which it can be speculated that an increased rachis PI was associated with improved vascular connections within the rachis and reduced resistance to assimilate supply to the distal spikelets during the floret survival period

(González et al., 2011). Alternatively, the negative relation among rachis specific weight and grain number could suggest that a reduction among length: DM on the rachis may result in physical restrictions to grain growth and/or spike photosynthesis.

2.4.3. Spring wheat ideotype for optimised partitioning

Since stem and spike growth overlaps during stem elongation, mainly during the rapid spike growth phase (Satorre & Slafer, 1999), the competition for assimilates between the spike and stem varies between internodes. Genetic variation in stem-internode partitioning and associations with spike growth have been reported in studies comparing tall versus semi-dwarf cultivars, as maximum stem growth rates have been reported to vary from 7 to 21 days after anthesis (Chen et al., 2013; Ehdaie et al., 2006). In the HiBAP, spike partitioning index was negatively associated with length of internode: peduncle < internode 2 < internode 3 and < plant height. Increased grain number per m^2 and harvest index were associated with reduced true-stem partitioning (internodes 2 and 3) recently in a CIMMYT elite spring wheat germplasm panel (Rivera-Amado, 2015). In this high biomass panel, DM spike per unit area was only strongly associated with reduced peduncle, internode 2 and 3 stem lengths. A negative relation is often found between grains per unit area and plant height, as tall plants invest relatively more assimilates in the stem (source) rather than in the spike (sink) impacting negatively on grain number and harvest index (Du et al., 2018). There are few previous reports related to genetic variation in internode partitioning between leaf sheath and true-stem in the literature. In the HiBAP, spike partitioning index was negatively associated with the DM partitioned to the true-stem of internode 2 and even more strongly with the true-stem of internode 3. At the same time, SPI was also more strongly negatively associated with internode 2 and 3 lengths than peduncle length again suggesting that reduced allocation of assimilates to stem internodes 2 and 3 was associated with higher SPI. However, these sections of the stem (int2TSPI and int3TSPI) were associated positively with grain yield in this study. This likely reflected that SPI, although positively associated with harvest index and grain number per unit area, was negatively associated with above-ground DM at both stages and that overall AGDM was a stronger driver for grain yield in this panel than harvest index and grain number. These results agree with those reported by Rivera-Amado et al. (2019) on 26 CIMMYT spring wheat elite lines. Concerning the determination of SPI, the competition for assimilates between the spike and these two internodes may be higher than between the spike and the peduncle as half of peduncle extension occurs after anthesis when rapid spike growth has ceased.

In the HiBAP there were associations between spike density and internode true-stem partitioning index; higher spike density increased assimilate partitioning to peduncle true-stem but decreased partitioning to internode 4 (true stem and leaf sheath). This could be result of reduced light interception in the lower canopy leaf layers with higher spike density. Present results indicated maintaining plant height but reducing stem internode 2 and 3 lengths and true-stem partitioning relative to other true-stem internodes could be a strategy to increase

SPI and HI. Since the basal internodes (int4+ and/or 5) are the most important for basal support (lodging resistance), this approach should also be consistent with maintaining lodging resistance in high yield potential cultivars. In the subset of 29 genotypes where SPI was used as the dependent variable in the stepwise regression analysis results were consistent with this hypothesis, showing internode2 true-stem partitioning index as a priority variable explaining phenotypic variation in SPI. The mechanism for reduced peduncle true-stem specific weight to increase DM partitioned to the grain may be as the result of the indirect association between spike density and pedTSSW. The present hypothesis relating to internode 2 and 3 could be examined further using plant growth regulators to shorten internode lengths (For further analysis see chapter 6). However, in relation to yield potential, the present results showed stem partitioning index and internode2 true-stem partitioning index were positively correlated with grain yield; these were likely indirect effects of positive associations between these traits and plant height which, in turn, was positively correlated with above-ground DM. For raising grain number, the stepwise analysis showed that fruiting efficiency, spike partitioning index and then AGDM at seven days after anthesis were the most critical target traits.

Present results showed improved harvest index, grain number and yield increases in high biomass cultivars could likely be achieved by selecting for reduced internode lengths and partitioning index of internode 2 and 3. Encouragingly, internode lengths made a meaningful contribution to raising harvest index and the total DM partitioned to the spike even after accounting for effects of plant height in the stepwise regression model offering scope for breaking the association between the ratio of grains to biomass produced and above-ground DM in CIMMYT spring wheat germplasm.

2.4.4. Implications for plant breeding programs

The present study indicated that a combination of plant height, length of stem internode 2, spikes per unit area, fruiting efficiency and spike partitioning index accounted for over 42% of the variation in harvest index and internode 2 true-stem partitioning index as a single trait accounted for 25% of the variation in harvest index suggesting these traits have value in plant breeding programs aimed at improving harvest index in high biomass backgrounds (Hawkesford et al., 2013; Rebetzke et al., 2012). To deploy these target traits high-throughput phenotyping (HTP) and/or genotypic markers for marker-assisted selection will be required, e.g. for stem DM internode partitioning and spike morphology traits, the current methodology was time-consuming. The implementation of phenotypic high-throughput methods can be employed to improve the efficiency of the selection of traits (Araus et al., 2018) which should be selected based on good phenotypic plasticity and heritability (Cooper & Bänziger, 2017; Sadras & Rebetzke, 2013). In this study, most of the grain partitioning traits had heritability > 50%, e.g. grain weight > grain number > harvest index >stem internode lengths > spike partitioning index> yield > fruiting efficiency, generally agreeing with other studies in wheat (Lopes et al., 2012; Sukumaran et al., 2017). Low heritability in certain traits such as above-

ground DM (at anthesis and physiological maturity), DM spike per unit area seven days after anthesis can be attributed to genetic causes (several genes controlling these complex traits) and large environment by genotype interaction. Data collected in the subsets for stem-internode partitioning and spike-component partitioning traits indicated scope to improve yield through the selection of shorter internode 2 and decreased rachis specific weight and/or awn partitioning index which may raise the ability that the spike has to translocate assimilates into grains. However, data collected on the subsets was not enough to conclude from a heritability perspective. Pyramid selection of these traits could also help to narrow the selection of parental crosses going into the breeding programme (Reynolds et al., 2017).

Phenotypic variation of many complex traits can be influenced by multiple DNA regions and the implementation of high-throughput genotypic methods such as SNP molecular marker arrays allows the possibility to associate a DNA region/sequence with a desired trait through appropriate experimental design and statistical analyses (Jonas & De Koning, 2013; Tester & Langridge, 2010). The recent development of an annotated version of the wheat genome (94% coverage) has given the opportunity to improve the precision of genetic analysis in breeding programs (IWGSC, 2018). In addition, the use of phenotypic + genotypic data makes a possible accurate selection in early generations reducing the amount of time and cost spend on trial increasing diversity; an example of this strategy will be introduced in chapter 4.

2.5. Conclusions

- Grain number within this high biomass panel was explained mainly through fruiting efficiency.
- Higher spike DM per unit area at GS65+7d was associated with shorter internode 2 length (phytomer below peduncle).
- Increases in fruiting efficiency were associated with decreased awn DM partitioning, and lower rachis DM partition was associated with higher grain weight and grain yield.
- Genetic diversity in modern CIMMYT genotypes has been increased with the introduction of landrace-derived and synthetic-derived backgrounds allowing higher biomass (landraces) and stem partitioning index (synthetics) but more research needs to be done to impact at grain yield level.
- The incorporation of next-sequencing data to developed precise molecular markers could empower the use of these novel traits, which are meticulous and time consuming to measure.

2.6. Supplementary material

Table S2.1. HiBAP genotypes names, subset and pedigree classification considering their breeding/crossing history.

	Genotype	Subset 1	Subset 2	HiBAP_ PGR	Detail group	General group	Number group
1	CIRNO C 2008	✖	✖		Elite	Elite	1
2	C80.1/3*QT4118//KAUZ/RAYON/3/2*TRCH/7/CMH79A.955/4/AGA/3/4*SN64/CNO67//INIA66/5/NAC/6/RIALTO	✖	✖		Elite-Int	Elite	1
3	SIETE CERROS T66	✖	✖	✖	Elite	Elite	1
4	PAVON F 76	✖		✖	Elite	Elite	1
5	SERI M 82				Elite	Elite	1
6	BACANORA T 88	✖	✖		Elite	Elite	1
7	ATTILA				Elite	Elite	1
8	BAVIACORA M 92				Elite	Elite	1
9	SERI/RAYON				Elite	Elite	1
10	BRBT1*2/KIRITATI				Elite	Elite	1
11	PFAU/WEAVER*2//TRANSFER#12,P88.272.2				Elite	Elite	1
12	KRICHAUFF	✖	✖	✖	Elite-Int	Elite	1
13	BECARD				Elite	Elite	1
14	SAUAL/WHEAR//SAUAL				Elite	Elite	1
15	WBLL1*2/4/BABAX/LR42//BABAX/3/BABAX/LR42//BABAX	✖			Elite	Elite	1
16	KFA/3/PFAU/WEAVER//BRAMBLING/4/PFAU/WEAVER*2//BRAMBLING	✖	✖	✖	Elite	Elite	1
17	KINGBIRD #1//INQALAB 91*2/TUKURU	✖			Elite	Elite	1
18	UP2338*2/4/SNI/TRAP#1/3/KAUZ*2/TRAP//KAUZ/5/MILAN/KAUZ//CHIL/CHUM18/6/UP2338*2/4/SNI/TRAP#1/3/KAUZ*2/TRAP//KAUZ				Elite	Elite	1
19	CMH79A.955/4/AGA/3/4*SN64/CNO67//INIA66/5/NAC/6/RIALTO	✖	✖		Elite-Int	Elite	1
20	C80.1/3*QT4118//KAUZ/RAYON/3/2*TRCH/7/CMH79A.955/4/AGA/3/4*SN64/CNO67//INIA66/5/NAC/6/RIALTO				Elite-Int	Elite	1
21	SOKOLL//PUB94.15.1.12/WBLL1				Syn+Lan	Syn+Lan	4
22	BCN/WBLL1//PUB94.15.1.12/WBLL1				Lan	Lan	2
23	WBLL1*2/4/SNI/TRAP#1/3/KAUZ*2/TRAP//KAUZ/5/KACHU #1				Elite	Elite	1
24	KRL 210	✖	✖		Elite	Elite	1

25	TECUE #1/2*WAXWING				Elite	Elite	1
26	CHEWINK #1	✖	✖	✖	Elite	Elite	1
27	PASTOR//HXL7573/2*BAU/3/WBLL1	✖			Elite	Elite	1
28	CHEN/AE.SQ//WEAVER/3/SSERI1	✖	✖	✖	Syn	Syn	3
29	SOKOLL/3/PASTOR//HXL7573/2*BAU/4/WBLL4//OAX93.24.35/WBLL1				Syn+Lan	Syn+Lan	4
30	SOKOLL/3/PASTOR//HXL7573/2*BAU/4/PARUS/PASTOR				Syn	Syn	3
31	SOKOLL/3/PASTOR//HXL7573/2*BAU/4/SOKOLL/WBLL1				Syn	Syn	3
32	PAVLOVKA/V15.89C//NAVJ07/3/ROLF07				Elite	Elite	1
33	SOKOLL/3/PASTOR//HXL7573/2*BAU/4/ATTILA/PASTOR				Syn	Syn	3
34	WBLL4//OAX93.24.35/WBLL1/5/CROC_1/AE.SQUARROSA (205)//BORL95/3/PRL/SARA//TSI/VEE#5/4/FRET2	✖			Syn+Lan	Syn+Lan	4
35	SOKOLL/WBLL1				Syn	Syn	3
36	CROC_1/AE.SQUARROSA (205)//BORL95/3/PRL/SARA//TSI/VEE#5/4/FRET2				Syn	Syn	3
37	MEX94.2.19//SOKOLL/WBLL1				Syn+Lan	Syn+Lan	4
38	1447/PASTOR//KRICHAUFF	✖	✖		Elite-Int	Elite	1
39	C80.1/3*QT4118//KAUZ/RAYON/3/2*TRCH				Elite	Elite	1
40	WBLL1*2/KURUKU	✖	✖		Elite	Elite	1
41	SERI/BAV92	✖			Elite	Elite	1
42	C80.1/3*QT4118//KAUZ/RAYON/3/2*TRCH				Elite	Elite	1
43	WHEAR/KUKUNA/3/C80.1/3*BATAVIA//2*WBLL1				Elite	Elite	1
44	MUTUS*2/AKURI				Syn	Syn	3
45	DPW 621-50	✖	✖		Elite	Elite	1
46	TRCH/5/REH/HARE//2*BCN/3/CROC_1/AE.SQUARROSA (213)//PGO/4/HUITES				Syn	Syn	3
47	C80.1/3*QT4118//KAUZ/RAYON/3/2*TRCH/4/BERKUT/KRICHAUFF				Elite-Int	Elite	1
48	MEX94.27.1.20/3/SOKOLL//ATTILA/3*BCN/4/PUB94.15.1.12/WBLL1				Syn+Lan	Syn+Lan	4
49	SOKOLL//PUB94.15.1.12/WBLL1				Syn+Lan	Syn+Lan	4

50	SERI/BAV92//PUB94.15.1.12/WBLL1	✖			Lan	Lan	2
51	SOKOLL//PUB94.15.1.12/WBLL1				Syn+Lan	Syn+Lan	4
52	CROC_1/AE.SQUARROSA (224)//OPATA/3/PUB94.15.1.12/WBLL1	✖	✖		Syn+Lan	Syn+Lan	4
53	BCN/WBLL1/6/CMH79A.955/4/AGA/3/4*SN64/CNO67//INIA66/5/NAC				Elite-Int	Elite	1
54	SERI/BAV92//JANZ				Elite	Elite	1
55	OR791432/VEE#3.2	✖	✖		Elite	Elite	1
56	ATTILA/3*BCN	✖			Elite	Elite	1
57	SOKOLL				Syn	Syn	3
58	PASTOR//HXL7573/2*BAU				Elite	Elite	1
59	SOKOLL/3/PASTOR//HXL7573/2*BAU/4/ASTREB				Syn	Syn	3
60	SOKOLL/3/PASTOR//HXL7573/2*BAU/4/WBLL4//OAX93.24.35/WBLL1				Syn+Lan	Syn+Lan	4
61	WBLL4//OAX93.24.35/WBLL1/5/CROC_1/AE.SQUARROSA (205)//BORL95/3/PRL/SARA//TSI/VEE#5/4/FRET2				Syn+Lan	Syn+Lan	4
62	MILAN/KAUZ//DHARWAR DRY/3/BAV92				Lan	Lan	2
63	BAV92/SERI				Elite	Elite	1
64	PASTOR//HXL7573/2*BAU/3/ATTILA/3*BCN/4/ATTILA/PASTOR				Elite	Elite	1
65	PUB94.15.1.12/FRTL/5/CROC_1/AE.SQUARROSA (205)//BORL95/3/PRL/SARA//TSI/VEE#5/4/FRET2				Syn+Lan	Syn+Lan	4
66	F2SR2-69//YANGLING SHAANXI/PASTOR	✖			Elite	Elite	1
67	PASTOR//HXL7573/2*BAU/3/WBLL1				Elite	Elite	1
68	BCN/WBLL1//PUB94.15.1.12/WBLL1				Lan	Lan	2
69	HE1/2*CNO79//BAV92				Elite	Elite	1
70	CROC_1/AE.SQUARROSA (205)//BORL95/3/PRL/SARA//TSI/VEE#5/4/FRET2				Syn	Syn	3
71	NAVOJOA M2007	✖			Elite	Elite	1
72	PASTOR//HXL7573/2*BAU/3/WBLL1				Elite	Elite	1
73	BABAX/LR42//BABAX/3/ER2000				Elite	Elite	1

74	SOKOLL/3/PASTOR//HXL7573/2*BAU					Syn	Syn	3
75	CHWL86/6/FILIN/IRENA/5/CNDO/R143//ENTE/MEXI_2/3/AEGILOPS SQUARROSA (TAUS)/4/WEAVER					Syn	Syn	3
76	BECARD					Elite	Elite	1
77	KACHU					Elite-dur	Elite	1
78	NELOKI	✖				Elite	Elite	1
79	PUB94.15.1.12/FRTL	✖				Lan	Lan	2
80	W15.92/4/PASTOR//HXL7573/2*BAU/3/WBLL1					Elite	Elite	1
81	BECARD/KACHU					Elite	Elite	1
82	TACUPETO F2001/SAUAL//BLOUK #1	✖				Elite	Elite	1
83	KUKRI	✖	✖			Elite	Elite	1
84	D67.2/PARANA 66.270//AE.SQUARROSA (320)/3/CUNNINGHAM/4/VORB					Syn	Syn	3
85	PVN//CAR422/ANA/5/BOW/CROW//BUC/PVN/3/YR/4/TRAP#1/6/WORRAKATTA/2*PASTOR/7/PRL/2*PASTOR					Elite	Elite	1
86	BECARD/KACHU					Elite	Elite	1
87	MUNAL #1	✖				Elite	Elite	1
88	CNO79//PF70354/MUS/3/PASTOR/4/BAV92*2/5/FH6-1-7	✖	✖		✖	Elite	Elite	1
89	PBW343*2/KUKUNA*2//FRTL/PIFED					Elite	Elite	1
90	KACHU #1/4/CROC_1/AE.SQUARROSA (205)//BORL95/3/2*MILAN/5/KACHU					Syn	Syn	3
91	BABAX/LR42//BABAX/3/VORB					Syn	Syn	3
92	OR791432/VEE#3.2//ATTILA/3*BCN	✖	✖		✖	Elite	Elite	1
93	SOKOLL/WBLL1					Syn	Syn	3
94	C80.1/3*QT4118//KAUZ/RAYON/3/2*TRCH/7/CMH79A.955/4/AGA/3/4*SN64/CNO67//INIA66/5/NAC/6/RIALTO/8/WBLL1*2/KURUKU					Elite-Int	Elite	1
95	CMH79A.955/4/AGA/3/4*SN64/CNO67//INIA66/5/NAC/6/RIALTO/7/BCN/WBLL1/8/C80.1/3*QT4118//KAUZ/RAYON/3/2*TRCH					Elite-Int	Elite	1

96	WBLL1//YANGLING SHAANXI/ESDA/3/ROLF07				Elite	Elite	1
97	HE1/2*CNO79//BAV92/3/ROLF07	✖			Elite	Elite	1
98	BCN/WBLL1//PUB94.15.1.12/WBLL1				Lan	Lan	2
99	C80.1/3*QT4118//KAUZ/RAYON/3/2*TRCH/4/BERKUT/KRICHAUFF				Elite-Int	Elite	1
100	WBLL1//PUB94.15.1.12/WBLL1				Lan	Lan	2
101	MEX94.27.1.20/3/SOKOLL//ATTILA/3*BCN				Syn+Lan	Syn+Lan	4
102	MTRWA92.161/PRINIA/5/SERI*3//RL6010/4*YR/3/PASTOR/4/BAV92				Elite	Elite	1
103	SOKOLL/WBLL1				Syn	Syn	3
104	PRIAMURSKAYA 93/2*TERREMOTO/3/ATTILA/BAV92//PASTOR/4/NAVJ07	✖			Elite	Elite	1
105	MEX94.27.1.20/3/SOKOLL//ATTILA/3*BCN/4/PUB94.15.1.12/WBLL1				Syn+Lan	Syn+Lan	4
106	BCN/WBLL1//ROLF07				Elite	Elite	1
107	C80.1/3*QT4118//KAUZ/RAYON/3/2*TRCH/7/CMH79A.955/4/AGA/3/4*SN64/CNO67//INIA66/5/NAC/6/RIALTO				Elite-Int	Elite	1
108	TACUPETO F2001/BRAMBLING*2//KACHU				Elite	Elite	1
109	WBLL1*2/KUKUNA	✖	✖	✖	Elite	Elite	1
110	WEEBILL1				Elite	Elite	1
111	ROELFS F2007				Elite	Elite	1
112	SERI/BAV92//PUB94.15.1.12/WBLL1				Lan	Lan	2
113	SOKOLL/WBLL1	✖	✖		Syn	Syn	3
114	QUAIU				Elite	Elite	1
115	BAJ #1				Elite	Elite	1
116	BORLAUG100 F2014				Elite	Elite	1
117	VOROBEY	✖	✖	✖	Syn	Syn	3
118	WBLL4//OAX93.24.35/WBLL1				Lan	Lan	2
119	SOKOLL/WBLL1	✖			Syn	Syn	3
120	PUB94.15.1.12/WBLL1				Lan	Lan	2
121	WBLL4//OAX93.24.35/WBLL1	✖	✖		Lan	Lan	2
122	BAV92/SERI	✖			Elite	Elite	1
123	W15.92/4/PASTOR//HXL7573/2*BAU/3/WBLL1				Elite	Elite	1
124	CNDO/R143//ENTE/MEXI_2/3/AEGILOPS SQUARROSA (TAUS)/4/WEAVER/5/2*JANZ/6/MISR2, EGY				Syn	Syn	3

125	FRANCOLIN #1/WBLL1	✖				Elite	Elite	1
126	ROLF07*2/5/REH/HARE//2*BCN/3/CROC_1/AE.SQUARROSA (213)//PGO/4/HUITES					Syn	Syn	3
127	FRET2/TUKURU//FRET2/3/MUNIA/CHTO//AMSEL/4/FRET2/TUKURU//FRET2					Elite	Elite	1
128	MUTUS//ND643/2*WBLL1					Elite	Elite	1
129	MUTUS*2/HARIL #1					Elite	Elite	1
130	QUAIU*2/KINDE	✖				Elite	Elite	1
131	DANPHE #1*2/CHYAK					Elite	Elite	1
132	ND643/2*WBLL1/4/WHEAR/KUKUNA/3/C80.1/3*BATAVIA//2*WBLL1					Elite	Elite	1
133	MUNAL*2/CHONTE					Elite	Elite	1
134	CHIBIA//PRLII/CM65531/3/MISR 2/4/MUNAL #1					Elite	Elite	1
135	NAC/TH.AC//3*PVN/3/MIRLO/BUC/4/2*PASTOR/5/KACHU/6/KACHU					Elite-Int	Elite	1
136	KACHU #1/4/CROC_1/AE.SQUARROSA (205)//BORL95/3/2*MILAN/5/KACHU	✖	✖			Syn	Syn	3
137	KACHU//WBLL1*2/BRAMBLING					Elite-dur	Elite	1
138	KACHU/BECARD//WBLL1*2/BRAMBLING	✖				Elite-dur	Elite	1
139	SUPER 152					Elite	Elite	1
140	SUP152*2/TECUE #1					Elite	Elite	1
141	BECARD/FRNCLN					Elite	Elite	1
142	FRET2*2/BRAMBLING//BECARD/3/WBLL1*2/BRAMBLING					Elite	Elite	1
143	KAUZ/PASTOR//PBW343/3/KIRITATI/4/FRNCLN	✖			✖	Elite	Elite	1
144	WBLL1*2/VIVITSI//AKURI/3/WBLL1*2/BRAMBLING	✖				Syn	Syn	3
145	SAUAL/3/ACHTAR*3//KANZ/KS85-8-4/4/SAUAL	✖				Elite	Elite	1
146	JANZ	✖	✖			Elite-Int	Elite	1
147	CMH79A.955/4/AGA/3/4*SN64/CNO67//INIA66/5/NAC	✖			✖	Elite-Int	Elite	1
148	CROC_1/AE.SQUARROSA (224)//OPATA	✖				Syn	Syn	3
149	BCN/RIALTO//ROLF07					Elite	Elite	1
150	MEX94.27.1.20/3/SOKOLL//ATTILA/3*BCN					Syn+Lan	Syn+Lan	4

Figure S2.1. HiBAP genotypes field experiment arrangement (including randomization) for Y16: 2015-16.

HiBAP Y16: 2015-16																				
1	2	3	4	5	6	7	8	9	10	11	12	13	14	15	16	17	18	19	20	Rep 1
40	39	38	37	36	35	34	33	32	31	30	29	28	27	26	25	24	23	22	21	
41	42	43	44	45	46	47	48	49	50	51	52	53	54	55	56	57	58	59	60	
80	79	78	77	76	75	74	73	72	71	70	69	68	67	66	65	64	63	62	61	
81	82	83	84	85	86	87	88	89	90	91	92	93	94	95	96	97	98	99	100	
120	119	118	117	116	115	114	113	112	111	110	109	108	107	106	105	104	103	102	101	
121	122	123	124	125	126	127	128	129	130	131	132	133	134	135	136	137	138	139	140	
36	22	132	116	5	20	41	110	52	125	150	149	148	147	146	145	144	143	142	141	
7	122	81	137	44	107	38	92	80	26	28	10	18	67	136	51	86	73	144	118	Rep 2
69	115	82	71	39	102	17	147	45	98	64	33	99	106	77	149	87	55	1	49	
134	109	62	113	40	94	126	50	2	27	78	119	140	83	68	150	123	103	12	56	
142	37	101	25	6	42	61	97	130	88	104	24	66	59	13	120	96	89	143	75	
91	65	79	19	48	105	90	138	57	141	111	47	127	84	9	135	93	53	21	34	
146	35	129	95	16	133	117	23	4	60	139	65	148	31	74	30	128	114	11	70	
58	72	15	145	8	29	43	112	131	124	85	46	76	3	108	121	32	63	100	14	
25	98	149	138	67	108	112	56	7	47	59	92	130	131	84	70	106	116	35	144	Rep 3
4	18	32	21	55	141	104	113	61	44	93	27	125	80	58	65	33	85	136	146	
17	118	94	121	87	105	24	133	37	74	68	10	39	29	120	79	16	127	99	88	
52	63	143	140	2	48	31	129	73	102	90	38	28	111	148	12	5	77	43	96	
40	71	14	124	91	6	150	81	132	53	100	114	86	60	110	8	50	19	26	78	
42	147	15	134	34	66	95	128	51	103	54	83	126	97	115	49	13	36	137	76	
122	9	30	142	20	75	117	64	109	45	11	82	41	72	3	119	62	101	23	135	
46	1	89	139	57	107	69	22	145	123	125	4	106	72	28	66	98	50	83	31	Rep 4
42	123	120	91	32	30	102	86	5	131	93	148	117	108	52	88	137	62	71	18	
9	128	78	43	36	146	92	82	105	67	49	34	23	10	100	90	104	124	70	140	
55	130	135	143	39	22	76	118	19	7	138	29	33	96	119	51	2	17	46	122	
1	56	26	14	79	116	133	147	61	126	149	59	127	37	27	139	48	115	3	12	
111	87	109	132	63	54	15	141	80	25	84	113	64	73	97	41	107	16	150	58	
60	112	81	69	13	121	77	142	21	134	110	53	94	11	85	68	44	145	35	75	
20	144	101	89	40	65	8	95	47	74	38	24	45	136	6	103	129	114	57	99	

Figure S2.2. HiBAP genotypes field experiment arrangement (including randomization) for Y17: 2016-17.

HiBAP Y17: 2016-17

138	85	76	122	39	88	144	81	126	149	132	36	92	80	54	7	21	29	116	84	37	117	119	53	41		108	139	64	36	37	26	95	38	5	67	74	133	61	97	70	117	98	39	131	121	51	87	108	115	125	
73	35	10	135	34	66	6	2	74	1	42	71	104	133	108	98	77	9	112	79	49	124	102	148	145		60	31	3	14	17	150	47	113	29	15	72	40	77	134	30	103	69	13	123	142	45	58	8	32	6	
30	96	120	69	64	141	107	109	128	150	127	68	15	12	61	14	136	91	131	59	86	3	38	48	32	Rep 2	85	71	16	19	144	138	65	35	56	96	116	136	80	86	130	99	11	120	101	140	91	146	137	83	28	Rep 4
100	65	24	142	114	62	99	25	83	19	46	47	33	110	97	17	40	43	8	113	129	111	123	16	60		22	148	114	7	73	81	50	145	33	62	49	25	122	100	12	94	34	106	20	93	147	41	66	78	102	
28	147	121	18	63	139	27	125	140	70	67	118	137	134	31	89	115	64	13	90	51	11	130	57	106		11	141	82	21	118	1	24	63	112	43	54	107	110	9	104	84	143	90	127	86	129	132	44	75	126	
103	45	75	20	22	56	82	143	52	87	55	146	78	105	5	72	23	95	58	4	50	44	101	93	26		10	79	4	2	53	109	68	52	23	42	27	57	46	18	92	124	149	128	135	76	88	55	119	59	48	
150	149	148	147	146	145	144	143	142	141	140	139	138	137	136	135	134	133	132	131	130	129	128	127	126		11	7	67	61	64	13	29	146	54	81	47	11	124	140	117	119	9	143	114	95	1	80	71	141	73	
101	102	103	104	105	106	107	108	109	110	111	112	113	114	115	116	117	118	119	120	121	122	123	124	125		125	33	65	79	127	24	38	75	145	82	46	12	116	20	72	25	96	121	26	36	15	58	34	39	126	
100	99	98	97	96	95	94	93	92	91	90	89	88	87	86	85	84	83	82	81	80	79	78	77	76	Rep 1	86	43	101	131	92	18	5	6	76	68	19	52	70	59	106	30	50	55	89	135	84	31	120	10	85	Rep 5
51	52	53	54	55	56	57	58	59	60	61	62	63	64	65	66	67	68	69	70	71	72	73	74	75		94	115	113	48	66	45	91	51	100	16	122	42	90	147	132	93	148	83	2	104	112	123	138	88	97	
50	49	48	47	46	45	44	43	42	41	40	39	38	37	36	35	34	33	32	31	30	29	28	27	26		130	137	23	103	98	87	128	69	8	108	150	14	77	49	37	107	44	56	3	57	110	134	105	63	144	
1	2	3	4	5	6	7	8	9	10	11	12	13	14	15	16	17	18	19	20	21	22	23	24	25		102	40	142	99	109	78	4	139	129	118	62	133	53	136	32	74	35	17	28	21	22	27	60	41	149	

Figure S2.3. Development stages at field level of the HiBAP experiment for Y16 and Y17.

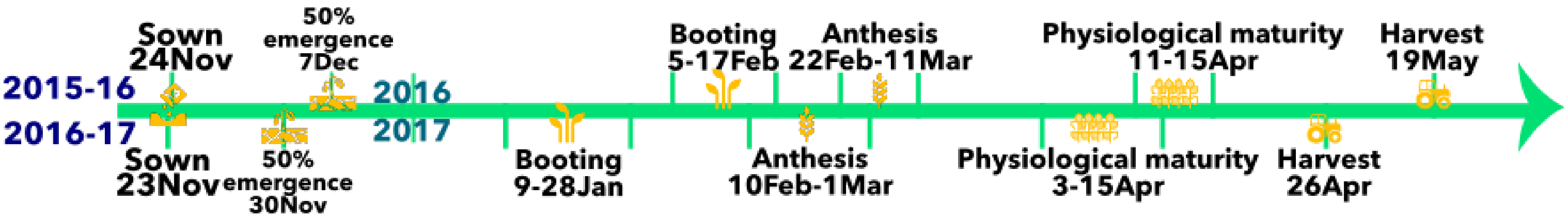


Figure S2.4. HiBAP genotype bed arrangement, two raised beds per genotype and four (Y16) or two (Y17) rows per bed.

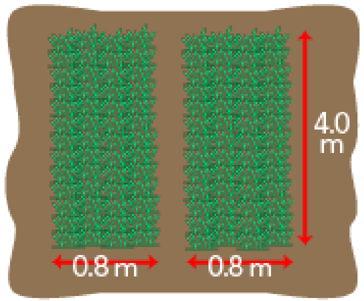


Table S2.2. Plot management, application of crop herbicide, fungicide and insecticide on the HiBAP for Y16 and Y17.

	Y16: 2015-16	Y17: 2016-17	
Herbicide	14/12/15 16/12/15	N/A	
Fungicide (Folicur)	04/02/16	26/01/17	10/03/17
	31/03/16	17/02/17	
Insecticide (Admire 750)	19/01/16	21/12/16	23/02/17
	19/02/16	18/01/17	
Fertilizer (Urea, 200 units)	06/01/16	21/12/16 (50 units) 19/01/17 (150 units)	

Table S2.3. Meteorological data and crop management over two seasons (Y16 and Y17) at NW Mexico.

		Y16: 2015-16	***Y17: 2016-17***
Planting date: 50% emergence:		November 24th December 7th	November 23th November 30th
Booting (GS41-GS49)	Mean Temperature	17.2°C	17.2°C
	Mean Solar radiation	206.1 MJ m^{-2}	194.4 MJ m^{-2}
	Mean Rain accumulated	0.04 mm	0mm
Anthesis (GS59-GS69)	Mean Temperature	18.8°C	17.2°C
	Mean Solar radiation	222.1 MJ m^{-2}	200.0 MJ m^{-2}
	Mean Rain accumulated	0.05 mm	1.6 mm
Grain filling (GS71-GS91)	Mean Temperature	19.7°C	19.1°C
	Mean Solar radiation	242.1 MJ m^{-2}	257.9 MJ m^{-2}
	Mean Rain accumulated	0.17 mm	0.03 mm

Table S2.4. Formulas used to calculate different partitioning traits at GS65+7d, grain yield and yield components (Pask et al., 2012).

Trait	Formula	Units
Above-ground dry matter ($AGDM_{A+7}$) at GS65+7d	Dry weight total Biomass (g) / width bed (m)	g m^{-2}
Above-ground dry matter (AGDM) at GS65+7d	Sum of all plant organs (spike, lamina and stem) DM	g per shoot[1]
Partitioning indices (PI)	DM plant organ (spike, lamina or stem) / AGDM	
Dry matter spike per unit area at GS65+7d	AGDM (g m^{-2}) * Spike Partitioning Index (SPI)	
Above-ground dry matter ($AGDM_{PM}$) at physiological maturity	Grain yield / Harvest Index (HI)	g m^{-2}
Grain yield (GY)	[(Plot grain weight (g) x grain moisture (%)) + (100 stems dry weight (g) x harvest index (HI) / Harvested area (m^{-2}))	
Thousand Grain Weight (TGW)	Dry weight of 200 (g) x 5	g
Harvest Index (HI)	Grain yield (g m^{-2}) / AGDM (g m^{-2})	
Grain Number (GN)	Grain yield (g m^{-2}) / TGW (g) x 1000	grains m^{-2}
Spikes per unit area (SM2)	$AGDM_{PM}$ / [(Dry weight 100 stems + DW 100 spikes) / 100]	spikes m^{-2}
Fruiting Efficiency (FE)	Number of grains m^{-2} (GN) / ($AGDM_{A+7}$ (g m^{-2}) and SPI)	grains g^{-1}

Table S2.5. Phenotypic ranges (BLUEs), least significant differences (LSD, *P=0.05*), significance (*p-values*) and broad-sense heritability (H^2) for 150 HiBAP genotypes in two seasons (Y16 and Y17) and cross-year (2015-16 and 2016-17).

	Traits	Units	Y16: 2015-16					Y17: 2016-17					Y16 and Y17							P(G×Y)
			Min	Mean	Max	LSD	P(G)	Min	Mean	Max	LSD	P(G)	H^2	Min	Mean	Max	LSD	P(G)	P(Y)	
C.T	Vegetative	°C	18.7	19.5	20.7	0.80	*	18.8	19.4	20.2	0.60	***	0.67	18.9	19.4	20.1	0.49	***	*	ns
	Grain filling		20.9	22.3	24.4	1.24	***	23.5	24.3	25	0.70	***	0.61	22.4	23.3	24.3	0.74	***	*	ns
Anthesis + 7 days (GS65+7d)	DTA	DAE	71	79	89	1	***	66	75	85	2	***	0.87	68	76	85	3	***	***	***
	$AGDM_{A+7\infty}$	g m^2	605	864	1092	161	***	658	859	1017	157	***	0.60	702	861	1006	130	***	***	*
	DM Lam∞	g $shoot^{-1}$	0.46	0.64	0.91	0.12	***	0.40	0.65	0.97	0.13	***	0.86	0.46	0.64	0.92	0.10	***	ns	***
	LamPI		0.18	0.22	0.30	0.04	*	0.16	0.20	0.26	0.03	***	0.68	0.17	0.21	0.26	0.03	***	**	ns
	DM Spk∞	g $shoot^{-1}$	0.52	0.78	1.10	0.21	***	0.55	0.89	1.33	0.23	***	0.86	0.56	0.83	1.10	0.16	***	*	ns
	SPI∞		0.19	0.83	0.36	0.03	***	0.21	0.27	0.38	0.04	***	0.75	0.21	0.27	0.32	0.03	***	ns	*
	DM Stem∞	g $shoot^{-1}$	0.91	1.48	2.00	0.34	***	1.03	1.75	2.40	0.39	***	0.89	0.98	1.62	2.08	0.27	***	***	ns
	StePI		0.46	0.51	0.56	0.03	***	0.41	0.53	0.62	0.04	***	0.76	0.46	0.52	0.57	0.03	***	*	***
	GA	cm^2 $shoot^{-1}$	61.4	123.6	242.8	38.9	***	75.1	128.6	218.0	31.5	***	0.78	81.5	125.7	203.0	30.7	***	ns	*
	$DMSpk_{A+7}$	g m^{-2}	167.9	231.4	305.6	71.2	ns	154.7	248.8	391.2	92.4	*	0.48	171.4	240.1	320.7	57.8	**	ns	ns
	SpkIspk	#	19	21	25	2	***	15	19	23	2	***	0.77	17	19	24	2	***	***	***
	FE∞	grains g^{-1}	37.1	56.7	92.1	17.3	ns	37.9	60.6	92.4	17.2	***	0.73	41.5	58.7	84.2	14.0	***	ns	*
	PH	cm	81.9	98.1	115.3	6.68	***	83.9	100.9	114.8	5.20	***	0.83	84.6	99.5	114.0	6.21	***	ns	***
	LnSpk∞		8.01	12.3	15.1	1.48	***	7.79	11.6	14.6	1.11	***	0.90	7.66	12.0	14.1	1.16	***	ns	**
	LnAwns		4.45	6.20	10.3	1.27	***	4.46	6.50	11.4	0.90	***	0.80	4.53	6.34	10.1	0.98	***	ns	***
	LnPed		28.3	35.1	41.5	3.78	***	29.7	39.8	47.6	3.08	***	0.84	29.0	37.4	42.8	3.51	***	*	***
	LnInt2		14.2	19.0	23.9	2.14	***	14.1	19.8	25.0	1.57	***	0.78	14.2	19.3	23.6	2.06	***	**	***
	LnInt3		8.75	14.0	17.3	1.80	***	9.39	13.5	16.2	1.21	***	0.79	9.93	13.7	16.7	1.64	***	ns	***
Physiological maturity (GS87)	DTM	DAEs	108	118	126	3	***	102	113	123	4	***	0.85	105	115	124	3	***	***	***
	$AGDM_{PM}$	g m^{-2}	1080	1472	2001	232	***	821	1144	1424	210	***	0.51	1105	1355	1642	206	***	**	***
	GY	g m^{-2}	449	632	838	66	***	410	559	637	46	***	0.60	485	596	705	71	***	ns	***
	TGW	g	30.2	45.6	55.4	2.33	***	29.6	42.2	52.9	1.80	***	0.94	30.0	43.9	53.8	2.92	***	***	***
	HI		0.39	0.48	0.53	0.04	***	0.39	0.46	0.53	0.05	***	0.80	0.40	0.47	0.53	0.04	***	ns	*
	GN∞	grains m^{-2}	10815	13961	17689	1550	***	9860	13384	17190	1152	***	0.83	10382	13643	16669	16727	*	ns	***
	SM2	spikes m^{-2}	266	343	490	63	***	206	248	379	60	***	0.86	234	303	411	46	***	**	ns

A+7: Anthesis + 7 days; **PM:** Physiological maturity; **C.T:** Canopy temperature; **DTA:** Days from emergence to anthesis; **AGDM:** Above-ground DM; **DM Lam:** Dry weight lamina; **LamPI:** Lamina partitioning index; **DM Spk:** Dry weight spike; **SPI:** Spike partitioning index; **DM Ste:** Dry weight stem; **StePI:** Stem partitioning index; **GA:** Green area; **DMSpk:** Spike DM per unit area; **PH:** Plant height; **LnSpk:** Length spike; **LnAwns:** Length awns; **Ped:** Peduncle; **Int2:** Internode 2; **Int3:** Internode 3; **DTM:** Days from emergence to physiological maturity; **FE:** Fruiting efficiency; **GY:** Grain yield (100% DM); **TGW:** Thousand grain weight; **HI:** Harvest index; **GN:** Grains per meter square; **SM2:** Spikes per meter square

***P(G)*:** Significance of the genotype; ***P(Y)*:** Significance of the year; ***P(G×Y)*:** Significance of the genotype x environment; **H^2**: Broad-sense heritability (cross-year analysis)

**P<0.05; **P<0.01; ***P<0.001; ns: non-significant;* ∞: cross-year (Y16 and Y17) adjusted mean using DTA as covariate

Table S2.6. Phenotypic ranges (BLUEs), least significant differences (LSD, *P=0.05*), significance (*p-values*) and broad-sense heritability (H^2) for subset 1 in two seasons (Y16 and Y17) and cross-year (2015-16 and 2016-17).

	Traits			Units	Y16: 2015-16 Min	Ave	Max	LSD	P(G)	Y17: 2016-17 Min	Ave	Max	LSD	P(G)	Y16 and Y17 H^2	Min	Ave	Max	LSD	P(G)	P(Y)	P(G×Y)
Anthesis + 7days (GS65+7d)	Ped	TS	DW	g shoot^{-1}	0.193	0.30	0.41	0.12	ns	0.26	0.40	0.50	0.13	ns	0.61	0.25	0.35	0.43	0.09	***	**	ns
			PI		0.15	0.20	0.27	0.05	**	0.17	0.24	0.32	0.04	***	0.71	0.17	0.22	0.29	0.04	***	**	*
			SW	g cm^{-1}	0.005	0.009	0.011	0.003	ns	0.006	0.010	0.014	0.004	**	0.64	0.006	0.009	0.01	0.002	***	*	*
		LS	DW	g shoot^{-1}	0.12	0.22	0.29	0.05	***	0.17	0.26	0.35	0.05	***	0.85	0.16	0.24	0.31	0.04	***	*	ns
			PI		0.10	0.15	0.20	0.04	***	0.12	0.15	0.21	0.03	***	0.64	0.11	0.15	0.20	0.03	***	ns	ns
			SW	g cm^{-1}	0.003	0.006	0.008	0.001	***	0.004	0.006	0.010	0.001	***	0.85	0.004	0.006	0.009	0.001	***	ns	ns
	Int2	TS	DW	g shoot^{-1}	0.14	0.26	0.35	0.09	***	0.17	0.31	0.32	0.10	***	0.76	0.17	0.28	0.38	0.07	***	*	ns
			PI		0.14	0.17	0.22	0.02	***	0.14	0.18	0.18	0.04	ns	0.66	0.14	0.18	0.22	0.03	***	ns	ns
			SW	g cm^{-1}	0.010	0.014	0.018	0.004	**	0.009	0.02	0.02	0.004	***	0.80	0.009	0.014	0.02	0.002	***	*	ns
		LS	DW	g shoot^{-1}	0.05	0.12	0.16	0.03	***	0.08	0.13	0.13	0.04	***	0.83	0.07	0.13	0.17	0.03	***	n	ns
			PI		0.05	0.08	0.10	0.02	ns	0.06	0.08	0.08	0.02	ns	N/A	0.07	0.08	0.09	0.01	ns	ns	ns
			SW	g cm^{-1}	0.003	0.006	0.008	0.001	***	0.004	0.007	0.006	0.002	***	0.85	0.003	0.006	0.008	0.001	***	ns	ns
	Int3	TS	DW	g shoot^{-1}	0.11	0.22	0.30	0.06	***	0.11	0.24	0.24	0.06	***	0.88	0.13	0.23	0.29	0.04	***	ns	ns
			PI		0.11	0.15	0.16	0.02	***	0.12	0.14	0.14	0.03	ns	0.17	0.12	0.14	0.15	0.02	***	ns	ns
			SW	g cm^{-1}	0.011	0.016	0.020	0.003	***	0.01	0.02	0.02	0.004	***	0.82	0.01	0.02	0.02	0.003	***	ns	ns
		LS	DW	g shoot^{-1}	0.05	0.09	0.13	0.03	***	0.04	0.08	0.08	0.03	***	0.77	0.05	0.08	0.12	0.02	***	ns	ns
			PI		0.05	0.06	0.10	0.02	ns	0.03	0.05	0.05	0.02	***	0.08	0.04	0.05	0.07	0.19	ns	*	ns
			SW	g cm^{-1}	0.004	0.006	0.010	0.002	ns	0.003	0.006	0.006	0.002	***	0.50	0.004	0.006	0.008	0.002	ns	ns	ns
	Int4+		DW	g shoot^{-1}	0.12	0.29	0.46	0.13	***	0.07	0.28	0.28	0.14	***	0.88	0.09	0.29	0.42	0.09	***	ns	ns
	Int4+		PI		0.12	0.19	0.25	0.04	***	0.07	0.16	0.16	0.05	***	0.80	0.09	0.17	0.23	0.04	***	*	ns

Ped: Peduncle; **Int2:** Internode 2; **Int3:** Internode 3; **Int4+:** Internode 4+; **TS:** True-stem; **LS:** Leaf-sheath; **DW:** Dry weight; **PI:** Partitioning index; **SW:** Specific weight
***P*(Gen):** Significance of the genotype, ***P(Y)*: Significance of the year, *P*(G×Y)**: Significance of the genotype x environment, **H^2:** Broad-sense heritability (cross-year analysis)
**P<0.05; **P<0.01; ***P<0.001; ns: non-significant*

Table S2.7. Phenotypic ranges (BLUEs), least significant differences (LSD, *P=0.05*), significance (*p-values*) and broad-sense heritability (H^2) for subset 2 in two seasons (Y16 and Y17) and cross-year (2015-16 and 2016-17).

	Traits		Y16: 2015-16					Y17: 2016-17					Y16 and Y17							P(GxY)
		Units	Min	Ave	Max	LSD	P(G)	Min	Ave	Max	LSD	P(G)	H^2	Min	Ave	Max	LSD	P(G)	P(Y)	
Anthesis + 7 days (GS65+7d)	GluDW	g spk^{1}	0.09	0.13	0.18	0.05	ns	0.08	0.13	0.17	0.03	***	0.85	0.09	0.13	0.17	0.03	***	ns	ns
	GluPI		0.17	0.21	0.23	0.02	***	0.17	0.20	0.25	0.04	*	0.68	0.18	0.21	0.24	0.03	**	ns	ns
	LeDW	g spk^{1}	0.12	0.17	0.24	0.07	ns	0.14	0.20	0.23	0.04	***	0.80	0.14	0.19	0.23	0.04	***	ns	ns
	LePI		0.25	0.28	0.31	0.02	**	0.27	0.30	0.33	0.04	ns	0.77	0.26	0.29	0.31	0.02	***	*	ns
	PaDW	g spk^{1}	0.05	0.07	0.10	0.03	*	0.05	0.07	0.09	0.03	ns	0.57	0.05	0.07	0.09	0.03	*	ns	ns
	PaPI		0.08	0.11	0.13	0.02	*	0.09	0.10	0.12	0.03	ns	0	0.09	0.11	0.12	0.02	ns	ns	ns
	RaDW	g spk^{1}	0.06	0.10	0.14	0.04	**	0.06	0.10	0.13	0.02	***	0.90	0.06	0.10	0.13	0.02	***	ns	ns
	RaPI		0.13	0.16	0.19	0.02	***	0.13	0.15	0.17	0.01	***	0.95	0.13	0.15	0.18	0.01	***	*	ns
	RaSW	g cm^{-1}	0.006	0.008	0.011	0.003	ns	0.006	0.009	0.010	0.002	ns	0.71	0.007	0.008	0.010	0.002	***	ns	ns
	AwDW	g spk^{-1}	0.11	0.15	0.23	0.06	ns	0.07	0.16	0.24	0.03	***	0.81	0.10	0.15	0.22	0.05	***	ns	ns
	AwPI		0.20	0.24	0.30	0.04	***	0.17	0.24	0.30	0.04	***	0.91	0.20	0.24	0.27	0.03	***	ns	ns

Glu: Gluma; **Le:** Lemma; **Pa:** Palea; **Ra:** Rachis; **Aw:** Awns; **DW:** Dry weight; **PI:** Partitioning Index; **SW:** Specific weight

***P*(G):** Significance of the genotype; ***P(Y)*:** Significance of the year; ***P*(G×Y):** Significance of the genotype x environment; **H^2:** Broad-sense heritability (cross-year analysis)

**P<0.05; **P<0.01; ***P<0.001; ns: non-significant*

Table S2.8. Cross-year (Y16 and Y17) adjusted means obtained from comparing the different pedigree groups of the HiBAP.

	Traits	Units	1: Elite		2: Landrace		3: Synthetic		4: Synthetic+ landrace	
C.T	Vegetative	°C	19.5	A	19.3	B	19.3	B	19.2	B
	Grain filling		23.3	A	23.1	B	23.7	A	23.3	A
Anthesis + 7days (GS65+7d)	DTA	DAE	76	B	79	A	76	B	76	B
	$AGDM_{A+7}$	g m^2	1032	B	1081	A	1030	B	1034	B
	DM Lam	g $shoot^{-1}$	0.63	B	0.70	A	0.63	B	0.71	A
	LamPI		0.21	B	0.22	A	0.21	B	0.21	B
	DM Spk	g $shoot^{-1}$	0.82	B	0.87	A	0.81	B	0.88	A
	SPI		0.27	A	0.26	B	0.26	B	0.27	B
	DM Stem	g $shoot^{-1}$	1.59	B	1.71	A	1.63	B	1.72	A
	StePI		0.52	B	0.52	B	0.53	A	0.52	B
	GA	cm^2 $shoot^{-1}$	121.3	C	142.4	A	127.7	B	142.4	A
	$DMSpk_{A+7}$	g m^{-2}	258.4	A	259.8	A	254.9	A	251.7	A
	FE	grains g^{-1}	51.5	A	46.0	B	49.0	A	44.5	B
	PH	cm	98.5	D	103.3	A	100.5	C	101.7	B
	LnSpk		12.0	C	12.8	A	11.5	D	12.3	B
	LnAwns		6.34	B	6.72	A	6.22	B	6.27	B
	LnPed		36.9	C	39.3	A	38.0	B	39.0	A
	LnInt2		19.4	A	19.0	B	19.5	A	19.3	AB
	LnInt3		13.6	C	14.0	AB	13.8	BC	14.1	A
Physiological maturity (GS87)	DTM	DAE	115	B	117	A	114	C	114	C
	$AGDM_{PM}$	g m^{-2}	1346	B	1394	A	1371	AB	1389	A
	GY	g m^{-2}	596	A	592	A	593	A	591	A
	TGW	g	42.6	C	45.7	B	45.6	B	48.2	A
	HI		0.47	A	0.45	C	0.46	B	0.46	B
	GN	grains m^{-2}	14046	A	13117	B	13062	B	12287	B
	SM2	spikes m^{-2}	307.3	A	287.7	B	301.5	A	283.5	B

A+7: Seven days after anthesis; **PM:** Physiological Maturity; **DTA:** Days from emergence to seven days after anthesis; **AGDM:** Above-ground DM; **LamPI:** Lamina Partitioning Index; **SPI:** Spike Partitioning Index; **StePI:** Stem Partitioning Index; **DMSpk:** DM Spike per unit area; **DTM:** Days from emergence to physiological maturity; **FE:** Fruiting Efficiency; **GY:** Grain Yield; **TGW:** Thousand Grain Weight; **HI:** Harvest Index; **GN:** Grain Number; **SM2:** Spikes per unit area

Means followed by the same letter are not significantly different (*P<0.05*) according to pairwise t tests.

Figure S2.5. Biplot for traits measured at GS65+7d (SPI: Spike Partitioning Index, FE: Fruiting Efficiency, $DMSpk_{A+7}$: DM spike per unit area) and physiological maturity (GY: Grain Yield, HI: Harvest Index, GN: Grain Number, SM2: Spikes per unit area) for subset 1 (29 genotypes). Values based on means of Y16 and Y17.
** For abbreviation meaning see table Table S2.6

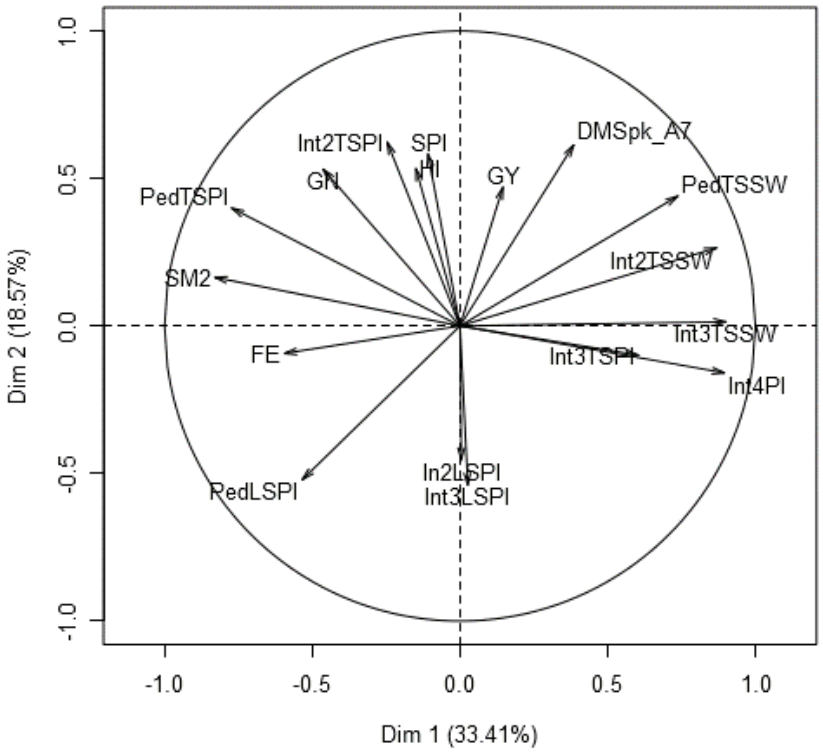
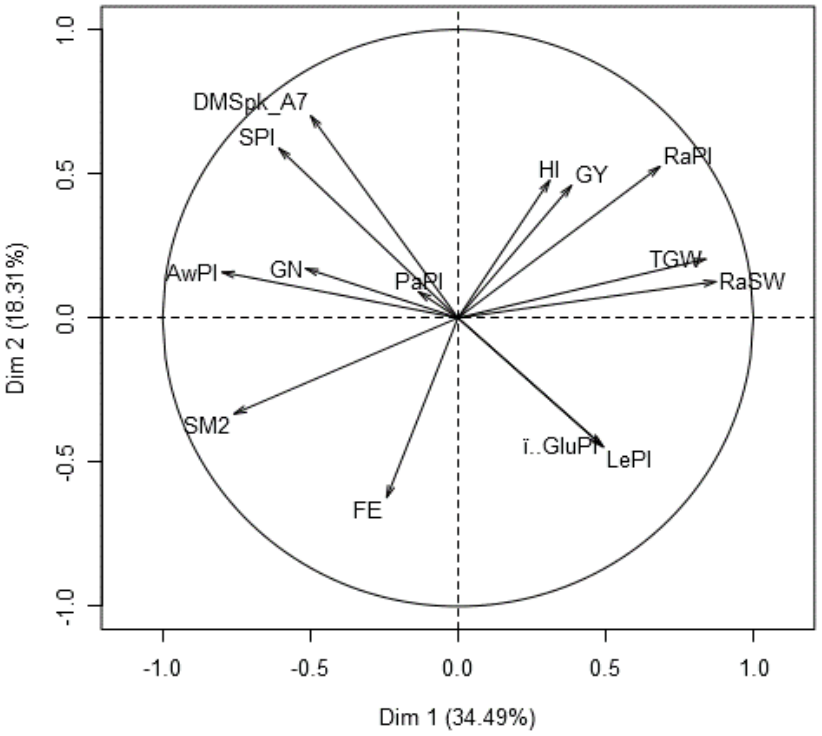


Figure S2.6. Biplot for traits measured at GS65+7d (SPI: Spike Partitioning Index, FE: Fruiting Efficiency, $DMSpk_{A+7}$: DM spike per unit area) and physiological maturity (GY: Grain Yield, HI: Harvest Index, GN: Grain Number, SM2: Spikes per unit area) for subset 2 (14 genotypes). Values based on means of Y16 and Y17.
** For abbreviation meaning see table Table S2.7



3. Enhancing dry matter partitioning to increase yield, grain number and harvest index in a doubled haploid winter wheat population

Understanding physiological traits and genetic gains to raise wheat yield potential have been critical that is why the necessity to understand how to raise grain yield considering the different environmental challenges and limitations that growing this cultivar is facing nowadays. Using a doubled-haploid (DH) winter wheat population with parents characterized as having moderate/high (Rialto) and high (Savannah) biomass production (**SxR DH**), grain partitioning traits were studied to identify avenues to boost harvest index (HI) and yield potential.

Averaging across seasons at physiological maturity grain yield (GY) ranged from 676 to 921 g m^{-2} (*P<0.001*), above-ground dry matter ($AGDM_{PM}$) from 1,443 to 1,941 g m^{-2} (*P<0.001*) and harvest index (HI) from 0.41 to 0.53 (*P<0.001*). Grain yield among genotypes was positively associated with AGDM (more strongly at PM than GS65+7d), grain number per area (GN), HI, plant height (PH) and fruiting efficiency (FE).

In both years, genetic variation was found for traits measured at GS65+7d with overall above-ground dry matter ($AGDM_{A+7}$) ranging from 1,654 to 2,779 g m^{-2} (*P<0.05*) and fruiting efficiency (FE) from 33 to 71.9 grains g^{-1} (*P<0.05*). Stem-internode lengths (peduncle, internode 2 and internode 3) were negatively associated with spike partitioning index (SPI) at GS65+7d (*P<0.001*), most strongly with internode 3 (int3), but were positively associated with stem internode partitioning (StePI) (*P<0.001*) and dry matter of spike at GS65+7d ($DMSpk_{A+7}$) (*P<0.001*). For lamina partitioning index (LamPI) weak negative associations were recorded with internode 2 and 3 lengths (*P<0.05*) but no relation was found with peduncle length.

Within spike DM partitioning analysis showed the following pattern for dry matter accumulation per spike: lemma > glume > rachis > palea. These results suggested that further increases in spike fertility could be obtained decreasing dry matter partitioning to the rachis.

To exploit future genetic gains in biomass, selection for these traits in wheat breeding will potentially allow breeders to maximize HI enhancing yield potential with the stable production of AGDM.

**This chapter will be submitted to a high impact journal, where authors contributed equally to the work presented.

Aleyda Sierra-Gonzalez[ab], Gemma Molero[b], Carolina Rivera-Amado[b], Matthew Reynolds[b] and John Foulkes[a]

[a]*Division of Plant and Crop Sciences, School of Biosciences, University of Nottingham, Leicestershire, LE12 5RD, UK*

[b]*CIMMYT International Maize and Wheat Improvement Center (CIMMYT), Km. 45, Carretera Mexico, El Batan, Texcoco, Mexico*

3.1. Introduction

Wheat has the second-highest cereal grain production, after maize, and its global production is forecast at 725.1 million tonnes for 2018/19 (FAO, 2018). Significant yield improvement was achieved at the Green Revolution as a result of the introduction of *Rht* (Reduced height) genes and rye translocation (Zhou et al., 2007), which resulted from a higher grain number per unit area (GN). Currently, genetic gains in yield worldwide are 0.5 to 1% per annum (Reynolds et al., 2017) and by 2050 population growth could reach between 9.3 and 10 billion people increasing the demand for wheat grain to at least 1.6% year (Peña-Bautista et al., 2017). However, yield rates of modern wheat varieties have decreased (Ho, 1988; Philipp et al., 2018; Rivera-Amado et al., 2019) or even in some countries reached a plateau (Rose et al., 2017). New breeding strategies need to be implemented to satisfy the demand for wheat grain production considering consequences of global warming (temperature rise, water availability, diseases) which could influence wheat development and as well genetic variability. To achieve this, scientists and breeders need to target those traits that are limiting yield potential by understanding better the physiological and genetic bases of biomass and grain partitioning (Leng & Hall, 2019).

3.1.1. Biomass and grain production

Crop productivity is related to the capacity that the plant has to accumulate biomass and then partition to the grains (Giunta et al., 2009). Biomass assimilation is the final product over the entire growing season where strong consistent positive associations have been found between this trait and grain yield. Using elite red winter wheat under varying water regimes, Thapa et al. (2019) reported that maintaining higher biomass production is essential for higher yield in a semi-arid environment. Optimum assimilation and distribution among plant organs could maximize yield potential as this is the result of compensating actions between i) number of spikes per unit area (SM2), ii) number of grains per unit area (GN) and grain weight (Arduini et al., 2006).

The introduction of semi-dwarf cultivars (genotypes carrying *Rht* genes, mainly from the cultivar Norin 10) into breeding programs provided a significant yield boost as more assimilates were available into sink organs increasing spike fertility (Webb et al., 1998). As a result of improved varieties, positive associations were found between year of release and plant above-ground DM production, on UK cultivars introduced from 1908 to 1986 Austin et al. (1989) found that harvest index was positively associated with yield progress, with only a slight non-significant increase in above-ground dry matter (AGDM) at harvest. For Chilean varieties released during the last decade, Lo Valvo et al. (2018) reported that increases in harvest index were proportionally higher than above-ground biomass, determining positive genetic gains in GY. Harvest index (HI: grain dry-matter / above-ground DM) has been widely reported to be associated with grain yield, as this trait indicates the efficiency of assimilate distribution to the grain (Fan et al., 2017; Zhang et al., 2012). Different values have been

reported for this trait, higher on winter wheat (0.61) than in spring wheat (0.51) (Dai et al., 2016; Rivera-Amado et al., 2019). For wheat, there is a hypothetical limit for HI of approximately 0.62 (Austin, 1980). Foulkes et al. (2011) assuming a further 10% in above-ground DM and a ratio of chaff to grain of 175 mg chaff grain^{-1} (estimated), harvest index could increase to 0.64 (winter wheat).

There is evidence that grain sink strength remains the critical yield-limiting factor under favorable conditions and that sink capacity will need to be improved (Foulkes et al., 2011); in modern wheat genotypes, it has been reported that grain number is the main responsible for increases in yield potential. On winter wheat cultivars Shearman et al. (2005) concluded that increases in grain yield (GY) were mainly due to more dry matter accumulation in the pre-anthesis phase and at harvest resulting in increments on the number of grain per unit area. Using 1850 Chinese winter wheat varieties, Qin et al. (2015) proposed that breeding efforts should focus on increasing grain size and grain number per spike without changing spike number per unit area, concluding that there is still scope to improve grain weight and grain number per spike. Grain number production is related to the assimilate available during floret survival from booting to anthesis while grain weight (TGW) depends on the photosynthetic sources available during grain filling period (García et al., 2014; Peltonen-Sainio et al., 2007). Due to the ability that grain number has to adapt to the environment (carbon and nitrogen accumulation), this trait could be increased through increasing the proportion of AGDM partitioned to the spike (SPI: spike DM / AGDM at anthesis) or the ratio of grains to spike DM at anthesis, known as the fruiting efficiency (FE: grains g^{-1}) (Slafer et al. 2015) (Equation 3.1):

$$GN = AGDM \times SPI \times FE \qquad [3.1]$$

where GN is the number of grain (per unit area basis); AGDM is the above-ground DM (per unit area); SPI is the ratio between the spike DM and the AGDM and FE is the number of grains per unit spike DM at anthesis.

Preferential allocation of assimilates to florets than to structural parts of the spike could increase fruiting efficiency (Garcia et al., 2014). Observed fruiting efficiency values in nine elite-modern wheat experiment, Elía et al. (2016) found that higher values were obtained where spike dry-matter weight was determined at anthesis rather than after leading to underestimation due to the initial growth of the grains. The causal relationship between grain number and spike dry-matter at anthesis is due to assimilates available for spike growth, as more resources become available at spike level the number of fertile florets will increase (Elía et al., 2016; Ferrante et al., 2017). Selecting for genotypes that allocate more resources towards florets could reduce the rate of floret primordia mortality (Garcia et al., 2019).

3.1.2. Enhancing pre-anthesis growth and grain number

The distribution of assimilates varies among organs been the stem the organ which more dry matter is partitioned (0.32 to 0.41), followed by the spike (0.21 to 0.26), then lastly leaf-lamina (0.18 to 0.23) and lastly leaf sheath (0.16 to 0.20) (Rivera-Amado et al., 2019). Stem elongation development (late reproductive phase) coincides with the onset of the rapid growth of stems and spikes resulting in competition for assimilates between them, determining the magnitude of floret mortality and hence the final number of floret primordia that will be fertile at anthesis (González et al., 2003). If competition for assimilates determines the grain number, it can be expected to correlate positively with spike DM and negatively with stem DM, or at least with the corresponding growth rates at the critical time of floret death (Bancal, 2008).

Increased assimilate partitioning to developing spikes and grains has historically had the most significant impact on improving yield potential in wheat during the past, which increased the harvest index (Philipp et al., 2018). Under optimal conditions (water, nutrients and radiation level) in Argentinian wheat cultivars, Abbate et al. (1997) stated that during the spike growth period the genetic variation in grain number is mainly determined by dry-matter partitioned to the spikes at anthesis. Similar findings were reported by Duan et al. (2018), in a winter wheat population in China, where the variation found among weight in spike and spike dry matter per unit area showed a significantly positive relationship with grain number from booting to anthesis.

The size of photosynthetic organs is an essential factor determining the extent of pre-anthesis growth, which strongly influences sink organs (Chen et al., 2019). Results from Argentina wheat cultivars, Buck Manantial and Eureka Ferrocarril Sur, showed an increase of DM partitioning to the spike at anthesis when the stem-elongation phase was lengthened by short photoperiod (Gonzalez et al., 2003). Increasing the amount of assimilates during mid-to-late stem extension increases the grain number per unit area; as a result, satisfying the potential growth of all organs (sinks) and reducing the stem and spike assimilate competition (Berry et al., 2003). Using a spring wheat population García et al. (2011) showed that grain yield per plant was higher when the duration of stem elongation phase was longer, due to improvement in floret primordia survival and grain number increases. In contrast, González-Navarro et al. (2016) found that there was no relation between the length of the stem elongation phase and spike dry weight at anthesis.

Another strategy to increase grain number is optimizing the distribution of dry-matter between the different stem internodes that made-up the stem. The internodes are the hollow parts of stems, mainly surrounded by leaf sheath, situated between nodes that reach their maximum length few days after anthesis (Cruz-Aguado et al., 2000). Upper internodes (those near the spike) segments have more influence on single-spike weight than basal internodes (Chen et al., 2019). The two upper internodes are only partially enclosed by the flag-leaf sheath and thus partly exposed to a high irradiance (Gebbing, 2003). This suggests that the peduncle

could be the primary source of stem photosynthesis assimilates for grain filling. The two basal internodes are reported to act as the most critical stem storage (source organs) supporting grain filling storing enough structural carbohydrates to support the development of the plant (Scofield et al., 2009). Using high biomass spring wheat genotypes, Rivera-Amado et al. (2019) concluded that decreased length of stem internodes 2 and 3 was correlated with increased spike partitioning index.

In this chapter the aim was to identify partitioning traits to increase grain number per unit area (GN), harvest index (HI) and grain yield (GY) in high biomass backgrounds using a UK winter wheat double-haploid population derived from a cross between Rialto (moderate/high yield potential) and Savannah (high yield potential). Field experiments were carried out over two seasons at University of Nottingham farm, Sutton Bonington campus (Leicestershire, U.K) under rain-fed conditions evaluating biomass and DM partitioning traits at GS65+7d and harvest and quantifying associations with HI and grain yield.

Chapter hypotheses:

- Genotypes with high above-ground dry matter (AGDM) will result in high potential yield but with low harvest index (HI).
- Grain number is determined by (i) the amount of above-ground dry matter at GS65+7d and/or (ii) percentage of dry matter partitioned to the spike
- There is a negative association found between grains m^{-2} (GN) and thousand-grain weight (TGW), genotypes with high yield tend to be more associated with GN rather than TGW.
- Relative stem-internode lengths are associated with spike partitioning index (SPI), DM of spike per unit area ($DMSpk_{A+7}$) influencing HI.
- Fruiting efficiency (FE) is associated with GN and determined by spike morphology partitioning (palea, lemma, glume, and rachis) at GS65+7d.

3.2. Materials and methods

3.2.1. Plant material and experimental design

The experiment was carried out over two seasons (Y16: 2015-16 and Y17: 2016-17) under rain-fed conditions using a randomized complete block design with two replicates at The University of Nottingham campus Sutton Bonington, Leicestershire, UK (52° 50' N, 1° 15' W). A Savannah x Rialto doubled-haploid population (**SxR DH**) comprised of 94 winter wheat lines derived from the F_1 between UK winter wheat parents Savannah and Rialto, which are UK semi-dwarf (*Rht-D1b*, formerly *Rht-2*), hard endosperm cultivars (Table S3.1). Rialto (RAGT seeds Ltd; Haven x Fresco) was first released in 1995 and is a high yield potential genotype with some potential for bread-making processes. Savannah (Limagrain UK Ltd; Riband x Brigadier) was first released in 1998 and is a high yielding feed wheat cultivar (Wilkinson et al., 2012). This population was used due to previous results showing high phenotypic expression and genetic variation in stay-green traits and in yield under drought and nitrogen stress in field

experiments in the UK and France (Atkinson et al., 2015). In both seasons, the experiment was sown in 1.625 x 6.0 m plots (Figure S3.1) using a seed rate of 350 seeds per m^2; the previous crop was winter oilseed rape for both years. In the first season (Y15-16) the trial was sown on 1 October 2015 and in the second season (Y16-17) on 19 October 2016 (Figure S3.2). Herbicides, fungicides, insecticides, fertilisers and plant growth regulators were applied to minimise the effects of weeds, diseases, pests and lodging (Table S3.2).

Weather means for temperature, accumulated rainfall and solar radiation were calculated for both seasons during booting (GS41-GS49), anthesis (GS59-GS69) and grain filling (GS71-GS91) stages (Table S3.2).

3.2.2. Crop measurements

Sampling and crop development

Samples were collected seven days after anthesis (GS65+7d) and at physiological maturity (PM, shoots with yellow-green peduncle, GS87) (Zadoks et al., 1974). The stages were taken as when 50% of the fertile shoots in the plot had reached the stage.

Biomass and dry matter partitioning at GS65+7d

At GS65+7d in both replicates, 10 randomly selected fertile shoots (those with a spike) were cut at ground level avoiding edge effects (at least 50 cm from side and ends of the plot). Green leaf area was determined on fresh material separating the leaf lamina from the stem and leaf sheath (all leaf lamina were bulked) using a planimeter (LI-3100C Area Meter: LiCOR, Lincoln). For the plant dry matter partitioning analysis (PI: Partitioning Index, ratio between component dry-matter and above-ground dry matter) this was done by separating each plant component into (i) spike, ii) leaf lamina and iii) stem (true stem+leaf sheath). The material for each plant component was dried for 48 h at 70°C and dry weight was recorded. Additionally, the lengths of each stem internode: i) peduncle, ii) internode 2 (internode below peduncle) and iii) internode 3 were recorded with a ruler (Figure 3.1).



Figure 3.1. Measurement of morphological characteristics (stem internode, flag leaf and spike length), on SxR DH shoots collected at seven days after anthesis (GS65+7d).

For 21 lines, parents were considered, (subset1; Table S3.1) selected to be representative of genetic variation of spike dry-matter partitioning in the panel the 12 shoots sampled at GS65+7d were further separated into true-stem (TS) and leaf sheath (LS) for each internode: peduncle (ped), internode 2 (int2), internode 3 (int3) and internode 4 and below (int4+). The dry weights were recorded for each component after oven drying at 70°C for 48 h. Finally, for 12, parents were considered, of the 21 genotypes (subset2; Table S2.1), the 12 spikes sampled at GS65+7d were dissected into: i) glume, ii) lemma, iii) palea, and iv) rachis. The different spike components were bulked for the 12 spikes and weighed separately after drying at 70°C for 48 h. For every internode and rachis specific weight (SW: linear density, phytomere and/or rachis DM per unit length) was calculated at this stage.

Plant and spike length measurements at post-anthesis

Plant height and spike length were measured in two replicates on seven shoots per genotype at the beginning of the grain-filling period. Plant height was measured from soil surface to the tip of the spike and spike length from the spike collar to the tip of the terminal spikelet.

Physiological maturity, grain yield and yield components

At physiological maturity (PM) in both replicates, approximately 75 fertile shoots were randomly selected and cut at ground level per plot avoiding edge effects (at least 50 cm from side and ends of the plot) and fresh weight (FW) of the total sample was measured. From the first shoot sample, a subsample was taken (20% of FW recorded), from which the leaf lamina (leaf sheath included) and spikes were separated from the stem and dry weight for each plant component was recorded after drying at 70 °C for 48 h. From the spikes collected on the subsample these were machine-threshed (Haldrup LT-20, Havnevej) in order to determine thousand-grain weight (TGW) by counting the grains using a seed counter (Pfeuffer contador, Kitzingen). After sampling, the plots were machine-harvested in a plot area of ~6 m^{-2}, and grain weight adjusted to 100% DM. From the data obtained spikes m^{-2} (SM2), grains m^{-2} (GN), harvest index (HI), final AGDM per unit area and fruiting efficiency (FE) were calculated (Table S2.4).

3.2.3. Statistical analysis

Statistical analysis (adjusted means, ANOVA, regression analysis and heritability) of phenotypic data was carried out using a randomized complete block design using the program MetaR, Windows R code-based platform program. For the combined analyses (cross-year means), the heritability was calculated as (Equation 3.2):

$$\mathbf{h^2} = \frac{\mathbf{\sigma^2 g}}{\frac{(\mathbf{\sigma^2 g + \sigma^2 ge})}{\mathbf{nlocs} + \mathbf{\sigma^2 e}}(\mathbf{nlocs})(\mathbf{nreps})} \quad [3.2]$$

where σg^2 and σe^2 are the genotype and error variance components, respectively, nreps is the number of replicates, σge^2 is the genotype × environment interaction variance component and nlocs is the number of locations in the analysis (Alvarado et al., 2015; Vargas et al., 2013).

For each trait, ANOVA and BLUEs (Best Linear Unbiased Estimator) were calculated for genotypes considering genotype as a fixed effect and replicates as a random effect. Combined analysis of variance across experiments (cross-year) was done considering genotypes and years as random effects.

GenStat 17th edition (VSN International) was used for calculating the Pearson's correlation coefficients, linear/non-linear regressions and stepwise multiple linear regressions between traits using the BLUEs obtained with MetaR. For the stepwise linear regression, where the variable selected to be explained was the dependent variable, and the variables tested in the model acted as independent variables

3.3. Results

Taking into account field data of two seasons (Y16: 2015-16 and Y17: 2016-17) significant genetic variation was found for grain partitioning related traits measured seven days after anthesis (GS65+7d) and at physiological maturity (GS87) (Table S3.3). Cross-year analysis reported significant phenotypic variation, where the genotypic effect (G) was significant for most of the traits while the year (Y) or G × Y significances were variable among traits measured. For this analysis (Table 3.1) 96 lines were included, with missing values entered for those genotypes omitted for Y16. Just in year Y16 (Table S3.1) only 90 genotypes were included as six DH lines which incurred flat lodging with low values for HI (0.23-0.32) were omitted from the analysis. Similarly, for the subsets of lines where detailed stem internode (Table S3.4) and spike morphology (Table S3.5) DM partitioning traits were measured. Regression and correlations analysis between traits measured showed interesting results which will benefit new venues to increase yield potential.

Table 3.1. Phenotypic ranges and means for 94 DH lines, least significant differences (LSD, *P=0.05*), significance (*p-values*) and broad-sense heritability (H^2) for SxR DH population. Values represent means of Y16 and Y17.

	Traits		***Y16 and Y17***									
		Units	**H^2**	**Min**	**Mean**	**Max**	**LSD**	***P(G)***	***P(Y)***	***P(G×Y)***	***Savannah***	***Rialto***
Anthesis + 7days (GS65+7d)	DTA	DAE	0.27	246	250	254	5	***	***	***	253	249
	$AGDM_{A+7}$	g m^2	0.26	1577	1986	2250	587	*	*	ns	1890	2477
	LamPI		0.25	0.15	0.17	0.19	0.02	*	ns	ns	0.14	0.18
	SPI		0.31	0.19	0.25	0.33	0.07	***	ns	***	0.31	0.20
	StePI		0.45	0.52	0.59	0.64	0.06	***	*	***	0.54	0.63
	$DMSpk_{A+7}$	g m^{-2}	0.12	369.6	540.9	743.6	233.2	ns	ns	ns	598.9	487.9
	FE	grains g^{-1}	0.25	30.8	44.7	68.0	17.4	*	*	**	35.3	49.6
Physiological maturity (GS87)	DTM	DAE	0.19	283	287	291	4.88	***	***	***	289	287
	$AGDM_{PM}$	g m^{-2}	0.35	1981	2151	2779	332	**	ns	ns	1794	2184
	GY	g m^{-2}	0.43	607	805	921	131	***	ns	***	834	892
	TGW	g	0.63	30.2	36.1	42.0	4.65	***	***	**	40.5	36.7
	HI		0.47	0.36	0.41	0.46	0.04	***	ns	ns	0.47	0.41
	GN	grains m^{-2}	0.64	16058	22723	28062	4141	***	ns	*	21092	24416
	SM2	spikes m^{-2}	0.44	412	557	733	138	***	ns	ns	470	570

A+7: Anthesis + 7 days; **PM:** Physiological Maturity; **DTA**: Days from Emergence to Anthesis; **AGDM**: Above-Ground Dry Biomass; **LamPI**: Lamina Partitioning Index; **DMSpk**: Spike DM at A+7d per unit area; **SPI**: Spike Partitioning Index; **StePI**: Stem Partitioning Index; **DTM**: Days from Emergence to Physiological Maturity; **FE**: Fruiting Efficiency; **GY**: Grain Yield (100% DM); **TGW**: Thousand Grain Weight; **HI**: Harvest Index; **GN**: Grains per meter square; **SM2**: Spikes per meter square

P(G): Significance of the genotype; ***P(Y):*** Significance of the year; ***P(G×Y):*** Significance of the genotype x environment; **H^2:** Broad-sense heritability (cross-year analysis)

**P<0.05; P<0.01; P<0.001; ns: non-significant*

3.3.1. Crop development

Averaging over seasons, date of anthesis (DTA) ranged amongst DH lines from 246 to 254 days after emergence (DAE) and date of physiological maturity (DTM) from 283 to 291 DAE. For this population parents showed similar DTA, Rialto at 249 and Savannah at 253 DAE and similarly for DTM at 287 and 289 DAE, respectively (Table 3.1). No genotypes showed transgressive segregation for DTA or DTM.

3.3.2. Grain yield and yield components

Averaging over two seasons, grain yield (GY) ranged from 676 to 921 g m^{-2} (*P<0.001*), with Rialto as the higher yield parent with 892 g m^{-2} compared with Savannah at 834 g m^{-2}. Genetic variation among DH lines for above-ground DM ($AGDM_{PM}$) was from 1443 to 1941 g m^{-2} (*P<0.01*) where Savannah produced 1606 g m^{-2} and Rialto 1686 g m^{-2}. For harvest index (HI) DH lines varied from 0.41 to 0.53 (*P<0.01*) where Savannah had higher HI (0.51) than Rialto (0.48). Grains per unit area (GN) varied from 18,807 to 28,061 (*P<0.01*) where Rialto overall produced more grains m^{-2} (28,021) than Savannah (23,963). Spike density (SM2) ranged amongst DH lines from 394 to 680 m^{-2}, with Rialto producing more (628 m^{-2}) than Savannah (513 m^{-2}). For the above-mentioned traits, just one genotype showed positive transgressive segregation (significantly greater than both parents) for SM2 (line 76: 780 spikes per m^2).

For the cross-year means, a strong positive linear relation was observed amongst the DH lines between grain yield (GY) and above-ground DM at this stage ($AGDM_{PM}$) (Figure 3.2a), same scenario presented between GY and harvest index (HI) (Figure 3.2b); differently to what was found between GY and thousand-grain weight (TGW) as between this traits no relation was found (Figure 3.2c). On the other hand, grain yield (GY) was highly associated with grain number per unit area (GN) (Figure 3.2d) contrasting to the negative relation recorded among the number of grains (GN) and weight (TGW) (Figure 3.2e) and the no relation found between GN and plant height (PH) (Figure 3.2f).

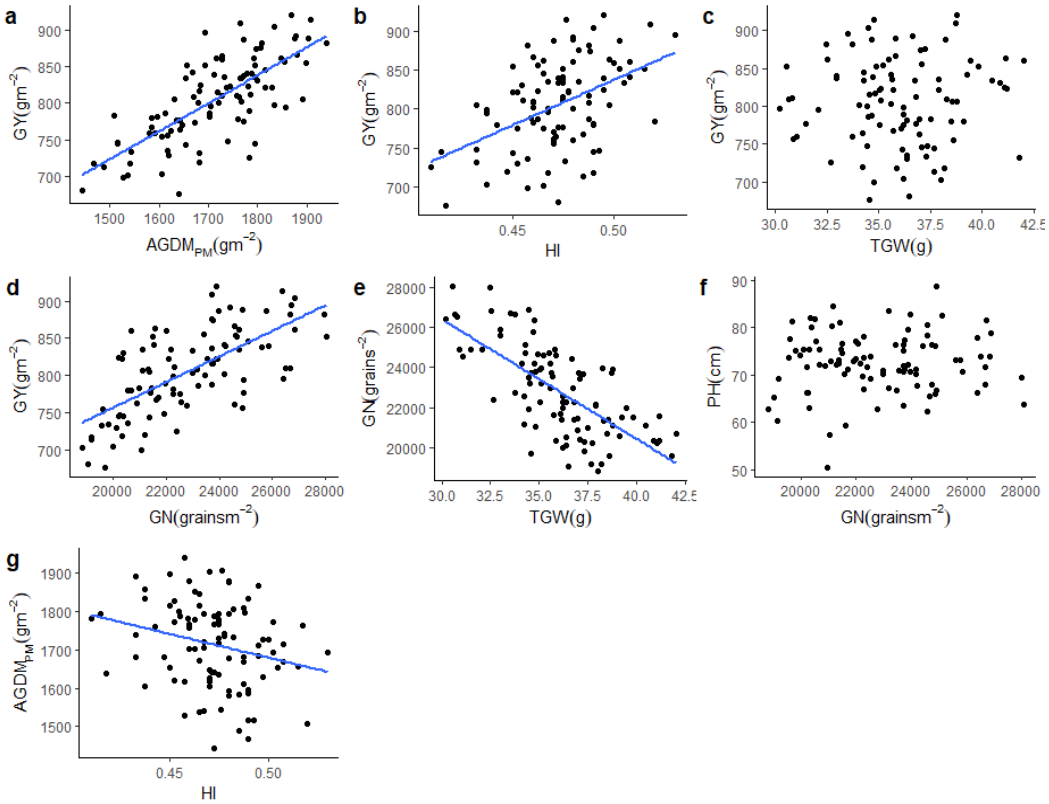


Figure 3.2. Linear regressions amongst 94 SxR DH lines (parents were excluded from the linear regression analysis) between physiological maturity traits:
a) Grain yield (GY) (100% DM) on above-ground DM at physiological maturity ($AGDM_{PM}$ y=0.33x+145.8, R^2=*0.59****
b) GY on HI: y=1348x+256.0, R^2=*0.18****
c) GY on thousand grain weight (TGW): y=-0.32x+815.2, R^2=*0.0002ns*
d) GY on grains m^{-2} (GN): y=0.02x+409.3, R^2=*0.49****
e) GN on TGW: y=-656.6x+46388, R^2=*0.51****
f) Plant height (PH) on GN: y=0.0006x+71.1, R^2=*0.005ns*
g) HI on $AGDM_{PM}$: y=-1729x+2688, R^2=*0.06**
**P<0.05*, ***P<0.01*, ****P<0.001*, *ns; non-significant*
Values presented are cross-year means (Y16 and Y17)

3.3.3. Biomass, DM partitioning and stem internode lengths at GS65+7d

Above-ground dry matter ($AGDM_{A+7}$) at GS65+7d ranged among DH lines over seasons from 1654 to 2779 g m^{-2} (*P<0.05*) where Rialto tended to produce more $AGDM_{A+7}$ at 2477 g m^{-2} than Savannah at 1890 g m^{-2}. Fruiting efficiency (FE) varied from 33.0 to 71.9 grains g^{-1} (*P<0.01*); contrasting values observed for Rialto and Savannah of 51.9 and 35.3 grains g^{-1}, respectively. For this trait, one line (46) had greater FE than both parents (71.9 grains g^{-1}). Genetic variation was found for the plant component partitioning indices (PI) been the stem the organ which accounted for the highest proportion of AGDM ranging amongst DH lines from 0.52 to 0.64 (*P<0.001*), followed by the spike from 0.19 to 0.33 (*P<0.001*) and leaf lamina from 0.15 to 0.19 (*P<0.05;* Table 3.1).

Plant height, stem-internode lengths and spike length were measured at GS65+7d (Figure 3.3); for stem internodes, the peduncle was the longest, then internode 2 and lastly internode 3. Plant height for Rialto was four centimeters greater than Savannah, for this trait two genotypes (lines: 12 and 88) showed significantly increased height compared to the parents (>83.2 cm). For the peduncle, Savannah was longer (23.1 cm) than Rialto (21.6 cm), and one genotype (line 25: 32.5 cm) showed significant positive transgressive segregation. For internodes 2 and 3 variation was not found between parents (15-16 cm for internode 2 and 11-12 cm for internode 3), but eight genotypes showed significantly higher values for both internode lengths than the two parents (>18.3 cm and >13.3 cm, respectively). For the spike length parents did not differ at 12 cm.

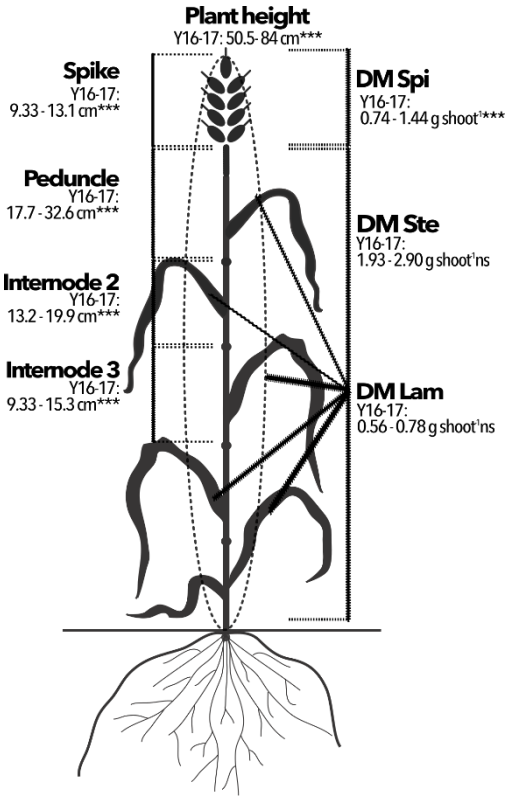


Figure 3.3. Genetic ranges from SxR DH genotypes for DM per $shoot^{-1}$ at GS65+7d (right) for spike (SPI), lamina (Lam) and stem (Ste) and spike and stem-internode lengths (left).
**P<0.05, **P<0.01, ***P<0.001, ns: non-significant*
Values presented are cross-year means (Y16 and Y17)

For the 94 DH lines, stem-internode lengths were related to the plant component partitioning indices (PI) where lengths of peduncle (LPed), internode 2 (LInt2) and internode 3 (LInt3) were linearly negatively associated with SPI (Figure 3.4a, d and g) but positively with StePI (Figure 3.4b, e and h) and for LamPI a weak negative on internode 2 and internode 3 or non-significant association among length of peduncle was found (Figure 3.4c, f and i).

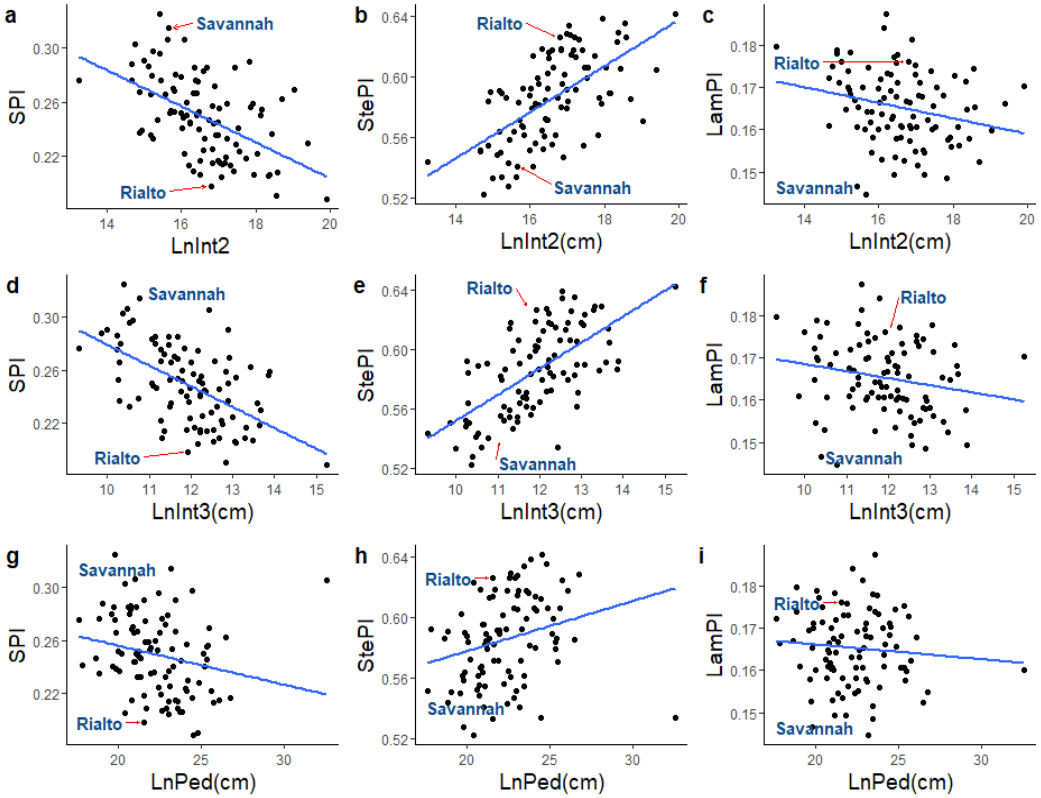


Figure 3.4. Linear regressions amongst the SxR DH population (parents were excluded from the linear regression analysis) between traits measured at GS65+7d:
a) Spike partitioning index (SPI) on stem (true stem + leaf sheath) internode 2 length (LnInt2): y=-0.01x+0.46, R^2=*0.27****
b) Stem partitioning index (StePI) on LnInt2: y=0.01x+0.34, R^2=*0.37****
c) Lamina partitioning index (LamPI) on LnInt2: y=-0.002x+0.20, R^2=*0.08**
d) SPI on stem internode 3 length (LnInt3): y=-0.02x+0.43, R^2=*0.30****
e) StePI on LnInt3: y=0.02x+0.38, R^2=*0.40****
f) LamPI on LnInt3: y=-0.0002x+0.19, R^2=*0.06**
g) SPI on peduncle length (LnPed): y =-0.003x+0.32, R^2=*0.06**
h) StePI on LnPed: y=0.003x+0.51, R^2=*0.08***
i) LamPI on LnPed: y=-0.0003x+0.17, R^2=*0.006ns*
**P<0.05, **P<0.01, ***P<0.001, ns: non-significant*
Values presented are cross-year means (Y16 and Y17)

3.3.4. Internode DM partitioning

For the 19 genotypes selected for subset 1 (Table S3.1) where detailed DM stem-partitioning traits were measured at GS65+7d (Table 3.2), genetic variation among was found for most of the traits measured except for int2LSPI and int3LSPI. True-stem (TS) accumulated more DM than leaf sheath (LS) PI following the specific DM PIs order of: int4+ > int2TS > int3TS > pedTS >pedLS > int2LS > int3LS. Stem-internode DM growth depends on the internode length and also the amount of DM per unit length (specific weight: g cm^{-1}), no genetic variation or GxY was found for TS internode SWs, although variation between years was recorded for int2TS (*P<0.05*) and int3TS (*P<0.001*). Basal stem internodes had greater SW than those near the spike: int3TSSW > int2TSSW > pedTSSW. For leaf-sheath SWs less variation was observed; pedLSSW was slightly higher than internode 2 and 3 LSSWs (Table 3.2; Figure S3.4).

Table 3.2. Cross-year genetic ranges (Min: Minimum, Mean, Max: Maximum), broad-sense heritability (H^2), and significance values for 19 SxR DH lines (subset 1) and parents (G), year (Y) and genotype x year (GxY) for true-stem (TS) and leaf-sheath (LS) DM partitioning indices (PI) and specific weight (SW). Values presented are cross-year means (Y16 and Y17).

Traits	Units	H^2	Min	Mean	Max	*P(G)*	*P(Y)*	*P(G×Y)*	*Savannah*	*Rialto*
PedTSPI		0.70	0.06	0.12	0.03	***	**	ns	0.06	0.06
Int2TSPI		0.77	0.06	0.09	0.02	***	*	ns	0.09	0.09
Int3TSPI		0.70	0.05	0.07	0.09	***	ns	*	0.08	0.09
PedLSPI		0.65	0.06	0.08	0.10	***	ns	ns	0.05	0.06
Int2LSPI		0.18	0.03	0.04	0.05	ns	ns	ns	0.04	0.05
Int3LSPI		0.25	0.02	0.03	0.04	ns	*	*	0.03	0.03
Int4+PI		0.79	0.11	0.20	0.28	***	ns	ns	0.17	0.25
PedTSSW		0.30	0.008	0.011	0.013	ns	ns	ns	0.013	0.013
Int2TSSW	g cm^{-1}	0.58	0.017	0.020	0.025	ns	*	ns	0.020	0.022
Int3TSSW		0.09	0.018	0.024	0.029	ns	***	ns	0.024	0.028

Ped: Peduncle; **Int2:** Internode 2; **Int3:** Internode 3; **Int4+:** Internode 4+; **TS:** True-stem; **LS:** Leaf-sheath; **DW:** Dry weight; **PI:** Partitioning index; **SW:** Specific weight

*P<0.05; **P<0.01; ***P<0.001; *ns: non-significant*

A highly significant linear relationship was found between stem-internode length and the respective TS DM per shoot[1] (Figure 3.5a) and specific weight (Figure 3.5b). On the other hand, there was no significant relation between the TS SW and internode length for any internode (Figure 3.5c); similarly to stem-internode PIs were not associated with spikes per unit area (Figure 3.5d).

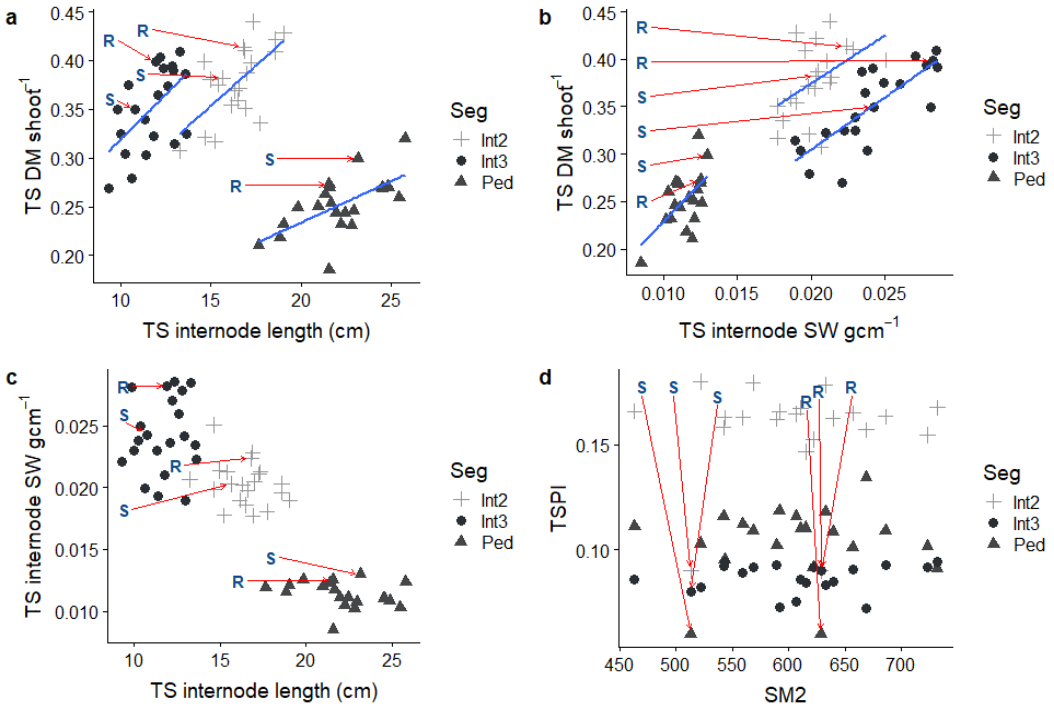


Figure 3.5. Linear regressions (parents were excluded from the linear regression analysis) amongst 19 lines of the SxR DH population (subset 1) between stem-internode traits:
Seg: Ped: Peduncle, Int2: Internode 2, Int3: Internode 3 and Int4+: Internode 4:
A) True stem (TS) DM shoot^{-1} on TS internode length (cm): Ped: y=0.007x-0.09, R^2=*0.22****; Int2: y=0.02x-0.08, R^2=*0.29****; Int3: y=0.02x+0.09, R^2=*0.34****
B) TS DM shoot^{-1} on TS internode specific weight (SW: g cm^{-1}): Ped: y=16.9x+0.06, R^2=*0.47****; Int2: y=13.4x+0.07, R^2=*0.45****; Int3: y=9.94x+0.06, R^2=*0.43****
C) TS internode SW (g cm^{-1}) on TS internode length (cm): Ped: y=0.0002x+0.02, R^2=*0.09ns*; Int2: y=0.0004x+0.03, R^2=*0.06ns*; Int3: y=0.0005x+0.04, R^2=*0.04ns*
D) TS stem partitioning index on spikes m^{-2} (SM2): Ped: y=4e-0.5x+0.05, R^2=*0.03ns*; Int2: y=5e-0.5x+0.08, R^2=*0.06ns*; Int3: y=7e-0.5x+0.06, R^2=*0.09ns*; Int4+: y=-0.0002x+0.12, R^2=*0.11ns*
**P<0.05*; ***P<0.01*; ****P<0.001*; ns: non-significant
Values presented are cross-year means (Y16 and Y17).

The correlations between stem internode traits, grain yield, harvest index, yield components, spike partitioning index and DM spike per unit area at GS65+7d are shown in Table 3.3 (Figure S3.3). For spike partitioning index (SPI) and grain number (GN) there was a negative association with internode 4+ (*P<0.001*) and central internodes, been stronger on internode 3 (*P<0.001*) than on internode 2 (*P<0.05*). On the other hand, for harvest index (HI) the only trait that showed a positive trend was peduncle true-stem specific weight (*P<0.10*) compared to the

negative trend found between grain yield and internode 3 leaf-sheath PI (P<0.10) and internode 3 true-stem specific weight (P<0.10). For spike DM per unit area ($DMSpk_{A+7}$) stem internodes far away were negatively associated: internode 4 (*P<0.05*) < internode 3 (*P<0.05*) < internode 2 (*P<0.05*). For spikes per unit area (SM2) there was a negative correlation with all internode TSSWs (*P<0.05*) and a positive correlation with int4PI (*P<0.01*). This segment of the stem was also negatively associated with spike DM per unit area ($DMSpk_{A+7}$)(*P<0.05*).

Table 3.3. Pearson's correlation coefficient between traits measured at GS65+7d, physiological maturity and stem partitioning traits among 19 DH lines (subset 1) of the SxR DH population (parents were excluded from the correlation analysis). Values presented are cross-year means (Y16 and Y17).

Trait	Correlation (r)					
	SPI	**HI**	**GY**	**GN**	**$DMSpk_{A+7}$**	**SM2**
PedTSPI	-0.09	0.10	0.22	0.24	-0.08	0.02
Int2TSPI	**-0.52***	-0.06	0.04	-0.25	**-0.53***	0.02
Int3TSPI	**-0.69*****	-0.20	0.02	**-0.43†**	**-0.65***	0.03
PedLSPI	-0.03	-0.05	-0.21	-0.10	-0.18	-0.14
Int2LSPI	0.25	0.11	-0.18	-0.10	-0.11	-0.09
Int3LSPI	0.16	-0.01	**-0.37†**	**-0.40†**	-0.22	-0.20
Int4PI	**-0.92*****	-0.26	0.29	-0.06	**-0.58***	**0.34†**
PedTSSW	0.38	**0.42†**	-0.34	-0.31	0.21	**-0.63*****
Int2TSSW	**0.40†**	0.23	**-0.58****	**-0.58****	0.11	**-0.60****
Int3TSSW	0.08	0.14	**-0.40†**	**-0.57****	0.06	**-0.54***

Ped: Peduncle, **Int2**: Internode 2, **Int3**: Internode 3, **Int4+**: Rest of internodes, **PI**: Partitioning Index, **SW**: Specific Weight, **SPI**: Spike Partitioning Index, **HI**: Harvest Index, **GY**: Grain Yield (100% DM), **GN**: Grain Number, **SM2**: Spikes per unit area

†*P<0.10*; **P<0.05*; ***P<0.01*; ****P<0.001*

3.3.5. Spike component DM partitioning

Spike morphological components DM were assessed for 12 genotypes (subset 2) where the order of DM accumulation per spike component was lemma > glume > rachis > palea (Table 3.3). Significant genetic variation was found for glume PI, rachis PI and rachis SW and genotype x year interaction was found for lemma and rachis PI.

Table 3.4. Cross-year genetic ranges (Min: Minimum, Mean, Max: Maximum), broad-sense heritability (H^2), and significance values for 10 DH lines (subset 2) and parents (G), year (Y) and genotype x year (GxY) for spike morphology DM partitioning indices (PI) and specific weight (SW). Values presented are cross-year means (Y16 and Y17).

Traits	H^2	Min	Mean	Max	*P(G)*	P(Y)	*P(G×Y)*	*Savannah*	*Rialto*
GluPI	0.55	0.25	0.27	0.28	*	***	ns	0.27	0.27
PaPI	0.30	0.15	0.16	0.18	ns	*	ns	0.16	0.20
LePI	N/A	0.29	0.33	0.35	ns	**	**	0.29	0.30
RaPI	0.52	0.19	0.20	0.22	*	**	*	0.21	0.21
RaSW (g cm^{-1})	0.60	0.010	0.013	0.016	*	**	ns	0.010	0.013

Glu: Gluma; **Le:** Lemma; **Pa:** Palea; **Ra:** Rachis; **Aw:** Awns; **DW:** Dry weight; **PI:** Partitioning Index; **SW:** Specific weight

**P*<0.05; ***P*<0.01; ****P*<0.001; *ns: non-significant*

The correlations between within spike partitioning traits and grain yield, harvest index, yield components, spike partitioning index and DM spike per unit area at GS65+7d are shown in Table 3.5 (Figure S3.4). For spike partitioning index (SPI) there was a negative association with glumePI (GluPI: *P<0.10*) and a positive association with rachisPI (*P<0.10*). RachisPI was positively associated with grain number (GN: *P<0.10*); while rachis SW (*P<0.001*) and palea PI (*P<0.10*) were negatively correlated with GN and also with grain yield (GY). In instance, rachis PI was positively associated with harvest index (HI: *P<0.05*) while glume PI was negatively related (*P<0.001*). Thousand-grain weight (TGW) was negatively associated with rachis PI (*P<0.05*) but positively with RaSW (*P<0.01*). Rachis SW was also negatively associated with spike DM per unit area ($DMSpk_{A+7}$) (*P<0.10*).

Table 3.5. Pearson's correlation coefficient between traits measured at GS65+7d, physiological maturity and stem partitioning traits among 12 DH lines (subset 2) of the SxR DH population (parents were excluded from the correlation analysis). Values presented are cross-year means (Y16 and Y17).

Traits	Correlations (r)						
	SPI	**FE**	**GN**	**HI**	**GY**	**TGW**	**$DMSpk_{A+7}$**
GluPI	**-0.24**†	0.15	0.12	**-0.66*****	0.01	-0.17	-0.11
PaPI	-0.01	-0.24	**-0.32**†	-0.05	-0.24	0.26	0.05
LePI	-0.15	-0.20	-0.23	0.12	-0.10	0.23	-0.14
RaPI	**0.38**†	0.28	**0.43**†	**0.54***	**0.34**†	**-0.32**†	0.23
RaSW	0.03	0.05	**-0.66*****	-0.20	**-0.60****	**0.56****	**-0.44**†

Glu: Glume; **Pa:** Palea; **Le:** Lemma; **Aw:** Awns; **Ra:** Rachis; **PI:** Partitioning Index; **SPI:** Spike Partitioning Index; **FE:** Fruiting Efficiency; **GN:** Grain Number; **HI:** Harvest Index; **GY:** Grain Yield; **TGW:** Thousand Grain Weight; **$DMSpk_{A+7}$:** Spike DM per unit area
$^{\dagger}P<0.10$; $^{*}P<0.05$; $^{**}P<0.01$; $^{***}P<0.001$

3.3.6. Correlations between partitioning traits, grain number, harvest index and grain yield

A strong negative linear relationship was found amongst the SxR DH lines between stem partitioning index (StePI) and lamina partitioning index (LamPI) and spike partitioning index (SPI). On the other hand, spike DM per unit area at seven days after anthesis ($DMSpk_{A+7}$) was positively associated with SPI but negatively with StePI. Strong negative associations were found between SPI and fruiting efficiency (FE), plant height (PH) and thousand-grain weight (TGW). For StePI a positive association was found with FE, PH and TGW. Positive associations were also found between LamPI and grain number (GN) but a negative association with TGW. Stem internode lengths (2 and 3) were positively associated with TGW, GY and FE but negatively with SPI. The above-ground dry matter at physiological maturity ($AGDM_{PM}$) was positively associated with grain yield (GY), but AGDM seven days after anthesis ($AGDM_{A+7}$) positive associations were found between GN and GY, but negatively associated with HI, FE and TGW. Additionally, FE was strongly associated with HI, GY and PH (Table 3.6).

Table 3.6. Pearson's phenotypic correlation coefficients between traits measured at GS65+7d and physiological maturity among the 94 SxR DH lines (parents were excluded from analysis). Values presented are cross-year means (Y16 and Y17).

Traits	GN	HI	TGW	GY	$AGDM_{PM}$	SPI	StePI	FE	PH	$AGDM_{A+7}$	LamPI	$DMSpk_{A+7}$	LnInt2	LnInt3	LnPed
GN	-														
HI	0.22*	-													
TGW	-0.72***	0.11	-												
GY	0.69***	0.44***	-0.01	-											
$AGDM_{PM}$	0.60***	-0.22*	-0.09	0.77***	-										
SPI	0.17†	0.01	-0.30**	-0.10	-0.10	-									
StePI	-0.24	0.05	0.41***	0.12	0.09	-0.96***	-								
FE	0.14	0.44***	0.03	0.26**	-0.03	-0.71***	0.63***	-							
PH	0.01	-0.12	0.25	0.30**	0.39***	-0.53***	0.57***	0.26**	-						
$AGDM_{A+7}$	0.50***	-0.38***	-0.28**	0.42***	0.73***	0.09	-0.07	-0.40***	0.14	-					
LamPI	0.20*	-0.19†	-0.33**	-0.05	0.05	-0.22*	-0.07	0.32	-0.09	-0.06**	-				
$DMSpk_{A+7}$	0.44***	-0.24	-0.37***	0.22*	0.42***	0.74***	-0.71***	-0.72***	-0.27**	0.71***	-0.19†	-			
LnInt2	-0.02	0.05	0.31**	0.32**	0.30**	-0.50***	0.60***	0.25**	0.72***	0.17†	-0.29**	-0.25**	-		
LnInt3	-0.11	-0.06	0.34***	0.21*	0.25	-0.54***	0.63***	0.23*	0.76***	0.16†	-0.25**	-0.27**	0.84***	-	
LnPed	0.08	-0.15	0.08	0.23*	0.32**	-0.25**	0.28**	0.05	0.68***	0.17†	-0.08**	-0.09**	0.50***	0.50***	-

A+7: Anthesis + 7 days; **PM:** Physiological Maturity; **GN**: Grains per m^{-2}; **HI**: Harvest Index; **TGW**: Thousand Grain Weight; **GY**: Grain Yield (100% DM); **$AGDM_{PM}$**: Above-Ground DM; **SPI**: Spike Partitioning Index; **StePI:** Stem Partitioning Index; **FE:** Fruiting Efficiency; **PH:** Plant Height; **LamPI**: Lamina Partitioning Index; **DMSpk**: Spike DM per unit area; **LnInt2**: Length Internode 2; **LnInt3**: Length Internode 3

*†P<0.10; *P<0.05, **P<0.01, ***P<0.001*

3.3.7. Stepwise regression analysis

The results of the associations between tested trait variables and each of grain yield (GY), harvest index (HI), spike partitioning index (SPI) and grain number (GN) (as the dependent variable) amongst 94 DH lines (parents were excluded from the analysis) from the stepwise linear regression model are shown in Table 3.7. As a single trait above-ground DM (AGDM) at physiological maturity explained 58.9% of the variation in GY, then adding to the model HI and peduncle length explained most of the remaining variation (98.8%). For HI, fruiting efficiency explained 35.8% of the variation and the proportion of variation explained increased to 54.9% when $AGDM_{A+7}$ and SM2 were added to the model. For SPI, 80.3% of the phenotypic variation was explained by FE, HI, plant height, GN and spikes per unit area (SM2). Lastly, GN variation was explained mainly through FE (42.4%) but adding SM2 to the model increased the proportion of variation explained to 71.9%.

For the subset 1 made up of 19 DH lines (parents were excluded from the analysis) a stepwise analysis was done, considering the same traits used as dependent variables as for the whole population, but including stem-internode traits in the tested variables (Table 3.7). For grain yield (GY), internode 2 true-stem SW explained most phenotypic variation (31.4%) as a single trait. Variation for harvest index (HI) was explained mainly through spikes per unit area (16.3%) and stem internode 2 and 3 lengths (32.6%). The phenotypic variation for spike partitioning index was explained through LInt3 (51.1%) and Int2TSPI, Int3TSPI and Int2TSSW (70.9%); whereas for grain number (GN), variation was accounted for by Int2TSSW, Int3TSPI, SM2 and LInt2 (67.5%).

Table 3.7. Stepwise multiple linear regression analysis testing GY, HI, SPI and GN as dependent variables different traits (parents were excluded from the analysis). Values presented are cross-year means (Y16 and Y17).

Traits	Variable selected	R	Prob	Variables tested in model
		Whole population: 94 DH lines		
GY	$AGDM_{PM}$	58.9	*<0.001*	$AGDM_{A+7}$, $AGDM_{PM}$, DTA, DTM, $DMSpkm^{-2}$, FE, PH, HI, LnInt2, LnInt3, LnPed, SPI, StePI, LamPI
	$AGDM_{PM}$, HI, LnPed	98.8	*<0.05*	
HI	FE	35.8	*<0.001*	PH, LnPed, LnInt2, LnInt3, SM2, SPI, FE, $AGDM_{A+7}$
	FE, $AGDM_{A+7}$, SM2	54.9	*<0.05*	
	FE, $AGDM_{A+7}$, SM2, LnPed, LnInt2, PH	60.1	*<0.05*	
SPI	FE	21.1	*<0.001*	GN, SM2, FE, HI, PH
	FE, HI	63.6	*<0.001*	
	FE, HI, PH	73.8	*<0.001*	
	FE, HI, PH, GN, SM2	80.3	*<0.001*	
GN	FE	42.4	*<0.001*	PH, LnInt2, LnInt3, LnSpk, SM2, SPI, StePI, FE
	FE, SM2	71.9	*<0.001*	
	FE, SM2, StePI, LnSpk, SPI	86.0	*<0.001*	
		Subset 1: 19 DH lines		
GY	Int2TSSW	31.4	*<0.01*	LnPed, LnInt2, LnInt3, PedTSPI, Int2TSPI, PedTSSW, Int2TSSW, Int3TSSW, Int3TSPI, SM2
HI	SM2	16.3	*0.05*	
	SM2, LnInt2, LnInt3	32.6	*0.05*	
SPI	LnInt3	51.1	*<0.001*	
	LnInt3, Int2TSPI, Int3TSPI, Int2TSSW	70.9	*<0.05*	
GN	Int2TSSW	30.6	*<0.001*	
	Int2TSSW, Int3TSPI	49.7	*<0.05*	
	Int2TSSW, Int3TSPI, SM2, LnInt2	67.5	*<0.05*	

A+7: Seven days after anthesis; **PM:** Physiological Maturity; **DTA:** Days from emergence to seven days after anthesis; **AGDM:** Above-ground DM; **LamPI:** Lamina Partitioning Index; **SPI:** Spike Partitioning Index; **StePI:** Stem Partitioning Index; **DMSpk:** DM Spike per unit area; **DTM:** Days from emergence to physiological maturity; **FE:** Fruiting Efficiency; **PH:** Plant Height; **TGW:** Thousand Grain Weight; **SM2:** Spikes per unit area; **GN:** Grains per unit area; **HI:** Harvest Index; **LnPed:** Length Peduncle; **LnInt2:** Length Internode 2; **LnInt3:** Length Internode 3; **TS:** True-Stem; **PI:** Partitioning Index; **SW:** Specific Weight

3.4. Discussion

3.4.1. Yield improvement in high biomass genotypes

Wheat breeding programs need to accelerate genetic gains to ensure that grain demand can be satisfied, for winter wheat yields have either remained stagnant or increased rates at a slow rate in breeding programs in the last 20 to 30 years (Senapati et al., 2019). For winter wheat genotypes limited studies have been published on the last years where yield improvement have been reached. For the SxR DH population, a strong association was found between grain yield and the above-ground dry matter (stronger at physiological maturity than

at anthesis + 7 days), agreeing with Shearman et al. (2005) findings, which attributed increase in grain yield as a result of more biomass produced with year of release among UK cultivars introduced from 1972 to 1995. Similarly, Siddique et al. (2018) comparing cultivars released from 1948 to 2012 in Australia suggested that total biomass was increased linearly with year of release (0.72% yr^{-1}) as a result of more grain number per spike and thousand-grain weight, likely due to higher net photosynthesis in modern wheat than older wheat.

In turn, Xiao et al. (2012) observed that grain yield gains from 1969 to 2006 in China were largely associated with the increase of above-ground DM and grain number and higher flag-leaf photosynthesis had benefited the production of carbohydrates in stems at anthesis. Increasing assimilate production at critical development stages could break-down or decrease the trade-off between harvest index and above-ground DM. For instance, Dai et al. (2016) concluded using different types of wheat (durum, spring, winter, soft white spring, soft white winter), that harvest index will not achieve high yield values unless constant biomass is maintained, high harvest index varieties were associated with lower biomass (5.2 t ha^{-1}) and grain yield (8.6 t ha^{-1}) than average harvest index varieties at biomass (17.0 t ha^{-1}) and yield (7.6 t ha^{-1}), respectively. Studying CIMMYT spring wheat cultivars released from 1966 to 2009, Aisawi et al. (2015) reported genetic gains in harvest biomass production, which were associated with reduced harvest index. In the present study, a negative association was observed between harvest index and above-ground DM at both seven days after anthesis and physiological maturity, suggesting that source and sink size must be jointly optimized when selecting for high harvest index and above-ground DM at harvest. In this context, Reynolds et al. (2017) demonstrated that creating strategic crosses to complement each other based on source-sink balance resulted in enhanced genetic gains.

Genetic variation in grain yield in the SxR DH population was explained mainly by grains per unit area rather than grain weight, traits that showed a negative association. For a spring wheat panel in NW Mexico, González-Navarro et al. (2016) observed that the trade-off between grain number and weight was a result of sink size limitation linked to carpel size. This trade-off could be the result of sink limitation related to grain position, grains in the basal-central spikelets were heavier than those in the apical and most basal spikelets (Li et al., 2016). These effects could also be partly due to the negative relationship found between grain weight and fruiting efficiency which may partly determine the relation between grain weight and number (Ferrante et al., 2015; Terrile et al., 2017). Current results showed that fruiting efficiency was positively associated with harvest index and this trait explained almost half of the genetic variation in grain number. Comparing five different winter wheat cultivars, Garcia et al. (2019) indicated that spike DM at anthesis explained differences in grain number, due to differences in dry matter partitioning to spikes before anthesis affecting the growth of floret primordia. Furthermore, Shearman et al. (2005) studied eight representative winter wheat cultivars introduced from 1972 to 1995 and reported genetic gains in grain number were related to

changes in grains per spike, as result of the introduction of *Rht* (Reduced height) genes; similar results were reported by Würschum et al. (2018). Therefore, further improvements in grain number must be focused on fruiting efficiency in addition to the efficient partitioning of assimilates to the spike to enhance fertile floret number.

3.4.2. Pre-anthesis growth, partitioning and determination of grain number

Modern wheat cultivars need to optimize DM allocation to the spike to increase grain number (González et al., 2014). The competition for assimilates between the spike and stem varies between internodes as maximum stem growth rates have been reported to vary from 7 to 21 days after anthesis (Ehdaie et al., 2006). In the present study, genetic variation in grain number was more strongly associated with the biomass produced at GS65+7d than the amount of DM partitioned to the spike (SPI); and was not associated with the fruiting efficiency (Fischer, 1984).

Assimilate competition during stem elongation appears mainly to occur between stem and spike as a result of the temporal growth overlap (Satorre & Slafer, 1999). Little research has been done at the stem phytomer partitioning level, but current results showed that true-stem PIs of middle internodes had stronger negative associations with SPI than the peduncle with the strongest association for stem internode 3. Indeed, half of the genetic variation in SPI was accounted for by the length of internode 3. Using UK winter wheat cultivars Shearman et al. (2005) showed that improvements in yield potential with the year of cultivar release from 1972 to 1995 had been mainly through changes in pre-flowering biomass accumulation, resulting in more assimilates available to the spike. In the present study, a positive relationship was found among DH lines between HI and peduncle and internode 2 (true-stem) PIs which likely was the result of an indirect association with biomass since both internode 2 and 3 PIs and above-ground biomass at GS65+7d increased with plant height. The stepwise regression showed that the specific weight of internode 2 true stem explained some of the variation in grain yield and grain number which was likely associated with a negative correlation between int2TSSW and spikes per m^2. Peduncle TSPI was also strongly positively associated with spikes per m^2 suggesting spike number played a role in determining TSPIs possibly through affecting the vertical distribution of light in the canopy, i.e. higher spike density reduced light transmission to the int4+ canopy layer increasing light interception by the peduncle.

In this population, the peduncle accounted for a considerable proportion of total stem length; the peduncle was reported to account for 0·33 to 0·47 of plant height in modern dwarf and semi-dwarf genotypes (Dodig et al., 2017) matching with results in this population. Therefore there is scope to change the relative partitioning between the peduncle and stem internodes 2 and 3 while broadly maintaining the overall plant height with regard to maintaining the optimum plant height range of ca, 70-100 cm in new cultivars. Pedro et al. (2012) using a mutant TILLING population characterized by extremes in source/sink ratios showed that

parents of a high grain number plant produced offspring of more grains per plant, on average than parents of a lower grain number per plant. This suggests that increasing the SPI could boost yield by allocating assimilates within the spike preferentially to the florets rather than structural components. In addition, it may be advantageous to decrease middle stem internodes rather than basal ones, which provide anchorage to avoid lodging (Gebbing, 2003; Piñera-Chavez et al., 2016).

3.4.3. Winter wheat ideotype for optimized partitioning

Present results showed that fruiting efficiency, spike partitioning index and stem internode lengths are essential traits to maximize HI (González-Navarro et al., 2015; Lo Valvo et al., 2018). Overall DM distribution in this population among the different organs was ranked stem > spike > lamina, similar to the findings on a high biomass modern CIMMYT spring wheat panel (Rivera-Amado et al., 2019). Some variation was found in the subset 1 in DM partitioning for every stem internode, with true-stem internodes accumulating DM in the order: internode 2 > internode 3> peduncle in contrast to the leaf sheath where internodes near the spike had more DM: ped > int2> int3. The different distribution of DM may reflect their roles, upper internodes (LS) will tend to be more important for light interception rather than those near the ground which confer structural support to the plant (TS) (Gebbing, 2003). Comparing 30 wheat cultivars widely grown in China since the 1940s with modern lines, Zhang et al. (2017) reported that changes in assimilate distribution to structural material in leaves have contributed to a higher photosynthetic rate resulting in higher production of DM. If we could diminish the trade-off existing between spike and stem in the critical period from booting to anthesis, when rapid spike growth coincides with the stem, there is the possibility to achieve stable harvest index values of ~0.55 or to approach closer to the theoretical maximum ~0.64, if at the same time above-ground DM production increases by 20% (Austin et al., 1989; Shearman et al., 2005).

The spike morphological analysis results showed that fruiting efficiency could be increased by reducing the DM allocated to the palea and/or lemma as both organs. However, this could affect the spike DM per unit area hence spike photosynthesis. Reducing the allocation of assimilates to these spike organs could impact photosynthesis rate and grain growth (Wang et al., 2018). Therefore, further research is needed to confirm this hypothesis. Although DM distributed to rachis was the only spike trait were positive trends were found with yield, grain number and to the ratio of grains and DM spike at GS65+7d, as for the rest of the spike organs negative links were recorded. It can be speculated that an increase in rachis partitioning index could help break the barrier of sink limitation in modern cultivars. Using two large-spike CIMMYT spring cultivars compared to a conventional cultivar Bacanora, Gaju et al. (2014) concluded that longer rachis length per spikelet enhanced grains per spike. With the use of genotypes with contrasting stem water-soluble carbohydrates (WSC), Dreccer et al. (2014) suggested that high WSC lines had more grains per spike associated with more florets per spike, implying fruiting efficiency may be related to sucrose levels in spikes exploring the

possibility of studying/modifying plant signalling, e.g. cytokinin concentration, to increase spike fertility (Foulkes et al., 2011).

3.4.4. Implications for plant breeding programs

Breeders select for many traits, including genetic variation among the progeny, in their efforts to improve yield potential for the target environment (Rebetzke et al., 2012). The deployment of traits, such as radiation-use efficiency (Tripathi et al., 2018), stomatal conductance (Motzo et al., 2013), boosting enzyme activity (Perdomo et al., 2017), photosynthesis capacity (Yang et al., 2007), as more information and results are available. Spike fertility could also be incorporated into breeding programs to match increasing source traits (Shearman et al., 2005). Pyramid trait selection is a strategy proposed by Reynolds et al. (2017) where crosses should combine complementary high heritability source-sink traits to achieve genetic gains. The selection for genotypes with shorter stem internode 2 and 3, as result of their association with spike partitioning index and harvest index, is a strategy that has not been used to date taking into account that the optimal plant height must be broadly maintained (Qin et al., 2015). The peduncle is not considered as a target phytomer since this internode extends partly after anthesis, therefore, competing less with spike during the critical spike growth phase pre-anthesis. Reducing partitioning to the central stem internodes may favor DM partitioning to sink organs increasing the number of fertile florets and combined with higher fruiting efficiency to boost grain number (Garcia et al., 2019).

Heritability is a critical parameter to consider while selecting traits for future crosses/progeny as this measures the phenotypic variance attributable to genetic causes under certain conditions (Khan & Naqvi, 2011). For most of the traits measured in this DH population heritability values were in the low to medium ranges (0.10 to 0.60) which could be attributed to the number of genotypes and repetitions that made-up the experiment and at the same time environmental conditions. Regarding the phytomers and spike traits measured on subset 1 and 2 these type of measurements needs to be precisely recorded which make them time-consuming and could have introduced variation. For the deployment of these novel target traits into breeding programs, high-throughput phenotyping (HTP) and/or genotypic markers for marker-assisted selection are required for a cost and time effective selection to achieve genetic gains, as for stem DM internode partitioning and spike morphology traits methodology used on this experiment was time-consuming. The introduction of these methodologies (genomics and phenomics) will allow scientists to gain a better understanding of the genetic basis facilitating the identification of high yielding lines for new strategic crosses of these traits.

3.5. Conclusions

- Gran yield variation in this DH population was mainly explained through above-ground dry matter at physiological maturity.
- Spike partitioning index did not translate to genetic gains as counter interaction of plant height on harvest index and above-ground dry matter.
- Positive trends were recorded between spike partitioning index and grain number but not between fruiting efficiency and grain number, although fruiting efficiency was positively associated with harvest index and grain yield.
- Spike partitioning index and harvest index could be increased through modest reductions of internode lengths as positive associations were with internodes 2 and 3; whilst considering that the optimal height range must be broadly maintained.
- Grain yield and number per unit area were negative related with internodes lengths, where for grain number leaf-sheath was stronger and for grain yield internode true-stem stood out.
- There is the possibility to increase fruiting efficiency and grain number reducing the among of assimilates to the rachis as this was the only spike organ positive related.
- Further methodologies, such as marker-trait associations, need to be implemented to make the use of this novel traits cost and time effective.

3.6. Supplementary material

Table S3.1. Savannah x Rialto (SxR) DH genotypes names and subset details.

Geno`type	Subset 1	Subset 2
1		
2		
3		
5		
6		
7		
8		
9	✖	✖
10		
11		
12		
13	✖	
14		
16	✖	✖
17		
18	✖	
19		
20	✖	✖
21		
23		
24		
25		
26		
27		
28		
29		
30		
31		
32		
33		
34		
35		
36	✖	✖
37		
38		
39		
40		
41		
42		
43		
44		
45		
46		
47	✖	
48	✖	
49		
50		
51		

Genotype	Subset 1	Subset 2
52	✖	✖
53	✖	✖
54		
55		
56		
57		
58		
59		
60		
61		
62	✖	
63		
64		
65		
66	✖	
67		
68		
69		
70		
71		
72		
73	✖	✖
74	✖	✖
76		
77		
78		
79	✖	✖
81		
82		
83		
84	✖	
85		
86	✖	✖
87		
88		
89	✖	
90		
91		
92		
93		
95		
96		
97		
98		
99		
100	✖	
Rialto	✖	✖
Savannah	✖	✖

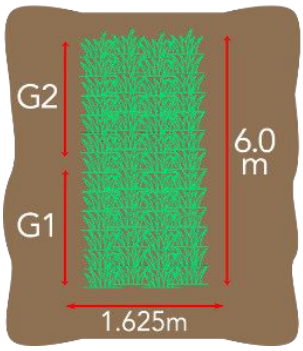


Figure S3.1. SxR DH bed arrangement (width and length) at field level: two genotypes (G) per bed.

Figure S3.2. Development stages at field level of the SxR DH experiment for Y16 and Y17.

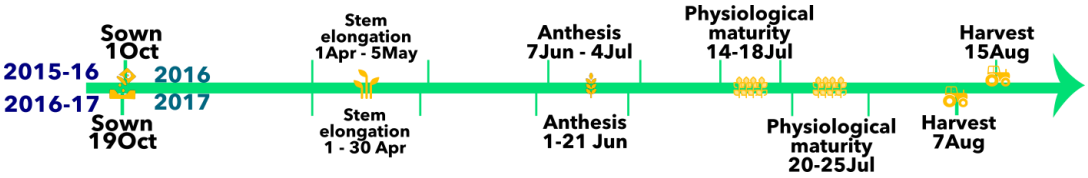


Table S3.2. Meteorological data and crop management over two seasons (Y16 and Y17) at NW Mexico.

		Y16: 2015-16	***Y17: 2016-17***
Planting date:		October 1st	October 19th
Booting (GS41-GS49)	Mean Temperature	7.72°C	9.15°C
	Mean Solar radiation	173.9 MJ m^{-2}	161.9 MJ m^{-2}
	Mean Rain accumulated	2.17 mm	0.43 mm
Anthesis (GS59-GS69)	Mean Temperature	13.7°C	16.9°C
	Mean Solar radiation	189.7 MJ m^{-2}	223.9 MJ m^{-2}
	Mean Rain accumulated	3.15 mm	1.8 mm
Grain filling (GS71-GS91)	Mean Temperature	16.6°C	15.6°C
	Mean Solar radiation	207.1 MJ m^{-2}	168.4 MJ m^{-2}
	Mean Rain accumulated	1.93 mm	8 mm

Table S3.3. Plot management, applications of crop herbicide, fungicide and insecticide on the SXR DH for Y16 and Y17.

	Y16: 2015-16		Y17: 2016-17	
Fertiliser	03/02/2016	Human extra @ 1l/ha	16/03/2017	116 kg/ha 34.5% Nitram 40kg/ha N
	16/03/2016	116 kg/ha 34.5% Nitram 40kg/ha N	24/03/2017	Opte-man @ 1l/ha
	17/03/2016	Human extra @ 1l/ha	03/04/2017	Opte-man @ 1l/ha
	05/04/2016	Human extra @ 1l/ha	07/04/2017	232 kg/ha 34.5% Nitram 80kg/ha N
	12/04/2016	232 kg/ha 34.5% Nitram 80kg/ha N	28/04/2017	Opte-man @ 1.5l/ha
	05/05/2016	Opti - M @ 1.0 l/ha	04/05/2017	174 kg/ha 34.5% Nitram 60kg/ha N
	09/05/2016	174 kg/ha 34.5% Nitram 60kg/ha N	26/05/2017	Magnor @ 1l/ha
	26/05/2016	Magnor @ 1l/ha		
Herbicide	02/10/2015	Movon @ 1l/ha + Defy @ 2l/ha + Backrow @ 200ml/ha	16/03/2017	116 kg/ha 34.5% Nitram 40kg/ha N
	01/04/2016	Chekker @ 180g/ha	24/03/2017	Opte-man @ 1l/ha
	26/05/2016	Cleancrop Gallifrey 3 @ 0.6l/ha	03/04/2017	Opte-man @ 1l/ha
			07/04/2017	232 kg/ha 34.5% Nitram 80kg/ha N
			28/04/2017	Opte-man @ 1.5l/ha
			04/05/2017	174 kg/ha 34.5% Nitram 60kg/ha N
			26/05/2017	Magnor @ 1l/ha
Fungicide	03/02/2016	Corbel @ 0.75l/ha	03/04/2017	Capalo @ 0.5l/ha + Phoenix @ 1l/ha
	05/04/2016	Cherokee @ 1.5l/ha	28/04/2017	Boogie Xpro @ 1.3l/ha + Pentangle @ 1l/ha + Kantor @ 0.2l/ha
	05/05/2016	Brutus @ 2.0 l/ha + Adexar @ 1.5 l/ha + Phoenix @ 1.5 l/ha	26/05/2017	Brutus @ 1l/ha + Imtrex @ 1l/ha
	26/05/2016	Phoenix @ 1.5l/ha + Brutus @ 1.2l/ha	16/06/2017	Kestrel @ 0.6l/ha + Kantor @ 0.2l/ha
	21/06/2016	Brutus @ 1l/ha + Kantor @ 0.3l/ha		
Insecticide	03/02/2016	Cleancrop Corsair @ 0.1l/ha		
PGR	05/04/2016	Adjust @ 1l/ha	03/04/2017	Adjust @ 1l/ha
	05/05/2016	Adjust @ 0.8 l/ha + Cleancrop Cutlass @ 0.2 l/ha	28/04/2017	Adjust @ 0.8l/ha

Table S3.4. Phenotypic ranges (BLUEs), least significant differences (LSD, *P=0.05*) and significance (*p-values*) for 94 DH lines and parents from the SxR DH population in two seasons (Y16 and Y17).

	Traits		***Y16: 2015-16***					***Y17: 2016-17***					***Savannah***		***Rialto***	
		Units	**Min**	**Mean**	**Max**	**LSD**	***P*(G)**	**Min**	**Mean**	**Max**	**LSD**	***P*(G)**	**Y16**	**Y17**	**Y16**	**Y17**
Anthesis + 7days (GS65+7d)	DTA	DAE	257	263	265	6	ns	232	237	243	1	***	265	240	260	238
	$AGDM_{A+7}$	g m^2	1338	1981	2315	900	ns	1230	1972	2640	738	ns	2039	1742	2929	2025
	DM Lam	g $shoot^{-1}$	0.60	0.71	0.90	0.15	*	0.52	0.62	0.74	0.11	ns	0.66	0.54	0.87	0.71
	LamPI		0.13	0.16	0.18	0.03	ns	0.14	0.17	0.20	0.03	*	0.14	0.15	0.17	0.19
	$SpkDM_{A+7}$	g m^{-2}	332.4	635.0	640.7	330.7	ns	247.6	453.3	668.1	200.6	***	668.9	528.9	572.6	403.2
	DM Spk	g $shoot^{-1}$	0.84	1.24	1.83	0.51	ns	0.50	0.82	1.59	0.22	***	1.54	1.14	1.03	0.76
	SPI		0.20	0.27	0.38	0.10	ns	0.17	0.23	0.32	0.03	***	0.33	0.30	0.20	0.19
	DM Ste	g $shoot^{-1}$	1.99	2.60	3.27	0.58	**	1.66	2.14	2.81	0.42	***	2.49	2.05	3.32	2.35
	StePI		0.47	0.57	0.64	0.08	*	0.51	0.60	0.66	0.03	***	0.53	0.55	0.64	0.62
	GA	g cm^{-1}	70.8	102.2	129.8	23.9	***	64.3	97.7	130.6	30.7	***	102.5	85	139.8	111
	FE	grains g^{-1}	20.6	34.2	59.8	16.3	*	27.5	54.0	81.9	20.0	***	26.9	43.7	41.6	57.5
	PH	cm	59.7	76.4	92.4	8.25	***	38.8	67.8	79.5	8.90	***	77.3	68.4	81.9	70.5
	LnFL		15.2	18.9	22.0	2.92	**	13.9	16.8	19.7	2.79	**	18.8	17.8	20.1	17.5
	LnSpk		10.1	11.9	14.3	1.66	***	8.61	11.0	12.8	1.39	***	12.2	11.2	13.8	11.7
	LnPed		17.2	22.1	27.2	2.81	***	17.0	22.5	43.0	6.10	***	22.3	24.0	22.4	20.7
	LnInt2		13.1	16.6	19.9	1.77	***	13.4	16.5	19.9	1.81	***	16.0	15.2	17.0	16.6
	LnInt3		8.95	11.6	14.9	1.98	***	9.54	12.2	15.5	1.58	***	10.9	10.7	11.7	12.2
Physiological maturity	DTM	DAE	298	300	303	3	ns	269	274	280	1	***	301	277	300	275
	$AGDM_{PM}$	g m^{-2}	1335	2071	2429	439	ns	1334	2005	2509	408	*	2232	1712	2688	2056
	GY (100% DM)	g m^{-2}	547	803	964	159	***	504	807	944	126	***	934	845	1081	841
	TGW	g	30.6	39.6	47.1	5.17	***	27.2	32.4	39.7	4.60	***	46.1	34.8	40.0	33.6
	HI	%	0.34	0.41	0.47	0.05	*	0.32	0.40	0.47	0.06	*	0.42	0.50	0.40	0.41
	GN	grains m^{-2}	12993	20467	26855	4932	***	16274	25111	32909	4553	***	20266	24287	27269	25047
	SM2	spikes m^{-2}	354	515	708	181	ns	395	603	811	182	**	493	504	645	577

A+7: Anthesis + 7 days; **PM:** Physiological Maturity**; DTA**: Days from emergence to anthesis; **AGDM**: Above-Ground Dry Biomass; **DM Lam**: Dry weight lamina; **LamPI**: Lamina Partitioning Index, **DMSpk**: Spike DM at A+7 per unit area; **DM Spk**: Dry weight spike; **SPI**: Spike Partitioning Index; **DM Ste**: Dry weight stem; **StePI**: Stem Partitioning Index; **GA**: Green Area; **PH**: Plant Height; **LnFL**: Length Flag Leaf; **LnSpk**: Length Spike; **Ped**: Peduncle; **Int2**: Internode 2; **Int3**: Internode 3; **DTM**: Days from emergence to physiological maturity; **FE**: Fruiting Efficiency; **GY**: Grain Yield; **TGW**: Thousand Grain Weight; **HI**: Harvest Index; **GN**: Grains per meter square, **SM2**: Spikes per meter square
***P*(G)**: Significance of the genotype
**P<0.05; **P<0.01; ***P<0.001; ns: non-significant*

Table S3.5. Phenotypic ranges (BLUEs), least significant differences (LSD, *P=0.05*) and significance (*p-values*) for 94 DH lines and parents from the SxR DH population (subset 1: 19 genotypes without parents) in two seasons (Y16 and Y17).

	Traits			***Y16: 2015-16***					***Y17: 2016-17***					***Savannah***		***Rialto***	
			Units	**Min**	**Mean**	**Max**	**LSD**	***P(G)***	**Min**	**Mean**	**Max**	**LSD**	***P(G)***	**Y16**	**Y17**	**Y16**	**Y17**
Anthesis + 7days (GS65+7d)	Ped	DM	g shoot^{-1}	0.22	0.27	0.35	0.07	*	0.16	0.23	0.40	0.16	ns	0.30	0.30	0.33	0.22
		TS PI		0.08	0.10	0.14	0.03	ns	0.08	0.13	0.17	0.02	ns	0.06	0.08	0.06	0.06
		SW	g cm^{-1}	0.010	0.012	0.015	0.002	ns	0.007	0.011	0.019	0.007	ns	0.013	0.012	0.014	0.010
		DM	g shoot^{-1}	0.20	0.23	0.29	0.05	*	0.13	0.19	0.40	0.17	ns	0.24	0.19	0.30	0.19
		LS PI		0.05	0.08	0.10	0.02	ns	0.06	0.08	0.10	0.01	ns	0.05	0.05	0.06	0.05
		SW	g cm^{-1}	0.009	0.010	0.012	0.002	*	0.004	0.009	0.019	0.007	ns	0.011	0.007	0.013	0.009
	Int2	DM	g shoot^{-1}	0.32	0.41	0.51	0.13	ns	0.24	0.35	0.53	0.16	ns	0.42	0.35	0.45	0.38
		TS PI		0.07	0.09	0.11	0.01	*	0.06	0.09	0.12	0.02	ns	0.09	0.09	0.09	0.10
		SW	g cm^{-1}	0.022	0.025	0.035	0.01	ns	0.009	0.15	0.025	0.007	ns	0.026	0.014	0.026	0.018
		DM	g shoot^{-1}	0.17	0.19	0.24	0.05	*	0.08	0.15	0.37	0.14	ns	0.17	0.14	0.25	0.15
		LS PI		0.02	0.04	0.05	0.01	ns	0.03	0.04	0.05	0.01	ns	0.04	0.04	0.05	0.04
		SW	g cm^{-1}	0.010	0.012	0.015	0.003	*	0.003	0.007	0.019	0.006	ns	0.014	0.005	0.010	0.007
	Int3	DM	g shoot^{-1}	0.29	0.39	0.49	0.11	*	0.21	0.31	0.51	0.15	ns	0.40	0.30	0.47	0.33
		TS PI		0.05	0.07	0.09	0.01	*	0.05	0.07	0.09	0.01	ns	0.09	0.08	0.09	0.09
		SW	g cm^{-1}	0.023	0.034	0.042	0.016	ns	0.008	0.014	0.024	0.007	ns	0.036	0.012	0.040	0.016
		DM	g shoot^{-1}	0.13	0.15	0.19	0.03	**	0.07	0.12	0.37	0.14	ns	0.14	0.11	0.15	0.14
		LS PI		0.02	0.03	0.05	0.01	ns	0.02	0.02	0.04	0.01	ns	0.03	0.03	0.03	0.04
		SW	g cm^{-1}	0.010	0.013	0.16	0.005	ns	0.003	0.006	0.018	0.007	ns	0.012	0.004	0.013	0.006
	Int4+DM		g shoot^{-1}	0.55	0.59	1.29	0.29	***	0.20	0.75	1.10	0.20	***	0.80	0.64	1.32	0.92
	Int4+PI			0.06	0.10	0.13	0.03	*	0.03	0.08	0.11	0.03	ns	0.17	0.17	0.25	0.24

Ped: Peduncle; **Int2**: Internode 2; **Int3**: Internode 3; **Int4+:** Internode 4+; **TS**: True-stem; **LS**: Leaf sheath; **DM**: Dry weight; **PI**: Partitioning index;` **SW**: Specific weight

P(G): Significance of the genotype

**P<0.05, **P<0.01, ***P<0.001, ns: non-significant*

Table S3.6. Phenotypic ranges (BLUEs), least significant differences (LSD, *P=0.05*) and significance (*p-values*) for 94 DH lines and parents from the SxR DH population (subset 2: 12 genotypes without parents) in two seasons (Y16 and Y17).

	Traits		***Y16: 2015-16***					***Y17: 2016-17***					***Savannah***		***Rialto***	
Anthesis + 7 days (GS65+7d)		**Units**	**Min**	**Ave**	**Mean**	**LSD**	***P(Gen)***	**Min**	**Mean**	**Max**	**LSD**	***P(Gen)***	**Y16**	**Y17**	**Y16**	**Y17**
	GluDM	g spk^{-1}	0.13	0.17	0.20	0.03	***	0.13	0.15	0.20	0.03	***	0.17	0.14	0.19	0.14
	GluPI		0.24	0.26	0.28	0.02	ns	0.26	0.27	0.29	0.02	ns	0.27	0.28	0.27	0.27
	LeDM	g spk^{-1}	0.18	0.23	0.29	0.05	**	0.16	0.20	0.26	0.05	*	0.22	0.17	0.20	0.19
	LePI		0.33	0.36	0.39	0.06	ns	0.34	0.37	0.38	0.02	ns	0.36	0.35	0.30	0.35
	PaDM	g spk^{-1}	0.08	0.11	0.14	0.05	ns	0.07	0.09	0.11	0.02	***	0.10	0.08	0.16	0.09
	PaPI		0.15	0.17	0.19	0.06	ns	0.14	0.16	0.17	0.01	*	0.17	0.16	0.23	0.17
	RaDM	g spk^{-1}	0.11	0.13	0.15	0.02	**	0.09	0.11	0.14	0.02	*	0.13	0.10	0.14	0.12
	RaPI		0.19	0.21	0.23	0.10	***	0.18	0.20	0.21	0.02	***	0.20	0.21	0.20	0.21
	RaSW	g cm^{-1}	0.009	0.011	0.013	0.002	ns	0.015	0.018	0.023	0.003	*	0.010	0.018	0.010	0.018

Glu: Gluma; **Le:** Lemma; **Pa:** Palea; **Ra:** Rachis; **Aw:** Awns; **DW:** Dry weight; **PI:** Partitioning Index; **SW:** Specific weight

***P*(G):** Significance of the genotype

**P<0.05, **P<0.01, ***P<0.001, ns: non-significant*

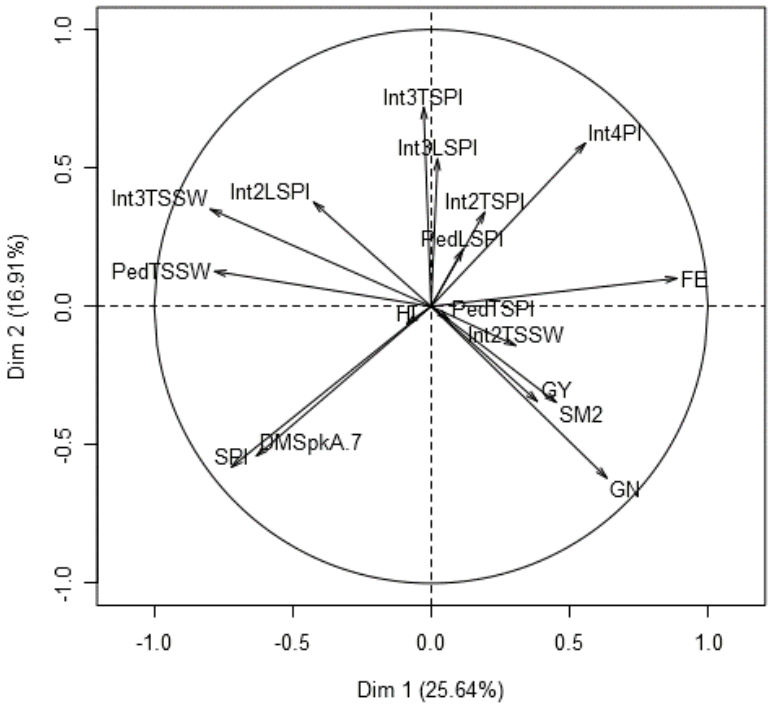


Figure S3.3. Biplot for traits measured at GS65+7d (SPI: Spike Partitioning Index, FE: Fruiting Efficiency, $DMSpk_{A+7}$: DM spike per unit area) and physiological maturity (GY: Grain Yield, HI: Harvest Index, GN: Grain Number, SM2: spikes per unit area) for subset 1 (19 DH genotypes, parents were excluded). Values based on means of Y16 and Y17.
** For abbreviation meaning see table Table S3.4

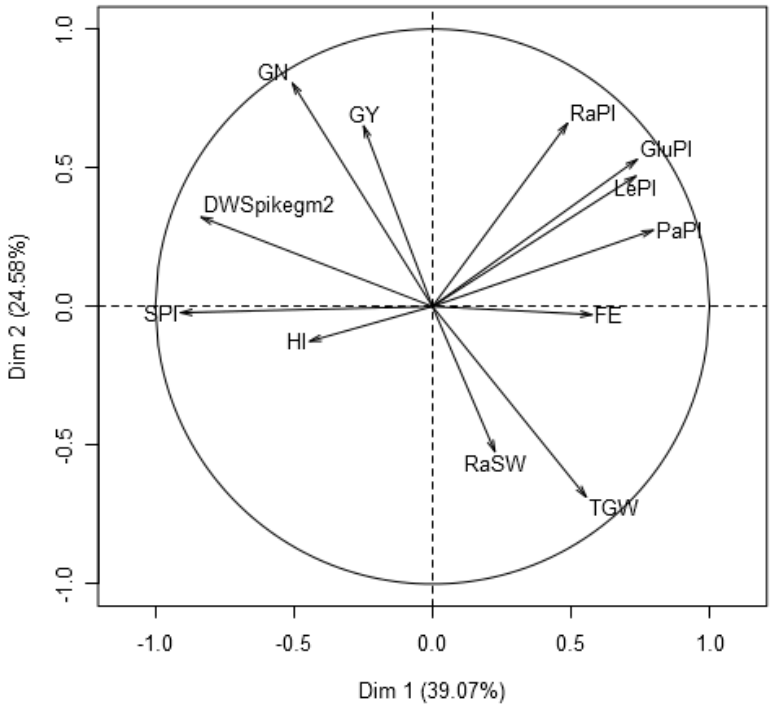


Figure S3.4. Biplot for traits measured at GS65+7d (SPI: Spike Partitioning Index, FE: Fruiting Efficiency, $DMSpk_{A+7}$: DM spike per unit area) and physiological maturity (GY: Grain Yield, HI: Harvest Index, GN: Grain Number, SM2: spikes per unit area) for subset 2 (12 DH genotypes, parents were excluded). Values based on means of Y16 and Y17.
** For abbreviation meaning see table Table S3.5

4. Genetic analysis of physiological traits to increase grain partitioning in a spring wheat high biomass association panel

Dry matter (DM) available during stem elongation and floret development are crucial for the determination of grain number (GN) in wheat which on modern cultivars tends to explain the variation in grain yield (GY). High-throughput technologies have allowed a better understanding of the genetic basis of yield potential and the development of molecular markers grain-partitioning related can lead to improved efficiency of breeding programs by the use of marker-assisted selection.

Phenotypic data on a high biomass spring wheat panel (**HiBAP**) grown under yield potential conditions (irrigation was supplied) was collected during two field cycles (Y16: 2015-16 and Y17: 2016-17) at seven days after anthesis (GS65+7d) and physiological maturity (GS87) in NW Mexico. For the obtention of genotyping data, using the 35K Wheat breeders' array, the generation of molecular markers (SNPs: Single Nucleotide Polymorphism) was done using leaf-lamina material at onset of stem extension for DNA extraction.

Genome-wide analysis (GWAS) reported 71 marker-trait associations (MTAs) explaining 8 to 18% of phenotypic variation. For the traits at GS65+7d, 33 MTAs were identified mainly on 6B and 1B regions related to spike fertility (FE) and DM of spike, stem and lamina. A total of 12 MTAs were linked to length-related traits which six correspond to plant height and the rest were distributed between awns, stem internode 3 identified, peduncle and spike lengths. At PM stage, a total of 26 MTAs were identified of which 7 corresponded to spike per unit area (SM2); most of the associations at this stage were recorded on chromosome 2B. A total of 78 candidate genes were identified near the marker-trait associations found (500,000 bp before/after the associations found), in flanking regions in traits including fruiting efficiency (FE), spike DM per unit area ($DMSpk_{A+7}$), lamina partitioning index (LamPI) and SPI.

The incorporation of these novel MTAs will allow breeders to develop new strategies, based on molecular markers, for the deployment of these traits in breeding programs to speed up the selection for grain partitioning for which either high-through phenotyping technology has not yet been developed, or it is not cost-effective.

**This chapter will be submitted to a high impact journal, where authors contributed equally to the work presented.

Aleyda Sierra-Gonzalez[ab], Gemma Molero[b], Carolina Rivera-Amado[b], Md Ali Babar[c], Matthew Reynolds[b] and John Foulkes[a]

[a]*Division of Plant and Crop Sciences, School of Biosciences, University of Nottingham, Leicestershire, LE12 5RD, UK*

[b]*CIMMYT International Maize and Wheat Improvement Center (CIMMYT), Km. 45, Carretera Mexico, El Batan, Texcoco, Mexico*

[c] *Agronomy Dept., University of Florida, Gainesville, FL, United States of America*

4.1. Introduction

Bread wheat is a versatile crop, being one of the three most essential cereals in the world. The average per capita consumption is increasing, and present grain yield progress is only 1% per year-region (Li et al., 2018; Reynolds et al., 2012) much lower than the 2.4% target (Crain et al., 2018). In addition, reduced amount of available water, urbanization, soil degradation and the fact that global wheat yields will be reduced by 6% for each 1°C of further global warming (Voss-Fels et al., 2019) presenting challenges for plant breeders to meet increased demand for wheat grain (Alonso et al., 2018; Zhang et al., 2017).

4.1.1. Physiological traits to increase grain partitioning

During the Green Revolution period, higher values of grain yield and harvest index were achieved due to the introduction of semi-dwarf (*Rht:* Reduced Height*)* genes. Varieties carrying these genes had stronger-shorter stems allowing them to support heavier spikes due to an increment of fertile florets translating into more grains per unit area (GN) (Hedden, 2003). Moreover, it has been reported that wheat genotypes with *Rht-B1b* and *Rht-D1b* genes resulted in poor emergence from deep sowing compared to tall lines without dwarf genes that exhibited heavy lodging and lower harvest index (HI) (Du et al., 2018). On the other hand, Rebetzke et al. (2012) reported that lines with the presence of *Rht4*, *Rht12* and *Rht13* were characterized as high biomass producers under deep sowing combined with greater grain partitioning which increased grain yield.

However, in the last 30 years CIMMYT spring wheat yields have raised associated with increases in AGDM but at a slower rate (Aisawi et al., 2015; Lopes et al., 2015) and in some regions yield progress has become stagnant (Brisson et al., 2010; Ray et al., 2012). In a recent study using a modern high yield CIMMYT spring wheat panel results suggested that the use of novel traits such as shorter stem internode 2 and 3 lengths exploiting within spike partitioning traits (decreased rachis DM and increased lemma DM) could boost harvest index in elite wheat breeding programs (Rivera-Amado et al., 2019). At the same time selection for fruiting efficiency -FE: grain number produced by unit of no-grain spike dry weight at anthesis or maturity- (Terrile et al., 2017) has been suggested as an avenue to increase yield potential in Argentina where although genotype × environment interaction and trade-off with spike dry weight at anthesis and grain weight may limit its usefulness.

4.1.2. Genome-wide association analysis for grain partitioning traits

Wheat breeding programs focus mainly on the development of two types of species: *T. aestivum* ssp. aestivum and *T. turgidum* ssp. durum (Jaradat, 2011). The use of existing data and multidisciplinary platforms need to be integrated for the identification of ideal parents that will contribute to yield progress. The incorporation of high-throughput phenotypic data and improvements in next-generation sequencing (NGS) have improved understanding of genetic basis the regulation/function of specific traits (Friesner et al., 2017).

Association mapping (AM) relies on identifying genomic regions associated with a particular phenotypic trait (Milner et al., 2016). In wheat, association mapping exploring linkage disequilibrium has improved in the last decade as the International Wheat Genome Sequencing Consortium (IWGSC) revealed an annotated reference sequence of the Chinese spring wheat variety, covering 94% of the genome containing 107,891 high-confidence gene models (Gorafi et al., 2018; IWGSC, 2018). The emergence of genome-wide association studies (GWAS) has allowed the study of diverse genetic pools having as output the explanation of the genetic architecture of agronomic traits (Chen et al., 2017; Sun et al., 2017). Identifying marker-trait associations (MTAs) for complex traits, such as grain yield (GY) is a challenging research area as this type of trait could be controlled by multiple genetic regions and highly influenced by the environment (Chang, & Jing, 2012). To control false positive interactions and/or spurious interactions, the implementation of population structure can increase the power of statistical associations, which may be due to geographical origins, local adaptation, breeding history and unequal relatedness among genotypes (Sorrells & Yu, 2009; Yu et al., 2006).

Population stratification was initially addressed using general linear models (GLM)-based methods such as structured association, genomic control and family-based tests of association. These methodologies estimate the proportion of genes identical by descent between any pair of individuals excluding closely related individuals (Schork et al., 2013). The introduction of mixed-linear model (MLM) has recently been demonstrated as an improved method simultaneously to account for population structure (fixed effect) and unequal relatedness (kinship-covariance; random) among individuals (Zhang et al., 2010). Additionally, principal component analysis (PCA) was recently proposed as a fast and effective way to summarise variation observed across all markers into a smaller number of underlying component variables (Wang et al., 2009). The loadings of each individual on each principal component describe the population membership or the ancestry of each individual (Zhu et al., 2008).

Several wheat GWAS studies have already been published mainly focusing on grain quality traits (Kristensen et al., 2018; Liu et al., 2018), and disease resistances (Gao et al., 2016; Juliana et al., 2018; Li et al., 2016) but relatively limited research has been done to date in yield-related traits. Using synthetic hexaploid wheat under drought conditions, Bhatta et al. (2018) reported 90 novels MTAs, of which 45 were present in genes, including MTA for grain yield and root traits, explaining from 1-32% of phenotypic variance. Guo et al. (2018) genotyped 215 wheat cultivars including 11 founder parents and 106 derivatives finding 117 significant associations for plant height, spike length, spikelet number per spike, grain number per spike, grain weight per spike, and thousand-grain weight under six irrigated environments where the phenotypic variation explained ranged from 2–13% and 25 MTAs were detected in two or more environments. Using a high biomass spring wheat panel

Molero et al. (2019) identified 94 SNPs significantly associated with yield, including phenology-related traits and RUE and biomass at various growth stages, which explained 7–17% of phenotypic variation. Common SNP markers were identified for grain yield, final biomass and radiation-use efficiency (RUE) during grain filling and from canopy closure to physiological maturity, on chromosomes 5A and 7A.

Development of molecular markers for spike fertility and grain partitioning in wheat will facilitate the selection process in breeding programs. In the present study using the Breeders 35K Axiom® array, which contains 35,143 SNPs and phenotypic data from a CIMMYT high biomass spring wheat panel collected over two seasons under fully irrigation conditions in NW Mexico a GWAS analysis was carried out to identify MTA and associated molecular markers for grain partitioning traits.

Chapter hypotheses:

- Novel MTAs, including co-located MTAs, can be identified for HI, GN and associated grain partitioning traits in a high biomass spring wheat panel using SNPs markers.
- Candidate genes for HI, GN and grain partitioning traits can be identified from SNP markers associated with MTAs.

4.2. Materials and methods

4.2.1. Plant material and experimental design

The experiments were carried out over two seasons (Y16: 2015-16 and Y17: 2016-17) under high yield potential conditions with an alpha-lattice design with four replicates at the Norman E. Borlaug experimental station near Ciudad Obregon, Sonora, Mexico (27°N, 110°W and 38 m above the sea level). A CIMMYT spring bread wheat High Biomass Association Panel (**HiBAP**) was used comprising 150 genotypes, including landrace-derivates, synthetic-derivatives and landrace + synthetic-derivatives and elite cultivars (Table S2.1). Agronomic details, such as sowing days and field management can be found in material and methods of chapter #2.

4.2.2. DNA extraction and genotyping

DNA extraction and SNP generation were done at the Earlham Institute (Norwich, United Kingdom) by Anthony Hall's research group following the methodology below as described by Molero et al. (2019).

Flag-leaf material from 148 genotypes was collected from 10 individual plants per genotype in the field in Y16 and pooled for DNA extraction using the DNeasy plant mini kit (Qiagen, Netherlands). DNA purity was measured using a NanoDrop 2000 (Thermofisher Scientific, United States) and quantified fluorometrically using the Quant-iTTM 425 assay kit (Life Technologies, United States).

SNP markers were generated using the 35K Wheat breeders array (Affymetrix, United States) (Allen et al., 2017) following the manufacturer's protocol. Allele clustering and subsequent

SNP calling was carried out using the Axiom Analysis Suite v2.0. Probe sequences for array loci were anchored to contigs from the Refseq-v1.0 Chinese Spring hexaploid wheat genome assembly using BWA (Li & Durbin, 2009).

4.2.3. High biomass spring wheat panel conformation

Population structure, k matrix and principal component analysis (PCA) were carried out following the methodology reported by Molero et al. (2019). In summary, familial relatedness of the panel was determined using Tassel applying a centred IBS method resulting in a K matrix scaled to give a reasonable estimate of additive genetic variance (Endelman & Jannink, 2012).

A consensus Q matrix was created from the independent STRUCTURE replicates using Clummpp 1.1.2 (Jakobsson and Rosenberg, 2007). Genotypes were allocated to their respective subpopulations from which they showed the highest estimated membership coefficient (Q). Distance-based cluster analysis was carried out using the hclust clustering algorithm in R as implemented by the Heatmap2 package.

PCA analysis was carried out using the Scikit-Lean package in python using 2386 LD-pruned SNPs. SNPs were LD pruned by removing the member of a SNP pair with the lowest MAF where the pair had an R^2 >critical LD value (0.30) within the distance LD decayed below that value in this population (8 Mbp).

4.2.4. Marker-trait analysis

Adjusted means (BLUEs) from cross-year analysis obtained from MetaR (reported on chapter #2) were used as input for TASSEL (version 5.2.50) to perform an association mapping analysis in which different models (Table 4.1) were applied in order to determine the amount of market-trait associations (MTAs) in this panel (Bradbury et al., 2007).

Table 4.1. Description of the implementation of different regression models used for the GWAS analysis.

General Linear Model (GLM) $y = X\beta+u$	Mixed Linear Model (MLM) $y = X\beta+Zu+e$
y: vector observations; X: design matrix; β: unknown vector containing fixed effects (genetic marker and population structure); u unobserved vector of random residuals **Population structure, familial relatedness not considered, was used as a covariate	y: vector observations; Z: design matrix, β: unknown vector containing fixed effects (genetic marker and population structure); u: vector of random additive genetic effects, e: unobserved vector of random residuals **Population structure (Q matrix), familial relatedness (K matrix) and principal component (PC) were used as a covariate

4.3. Results

Marker-trait associations (MTAs) were scored in most of the chromosomes for this spring wheat panel (HIBAP) using the phenotypic data gather over two seasons (Y16: 2015-16 and Y17: 2016-17) at different growth stages (seven days after anthesis: GS65+7d and at physiological maturity (Chapter #2). Taking into reference the location of the MTAs found using different models (general/mixed linear models) and covariates (population structure) candidate genes are reported which will allow the understanding of the genetic basis behind complex traits.

4.3.1. Population structure, linkage disequilibrium and principal component analysis

A total of 35,143 single nucleotide polymorphism (SNPs) were anchored to the reference wheat genome sequence (IWGSC, 2018). Residual heterozygous calls were entered as missing values and markers with a minor allele frequency (MAF) of 5% were removed resulting in 9,267 SNPs markers of which genome B contributed 3,486, then A with 3,486 and D with 1,230 (Figure 4.1b). Most markers belonged to chromosome 2 (1,706) and chromosome 4 had the least markers (680) (Figure 4.1a).

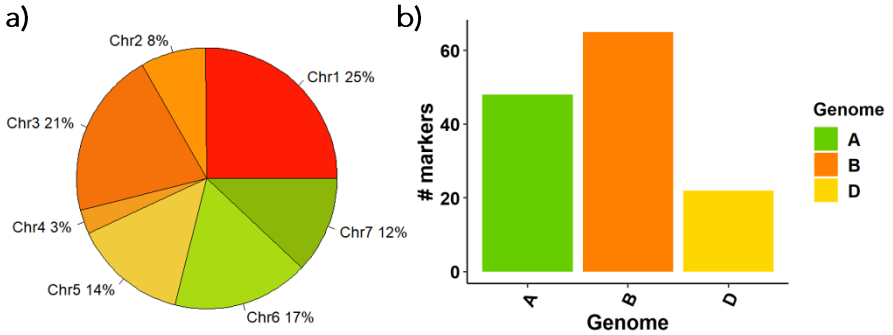


Figure 4.1. Significant (-$\log_{10}$<3) marker trait associations (MTAs) distribution among 148 genotypes by a) chromosome and b) genome.

STRUCTURE software (Porras-Hurtado et al., 2013) was used to infer the population structure of the panel. This approach assumed a model in which there are K populations, number of populations being unknown, each of which is characterised by a set of allele frequencies at each locus (Pritchard et al., 2000). Clustering was performed assuming that the number of clusters was between 1-10, showing that two was the optimal (some evidence for three), with one group with 98 and another group with 50 genotypes, which at the same time could be further subdivided into four and two sub-lineages, respectively (Figure 4.2). The two genotypes that were not included the analysis were due to missing genotype data.

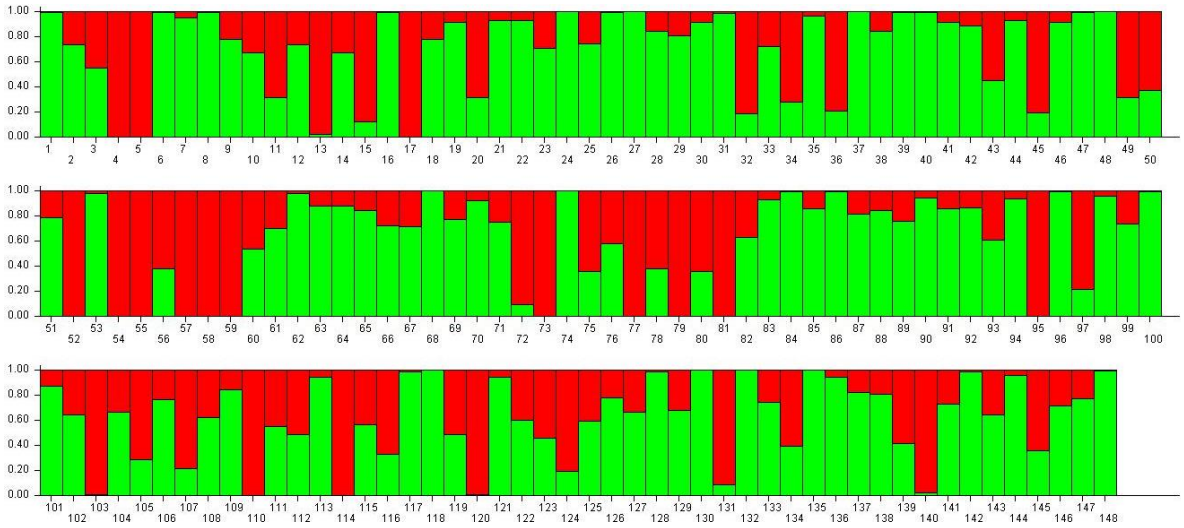


Figure 4.2. HiBAP structure distribution of main two populations (by hierarchical clustering) between 148 genotypes using structure software (red: landrace background, green: elite background).

The distinction between the two main subpopulations was also identified using PCA, demonstrating that subpopulation 2 (Figure 4.3) was mainly composed of lines with landrace or synthetic wheat or both in their pedigree history. Population structure was used for analysing marker-trait associations (MTAs) to reduce the number of false positives.

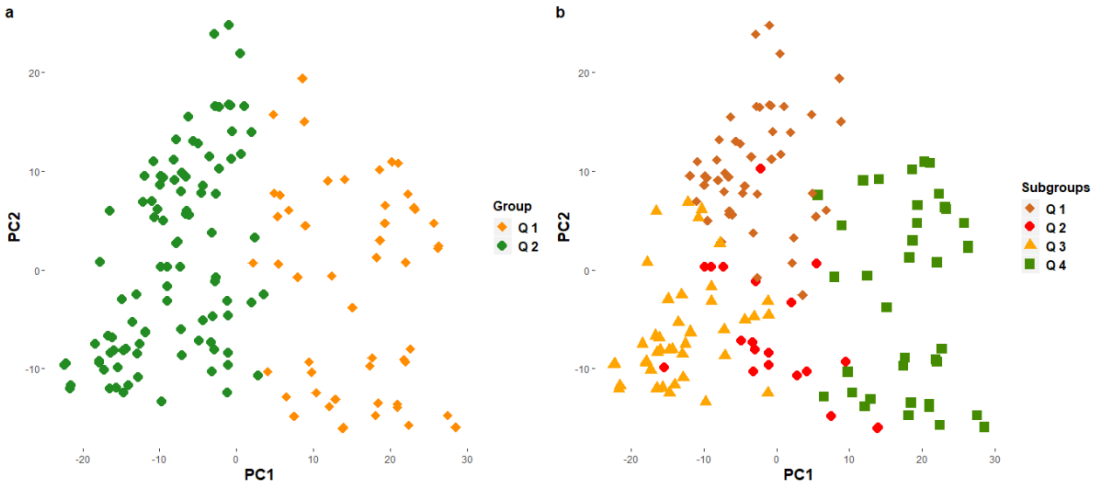


Figure 4.3. HiBAP clusters based on PCA considering pedigree background: a) 2 main groups (elite and landrace-synthetic derivates) and b) 4 groups: elite, landrace-derivates, synthetic-derivates and synthetic+landrace-derivates.

The extent of LD and the average trend of LD decay rate were estimated based on pairwise LD squared correlation coefficients (R^2). Across the whole genome, the average R^2 value was 0.105 with 33.3% of the pairwise comparisons being statistically significant at *P<0.01* and 1.9% of marker pair combinations in full linkage (R^2=1.0). The A genome showed an average R^2 of 0.097, 31.7% of pair-wise comparisons were significant and 1.17% of marker pairs were in complete linkage. The B genome showed an average R^2 of 0.107, 34.2% of pair-wise comparisons were significant and 2.17% of marker pairs were in complete linkage. The D

genome showed an average R^2 of 0.132, 34.3% of pair-wise comparisons were significant and 3.45% of marker pairs were in complete linkage. Chromosome 1 had the highest average R^2 (0.134) and highest proportion of pairs in complete LD (4.9%) with chromosome 7 showing the lowest for this metric with 0.081 and 0.6%, respectively.

In order to determine the resolution of any MTA identified in this study LD decay for the population was evaluated at the genome and subgenome level. The critical LD value of 0.301 for the population was determined by taking the 95th percentile of the square root normalised distribution of unlinked R^2 values. LD decayed below 0.301 at 8 Mbp for the whole genome and at 7 Mbp, 8.6 Mbp and 12.4 Mbp for the A, B and D sub-genomes, respectively. Whole-genome initial LD was 0.62 and LD decayed to 50% of this value at 7.2 Mbp. Initial LD values decayed to 50% at 8.6 Mbp 10.4 Mbp and 11.1 Mbp for the A, B and D sub-genomes.

4.3.2. Genome-wide association analysis

Due to the complexity of the traits analysed and the diversity of this panel several models were implemented to detect marker-trait associations (MTAs). From 148 genotypes (as there were no data for two genotypes) BLUEs (Best Linear Unbiased Estimators) for 16 traits from two field seasons (Y16 and Y17) were associated with 9,267 filtered SNPs resulting in several MTA with -log p value of 3 or greater (*P<0.001*) depending the model used (Yu et al., 2006) (Table 4.4).

Table 4.4. Summary of GWAS results obtained using a threshold of $-\log_{10} > 3$ under different models.

Model			# of significant MTAs	AveMarkerR^2	Ave ($-\log_{10}$)
GLM_1	Naïve	P+S	13,049	N/A	0.07-0.36
GLM_2	Naïve+Q4	P+S+Q_{1-4}	4,619	N/A	0.05-0.25
MLM_1	K	P+S+K	270	7-16%	3.0-5.4
MLM_2	PC2+K	P+S+PC_{1-2}+K	255	7-16%	3.0-5.6
MLM_3	PC3+K	P+S+PC_{1-3}+K	230	7-17%	3.0-5.8
MLM_4	PC4+K	P+S+PC_{1-4}+K	255	7-17%	3.0-5.7
MLM_5	PC5+K	P+S+PC_{1-5}+K	215	7-16%	3.0-5.6
MLM_6	Q3+K	P+S+Q_{1-3}+K	301	7-16%	3.0-5.3
MLM_7	Q4+K	P+S+Q_{1-4}+K	245	6-16%	2.5-5.6

GLM: General Linear Mixed; **MLM:** Mixed Linear Model; **Ave:** Average; **P:** Phenotype data (adjusted cross-year means: BLUEs); **S:** Genetic markers (SNPs); **Q:** Population structure matrix; **PC:** Principal Component; **K:** Familial relatedness matrix

Without a population structure and relatedness (genetic background: Q and K matrices) more significant markers were detected (Figure 4.4a) on the naïve model (GLM_1) than the rest since it was less stringent leading to underestimation of the distribution (Figure 4.4b) resulting in numerous false observations.

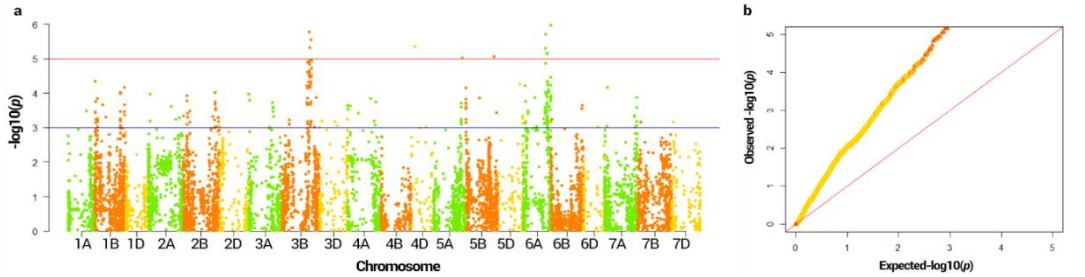


Figure 4.4. GWAS for grain yield using naïve model (GLM_1) model: a) Manhattan plot with two -log_{10} *p-values* cut-offs (blue/red line) plotted against the chromosomes position and b) QQ plot with -log_{10} transformed p-values.

Still considering a general linear model (GLM_2) but implementing the number of subgroups into which the panel could be divided (K=4), based on the relatedness of each genotype to each population, fewer markers were registered (Figure 4.5a) but still, the QQ plot showed that values were higher than expected (Figure 4.5b). This behavior was shown for most of the traits where significant markers were scored suggesting that the associations found using this specific model did not fit the data analyzed.

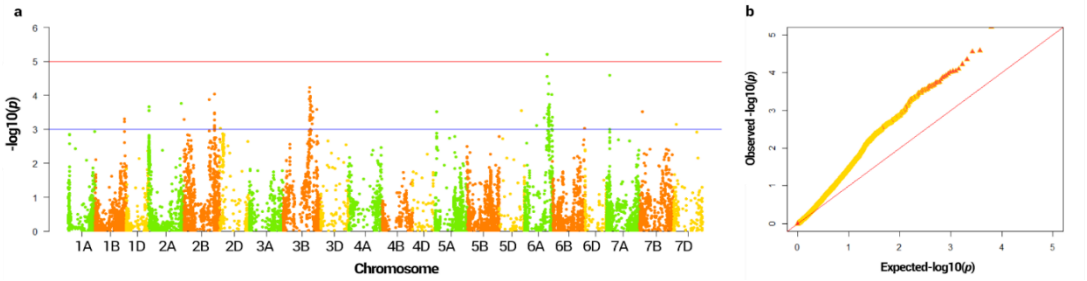


Figure 4.5. GWAS for grain yield using naïve model + Q_{1-4} (GLM_2) model: a) Manhattan plot with two -log_{10} *p-values* cut-offs (blue/red line) plotted against the chromosomes position and b) QQ plot with -log_{10} transformed p-values.

Using the mixed linear model considering as co-variates the principal component (PC), Q and/or K values (Table 4.4: MLM_{1-7}), a total of 71 MTAs, including co-located MTAs, with a -log_{10} *p-value* of 3 or higher (*P<0.001*) were detected which explained from 6 to 17% of the phenotypic variation. From the 16 traits analysed, 71 scored MTAs, with seven days after anthesis the stage with the largest number of associations detected. At the chromosome level chromosome 6 (18) scored the most MTAs compared to chromosome 4 which had the least (3). At genome level, 31 MTAs were found on genome A, then B with 33 and finally D with 7 (Table 4.5; Figure 4.6; Table S4.1).

Table 4.5. Summary of the marker-trait associations (MTAs) obtained on the HiBAP at GS65+7d and physiological maturity and their location at chromosome and genome level.

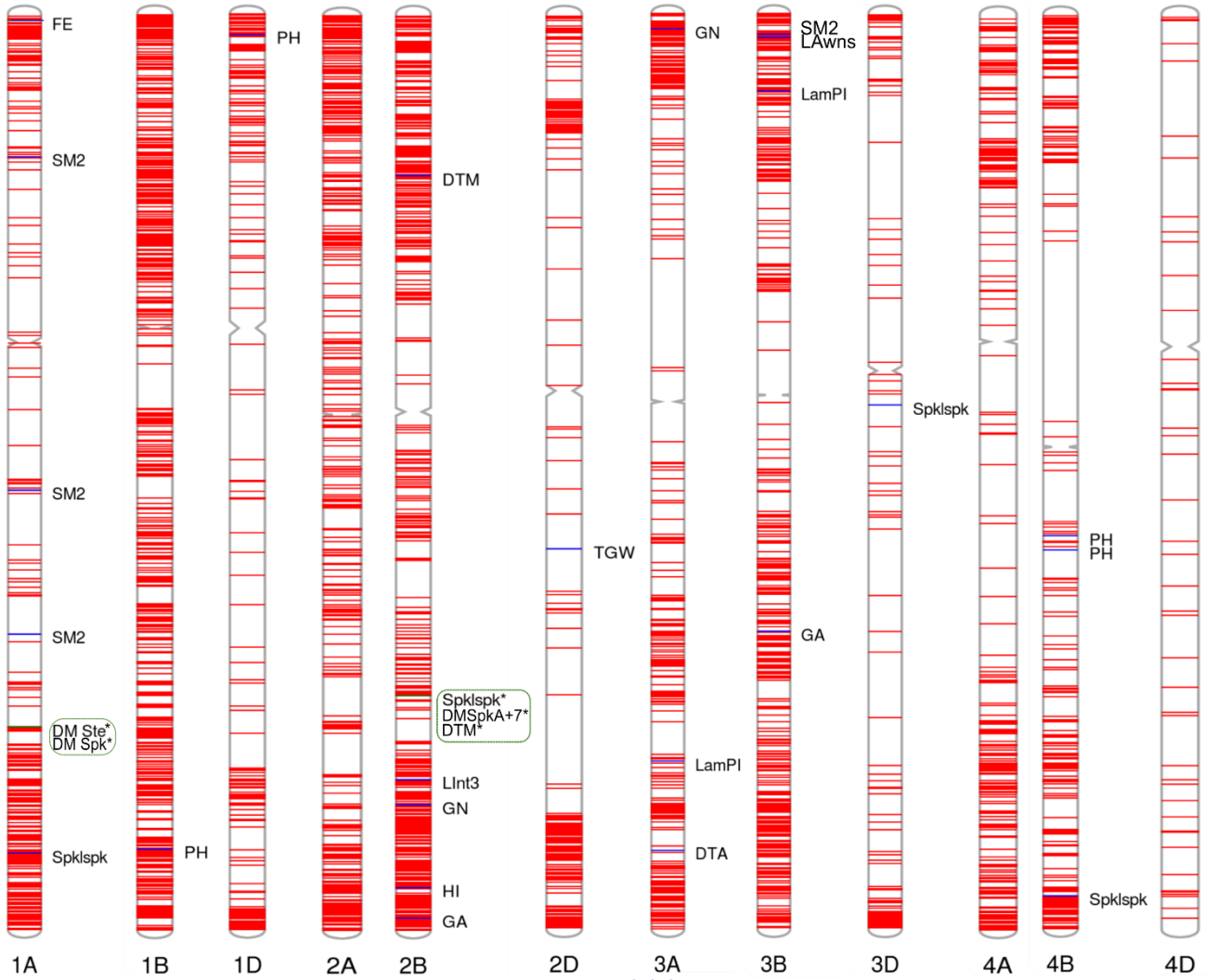
Stage	Trait	Total MTAs	Multitrait	Location	AveMarker R^2
Anthesis + 7days (GS65+7d)	DTA	2	1	3A(1), 6B(1)*	0.08
	DM Lam	2	0	6B(1), 6D(1)	0.09
	DM Spk	2	2	1A(1)*, 6B(1)*	0.09
	$DMSpk_{A+7}$	1	1	2B(1)*	0.09
	DM Ste	3	2	1A(1)*, 6B(2)*, 6D(1)*	0.02
	FE	2	-	1A(1), 5A(1)	0.08
	GA	7	-	2B(1), 3B(1), 5A(1), 6A(2), 7A(1)	0.09
	PH	5	-	1B(1), 1D(1), 4B(2), 6A(1)	0.08
	LamPI	4	-	3A(1), 3B(1), 5B(1), 7B(1)	0.10
	LnAwns	1	-	3B(1)	0.08
	LnInt3	1	-	2B(1)	0.09
	LnPed	1	-	7A(1)	0.08
	LnSpk	3	-	5A(1), 5B(1), 7A(1)	0.14
	SPI	1	-	7A(1)	0.09
	Spklspk	5	1	1A(1), 2B(1)*, 3D(1), 4B(1), 7A(1)	0.10
Physiological maturity (GS87)	$AGDM_{PM}$	6	2	5A(1)*, 6A(1), 7A(2)*, 7B (1), 7D(1)	0.10
	DTM	2	1	2B(2)*	0.09
	GN	3	1	2B(1), 3A(1), 7B(1)*	0.09
	HI	2	-	2B(1), 6A(1)	0.10
	SM2	7	1	1A(3), 3B(1), 6B(2)*, 7B(1)	0.09
	TGW	3	2	2D(1), 6D(1)*, 7B(1)*	0.08
	GY	3	2	5A(1)*, 6A(1), 7A(1)*	0.09

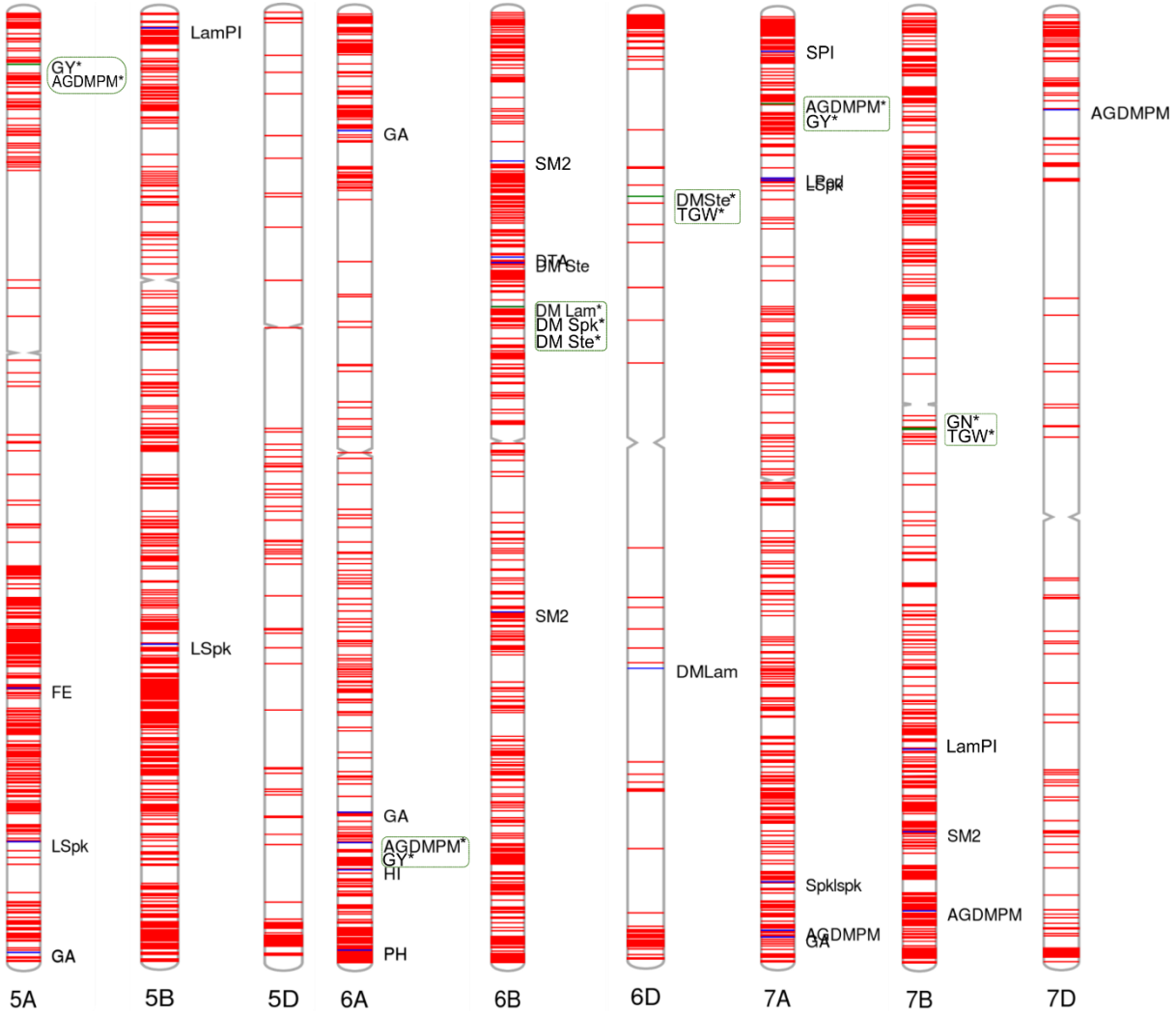
A+7: Anthesis + 7 days; **PM:** Physiological maturity; **DTA:** Days from emergence to anthesis; **AGDM:** Above-ground DM; **DM Lam:** Dry weight lamina; **LamPI:** Lamina partitioning index; **DM Spk:** Dry weight spike; **SPI:** Spike partitioning index; **DM Ste:** Dry weight stem; **StePI:** Stem partitioning index; **WSC**: Stem (true stem+leaf sheath) water-soluble carbohydrate; **$DMSpk_{A+7}$:** Spike DM at A+7d per unit area; **Spklspk:** Spikelets per spike; **GA:** Green area; **PH:** Plant height; **LnAwns :** Length awns; **LnPed :**Length peduncle; **LnInt2**: Length internode 2; **LnInt3**: Length internode 3; **DTM**: Days from emergence to physiological maturity; **FE**: Fruiting efficiency; **GY**: Grain yield (100% DM); **TGW**: Thousand grain weight; **HI**: Harvest index; **GN**: Grains per meter square; **SM2**: Spikes per meter square

*Multi-trait markers

At seven days after anthesis (GS65+7d), including those length-related, 41 markers were identified where 26 were recorded on physiological maturity. From this MTAs six were common MTAs for DM Spk/DM Ste (1A), $DMSpk_{A+7}$/Spklspk/DTM (2B), DM Lam/DM Spk/DM Ste/SM2 (6B), DM Ste/TGW (6D), $AGDM_{PM}$/GY (7A) and GN/TGW (7B).

Figure 4.6. Chromosomal locations of SNPs (red lines), single MTAs (blue lines) and multi-trait MTAs (green lines) identified on the HiBAP based on cross-year means in Y16 and Y17.




GY*
AGDMPM*
FE
LSpk
GA
LamPI
LSpk
GA
GA
AGDMPM*
GY*
HI
PH
SM2
DM Lam*
DM Spk*
DM Ste*
SM2
DMSte*
TGW*
DMLam
SPI
AGDMPM*
GY*
Spklspk
AGDMPM
GA
GN*
TGW*
LamPI
SM2
AGDMPM
AGDMPM
5A
5B
5D
6A
6B
6D
7A
7B
7D

With the position (base pair) of each marker Manhattan plots were generated for several traits to represent the major MTAs found. These plots show the distribution of each marker considering two $-\log_{10}$ *p-values* thresholds, $P<0.001$ shown by the blue line and $P<0.00001$ by the red line, across the seven chromosomes and three genomes. QQ plots were used to represent the distribution of observed and expected transformed p-values for each trait plotted on the Manhattan plot (Figures S4.2 a&b).

4.3.3. Candidate genes

The identification of candidate genes was done using a genome-scale knowledge network: KnetMiner which integrates agronomic data for gene discovery (Hassani-Pak et al., 2016). Potential candidates were identified using the MTAs as input considering especially the location of the MTA on the genome as this was the midpoint for the start and end position in the search bar (500,000 bp before the MTA actual position marked as start and 500,000 bp after the MTA as end point).

For some of the traits mentioned in this chapter ($AGDM_{PM}$, DTA, GN, SM2, spklspk), potential candidate genes were already reported by Molero et al. (2018). For the partitioning and length-related traits measured seven days after anthesis (not addressed by Molero et al., 2019) a total of 78 potential candidate genes over 12 traits were identified, of which 39 had a determined gene name, while the rest had an accession name/number assigned as several genes were linked (Table 4.6). For dry-matter accumulation at GS65+7d (DM spike, stem and lamina) most of the candidate genes found were related to stem WSC storage, heading time, lignin content, plant height, stem elongation. In the case of green area per shoot[1] several candidate genes were located on chromosome 6A associated with leaf size, curling, length, chlorophyll content and stomatal opening. For the MTAs on chromosome 7B for LamPI, candidate genes for spike fertility were found related to spike number, seed size, stem elongation and grain number. For length-related traits (PH, LnPed and LnInt3) genes were identified related to plant height, tiller number, storage and grain filling period.

Table 4.6. List of potential genes identified on the MTAs scored on the HiBAP using KnetMiner.

Trait	Chr	Gene name/Accession	Traits involved
DM Spk/ DM Ste	1A	AKT2	Stem elongation, storage, seed dormancy, stomatal opening, spikelet fertility
		PATL1	Storage
		PCBER1	Anthesis time, spike length, days to heading, floral organ identity
FE	1A	PNSL5	Stem elongation, seed size, plant height, stem length
		TRAESCS1A02G007600	Heading time
$DMSpk_{A+7}$	2B	TRAESCS2B02G417000 TRAESCS2B02G417100 TRAESCS2B02G417300 CCS	
GA	2B	TRAESCS2B02G612100	Leaf length, chlorophyll content, leaf shape
LamPI	3A	RABA2D TRAESCS3A02G364100	Photosynthetic rate, glucose content
GA	3B	TRAESCS3B02G351400 FH	
LamPI	3B	GTE8 TRAESCS3B02G103300 ATL63 TRAESCS3B02G103200 TRAESCS3B02G102800 URH2	Leaf role, leaf size, leaf curling, chlorophyll content
FE	5A	AKR2	Storage
		TRAESCS5A02G296900 TRAESCS5A02G295900 TRAESCS5A02G297000	Grain number
		LCAT3	Anthesis time
GA	5A	HSFC1 TRAESCS5A02G548700	Leaf size, chlorophyll content, leaf shape
LamPI	5B	LRR XI-23	Leaf thickness, leaf size, stomatal opening, leaf number, chlorophyll content, leaf shape
		CEPR1	Leaf length, starch mobilization, chlorophyll content, leaf shape
		TRAESCS5B02G012000 TRAESCS5B02G011300	
GA	6A	SPY	Leaf curling, stomatal opening, leaf shape
		HAC1	Leaf roll, leaf size, leaf gloss,
		PEX5	Chlorophyll content
		TULP2	Leaf curling, flag leaf width, stomatal opening
		SYP21	Leaf size, leaf roll
		ARID3	Flag leaf lamina width, stomatal opening, respiration rate, leaf number, water-use efficiency, chlorophyll content, specific leaf area
		AHL29	Leaf curling, specific leaf area, photosynthetic ability, leaf chlorophyll content, leaf position, leaf angle
		TRAESCS6A02G270800	
DM Spk/ DM Ste/ DM Lam/	6B	AGD12 TRAESCS6B02G190600	
		CCR2	Lignin content
		TRAESCS6B02G175400	Plant height
		TRAESCS6B02G190600	
DM Lam	6D	TRAESCS6D02G233200 APC8	
		TRAESCS6D02G233000	

Trait	Chr	Gene name/Accession	Traits involved
DM Ste	6D	TRAESCS6D02G127600	Stem elongation
SPI	7A	PAP24 TRAESCS7A02G102400 NAP1;1 TRAESCS7A02G101900	Spike number
LamPI	7B	RPA2A ERF7 TRAESCS7B02G343300 PAGR TRAESCS7B02G346700 ARF10 TRAESCS7B02G345300 RPM1 TRAESCS7B02G333100 TRAESCS7B02G335700 TRAESCS7B02G340300 ASNAP2	Leaf size Leaf width
PH	1D	WNK3 TRAESCS1D02G028300	Storage, plant height, relative growth rate, Plant height, tiller number
LnInt3	2B	ABCC15	Grain filling period
PH	6A	MYB112	Plant height
LnPed	7A	TRAESCS7A02G172400	Plant height

DM Spk: Dry weight spike (g per shoot^{-1}); **DM Ste:** Dry weight stem (g per shoot^{-1}); **DM Lam:** Dry weight lamina (g per shoot^{-1}); **FE:** Fruiting Efficiency (grains g^{-1}); **DMSpk$_{A+7}$:** Spike DM per unit area (g m^{-2}); **GA:** Green Area (cm^2 shoot^{-1}); **LamPI:** Lamina Partitioning Index; **PH:** Plant Height (cm); **LnInt3:** Length Internode 3 (cm); **LnPed:** Length Peduncle (cm)

4.4. Discussion

Wheat has three genomes, seven chromosomes and large segments of repetitive DNA (>80%) making the identification of genetic regions that underlie most complex traits challenging (Wang & Xia, 2015). Next-generation sequencing and current technology are expanding at accelerating rates allowing the discovery of genetic trait variation on novel traits (such as dry-matter partitioning) and its associations with SNPs with increasing speed, effectiveness and the introduction of new genetic backgrounds into breeding programs (Borrelli et al., 2015).

4.4.1. Genetic and phenotypic variation in the high biomass association panel

The HIBAP panel was comprised mainly of elite cultivars but also included synthetic-derivates, synthetic + landrace-derivatives and landrace-derivates. Cross-year results presented in Chapter 2 confirmed that the incorporation of the landrace and synthetic backgrounds into elite lines resulted in higher above-ground dry matter at physiological maturity ($AGDM_{PM}$) and grain weight, respectively. This is an example of how plant pre-breeding has widened genetic diversity increased variation and improving yield-related traits (Rebetzke et al., 2018). However, no yield advantage was observed due to decreased harvest index and grain number, coinciding with the results reported mainly at physiological maturity (harvest index and yield components) by Molero et al. (2019) using the same panel (HiBAP) and genotypic data.

Present results on this panel suggested that higher biomass at seven days after anthesis (GS65+7d) was associated with higher lamina partitioning (LamPI) in landrace-derived lines and higher stem partitioning (StePI) in synthetic-derived lines, resulting in both cases in relatively less investment in spike DM (SPI). The diverse and complex genetic structure of wheat landraces is an evolutionary response to survival and adaptation, especially under low potential growing conditions (Jaradat, 2011). By itself this type of genotype may not be a viable option for crossing directly into wheat programs due to unadapted backgrounds. However, the introduction of traits from landrace-derivates into modern cultivars could bring beneficial effects diversifying genetic pools providing it is not associated with the addition of undesired traits (Ozdemir et al., 2015). Synthetic wheat genotypes, crosses between durum wheat and wild goat grass, are designed and maintained to widen genetic variation for yield components, mainly at spike level (size, number, shape, length, etc) and to increase resistance to pathogens, diseases and abiotic stress (Breseghello & Sorrells, 2006; Li et al., 2014). Using 795 hexaploid wheat accessions, a combination of bread and spelt landraces in winter/spring material, Müller et al. (2018) suggested that novel traits such as frost tolerance, snow mould resistance and early maturing genes could be introduced into modern varieties to increase diversity and genetical stability. This will result in enrichment of adaptation alleles breaking the homogenous breeding cycle (Rebetzke et al., 2018).

Grain yield in the HIBAP panel was strongly correlated with above-ground DM at physiological maturity which explained more of the genetic variation in grain yield than harvest index. However, a trade-off was found between above-ground DM at physiological maturity ($AGDM_{PM}$) and harvest index (HI) suggesting that selecting for lines achieving greater biomass may not increase grain yield significantly unless HI can be maintained or ideally increased (Duan et al., 2018; Foulkes et al., 2007; Giunta et al., 2009). The positive relation found between $AGDM_{PM}$ and plant height may be partly a result of the planting system (raised bed) used as discussed in Chapter 2. In the HIBAP, taller plants had higher biomass, but this was associated with increased stem partitioning and lower HI. Overall plant height (PH) was not associated with grain yield. On semi-dwarf isogenic lines (*Rht* genes) Addisu et al. (2010) reported that semi-dwarfing alleles failed to increase yield but did increase HI which showed a trade-off with above-ground DM due to reduced light interception. Alternatively, another avenue to increase harvest index in high biomass backgrounds may be improving the fruiting efficiency (Sonder et al., 2017).

Results in this panel showed that spike partitioning index and fruiting efficiency were positively associated with harvest index and grain number which were both, in turn, linearly related with grain yield (see Chapter 2 for detailed discussion of the physiological determinants of SPI and FE). In summary, the association between spike partitioning index (SPI) and grain number could be related to more assimilates being available to the spike during the booting to anthesis period, enhancing floret survival and grains per spike (González et al., 2011). Higher SPI and

HI were each correlated with a shorter length of stem internode 2 and reduced DM partitioning to stem internode 2. Similar results were reported in a panel of modern high yielding CIMMYT spring wheat cultivars and advanced lines with high biomass expression (Rivera-Amado et al., 2019). Using winter wheat varieties under rainfed conditions, Chen et al. (2019) reported that the length of peduncle and stem internode 2 showed higher correlations with the spike weight than other internodes, particularly the peduncle. It could be the case that stem internode 2 and 3 compete more strongly with the spike for assimilate during the rapid spike growth phase from booting to anthesis than other internodes. Therefore, it is important to identify marker-trait associations for grain partitioning traits (spike fertility related) and stem internode lengths, specifically internode 2 and 3, to enhance yield potential through raise grain number, harvest index and grain yield.

4.4.2. Marker-trait associations

Genetic studies in wheat reporting on partitioning traits at flowering are limited, mainly using next-generation sequencing data. Having a high-quality wheat reference genome (IWSC, 2016) allows a better understanding of specific genomic regions regulating physiological traits and their interactions. Using the data collected over two seasons it was possible to link 42 genetic regions to 16 different traits explaining from 7 to 16% of the phenotypic variation. These results enabled the identification of candidate genes which could potentially be incorporated into breeding programs.

Detection of marker-trait associations through the use of high-quality phenotypic data and statistical methods have evolved as new sequencing platforms are allowing more precise data. Several statistical methods have been developed using different covariates to increase the power of GWAS analysis enabling recognition of small effects caused by complex traits eliminating false-positive associations between markers and phenotypic information (Zhang et al., 2010). This improvement could be achieved by incorporating multiple backgrounds as a random effect in a mixed model, taking into consideration relatedness and similarities between individuals avoiding spurious association caused by differences in relatedness between pairs of individuals (Li et al., 2014; Singh & Singh, 2015). In the present study with the use of the general linear model, a higher number of MTAs were obtained compared to the model in which the population structure was considered. More precise MTAs were scored using a mixed linear model (MLM) where different variables were tested to see how the interaction between the relatedness and different levels of population structure affect the detection of market-phenotype association. Similarly, Bordes et al. (2014) for two doubled-haploid populations population reported 194 MTAs associated with grain yield (scored on 1BS, 3B, 6A and 7B) and 134 for heading data (scattered across the wheat genome, except for 4B and 5D), where MLM improved the power of the study. This last model was found to be the most efficient. Liu et al. (2015) using 322 *Ae. tauschii* accessions reported 12,444 significant markers for phosphorus-deficiency-tolerance traits were detected by the GLM and 28 by MLM from which just 18 were

detected by both methods (threshold: − log10(p) = 3.84). In this study from the 118 MTA detected through MLM 79 also detected using the GLM (naïve).

In the HIBAP, the present analysis was able to detect novel genetic regions on 1A, 2B, 7A and 7B related to grain partitioning traits for potential application in breeding for yield potential. Furthermore, several studies have been published on phenology, biomass, plant height, and yield-related MTAs identified using different genotypes of wheat under different environmental conditions, agreeing with results found in this study. Using different wheat accessions (landraces, synthetics and advanced) under rainfed conditions, Wolters et al. (2019) reported MTAs for plant height (6A) and grain yield (5A) which were consistent with the MTAs found for the HiBAP. In soft wheat lines grown in the mid-Atlantic and Midwest USA regions several MTAs were reported for grain number (7B), days to maturity (2B), spikes per unit area (1A), thousand-grain weight (6D and 7B) and grain yield (6A and 7A) (Ward et al., 2019), similarly to those detected in the current panel.

For the MTAs for length-related traits identified in the HiBAP, previous studies have reported similarly positioned loci for plant height (1B and 4B), length peduncle (7A) and length spike (7A) (Ogbonnaya et al., 2017; Turuspekov et al., 2017). However, the present study is the first where loci are reported for spike fertility-related traits (DM spike, fruiting efficiency and spike partitioning index), stem internode 3 length, awns length and for green area per shoot at GS65+7d. The identification of these new MTAs hopefully will be corroborated in further studies. Wang et al. (2017) reported MTAs for flag-leaf stay green on 6A and 7A which may correspond with the MTAs reported in this panel for green area per shoot on 6A and 7A.

In the present study co-located MTAs were identified on 1A for spike DM per shoot and stem DM per shoot at GS65+7d and on 2B for spike DM per unit area ($DMSpk_{A+7}$) and spikelets per spike (spklspk). The competition between plant components for assimilates during stem elongation could mechanistically explain the co-located MTAs found on 1A and 2B. The MTA on 1A may be similar to an MTA for spike length of the main shoot at anthesis reported by Guo et al. (2018) who concluded that manipulating this trait (under genetic control) specific developmental stages could increase spike DM in wheat. The MTA on chromosome 2B for $DMSpk_{A+7}$ and spikelets per spike could be related to the *Ppd-B1* locus for photoperiod sensitivity on chromosome 2BS in wheat (Ammar et al., 2017). Detailed study needs to be done to corroborate this MTA, but selecting the right allelic combination at *Ppd-1* loci to optimise the phenology and grain partitioning could be important to maximise grain yield. At physiological maturity co-located MTAs for above-ground DM and grain yield were found on both 5A and 7A and co-located MTAs for number and thousand-grain weight were found on 7B. For co-located association among grain yield and above-ground DM there is evidence that gene/genes clusters have a pleiotropic effect on source traits and overall yield in winter wheat (Mason et al., 2013).

4.4.3. Next steps: marker-trait validation

New high-sequencing tools and high-throughput phenotype platforms have enabled the identification and discovery of specific genomic regions underlying complex traits resulting in more genetic gain compared to standard phenotypic selection (Crain et al., 2018). This progress goes hand in hand with the incorporation of databases such as Knetminer permitting the identification of putative genes near the MTAs scored bringing the possibility to accelerate gene discovery using PCR-KASP (Kompetitive Allele Specific PCR). In wheat some reports have already been published, Kumar et al. (2019) reported at least two regions controlling grain texture (*Qssoft.wwql-4B.1 and Qssoft.wwql-5A.1*), Rasheed et al. (2016) developed and validated KASP involved in grain traits, disease resistance and grain-bread making quality. For disease related, Mu et al. (2019) and Mago et al. (2019) reported on stripe and stem rust resistance genes located on 1DS and 6D, respectively. As mentioned above, research on grain partitioning traits in wheat is limited. From the present results, the generation of KASP markers could be developed for key traits, and their haplotypes determined and validated in at least one DH mapping population. Validation could be done by phenotyping those genotypes that express the haplotype for the desired trait and lately the genotype with the desired trait could be incorporated into breeding programs using the pyramid crossing scheme suggested by (Reynolds et al., 2017).

Candidate genes reported in this study require further validation, by generation and characterization of mutant genotypes, before their introduction into breeding programs, as for some of the regions, not enough information is presently available in wheat. For some MTAs for co-located traits such as DM spk/DM ste/DM lam, further study is required to investigate whether they represent pleiotropic effects of a single gene or effects of two or more closely linked genes. The use of TILLING (Targeting Induced Local Lesions In Genomes) mutants will allow the validation of different alleles of the candidate genes reported and the generation of KASP markers.

Such markers could significantly accelerate the characterization of crossing parents as well as advanced lines in marker-assisted selection and can complement the inflexible, high-density SNP arrays (Rasheed et al., 2016). The incorporation of these partitioning-based traits into breeding programs, such as stem-partitioning indices, internode lengths and fruiting efficiency, has significant scope to accelerate gains in harvest index and yield potential.

4.5. Conclusions

- Genetic variation and medium to high heritability values were recorded for the partitioning traits measured at GS65+7d and physiological maturity.
- Fruiting efficiency, spike partitioning index (SPI) and grain number (GN) showed a positive linear association with harvest index which, in turn, was linearly related with grain yield.

- Higher spike partitioning index and harvest index were associated with a shorter relative length of stem internode 2 (internode below peduncle) and reduced dry-matter partitioning to stem internode 2.
- The implementation of covariates into genetic analysis increased the accuracy and power of the association.
- A significant number of novel marker traits associations, mainly for DM partitioning and spike fertility, (1A, 2B, 5A, 6A, 6B and 7A) were stable among grain partitioning traits measured at GS65+7d and physiological maturity.
- Marker traits associations were identified providing useful genetic information for the location of potential candidate genes such as DM spike, DM stem, lamina partitioning index, fruiting efficiency (chromosome 1, 5 and 7) which will be useful for further fine-mapping of the target genes.

4.6. Supplementary material

Table S4.1. Cross-year (Y16 and Y17) significant SNPs for traits at GS65+7d and physiological maturity using a genome-wide association analysis (GWAS).

Stage	Trait	Marker	Chr	Pos (bp)	p-value	Log trans	Marker R^2
Anthesis + 7 days (GS65+7d)	DTA	AX-95087924	3A	686127775	9.32E-04	3.03	0.08
		AX-94443799	6B	185673725	4.57E-04	3.34	0.09
	DM Lam	AX-95119680*	6B	223259475	8.11E-04	3.09	0.09
		AX-94676072	6D	327365593	6.97E-04	3.16	0.09
	DM Spk	AX-94413932*	1A	462794136	6.38E-04	3.20	0.08
		AX-95119680*	6B	223259475	4.03E-04	3.39	0.10
	$DM\ Spk_{A+7}$	AX-94836731*	2B	596412191	5.10E-04	3.29	0.09
	DM Ste	AX-94740723	6B	189296798	3.26E-04	3.49	0.10
		AX-95195224	6D	91390591	2.91E-04	3.54	0.10
		AX-94413932*	1A	462794136	6.98E-04	3.16	0.08
		AX-95119680*	6B	223259475	2.56E-04	3.59	0.10
	FE	AX-95259248	1A	4063342	7.06E-04	3.15	0.08
		AX-94536798	5A	504778781	8.45E-04	3.07	0.08
		AX-94882514	2B	790751816	2.96E-04	3.53	0.09
	GA	AX-94770277	3B	561094873	6.17E-04	3.21	0.08
		AX-94560945	5A	702461319	0.00102	2.99	0.08
		AX-94974293	6A	520354792	3.81E-04	3.42	0.09
		AX-95660165	6A	76523894	5.75E-04	3.24	0.08
		AX-94512150	7A	717823111	7.93E-04	3.10	0.09
	LamPI	AX-94481094	3A	613393005	4.56E-04	3.34	0.09
		AX-94857800	3B	69818526	0.00101	3.00	0.08
		AX-94570703	5B	11456877	1.42E-05	4.85	0.14
	SPI	AX-94635917	7B	603340669	1.53E-04	3.81	0.10
		AX-95079601	7A	62527487	6.71E-04	3.17	0.09
	Spklspk	AX-94651424	1A	544723326	9.35E-05	4.03	0.11

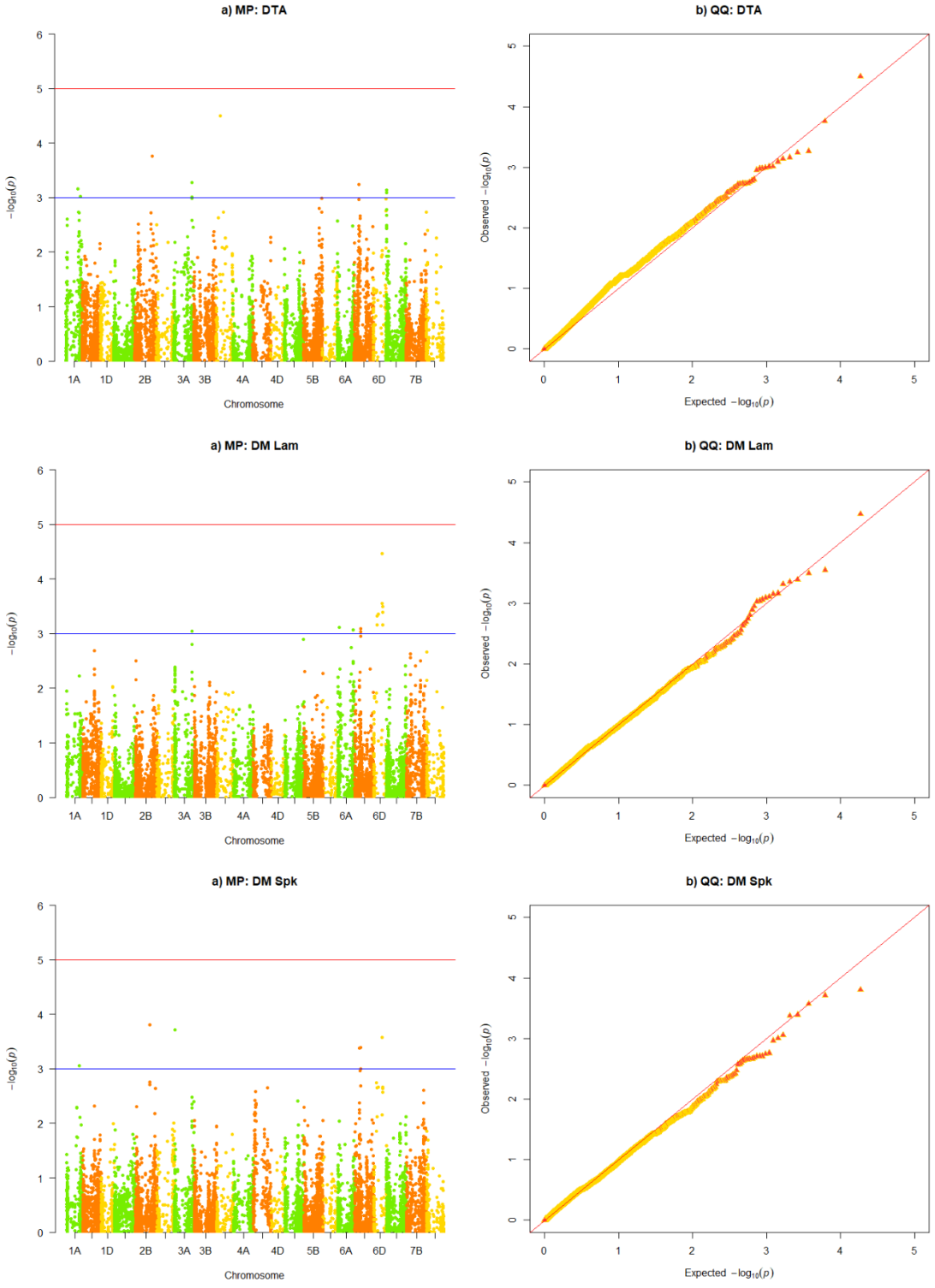
	AX-94552356	3D	263354244	7.93E-04	3.10	0.09
	AX-95173991	4B	649492569	1.48E-04	3.83	0.10
	AX-94512826	7A	674277268	9.69E-05	4.01	0.11
	AX-94836731*	2B	596412191	3.84E-04	3.42	0.09
	AX-94661194	1B	628795065	4.51E-04	3.35	0.09
	AX-94825835	1D	11049882	7.61E-04	3.12	0.07
PH	AX-94880955	4B	384292938	9.40E-04	3.03	0.07
	AX-94980498	4B	394603091	9.36E-04	3.03	0.07
	AX-94554119	6A	610348953	2.27E-04	3.64	0.09
LAwns	AX-94537116	3B	18559056	7.58E-04	3.12	0.08
LInt3	AX-94680690	2B	669347094	6.59E-04	3.18	0.09
LPed	AX-94411551	7A	126951591	7.50E-04	3.12	0.08
	AX-95132498	5A	619685320	4.77E-06	5.32	0.15
LSpike	AX-94539975	5B	474973041	5.39E-06	5.27	0.16
	AX-94916259	7A	129260071	9.36E-05	4.03	0.11

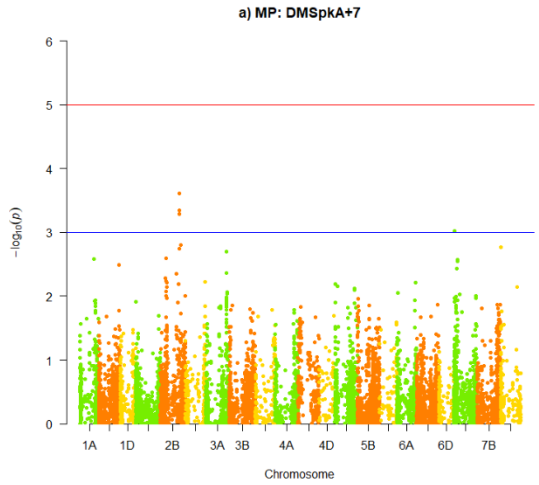
Stage	Trait	Marker	Chr	Pos (bp)	p-value	Log trans	Marker R^2
Physiological Maturity (GS87)	$AGDM_{PM}$	AX-94522599	6A	539866180	3.33E-04	3.48	0.09
		AX-94958668	7A	712423177	5.48E-04	3.26	0.09
		AX-94494622	7B	709528334	6.10E-04	3.21	0.09
		AX-94880213	7D	64270964	4.40E-04	3.36	0.09
	DTM	AX-95158872*	5A	37836752	2.53E-04	3.60	0.10
		AX-94525122*	7A	68846954	9.16E-05	4.04	0.12
		AX-94836731*	2B	596412191	5.54E-04	3.26	0.09
		AX-95685212	2B	141641152	4.38E-04	3.36	0.09
	GN	AX-94461881	2B	691780758	7.76E-05	4.11	0.12
		AX-94385986	3A	12778481	9.15E-04	3.04	0.08
		AX-95192986*	7B	328802260	4.58E-04	3.34	0.08
	HI	AX-94728242	2B	763862898	6.17E-04	3.21	0.08
		AX-94546552	6A	557715847	5.59E-05	4.25	0.12
	SM2	AX-94630858	1A	92567883	1.74E-04	3.76	0.10
		AX-94873875	1A	308813822	5.23E-04	3.28	0.08
		AX-94404955	1A	402232673	9.12E-04	3.04	0.07
		AX-94512327	3B	21331548	0.00025	3.60	0.11
		AX-95119680	6B	223259475	1.41E-04	3.85	0.11
		AX-94913939	7B	647148119	5.47E-04	3.26	0.09
	TGW	AX-94659739	2D	381335181	0.00166	2.78	0.07
		AX-95195224	6D	91390591	2.30E-04	3.64	0.10
		AX-95192986*	7B	328802260	8.35E-04	3.08	0.08
	GY	AX-94518269	6A	596085114	3.37E-04	3.47	0.10
		AX-95158872*	5A	37836752	7.69E-04	3.11	0.08
		AX-94525122*	7A	68846954	3.22E-04	3.49	0.10

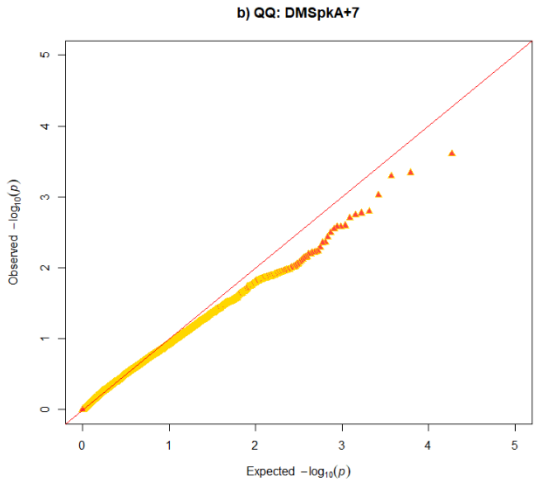
A+7: Anthesis + 7 days; **PM:** Physiological maturity; **DTA:** Days from emergence to anthesis; **AGDM:** Above-ground DM; **DM Lam:** Dry weight lamina; **LamPI:** Lamina partitioning index; **DM Spk:** Dry weight spike; **SPI:** Spike partitioning index; **DM Ste:** Dry weight stem; **StePI:** Stem partitioning index; **WSC**: Stem (true stem+leaf sheath) water-soluble carbohydrate; **$DMSpk_{A+7}$:** Spike DM at A+7d per unit area; **Spklspk:** Spikelets per spike; **GA:** Green area; **PH:** Plant height; **LnAwns :** Length awns; **LnPed :**Length peduncle; **LnInt2**: Length internode 2; **LnInt3**: Length internode 3; **DTM**: Days from emergence to physiological maturity; **FE**: Fruiting efficiency; **GY**: Grain yield (100% DM); **TGW**: Thousand grain weight; **HI**: Harvest index; **GN**: Grains per meter square; **SM2**: Spikes per meter square

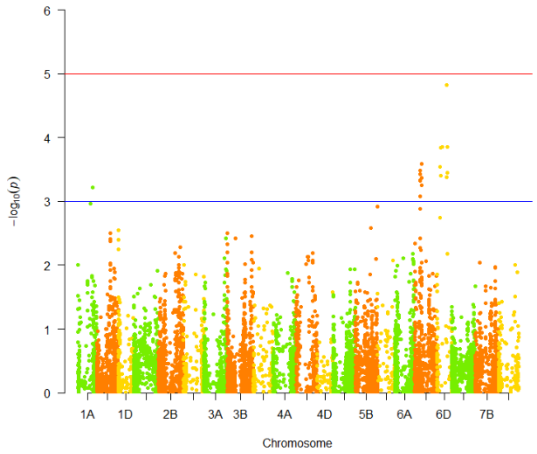
*Multi-trait markers

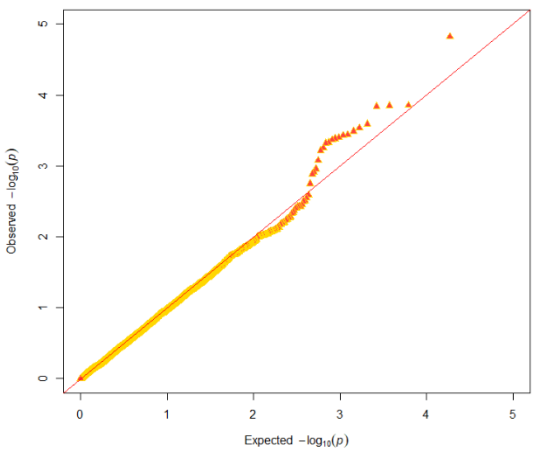
Figure S4.2. Manhattan and QQ plots generated for different traits analyzed using MLM models.

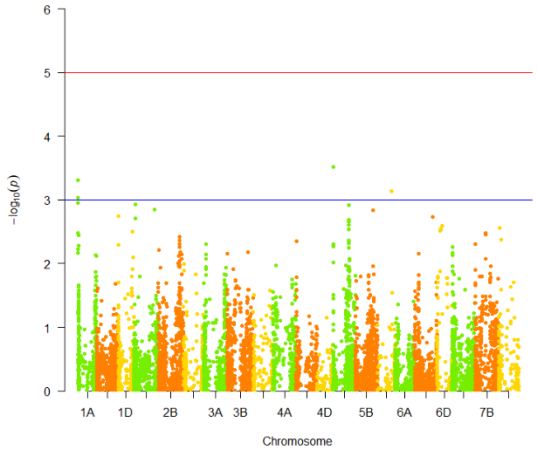


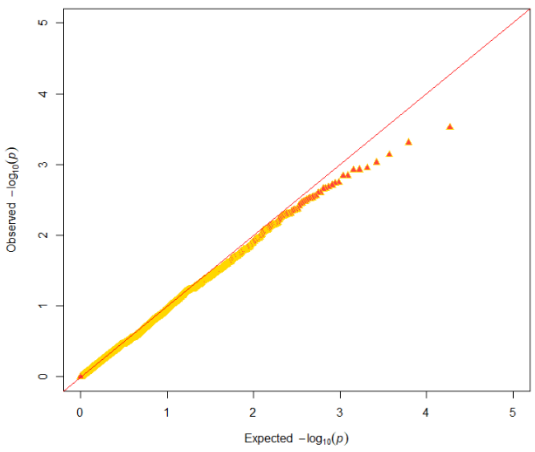

a) MP: DMSpkA+7
$-\log_{10}(p)$
0
1
2
3
4
5
6
1A
1D
2B
3A
3B
4A
4D
5B
6A
6D
7B
Chromosome

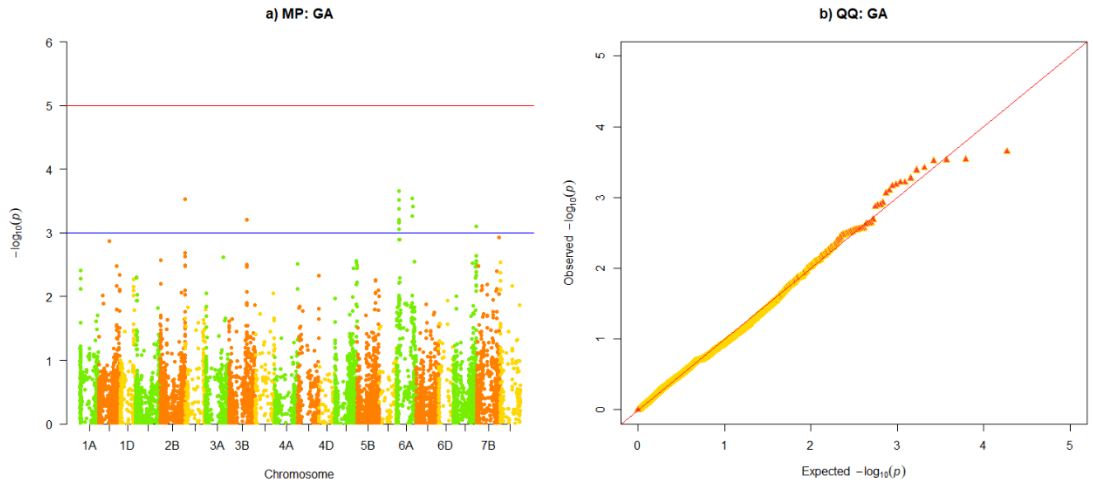

b) QQ: DMSpkA+7
Observed $-\log_{10}(p)$
Expected $-\log_{10}(p)$
0
1
2
3
4
5

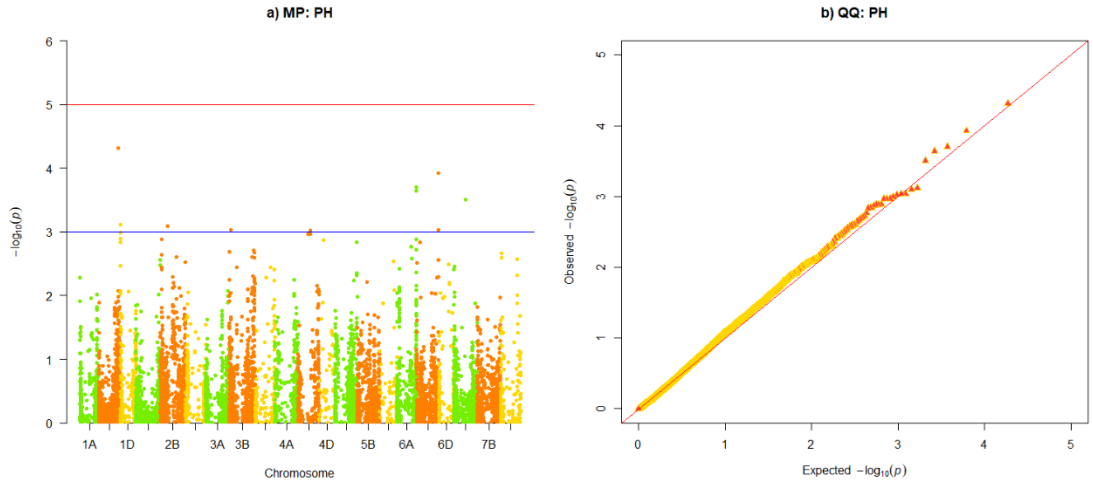

a) MP: DM Ste
$-\log_{10}(p)$
0
1
2
3
4
5
6
1A
1D
2B
3A
3B
4A
4D
5B
6A
6D
7B
Chromosome

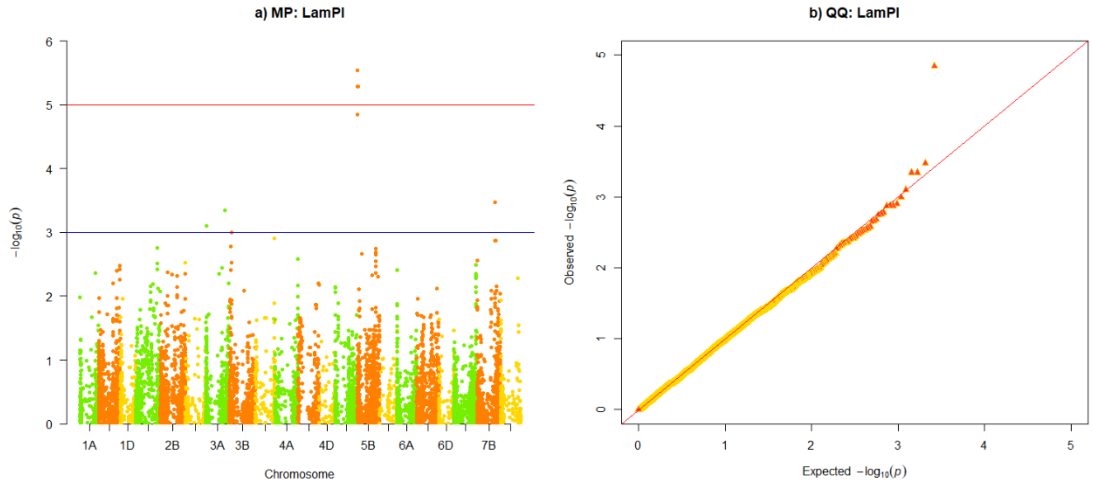

b) QQ: DM Ste
Observed $-\log_{10}(p)$
Expected $-\log_{10}(p)$
0
1
2
3
4
5

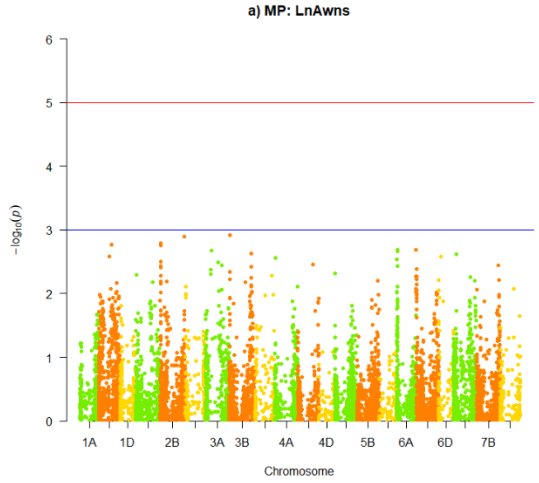

a) MP: FE
$-\log_{10}(p)$
0
1
2
3
4
5
6
1A
1D
2B
3A
3B
4A
4D
5B
6A
6D
7B
Chromosome

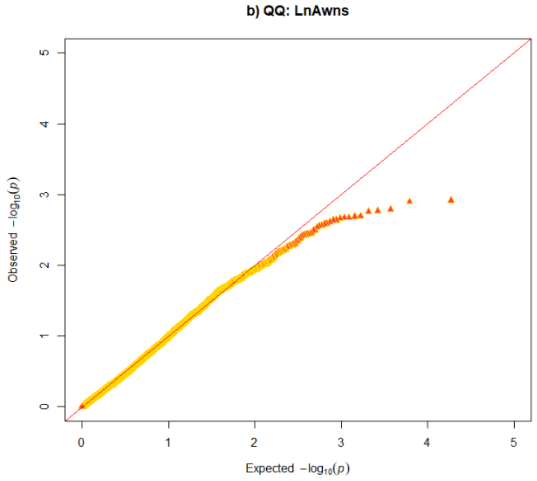

b) QQ: FE
Observed $-\log_{10}(p)$
Expected $-\log_{10}(p)$
0
1
2
3
4
5

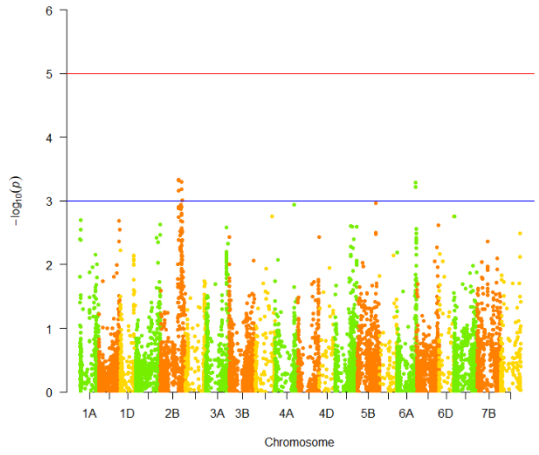

a) MP: GA
b) QQ: GA
$-\log_{10}(p)$
Chromosome
1A 1D 2B 3A 3B 4A 4D 5B 6A 6D 7B
Observed $-\log_{10}(p)$
Expected $-\log_{10}(p)$

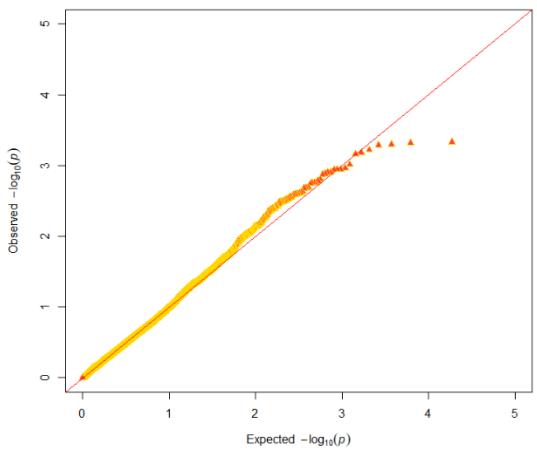

a) MP: PH
b) QQ: PH
$-\log_{10}(p)$
Chromosome
1A 1D 2B 3A 3B 4A 4D 5B 6A 6D 7B
Observed $-\log_{10}(p)$
Expected $-\log_{10}(p)$

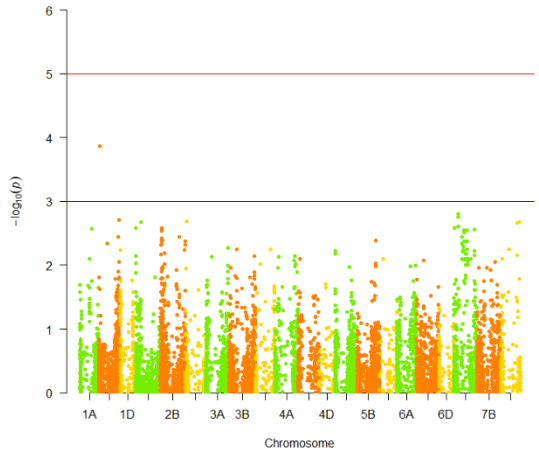

a) MP: LamPl
b) QQ: LamPl
$-\log_{10}(p)$
Chromosome
1A 1D 2B 3A 3B 4A 4D 5B 6A 6D 7B
Observed $-\log_{10}(p)$
Expected $-\log_{10}(p)$

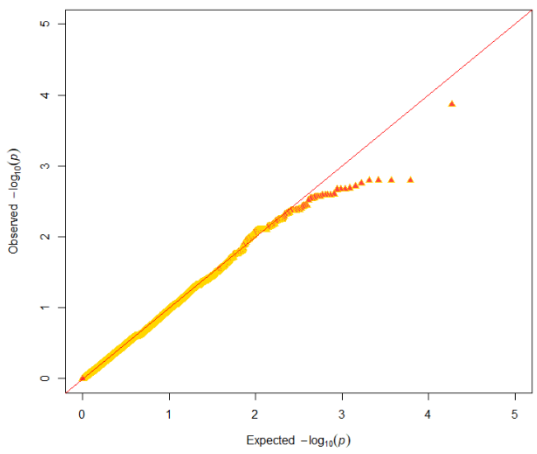

a) MP: LnAwns
$-\log_{10}(p)$
1A 1D 2B 3A 3B 4A 4D 5B 6A 6D 7B
Chromosome

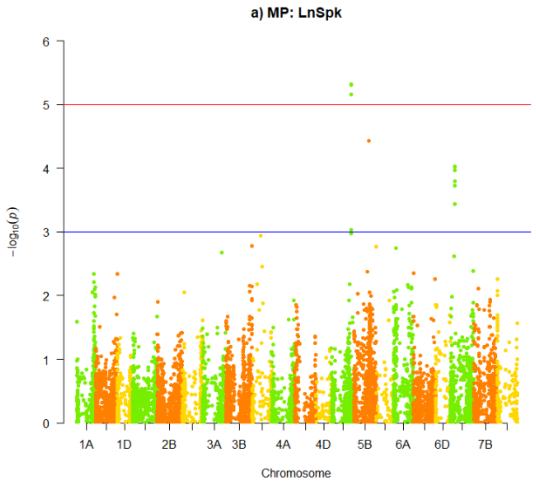

b) QQ: LnAwns
Observed $-\log_{10}(p)$
Expected $-\log_{10}(p)$

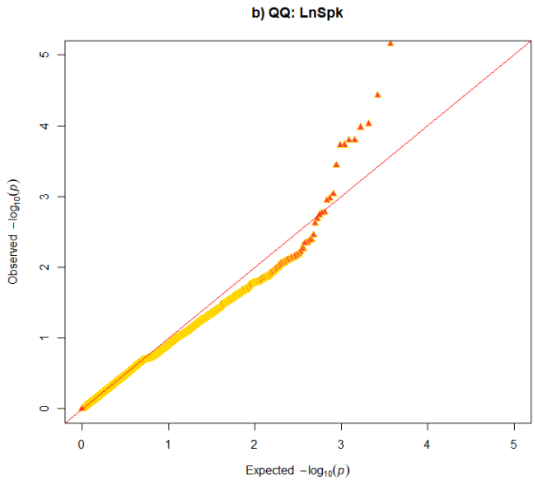

a) MP: LnInt3
$-\log_{10}(p)$
1A 1D 2B 3A 3B 4A 4D 5B 6A 6D 7B
Chromosome

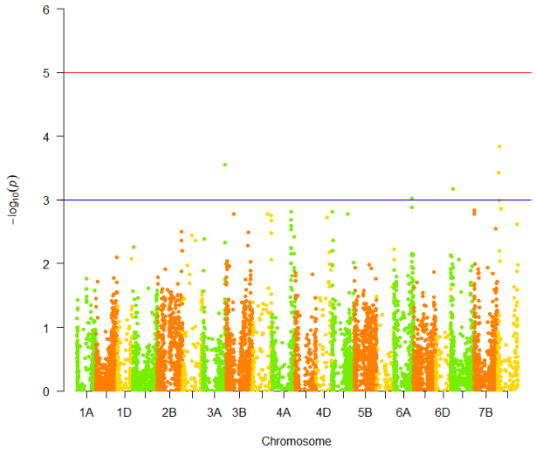

b) QQ: LnInt3
Observed $-\log_{10}(p)$
Expected $-\log_{10}(p)$

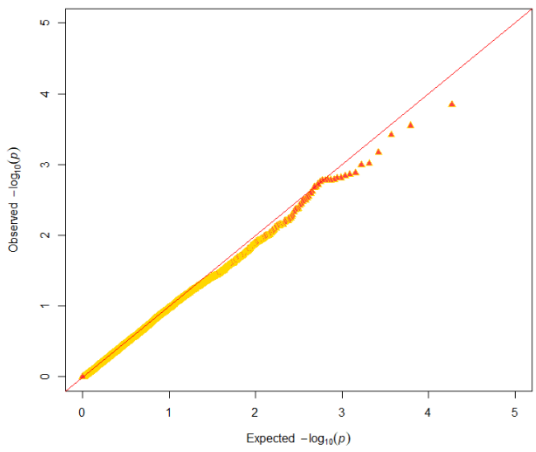

a) MP: LnPed
$-\log_{10}(p)$
1A 1D 2B 3A 3B 4A 4D 5B 6A 6D 7B
Chromosome

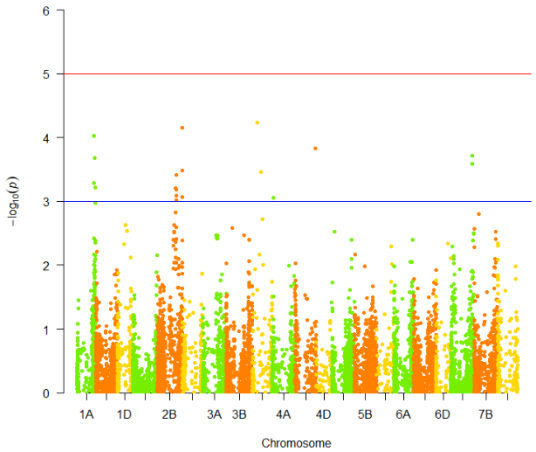

b) QQ: LnPed
Observed $-\log_{10}(p)$
Expected $-\log_{10}(p)$

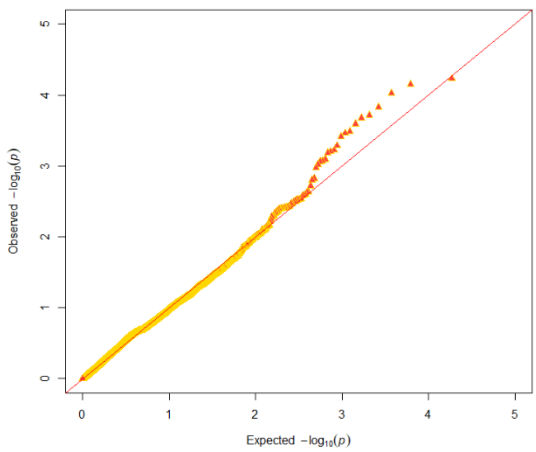

a) MP: LnSpk
$-\log_{10}(p)$
0
1
2
3
4
5
6
1A
1D
2B
3A
3B
4A
4D
5B
6A
6D
7B
Chromosome

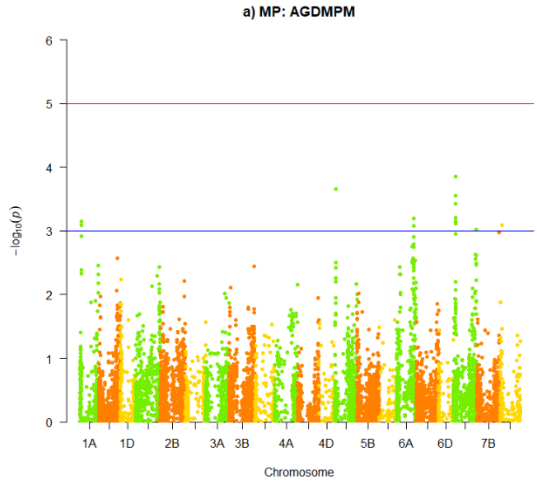

b) QQ: LnSpk
Observed $-\log_{10}(p)$
Expected $-\log_{10}(p)$
0
1
2
3
4
5

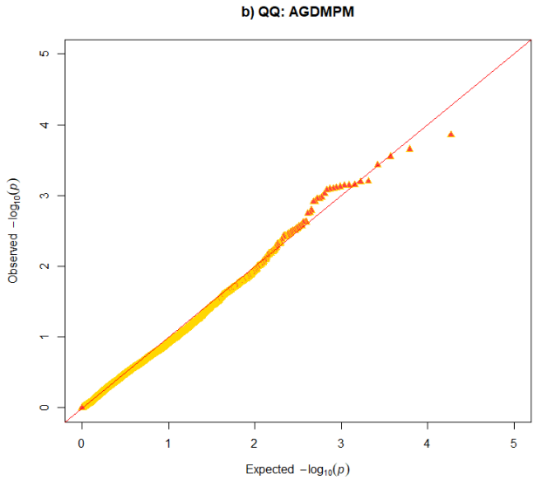

a) MP: SPI
$-\log_{10}(p)$
0
1
2
3
4
5
6
1A
1D
2B
3A
3B
4A
4D
5B
6A
6D
7B
Chromosome

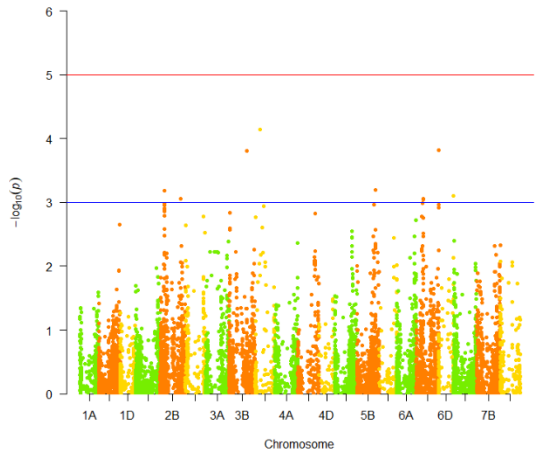

b) QQ: SPI
Observed $-\log_{10}(p)$
Expected $-\log_{10}(p)$
0
1
2
3
4
5

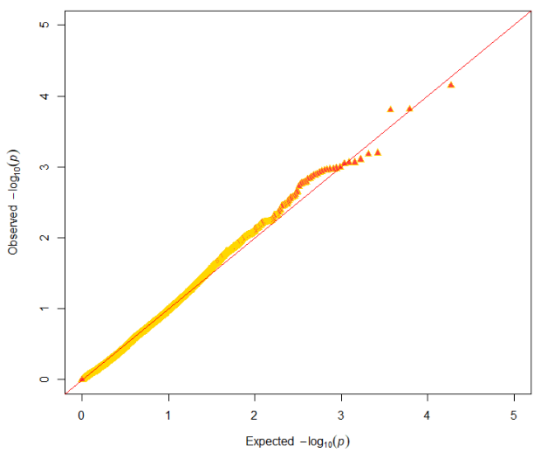

a) MP: SpkIspk
$-\log_{10}(p)$
0
1
2
3
4
5
6
1A
1D
2B
3A
3B
4A
4D
5B
6A
6D
7B
Chromosome

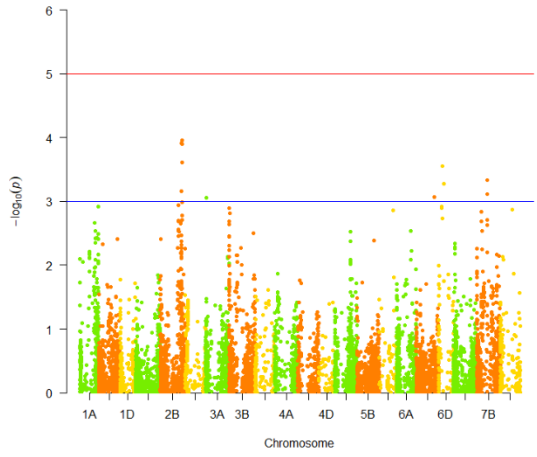

b) QQ: SpkIspk
Observed $-\log_{10}(p)$
Expected $-\log_{10}(p)$
0
1
2
3
4
5

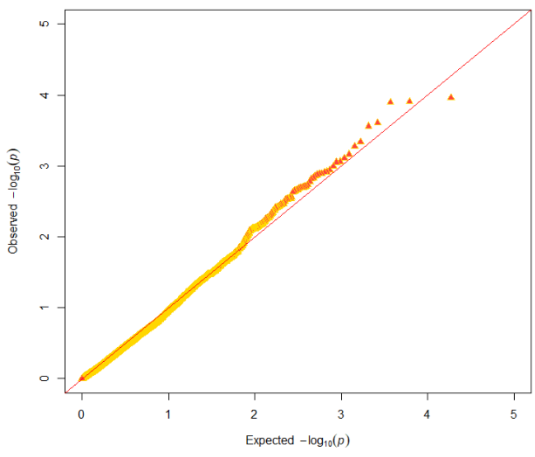

a) MP: AGDMPM
$-\log_{10}(p)$
0
1
2
3
4
5
6
1A
1D
2B
3A
3B
4A
4D
5B
6A
6D
7B
Chromosome

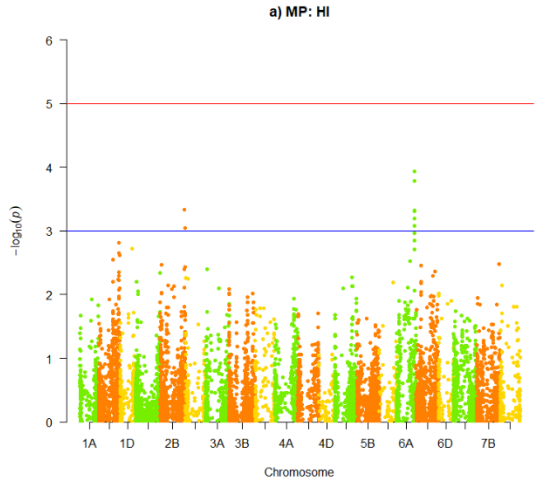

b) QQ: AGDMPM
Observed $-\log_{10}(p)$
Expected $-\log_{10}(p)$
0
1
2
3
4
5

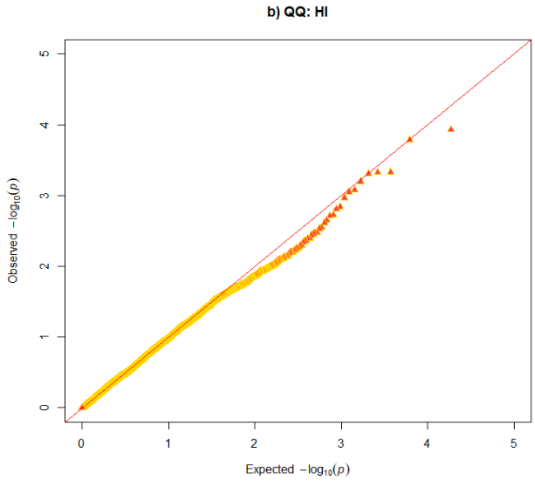

a) MP: DTM
$-\log_{10}(p)$
0
1
2
3
4
5
6
1A
1D
2B
3A
3B
4A
4D
5B
6A
6D
7B
Chromosome

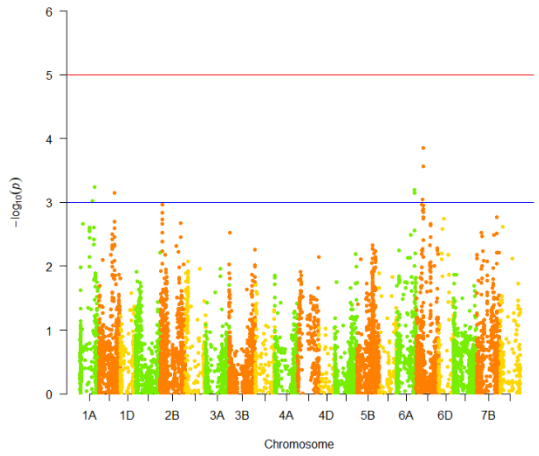

b) QQ: DTM
Observed $-\log_{10}(p)$
Expected $-\log_{10}(p)$
0
1
2
3
4
5

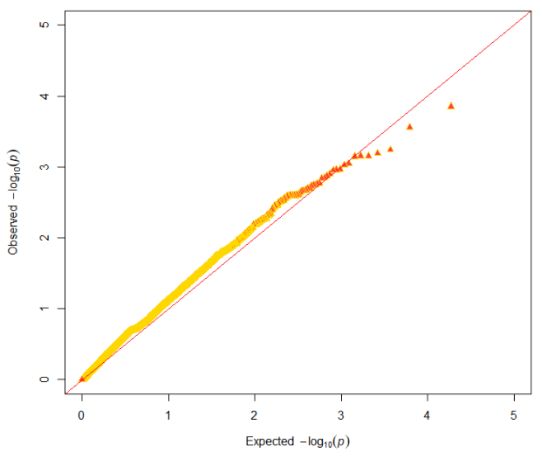

a) MP: GN
$-\log_{10}(p)$
0
1
2
3
4
5
6
1A
1D
2B
3A
3B
4A
4D
5B
6A
6D
7B
Chromosome

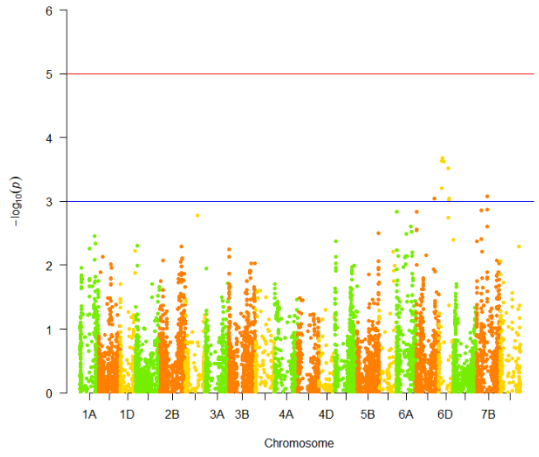

b) QQ: GN
Observed $-\log_{10}(p)$
Expected $-\log_{10}(p)$
0
1
2
3
4
5

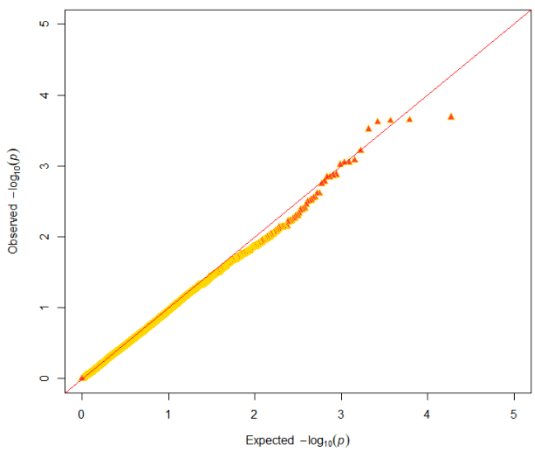

a) MP: HI
−log10(p)
Chromosome
1A 1D 2B 3A 3B 4A 4D 5B 6A 6D 7B

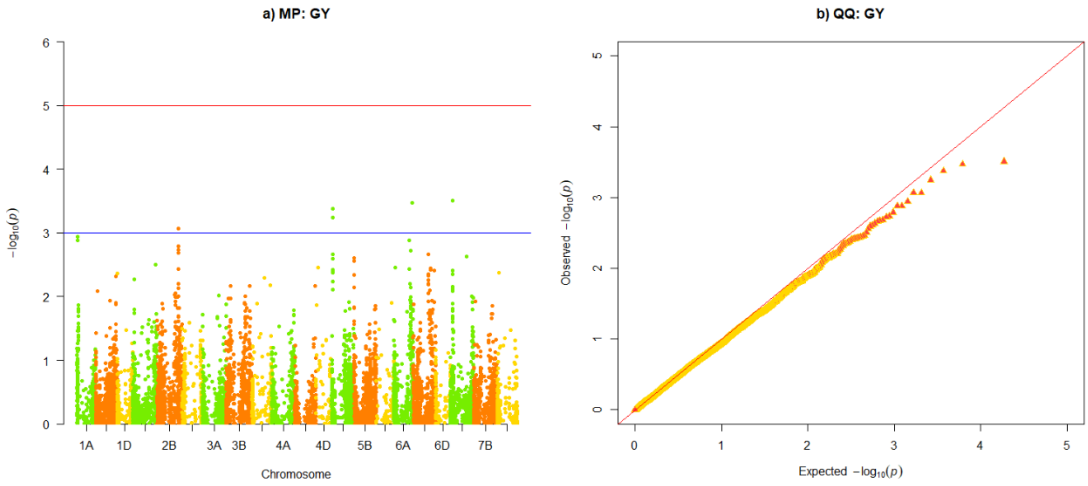

b) QQ: HI
Observed −log10(p)
Expected −log10(p)


a) MP: SM2
−log10(p)
Chromosome
1A 1D 2B 3A 3B 4A 4D 5B 6A 6D 7B


b) QQ: SM2
Observed −log10(p)
Expected −log10(p)


a) MP: TGW
−log10(p)
Chromosome
1A 1D 2B 3A 3B 4A 4D 5B 6A 6D 7B


b) QQ: TGW
Observed −log10(p)
Expected −log10(p)


a) MP: GY
b) QQ: GY
$-\log_{10}(p)$
Chromosome
1A
1D
2B
3A
3B
4A
4D
5B
6A
6D
7B
Observed $-\log_{10}(p)$
Expected $-\log_{10}(p)$

5. Characterization of partitioning and yield-related QTL in a doubled haploid winter wheat population

Winter wheat mostly grown under rain-fed conditions is vulnerable to climate change as any other crop. The implementation of new sequencing technologies has allowed the detection of genetic regions behind complex traits, but still progress needs to be done to optimize the partitioning of biomass to the grain to boost genetic gains in wheat. The use of marker-assisted selection opens avenues to selection for grain partitioning traits in breeding programs where measurements are time-consuming, and high-throughput phenotypic methods are not presently available.

Using 94 doubled-haploid lines derived from parents characterized as moderate/high (Rialto) and high (Savannah) yield potential, dry matter partitioning traits at seven days after anthesis (GS65+7d) and physiological maturity (PM) were assessed during two seasons (Y16: 2015-16 and Y17: 2016-17). Using the phenotypic data collected a quantitative trait loci (QTL) analysis of grain-partitioning traits was carried. A total of 80 QTL were identified of which 54 corresponded to GS65+7d traits (spike fertility, DM distribution, length-related, crop development) and the rest to physiological maturity (AGDM, GN, HI, GY). The present analysis revealed a QTL cluster on chromosome 3A at 69.4-94.5 cM which could play a crucial role in spike DM partitioning at GS65+7d and optimizing DM partitioning amongst the stem internodes. Markers found in this population will eventually facilitate further studies for fine mapping, candidate gene discovery and marker-assisted selection (MAS) in wheat breeding.

**This chapter will be submitted to a high impact journal, where authors contributed equally to the work presented.

Aleyda Sierra-Gonzalez[ab], Gemma Molero[b], Carolina Rivera-Amado[b], Matthew Reynolds[b] and John Foulkes[a]

[a]*Division of Plant and Crop Sciences, School of Biosciences, University of Nottingham, Leicestershire, LE12 5RD, UK*

[b]*CIMMYT International Maize and Wheat Improvement Center (CIMMYT), Km. 45, Carretera Mexico, El Batan, Texcoco, Mexico*

5.1. Introduction

Wheat contributes 153,800 MT (megatonne) per annum to global cereal yield production in Europe (USDA, 2019), but a significant increase in crop productivity is needed to satisfy the predicted demand considering the various challenges presented, such as climate change and population growth (Semenov et al., 2014). Yield potential can be explained as the product of light interception, radiation-use efficiency (RUE) and harvest index (HI) which requires favourable environmental conditions and good agronomic practices to maximise genetic gains (Reynolds et al., 2009).

During the Green Revolution increases of yield occurred with the introduction of *Rht* genes resulting in plants with more grains as the distribution of dry matter (DM) between the organs was enhanced in favour of the spike (Evenson, 2003). As a consequence of this period, spring wheat yields in Mexico increased roughly 25% from 1960 to 1980 (Lobell et al., 2005) and winter wheat yields in China from 44 to 01% from 1940 to 2008 (Xiao et al., 2012). Nowadays there is evidence that in some countries genetic gains in wheat production have reached a plateau level as agricultural management and climate change have influenced yield throwing into question whether the required 2.4% increase per year will be reached (Crain et al., 2018; Terrile et al., 2017). Therefore, there is a necessity to boost breeding strategies through improved understanding of the physiological basis of genetic gains in yield.

5.1.1. Physiological traits to increase grain partitioning

Grain yield is a quantitative trait which represents the final product of many physiological processes occurring in the stem, spike and leaves. At the same time, this complex trait can be dissected into different components such as spike number per unit area (SM2), spikelet number per spike, grain number per spikelet and 1000-grain weight (TGW) (Kuchel et al., 2007).

Genetic gains in wheat yield depend mainly on the amount of above-ground DM (AGDM) and its partitioning to the grain. Lo Valvo et al. (2018) emphasised that progress in yield of bread wheat varieties released between 1918 to 2011 in Argentina was through gains in AGDM and reduced plant height leading to increments in harvest index (HI: ratio between grains per unit area and AGDM). However, other recent studies in Mexico (Aisawi et al., 2015; Lopes et al., 2012) indicate that recent yield gains were mainly associated with the total above-ground biomass produced by the plant. There is evidence that grain yield of modern wheat genotypes is often sink-limited rather than source-limited (availability of assimilates) (Maydup et al., 2012; Philipp et al., 2018). Therefore, increasing grain number remains a top priority in wheat breeding programs aimed to boost yield potential.

For optimal partitioning, only the biomass necessary for resource capture (source) and physical support should be allocated to the leaves, stem and chaff and all remaining DM should be mobilized into grain (sink) (Sylvester-Bradley et al., 2012). Increasing assimilate availability to

developing spikes has been strongly associated with an increase in the number of grains per unit area (González et al., 2005).

5.1.2. Quantitative trait loci for grain partitioning traits

Conventional breeding is based on raising the upper and stable limit of yield potential by combining complementary features to produce genotypes for a given target environment (Reynolds et al., 2009). This strategy has been useful providing an improved understanding of yield in specific conditions, but different approaches need to be implemented to fulfil production increases with the challenges that crop productivity is facing nowadays (Rasheed & Xia, 2019). Genome-scale sequencing technologies have allowed the identification of genetic regions and provide a convenient low-cost tool to study high-genomic specific regions with relatively low genotyping error rates (Ayalew et al., 2019). The incorporation of marker-assisted selection (MAS) into breeding programs reduces time/cost and improves the efficiency and precision of recognising and evaluating the effect that a gene/allele has in the expression of a trait (Landjeva et al., 2007; Nelson et al., 1995; Sa 2009).

Yield-based traits are genetically complex, requiring large populations to accumulate favourable alleles for adequate expression of the character (Rebetzke et al., 2017); genetically these traits are controlled by numerous genes with additive effects and genotype by environment interactions. Some crop traits, such as grain weight and plant height, are more stably inherited compared to others including grain number per unit area and root or shoot biomass that are more variable and show stronger genotype by environment interactions (Rustgi et al., 2013). Grain yield is perhaps the most commonly studied but poorly understood trait related to agronomic performance of wheat but, given its polygenic nature, this trait and its related characteristics usually show a low heritability (Zhang et al., 2010). Different approaches can be used in molecular marker studies depending on the genetic architecture, type of sequencing used to generate the markers, number of individuals and goal of the analysis.

Recently, dissecting the genetic basis of crop improvement by associating genomic information with phenotypic measurements has accelerated the development of strategic crosses in breeding programs. Most of the literature to date focuses on disease resistance (Liu et al., 2018), grain quality (Kristensen et al., 2018; Zhang et al., 2015) and grain yield-related traits. Using a DH population derived from two high yield genotypes, Wang et al. (2018) reported genetic regions of importance for tillers per unit area and fertile spikelets per spike on chromosomes 4A, 5A and 6A, results agree with those reported by Kato et al. (2000) who suggested that chromosome 5A of wheat is known to carry a number of genes affecting adaptability and productivity. Using different environments and 203 winter wheat varieties, Guan et al. (2018) on a double haploid population detected 39 stable QTL using on chromosomes 1B, 2A, 2B, 2D, 3A, 4A, 4B, 4D, 5A, 6A, and 7A for various traits, including grain yield, grain number per spike, thousand grain weight and grain weight per spike outstand,

from which three QTL were linked to dwarfing genes which had a pleiotropic effect on yield component traits. Examining the trade-off behind grain number and weight, Zhai et al. (2018) using 191 recombinant inbred lines (RILs) located a QTL on 6A that increased TGW by 8% by decreased grain number per spike by 3% and at the same time five more genomic regions were reported (1B, 3A, 3B, 5B and 7A).

To incorporate novel traits into breeding programs the identification of quantitative trait loci (QTLs) was carried out for a winter wheat high biomass population over two seasons to understand the genetic basis behind grain partitioning traits measured seven days after anthesis (GS65+7d) and at physiological maturity.

Chapter hypothesis:

- Novel QTLs, including co-located QTLs, can be identified for harvest index, grain number and grain partitioning traits in the DH progeny, derived from a cross between two high/moderate biomass parents (Savannah and Rialto), sown under rain-fed conditions over two seasons.

5.2. Materials and methods

5.2.1. Plant material and experimental design

The experiment was carried out over two seasons (Y16: 2015-16 and Y17: 2016-17) under rain-fed conditions using a randomised complete block design with two replicates at The University of Nottingham campus Sutton Bonington, Leicestershire, UK (52° 50' N, 1° 15' W). A Savannah x Rialto doubled-haploid population (**SxR DH**) comprised of 94 winter wheat lines derived from the F_1 between UK winter wheat parents Savannah and Rialto, which are UK semi-dwarf (*Rht-D1b*, formerly *Rht-2*), hard endosperm cultivars (Table S3.1). Rialto (RAGT seeds Ltd; Haven x Fresco) was first released in 1995 and is a high yield potential genotype with some potential for bread-making processes. Savannah (Lime Grain UK Ltd; Riband x Brigadier) was first released in 1998 and is a high yielding feed wheat cultivar (Wilkinson et al., 2012). This population was used due to previous results showing high phenotypic expression and genetic variation in stay-green traits and in yield under drought and nitrogen stress in field experiments in the UK and France (Atkinson et al., 2015). Agronomic details, such as sowing days and field management can be found in material and methods of chapter #3.

5.2.2. Construction of genetic linkage map

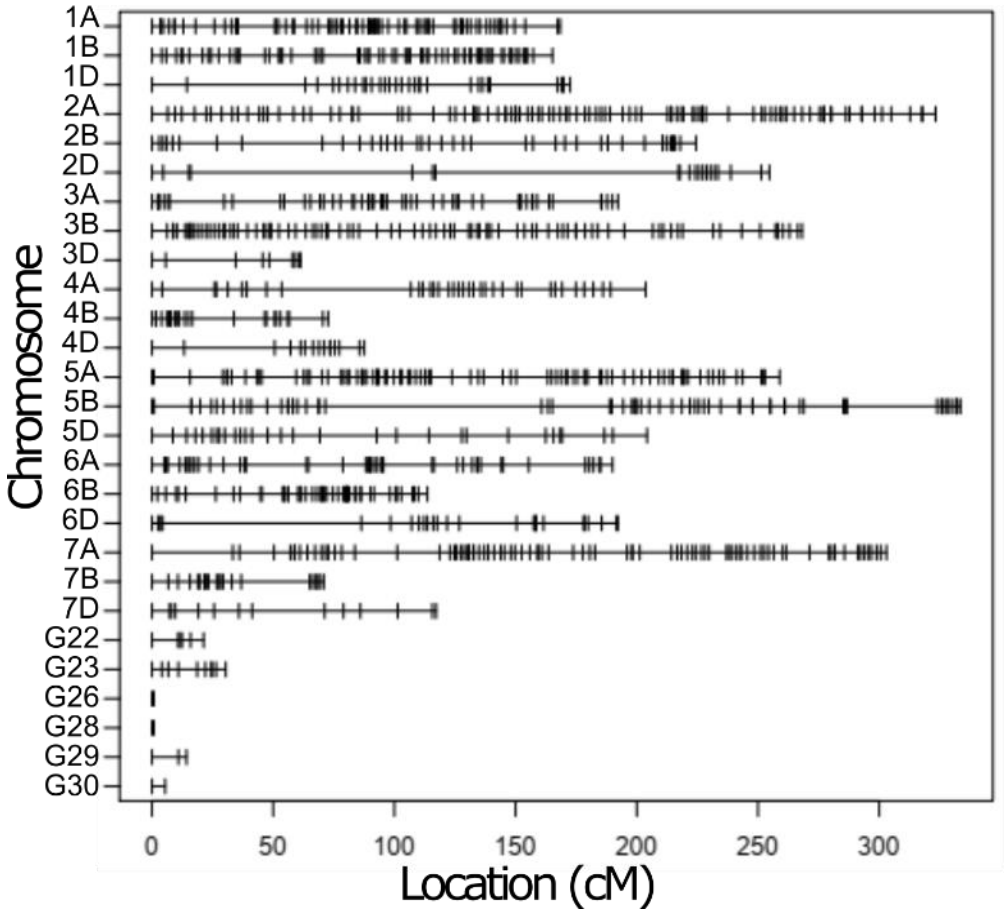
The genetic map used for QTL analysis was provided by the John Innes Centre (JIC) and available at the website CerealDB (BBSRC, 2013). This map was based on SNP-based KASP assays for a set of wheat markers commonly used in marker-assisted selection (MAS) in collaboration with CIMMYT, USDA, University of Sydney, INRA and JIC. The complete map is constituted of 9,379 markers (Table 5.1) mainly located in genome A (48.7%), then B (43.1%) and finally D (8.2%).

Table 5.1. Marker number (M), map length (cM: centimorgans) and density in each chromosome and genome for the complete SxR DH genetic linkage map.

Chromosome	# markers (M)	Map length (cM)	Map density (cM/M)
1A	660	222.5	0.34
1B	640	191.2	0.30
1D	236	181.9	0.77
2A	1029	330.1	0.32
2B	931	212.7	0.23
2D	64	188.6	2.95
3A	560	220.3	0.39
3B	760	360.6	0.47
3D	16	67.6	4.23
4A	179	191.6	1.07
4B	168	93.5	0.56
4D	65	76.8	1.17
5A	882	393.9	0.45
5B	471	316.7	0.67
5D	174	237.8	1.37
6A	633	192.9	0.30
6B	859	136	0.16
6D	131	161.7	1.23
7A	617	298	0.48
7B	158	75.7	0.48
7D	66	132.4	2.00
Grouped	140	70.5	0.50
		Genome	
A	4,500	1,849.3	0.41
B	3,987	1,386.4	0.35
D	752	1,046.8	1.39
Total	**9,239**	**4,282.5**	**2.15**

From the 9,379 markers all repeated, redundant markers and closer than 0.5cM were excluded resulting in 1,050 markers from which 27 linkage groups were mapped (Figure 5.1) based on map distance calculation using the Haldane's mapping function (Haldane, 1919).

Figure 5.1. SxR DH genetic map showing all the unique markers in each linkage group.



QTL identification and plotting of logarithm of odds (LOD) scores were conducted using the R package rqtl (Broman et al., 2003) using cross-year phenotypic data (91 DH lines, parents were excluded). This method used a single QTL model employing the extended Haley-Knott method on the 91 genotypes, as for three genotypes there was no genomic information available. Significant thresholds were calculated from the data distribution. Final QTL LOD scores and effects were calculated from a multiple QTL model, using the QTL detected in the initial scan. LOD scores of >3.0 were considered significant (*P<0.05*) and LOD scores of >2.0 putative (*P<0.10*).

5.3. Results

Using the adjusted means from the phenotypic traits measured over the two seasons (Y16: 2015-16 and Y17: 2016-17) quantitative trait loci (QTLs) were found for most of the traits measured. Seasonal (Y16 and Y17) phenotypic results for traits at both assessment stages can be found in chapter #3.

5.3.1. QTL analysis

SxR DH: QTL Y16

A total of 21 QTLs were identified in 2015-16, from these, 13 were detected at seven days after anthesis which seven of them were length-related and eight at physiological maturity (Table 5.4).

At GS65+7d, one QTL was identified for spike DM per shoot^{1} on chr 7B (LOD: 2.95) accounting for 14.3% of phenotypic variation with spike DM increased by the Savannah allele. Two QTL were identified on chr 2A (LOD: 2.00) and 2D (LOD: 2.30) for stem DM per shoot^{1} each explaining 10% of phenotypic variation with increasing expression with the Savannah allele. On 4A (LOD: 1.98) a QTL was found for FE explaining 9.86% of variation associated with higher expression of the Savannah allele. For partitioning indices, two QTLs were identified on 3A, one for SPI (LOD: 3.19) and the other for StePI (LOD: 4.38) explaining 15.4 and 20.5% of phenotypic variation, respectively, with higher expression through Savannah and Rialto alleles, respectively (Table 5.4).

Seven length-related QTLs were identified, mainly on chr 3A for plant height (LOD: 5.80), stem internode 2 (LOD: 4.87), stem internode 3 (LOD: 7.08) and peduncle (LOD: 4.50) lengths explaining 15 to 30% of phenotypic variation; the expression of these traits was increased through Rialto alleles. On chr 6A, QTLs were identified for plant height (LOD: 5.10) and peduncle length (LOD: 5.00) each explaining 18% of variation with expression increased with Savannah alleles. One QTL was associated with flag-leaf length on chr 6D (LOD: 3.13) explaining 15.1% of phenotypic variation, with flag-leaf length increasing with the Savannah allele (Table 5.4).

At physiological maturity, eight QTLs were found including two for grain yield on chr 1D (LOD: 3.30) and chr 7D (LOD: 2.20) explaining 14.8% and 9.6% of the variation, respectively, with trait expression increased through Rialto and Savannah alleles, respectively. On chr 7A two QTLs were found, one for $AGDM_{PM}$ (LOD: 2.35) and the other for SM2 (LOD: 2.35) each explaining 11.6% of variation with the Rialto allele increasing trait expression; and three QTLs were identified on 3B for GN (LOD: 4.75), HI (LOD: 2.16) and TGW (LOD: 3.77) explaining from 2 to 4% of variation with increasing values attributed to Savannah alleles (first two traits) and to the Rialto allele for TGW (Table 5.4).

Table 5.4. QTLs identified per chromosome (chr) with the specific location (cM) and its percentage of variation (PVE) for season 2015-16 (Y16) for 25 traits measured at GS65+7d and PM on 91 lines of the SxR DH population.

Stage	Trait	Chr	Pos (cM)	LOD	PVE (%)	Add effect	Nearest marker	Parent Increasing
Anthesis + 7d (GS65+7d)	DM Spk	7B	67.4	2.95	14.3	-0.16	BS00010355	A
	DM Ste	2A	294.0	2.00	9.10	-0.13	Excalibur_c49875_479	A
		2D	0.0	2.30	10.5	-0.16	BS00018412	A
	FE	4A	10.0	1.98	9.86	-4.16	BS00023164	A
	SPI	3A	79.0	3.19	15.4	-0.03	wsnp_Ex_rep_c106152_90334299	A
	StePI	3A	80.0	4.38	20.5	0.03	BS00095423_51	B
	PH	3A	77.8	5.80	20.9	6.11	wsnp_Ex_rep_c106152_90334299	B
		6A	93.0	5.10	18.0	-5.89	GENE.3659_162	A
	LFL	6D	104.0	3.13	15.1	-1.06	BS00047195_51	A
	LnInt2	3A	83.5	4.87	22.5	1.24	wsnp_Ex_rep_c106152_90334299	B
	LnInt3	3A	77.8	7.08	31.0	1.28	wsnp_Ex_rep_c106152_90334299	B
	LnPed	3A	94.5	4.50	16.4	1.86	GENE.1167_104	B
		6A	89.0	5.00	18.2	-2.06	Jagger_c2853_75	A
Physiological Maturity (GS87)	$AGDM_{PM}$	7A	189.0	2.35	11.6	131.1	BS00102772_51	B
	GN	3B	156.8	4.75	22.0	-2625.1	Tdurum_contig33192_76	A
	HI	3B	151.0	2.16	10.7	0.0	IAAV5855	A
	SM2	7A	122.9	2.35	11.6	53.3	Excalibur_c16355_712	B
	TGW	3B	138.3	3.77	17.9	2.84	BS00108055_51	B
	GY	1D	103.0	3.30	14.8	55.0	GENE.0524_302	B
		7D	117.3	2.20	9.60	-39.5	wsnp_Ku_c416_869895	A

DM Spk: Dry matter spike (g per shoot^{1}); **DM Ste:** Dry matter stem (g per shoot^{1}); **FE:** Fruiting Efficiency (grains g^{1}); **SPI:** Spike Partitioning Index; **StePI:** Stem Partitioning Index; **PH:** Plant Height (cm); **LnFL:** Length Flag Leaf (cm); **LnInt2:** Length Internode 2 (cm); **LnInt3:** Length Internode 3 (cm); **LnPed:** Length Peduncle (cm); **$AGDM_{PM}$:** Above-Ground Dry Matter (g m^{-2}); **GN:** Grain Number per unit area; **HI:** Harvest Index; **SM2:** Spikes per unit area; **TGW:** Thousand Grain Weight (g); **GY:** Grain Yield (g m^{-2}); **Chr:** Chromosome; **Pos:** Position (cM); **Lod**: Log Likelihood Score; **PVE**: Percentage of Variation Explained; **Add effect**: Additive Effect (μA- μB/2) Savannah is A and Rialto is B

SxR DH: QTL Y17

For 2016-17 a total of 26 QTLs were found, including 17 at GS65+7d from which nine were length-related and nine at physiological maturity (Table 5.5). At GS65+7d, four QTLs were located on chr 4D corresponding to DTA (LOD: 3.39), $DMSpk_{A+7}$ per unit area (LOD: 3.30), green area per shoot[1] (LOD: 3.40) and StePI (LOD: 2.20) explaining from 9 to 15% of variation with increased variation linked with the Rialto allele for the first two traits and with Savannah for green area per shoot and StePI. Three QTLs were found on chr 3A, one for DM Ste per shoot[1] (LOD: 4.70) explaining 21% of phenotypic variation with positive expression related with the Rialto allele, another for LamPI (LOD: 2.64) with positive expression linked to the Savannah allele and the last for StePI (LOD: 3.10) explaining 13% of phenotypic variation with increasing values through the Rialto allele. One QTL was located on 1B associated with green area per shoot[1] (LOD: 3.40) explaining 13% of variation with positive variation linked to the Rialto allele (Table 5.5).

A total of nine QTLs were identified for length-related traits, three for PH located on 3A (LOD: 9.6), 6A (LOD: 6.9) and 7D (LOD: 2.8) explaining 28, 19 and 7% of variation, respectively with positive expression linked with Rialto and Savannah alleles (6A & 7D). For spike length on chr 2B (LOD: 3.52) a QTL was recorded with increasing values associated with the Rialto allele which explained 16% of the phenotypic variation. A QTL for flag-leaf length was found on 6D (LOD: 2.83) which explained 13% of the variation with trait expression increasing with the Savannah allele. Two QTLs were found for peduncle length on 3A (LOD: 1.60) and 6A (LOD: 1.80) explaining 7% of the variation with length increased by the Rialto and Savannah alleles, respectively. For stem internode 2 and 3 lengths one QTL on 3A (LOD: 4.82 and 7.22), for each internode was found, explaining 21 and 30% of the variation with increasing length linked to the Rialto alleles (Table 5.5).

At physiological maturity three QTLs were identified on chr 2A corresponding to $AGDM_{PM}$ (LOD: 2.01), HI (LOD: 3.7) and SM2 (LOD: 2.37) with higher expression of HI associated with the Savannah allele and explaining 17% of variation; higher expression of the QTLs for $AGDM_{PM}$ and SM2 was related to the Rialto allele explaining 9 and 11% of variation, respectively. On chr 2D a QTL was found for DTM (LOD: 3.31) explaining 15% of variation with values increased through the Rialto allele. On chr 7D, a QTL for grain yield was found with higher yield related to the Savannah allele explaining 12% of the variation. On the linkage group 23 a QTL for TGW was found explaining 12% of variation with higher expression linked to the Savannah allele. On linkage group 23 and 3A, two QTLs were identified for GN each explaining 8% of the variation with higher expression linked to the Savannah and Rialto alleles, respectively (Table 5.5).

Table 5.5. QTLs identified per chromosome (chr) with the specific location (cM) and its percentage of variation (PVE) for season 2016-17 (Y17) for 25 traits measured at GS65+7d and PM on 91 lines of the SxR DH population.

Stage	Trait	Chr	Pos (cM)	LOD	PVE (%)	Add effect	Nearest marker	Parent Increasing
Anthesis + 7d (GS65+7d)	DTA	2D	16.0	3.29	15.8	2.71	BS00049876_51	B
	$DMSpk_{A+7}$	2D	13.0	3.10	15.0	80.5	IAAV7407	B
	DM Ste	3A	69.4	4.10	19.3	0.19	BS00007502_51	B
	FE	4A	37.1	2.39	11.8	-7.47	wsnp_RFL_Contig3501_3652740	B
	LamPI	3A	82.7	2.78	13.6	-0.01	BS00095423_51	A
	GA	1B	154.8	3.10	11.9	11.3	BS00028318_51	B
		2D	12.0	1.60	6.1	-10.7	BS00018412	A
		5A	65.2	2.00	7.5	-10.5	BS00047241	B
	SPI	2D	16.0	2.31	11.4	0.03	BS00049876_51	B
	StePI	3A	60.0	2.91	14.1	0.03	Kukri_rep_c102131_891	A
	PH	3A	83.5	9.60	27.8	7.49	wsnp_Ex_rep_c106152_90334299	B
		6A	86.0	6.90	18.7	-5.65	BS00103842_51	A
		7D	41.0	2.80	6.8	-4.68	IAAV4624	A
	LFL	6D	108.0	2.83	13.0	-0.95	BS00047195_51	A
	LnInt2	3A	94.0	4.82	21.0	1.15	wsnp_Ex_rep_c106152_90334299	B
	LnInt3	3A	92.0	7.22	29.8	1.22	wsnp_Ex_c13949_21828493	B
	LnPed	3A	94.5	1.60	6.7	2.23	wsnp_RFL_Contig2699_2402527	B
		6A	36.4	1.80	7.3	-2.31	RFL_Contig2954_581	A
	LnSpk	2B	215.0	3.52	15.8	0.61	Ra_c1501_1220	B

Stage	Trait	Chr	Pos (cM)	LOD	PVE (%)	Add effect	Nearest marker	Parent Increasing
Physiological Maturity (GS87)	$AGDM_{PM}$	2A	228.5	2.01	9.37	111.2	BS00107533	B
	DTM	2D	16.0	3.31	15.0	2.70	BS00049876_51	B
	GN	3A	33.3	1.90	7.90	-1786.2	BS00049032_51	A
		G23	30.4	2.00	8.40	1853.3	BS00046264	B
	HI	2A	132.6	3.70	16.6	-0.02	Excalibur_rep_c103108_709	A
	SM2	2A	170.8	2.37	11.0	52.6	Kukri_c45015_145	B
	TGW	G23	30.4	2.56	11.8	-1.92	BS00046264	A
	GY	7D	0.0	2.50	11.5	-46.7	BS00021859	A

DTA: Days to anthesis; **$DMSpk_{A+7}$:** Dry matter spike at GS65+7d per unit area (g m^{-2}); **DM Ste:** Dry matter stem (g per $shoot^{-1}$); **FE:** Fruiting Efficiency (grains g^{-1}); **LamPI:** Lamina Partitioning Index; **GA:** Green Area (g cm^{-1}); **SPI:** Spike Partitioning Index; **StePI:** Stem Partitioning Index; **PH:** Plant Height (cm); **LnFL:** Length Flag Leaf (cm); **LnInt2:** Length Internode 2 (cm); **LnInt3:** Length Internode 3 (cm); **LnPed:** Length Peduncle (cm); **LnSpk:** Length Spike (cm); **$AGDM_{PM}$:** Above-Ground Dry Matter (g m^{-2}); **DTM:** Days to maturity; **GN:** Grain Number per unit area; **HI:** Harvest Index; **SM2:** Spikes per unit area; **TGW:** Thousand Grain Weight (g); **GY:** Grain Yield (g m^{-2}); **Chr:** Chromosome; **Pos:** Position (cM); **Lod**: Log Likelihood Score; **PVE**: Percentage of Variation Explained; **Add effect**: Additive Effect (μA- μB/2) Savannah is A and Rialto is B

SxR DH: QTL Y16 & Y17

QTL analysis for cross-year (Y16 & Y17) means revealed a total of 33 QTL, 23 at GS65+7d been 13 length-specific and seven at PM (Table 5.6; FigureS5.1). Most of the QTLs were found on genome A (20), then genome D (10) and genome B (3); at the chromosome level QTL were identified on 6 chromosomes with chr 3 with the most (12) and chr 4 with the least (1).

At seven days after anthesis (GS65+7d), two QTLs were identified for DTA on 2D (LOD: 2.70) and 3D (LOD: 2.60), explaining 11% of the variation with higher expression associated with the Rialto and Savannah alleles, respectively. For StePI two QTLs were found, one on 3A (LOD: 6.20) which explained 23% of the variation with higher expression with Rialto and the other on chr 3D (LOD: 3.50) explaining 12% of variation with higher expression linked with the Savannah allele. One QTL was found on 3A (LOD: 3.07) for stem DM per shoot^{1} explaining 14% of variation with higher expression with the Rialto allele and another for spike DM per shoot^{1} on 7B (LOD: 3.49) explaining 16% of the variation with higher expression linked with the Savannah allele. Another two QTLs were identified for partitioning indices, one for lamPI on chr 6D (LOD: 2.25) explaining 11% of the variation and the other on chr 3A (LOD: 4.45) for SPI explaining 20% variation both with higher expression related with the Savannah allele. On chr 2D (LOD: 2.51) a QTL was found for spike DM per unit area which explained 12% of phenotypic variation with higher expression associated with the Rialto allele; two further QTLs were found with higher expression associated with the Savannah allele. At 4A one QTL(LOD: 2.25) was located for FE and the other on 5A (LOD: 3.85) for green area per shoot^{1}, explaining 17% and 11% of phenotypic variation, respectively (Table 5.6).

For length-related QTLs, one QTL was found on chr 6D (LOD: 4.74) for flag-leaf length explaining 21% of the phenotypic variation with higher expression through the Savannah allele. On 7A (LOD: 3.36) a spike length QTL was found explaining 16% of the variation with longer spikes associated with the presence of Rialto allele. Two QTLs were identified for plant height, one on 3A (LOD: 8.80) explaining 28% of the variation with higher expression with the Rialto allele and the other on 6A (LOD: 6.40) explaining 19% variation with the Savannah allele increasing plant height. For peduncle length, two QTLs were found on chr 3A (LOD: 4.90) and chr 6A (LOD: 4.20), explaining 18% and 15% of phenotypic variation, respectively, with higher expression associated with Rialto and Savannah alleles, respectively. Three QTLs were associated with stem internode 2 length located on 3A (LOD: 6.60), 6A (LOD: 3.70) and 6D (LOD: 3.50) explaining 21%, 11% and 10% of variation, respectively, with higher expression of with Rialto allele for the QTLs on 3A and 6A and with Savannah for the QTL on 6D. For stem-internode 3 length four QTLs were found on 2A, 3A, 6A and 6D (LOD: 4.20), with the QTL on 3A (LOD: 3.20) explaining 26% of the variation with longer stem internode 3 length through the Rialto allele. The other three QTLs explained around 10% of the variation, 2A (LOD: 3.50) and 6A (LOD: 5.10) with higher expression linked to the Savannah allele for the QTL on 2A and 6A and to the Rialto allele for the QTL on 6D (Table 5.6).

At physiological maturity, one QTL was identified for physiological maturity date on chr 2D (LOD: 4.06) explaining 19% variation with higher expression associated with the Rialto allele. For grains per unit area (GN) two QTLs were identified, one on 3A (LOD: 2.90) explaining 11% of the variation and the other on 3B (LOD: 4.80) explaining 19%, both with the Savannah allele increasing trait expression. One QTL was found on chr 7D (LOD: 2.55) for grain yield explaining 12% of variation with yield increased through the Savannah allele. For harvest index, one QTL was found on chr 2A (LOD: 3.39) explaining 16% of the variation with HI increased through the Savannah allele. A QTL was found on chr 2D (LOD: 2.86) for spikes per unit area explaining 14% of the variation with higher expression through the Rialto allele. On chromosome 3B (LOD: 2.91) a QTL was identified for thousand-grain weight explaining 14% of the variation with higher TGW associated with the Rialto allele (Table 5.6).

Table 5.6. QTLs identified per chromosome (chr) with the specific location (cM) and its percentage of variation (PVE) for cross-year data (Y16 & Y17) on 25 traits measured at GS65+7d and PM on 91 lines of SxR DH population.

Stage	Trait	Chr	Pos (cM)	LOD	PVE (%)	Add effect	Nearest marker	Parent Increasing
Anthesis + 7d (GS65+7d)	DMSpk	7B	65.1	3.49	16.2	-0.11	BS00010355	B
	DMSte	3A	69.4	3.07	14.4	0.15	Kukri_rep_c102131_891	B
	DTA	2D	16.0	2.70	11.1	1.69	BS00049876_51	B
		3A	69.4	2.60	10.7	-1.67	BS00007502_51	A
	FE	4A	14.0	2.25	10.8	-4.54	wsnp_RFL_Contig3501_3652740	A
	GA	5A	66.0	3.85	17.7	-8.30	Excalibur_rep_c95828_165	A
	LamPI	6D	98.4	2.35	11.2	-0.01	BS00022856	A
	SPI	3A	61.0	4.45	20.2	-0.03	BobWhite_c28464_814	A
	$DMSpk_{A+7}$	2D	16.0	2.51	11.9	59.9	BS00049876_51	A
	StePI	3A	79.0	6.20	23.0	-0.02	BobWhite_c28464_814	B
		3D	45.7	3.50	11.9	-0.03	IAAV5136	A
	LnFL	6D	107.1	4.74	21.3	-0.98	wsnp_BQ161779D_Ta_2_1	A
	LnInt2	3A	78.0	6.60	21.2	0.77	wsnp_Ex_rep_c106152_90334299	B
		6A	84.0	3.70	11.1	1.24	RFL_Contig1038_942	B
		6D	121.8	3.50	10.2	-0.93	GENE.4060_219	A
		2A	292.8	3.50	7.6	0.61	Kukri_c209_999	A
	LnInt3	3A	79.0	10.20	26.4	1.27	wsnp_Ex_rep_c106152_90334299	B
		6A	84.0	5.10	11.3	-0.83	BobWhite_c8879_142	A
		6D	122.0	4.20	9.1	-0.70	GENE.4060_219	B
	LnPed	3A	94.5	4.90	17.7	1.99	wsnp_RFL_Contig2699_2402527	B
		6A	84.0	4.20	14.8	-1.82	Jagger_c2853_75	A
	LnSpk	7A	303.0	3.36	15.6	0.56	GENE.4717_210	B
	PH	3A	79.0	8.80	27.5	7.35	wsnp_Ex_rep_c106152_90334299	B
		6A	86.0	6.40	18.9	-6.11	GENE.3659_162	A

Stage	Trait	Chr	Pos (cM)	LOD	PVE (%)	Add effect	Nearest marker	Parent Increase
Physiological Maturity (GS87)	DTM	2D	16.0	4.06	18.6	1.75	BS00049876_51	B
	GN	3A	33.3	2.90	11.0	-2080.1	BS00049032_51	A
		3B	171.4	4.80	19.4	-1553.9	RAC875_c62223_86	A
	GY	7D	117.3	2.55	12.1	-41.88	wsnp_Ku_c416_869895	A
	HI	2A	151.7	3.39	15.8	-0.02	Excalibur_c5121_930	A
	SM2	2D	8.0	2.87	13.5	46.1	Kukri_c2912_2029	B
	TGW	3B	136.0	2.91	13.7	1.91	wsnp_Ex_c1097_2105311	B

DM Spk: Dry matter spike (g per shoot^{-1}); **DM Ste:** Dry matter stem (g per shoot^{-1}); **DTA:** Days to anthesis; **FE:** Fruiting Efficiency (grains g^{-1}); **GA:** Green Area (g cm^{-1}); **LamPI:** Lamina Partitioning Index; **SPI:** Spike Partitioning Index; **DMSpk$_{A+7}$:** Dry matter spike at GS65+7d per unit area (g m^{-2}); **StePI:** Stem Partitioning Index; **LnFL:** Length of Flag Leaf (cm); **LnInt2:** Length Internode 2 (cm); **LnInt3:** Length Internode 3 (cm); **LnPed:** Length Peduncle (cm); **LnSpk:** Length Spike (cm); **PH:** Plant Height (cm); **DTM:** Days to maturity; **GN:** Grain Number per unit area; **GY:** Grain Yield (g m^{-2}); **HI:** Harvest Index; **SM2:** Spikes per unit area; **TGW:** Thousand Grain Weight (g); **Chr:** Chromosome; **Pos:** Position (cM); **Lod**: Log Likelihood Score; **PVE**: Percentage of Variation Explained; **Add effect**: Additive Effect (μA- μB/2) Savannah is A and Rialto is B

SxR DH: co-located QTL

A total of nine loci were recorded with co-located QTLs on chromosomes 2D, 3A, 6A and group 23 between the single year and cross-year analyses. On chr 2D at 15.96 cM there were three traits which shared the same QTL position StePI Y17, DTA Y16 & Y17 and $DMSpk_{A+7}$ per unit area Y16 & Y17 explaining from 9 to 12% of the variation with positive effects through the presence of the Savannah allele for StePI and the Rialto allele for DTA and $DMSpk_{A+7}$. Also on chr on 2D at 16 cM were co-located QTL for DTA Y16, DTM Y16 and DTA Y16 & Y17 explaining 15 to 19% with increased trait expression with the presence of the Rialto allele (Figure S5.1).

On chr 3A at 69.37 cM there were co-located QTL for DTA Y15 & Y17 and DM Ste Y17 explaining 11 to 21% of the phenotypic variation, with trait expression increased through the Rialto allele. Also on chr 3A at 77.8 cM QTLs were co-located for LInt3 Y16 and PH Y16 explaining 31 and 21% of the variation, respectively, with higher trait expression through Rialto. Near this location on 3A at 79cM stePI Y16 & Y17, SPI Y16, and LInt3 and PH both in Y16 & 17 were co-located explaining from 15 to 28% of variation, with trait expression increased by the Savannah allele for SPI and the Rialto allele for the rest. Another co-location was identified at 83.5 cM on 3A for LInt2 Y16 and PH Y17 explaining 23 and 28%, respectively of the variation with traits increased by the Rialto allele. Lastly for LPed on Y16 and Y16 and Y17 a co-location was found at 94.5 cM explaining 22 and 23% variation, respectively with increases through the Rialto allele (Figure S5.1).

Most of the markers colocated on chr 6A corresponded to stem-internode lengths with length increased through the Savannah allele; at 84 cM LInt2 Y16 & Y17, LInt3 Y16 & Y17 and LPed Y16 & Y17 explaining from 11 to 15% of variation and at 86cM PH Y16 and Y16 & 17 explaining 18 and 19% of variation, respectively (Figure S5.1).

For group 23, QTLs for GN Y16 and TGW Y16 were co-located at 30.4 cM explaining 8 and 12% of the variation, respectively with trait expression increased by Rialto and Savannah, respectively (Figure S5.1).

5.4. Discussion

Grain yield is a complex quantitative trait influenced by the genetic variation of many other traits, for winter wheat raising yield potential is fundamental since its high yields are necessary for the worldwide supply (Rose et al., 2017). Improved understanding of the physiological and genetic bases of yield production relating to partitioning traits seven days after anthesis and at physiological maturity will help develop better breeding strategies for raising harvest index and yield potential.

5.4.1. Genetic and phenotypic variations among high biomass progeny

Improvement of yield potential can be achieved by increasing grain number per unit area or thousand-grain weight (Qin et al., 2015). For the SxR DH population, grain yield variation was explained mainly through grain number. Results showed that yield variation was related

with both above-ground DM and harvest index, been similar to Shearman et al. (2005) findings using eight winter wheat representative UK cultivars introduced from 1972 to 1995 where yield was linearly associated increases on harvest index with year of release. Examining the association between grain number per m^2 and yield, Philipp et al. (2018), in 180 elite varieties (German Federal ex situ Genebank) and 210 European elite varieties (GABI-WHEAT and VALID projects), found that breeding increased grains per spike (30%), spikes per m^2 (14%) but only contributed a small increment (3%) in grain weight. The latter effect was due to a trade-off between grain number and weight which is often observed in wheat populations. This was also observed in this DH population. The fact that grain number is dominant overweight maybe because this trait is more plastic; present results supported that yield is predominantly sink limited under optional conditions, and grain number is the primary determinant of sink (Peltonen-Sainio et al., 2007).

The negative association between above-ground DM at physiological maturity and harvest index may be the result of inefficient use of assimilates, suggesting scope for extra DM could be allocated to the grain (sink) if traits favoring grain partitioning can be identified and their genetic regulation determined. The results at seven days after anthesis indicated that modern UK winter wheat genotypes show a trade-off between spike and stem DM partitioning, likely as these two organs develop almost simultaneously during stem elongation. Decreasing the competition from the stem could increase spike fertility, which could be driven by shortening stem-internode lengths. Attention will be required with the use of length-related traits as they may also indirectly alter related traits; these correlations and heritability will affect genetic variance (Philipp et al., 2018). In this population, the length of each internode was positively associated with grain yield, while stem internode 2 and 3 were also related to fruiting efficiency. The production of grain number was mainly driven by the total amount of biomass produced by the plant at seven days after anthesis but was also partially explained through the positive association among spike partitioning index and DM spike per unit area. Results also indicated fruiting efficiency as a complementary trait to boost yield by enhancing grain number.

5.4.2. Detection of stable partitioning and grain yield QTLs

In wheat, many QTLs have been reported for disease resistance, grain quality-related traits and yield but today limited information is available on DM partitioning traits. The use of QTL mapping in early generations has allowed the detection of beneficial alleles and their transfer through marker-assisted selection and/or genomic selection (Soriano et al., 2017). The results presented in this study are the first attempt to dissect at the molecular level partitioning traits measured at around anthesis. A total of 80 QTLs, for seasonal and cross-year trait means, were recorded across 15 chromosomes using 1,050 filtered markers with two years data over 25 traits measured at seven days after anthesis and physiological maturity. New rapid, cost-effective genotyping technologies allow the identification of more precise genetic regions

including the integration of an annotated wheat map (IWGSC, 2018) which could prioritize the selection of loci for breeding programs for QTL cloning.

Exciting QTLs regions were found among seven chromosomes (2A, 2D, 3A, 3B, 4A, 6A and 6D) from which most of the co-located markers were on chromosome 3A corresponding to length-related traits and DM partitioning. These locations will require fine genetic mapping to clarify whether they represent multiple loci with small effects or effects of a single gene. It is essential to take into account that the co-location of two or more QTL could be indicative of pleiotropic or linkage effects (Pinto et al., 2010) which could indicate mechanistically associated traits in the QTL cluster. Some previous studies have reported QTLs for plant height and peduncle length, but their findings did not match with current results (Daoura et al., 2014; Heidari et al., 2012; Sun et al., 2017).

Grain yield is a trait strongly influenced by genotype x environmentS interaction controlled by a large number of small QTL (Bennett et al., 2012). The easiest way to study this trait is to dissect it into components such as grain number, thousand-grain weight, spike number per unit area and grain number per spike and assess the contribution of each locus to the trait variability. A region on chromosome 7D at 117.3 cM increased through Savannah allele was linked to grain yield which showed stability across both years. Using a recombinant inbred lines (RIL) from the cross between Renan and Récital characterized as high yield potential parents (grain weight-related), Groos et al. (2003) detected a stable QTL in 7D explaining nearly 15% of the phenotypic variation. On chromosome group 3, several loci were identified for grain number and weight; for the QTL on 3A for grain number at 33.3 cM positive variations was attributed to the Savannah allele and for those on 3B (grain number and thousand-grain weight) to Rialto allele. Using RILs Zhai et al. (2018) also reported a stable QTL on 3A (113.8–139.8 cM). The QTLs on 3B were identified for the cross-year analysis (Y16 & Y16) and for Y16. For traits such as above-ground DM, spikes per unit area, harvest index and days to maturity some regions were linked but were not uniform across seasons probably due to environmental effects.

For DM partitioning traits, especially at anthesis stage, not enough research has been done. Results obtained using this high biomass doubled-haploid population propose a couple of genetic loci related to spike fertility and DM partitioning. In chromosome 2D several DM production traits were found, QTLs for DMSte (Y16), $DMSpk_{A+7}$ (Y16-17) and DTA (Y17 & Y16-17), were identified on this chromosome. Using a winter wheat DH population (Buster x Charger), Gonzalez-Navarro (2017) reported a genetic loci in chromosome 2D related to stem elongation. The finding of this region could be result of the presence of the *Ppd* (photoperiod) gene in this chromosome which influences the floral developmental stages (Guo et al., 2018). Another couple of interesting QTLs were identified on 3A for stem partitioning index (Y16 & Y17), 4A for FE (Y16 & Y16-17) and on 7B for DMSpk (Y16 & Y16-17). For this last region related to spike DM, Griffiths et al. (2015) found a QTL in this same chromosome, using a recombinant

DH population, concluded that these loci were responsible to regulate grain weight contributing to yield stability.

5.4.3. Implications of detected QTLs

Present QTL results will potentially allow the introduction of novel grain partitioning traits into breeding programs representing potential targets for marker-assisted breeding to increase genetic gains. Distribution of most of the QTLs showed continuous variation, and most of them had moderate-high heritability. For a trait of moderate heritability one strategy is to break it into simple traits of higher heritability with several QTLs with substantial effect contributing to the expression of a specific phenotype (Hospital, 2009). This is the case for grain yield (Bhatta et al., 2018; Rajala et al., 2009; Turuspekov et al., 2017); but could also be the case for stem partitioning index which had moderate heritability (h^2<0.40). Low heritability (H^2) values cause the estimates of QTL location to have large confidence intervals suggesting that the QTL position may be within a range ±10–20 cM unless the QTL effect is significant enough to reduce the confidence interval to less than about 10 cM (Kearsey, 1998). This was the case for length-related QTLs and several QTLs for grain number, above-ground DM and spike DM per unit area at seven days after anthesis, for the rest of the traits, grain yield, yield components and DM partitioning values were below 0.2. Plant height and stem internode 2 and 3 lengths had high heritability (H^2>0.80), suggesting that phenotype of the individuals was a good predictor of the genotype (Visscher et al., 2008).

The QTLs discussed above were mainly those which were stable across years, for the other QTLs reported further studies are required to understand better the bases of the interaction with the environment to allow their deployment inbreeding programs. The incorporation of the novel traits presently reported, such as internode length and fruiting efficiency, through marker-assisted selection could allow breeders to design new strategic crosses to combine novel traits raise grain partitioning and yield potential in their programs.

5.5. Conclusions

- The redistribution of assimilates during stem elongation and floret development could be achieved by decreasing internode length (2 and 3), benefitting spike growth with more DM to produce extra fertile florets to increase grain number.
- Phytomer lengths (stem internode 2 and 3) were negatively correlated with spike fertility-related traits.
- A trade-off was observed between the fruiting efficiency and the total amount of DM partitioned to the spike.
- Grain number was associated with grain yield, amount of above-ground DM and harvest index.
- Nine stable grain partitioning QTLs were identified (3A: stem partitioning index; plant height, peduncle length and stem internode 2 and 3; 6A: plant height and peduncle length;

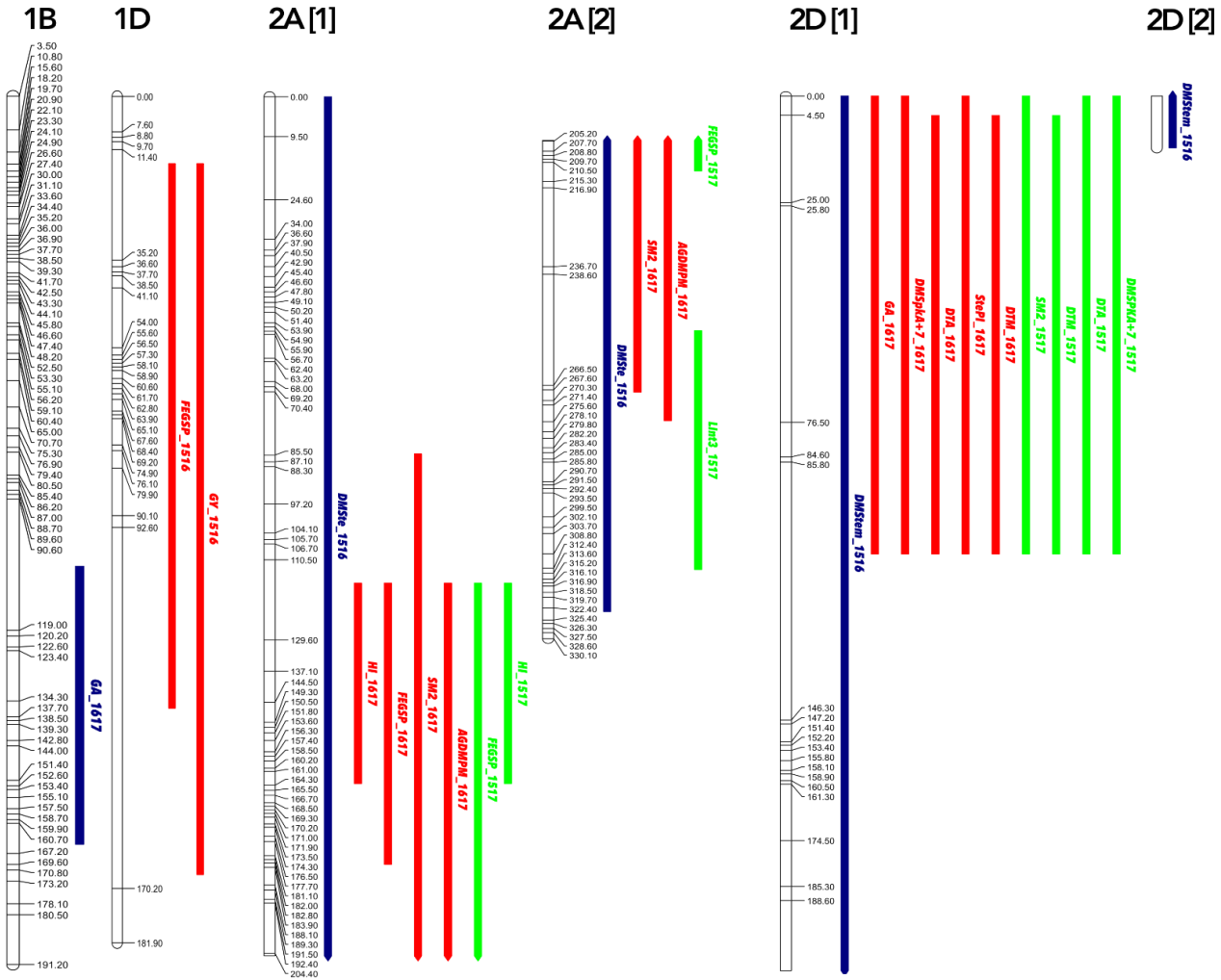
6D: flag leaf length; 7D: grain yield) which were consistent between seasonal and cross-year analysis

- Fine mapping is required for the co-localized QTLs on chromosome 3A (DM partitioning and length-related) to assess the 'real' QTL effects to understand the molecular mechanisms behind this cluster region.

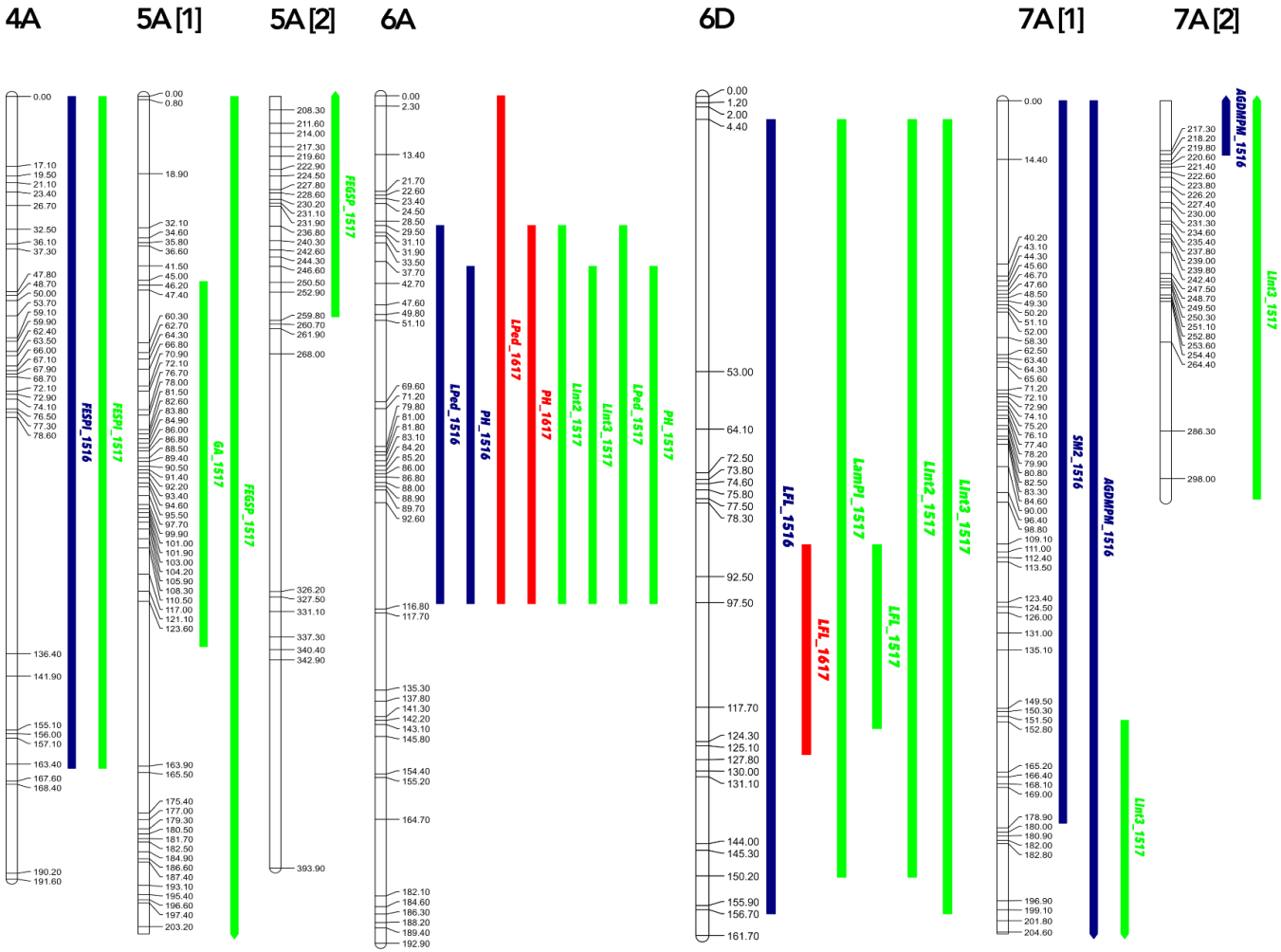
.

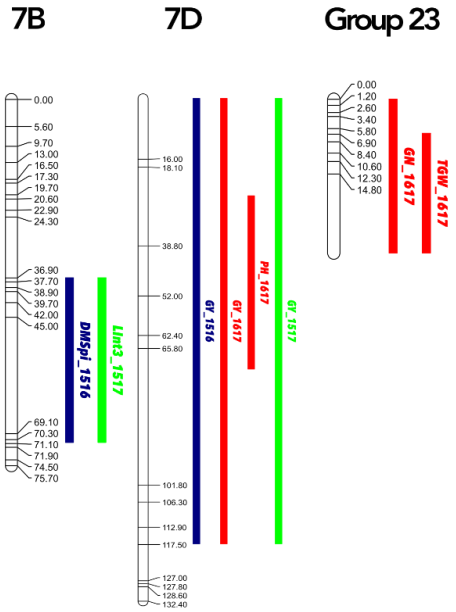
5.6. Supplementary material

Figure S5.1. Relevant QTLs (cM) identified on each wheat chromosome for the different traits measured seven days after anthesis and at physiological maturity across cross-year means for the SxR DH population based on cross-year means (Y16 and Y17)



3A [1]
3A [2]
3B [1]
3B [2]
3D
0.00
1.50
2.80
4.00
5.10
6.00
10.50
11.30
41.70
44.20
59.60
60.40
67.20
68.90
74.60
77.00
79.30
80.20
100.40
102.10
103.30
104.50
105.70
108.40
110.00
110.90
112.50
120.90
123.20
124.80
125.60
131.60
134.30
135.10
136.30
144.90
147.30
148.60
149.40
158.80
165.80
169.70
182.20
183.40
184.20
185.30
186.40
188.10
188.90
195.00
196.20
PH_1516
Lint3_1516
SPI_1516
StePI_1516
Lint2_1516
LPed_1516
GN_1617
StePI_1617
DMSte_1617
LamPI_1617
PH_1617
Lint3_1617
Lint2_1617
LPed_1617
GN_1517
SPI_1517
DMSte_1517
DTA_1517
Lint2_1517
Lint3_1517
StePI_1517
PH_1517
LPed_1517
214.90
215.70
216.90
217.80
220.30
0.00
61.40
65.40
69.30
80.60
82.10
83.30
84.80
96.70
97.70
100.10
105.10
106.70
107.60
109.20
110.00
111.30
112.40
113.50
114.30
115.40
116.30
117.40
119.70
120.80
123.30
125.60
126.80
127.80
128.60
129.40
131.90
132.70
134.70
135.70
136.50
138.20
139.00
139.80
143.10
145.50
146.40
148.00
154.50
159.40
161.80
167.70
169.30
178.80
180.50
182.70
184.90
185.70
190.80
192.40
193.60
197.10
198.00
199.00
203.70
204.60
TGW_1516
HI_1516
GN_1516
TGW_1517
GN_1517
205.70
207.00
210.50
212.90
214.60
216.20
218.70
220.30
222.00
226.20
230.80
235.20
238.50
260.00
262.50
296.40
297.50
298.40
300.10
300.90
304.30
325.70
327.90
333.80
345.90
351.60
352.80
354.00
356.30
357.10
359.40
360.60
TGW_1517
0.00
5.80
36.00
51.20
53.50
62.90
65.20
66.80
67.60
StePI_1517


4A
5A [1]
5A [2]
6A
6D
7A [1]
7A [2]
FESPI_1516
FESPI_1517
GA_1517
FEGSP_1517
LPed_1516
PH_1516
LPed_1617
PH_1617
Lint2_1517
Lint3_1517
LFL_1516
LFL_1617
LamPI_1517
LFL_1517
SM2_1516
AGDMPM_1516


7B
7D
Group 23
0.00
5.60
9.70
13.00
16.50
17.30
19.70
20.60
22.90
24.30
36.90
37.70
38.90
39.70
42.00
45.00
69.10
70.30
71.10
71.90
74.50
75.70
DMSpl_1516
Lint3_1517
16.00
18.10
38.80
52.00
62.40
65.80
101.80
106.30
112.90
117.50
127.00
127.80
128.60
132.40
GY_1516
GY_1617
PH_1617
GY_1517
0.00
1.20
2.60
3.40
5.80
6.90
8.40
10.60
12.30
14.80
GN_1617
TGW_1617

6. Optimising dry-matter partitioning using plant growth regulators in a high biomass spring wheat background

Assimilates available for spike growth during stem elongation and floret survival play an important role in determining the number of fertile florets hence grain number and yield potential. Stem carbohydrate reserves play an important role in determining grain yield as efficient accumulation and mobilization of DM could enhance spike fertility resulting in genetic gains. Results gathered in chapter 2 of the current thesis suggested that decreasing the length of central internodes genetic gains could be achieved.

Plant growth regulators (PGR) are synthetic compounds used on crops to impact on agronomic yield components by altering the plant development and growth. In winter wheat cultivars has increased plant productivity by reducing stem elongation and creating better root anchorage, therefore, decreasing lodging and increasing spike growth and yield. The use of growth retardants on spring wheat is a novel topic as the morphology of this cultivar is not expose to lodge.

In this chapter, the use of a PGR was tested on 12 high biomass spring wheat cultivars (HiBAP subset) to decrease stem internode elongation benefiting the spike with more assimilates available during critical growth periods to improve yield production. Genetic variation in response to gibberellic acid (GA) PGR (Moddus 250 CE) genotypes was recorded among treatments (control and PGR) and genotype x treatment interaction for traits measured at booting (GS41), GS65+7d and PM.

Cultivars where PGR was sprayed during stem elongation phase presented a reduction of almost 40% in plant height, with the peduncle the most affected internode. Genetic variation found between the reduction of internode lengths and spike partitioning index (SPI) within the genotypes response suggests that spike growth is more sensitive to internodes distant from the spike. The reduction of yield potential was lower due to poor spike fertility as the number of grains per unit area (GN) and the ratio of grains set per unit spike dry weight at anthesis (FE: Fruiting Efficiency) was reduced almost 50%. On the other hand, traits such as DM per spike, spike partitioning index (SPI) and harvest index (HI) did not show significant variation between control and PGR blocks. Yield decreases could be partly attributed to phytotoxicity (chlorosis) in plants where the PGR was applied when the first internode was at least one centimeter above the ground.

With the use of PGR yield potential could be improved, as this has been tested on winter wheat, but further research is required on spring wheat cultivars. This with the aim to determine appropriate product concentration and application timing for the effective use of PGR.

6.1. Introduction

Wheat is one of the three most important cereals worldwide and the FAO has estimated that for 2018/2019 the production of this crop will decrease while demand will increase (1.2%) (FAO, 2019). From 1960 to 2000 genetic gains in wheat yield (~208%) were achieved in large part as a result of the introduction of cultivars carrying *Rht* (reduced height) genes (Pingali, 2012). Before this period, wheat genotypes were characterized as tall plants (lodging-prone), with small spikes and moderate grain density disease/pest resistance which were adapted to survive under extreme environments requiring low nutrients (Gustafson et al., 2009; Shewry, 2009).

In the last decade, food security has been negatively impacted by population increase and environmental conditions (increased temperatures and reduced water availability) (Asseng et al., 2015) resulting in yield stagnation in some regions (Brisson et al., 2010; Ray et al., 2012). Recent advances in technology such as high-throughput phenotyping (Rebetzke et al., 2018), and implementation of crop simulation models (Bolger et al., 2019) have allowed a better understanding of the optimization of resources required to achieve genetic gains on wheat. Higher yield potential is related to the capacity that the plant has to accumulate biomass and then partition the dry matter to the grains (Giunta et al. 2009), but the latter may not be optimized due to assimilate competition between the stem and spike during stem elongation.

6.1.1. Spike/stem dry-matter distribution

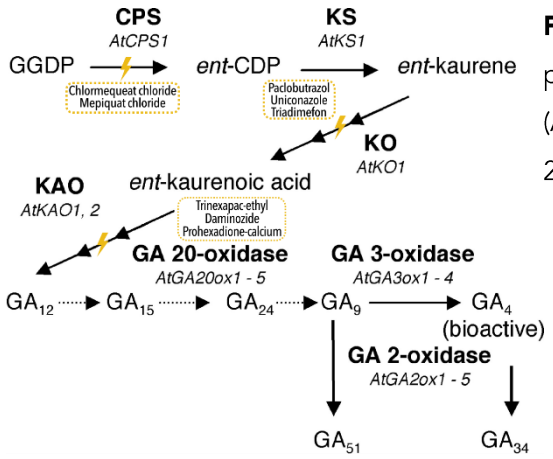
Dry matter (DM) partitioning is the result of assimilate transport of assimilates from source organs via a flow path to sink organs (Marcelis, 1996). The production of spike DM plays a fundamental role in the determination of fertile florets as a result of the interplant assimilate competition between the stem and the spike during stem elongation when grain number per unit area is fixed (Foulkes et al., 2011).

Wheat stems are erect and cylindrical joined by four to five nodes on spring wheat and from five to six nodes in winter varieties (Knapp et al., 1987; Weightman et al., 1997). The stem internodes are the hollow carbohydrate storage parts of stems, mainly surrounded by leaf sheath, situated between nodes that reach their maximum length a few days after anthesis (Cruz-Aguado et al., 2000; Schnyder 1993). Stem growth starts with a vigorous extension of internodes in sequence; when the extension is half completed the above internode will start to grow, ending with the peduncle (Lupton, 2014). Therefore lower internodes tend to store assimilates for longer compared to the peduncle (Krenzer et al., 1995, Schnyder, 1993). Increased grain number (GN) and harvest index (HI) was associated with reduced true-stem partitioning to internodes 2 and 3 recently in 26 CIMMYT elite spring wheat germplasm (Rivera-Amado et al., 2019).

6.1.2. Plant growth regulators and their action

Plant growth regulators (PGR) have been developed to antagonistically to the synthesis of gibberellic acid (GA) and auxins, hormones responsible for stem elongation (Rademacher, 2000). These synthetic compounds are used in crops to reduce plant height by repressing internode elongation and improve stem quality (increases of sclerenchyma and parenchyma cells and lignin content) resulting in non-lodged plants with a higher yield (Amram et al., 2015; Kleczewski & Whaley, 2018; Zhang et al., 2017). Higher productivity is also achieved as a result of re-distribution of assimilates decreased, plant height lowering the rate of pre-anthesis abortion of distal florets in each spikelet and increasing the total number of florets viable at anthesis (Pirahmadi et al., 2016). Therefore, genotypes with semi-dwarf genes (*Rht*) characterized by shorter plants with smaller leaves but increased photosynthetic rates may be comparable to cultivars where PGR is applied. Examing wheat isogenic lines carrying different *Rht* genes (*Rht4*, *Rht5*, *Rht8*, *Rht12* and *Rht13*), Rebetzke et al. (2012)reported the reduction of plant height from 17 to 55%, compared to the control cultivars, benefiting grain production by 9 to 27%. Yield advantages of *Rht* lines derive from increased partitioning of assimilates to the developing spike associated with reduced stem elongation growth (Fischer & Stockman, 2006).

Growth regulators which are antagonistic to gibberellins can be divided into three classes depending on the mechanism of inhibition of GA biosynthesis (Sun, 2008) (Figure 6.1). The first class known as quartenary ammonium (chlormequat chloride, mepiquat chloride and chlorophenium chloride) block the ent-kaurene synthesis from geranylgeranyl diphosphate. The second group consists of heterocyclic compounds which inhibit the oxidation of ent-kaurene to ent-kaurenoic acid by the P450 monooxygenases during stage 2 of gibberellin biosynthesis (ancymidol, tetcyclases, and triazole-type). The last class includes acylcyclohexanediones and inhibit 2-oxoglutarate-dependent dioxygenases at stage three of gibberellin biosynthesis (Espindula et al., 2009).



CPS: *ent*-copalyl diphosphate synthase, ent-CDP: *ent*-copalyl diphosphate, GGDP: geranyl diphosphate, KAO: *ent*-kaurenoic acid oxidase, KO: *ent*-kaurene oxidase, KS: *ent*-kaurene synthase

Figure 6.1. Gibberellin acid biosynthesis and points of inhibition by plant growth retardants (Adapted from: Sun, 2008 & Rademacher, 2000).

Moddus 250EC is a synthetic trinexapac-ethyl (TE) based compound, which blocks the enzymes produced late in the biosynthesis of gibberellin acid (Figure 6.1) and was introduced as a growth inhibitor in 1998 (Sezer et al., 2016). Studies have reported yield increases if the product is applied in good environmental conditions (high retention and absorption) at the appropriate developmental timing, the optimum windows starts from the first node is at least one cm above tillering node until second internode is detectable (Lancashire et al., 1991). This retardant is reported to decrease dry matter production and internode length, but increase stem diameter, number of spikes per unit area and grain yield and at the same time influence photosynthesis level through the increase of leaf chlorophyll content and root growth and development (Ervin & Koski, 2001; Matysiak, 2006).

In wheat chlormequat, trinexapac-ethyl and paclobutrazol presented good results in reducing plant height (Espindula et al., 2009). Combining two different types of PGRs (chlormequat and trinexapac-ethyl) on six spring wheat cultivars grown under a greenhouse environment Zhang et al. (2017) observed no lodging plants as consequence of a reduction in plant height (22 to 48%). This was caused by the shortening of the second internode but yield losses were registered when the regulators were applied when the first internode was detectable (GS31). In barley plants, no significant impact was detected on grains per spike or yield when TE was applied (Miziniak et al., 2017). When TE was applied at GS30 in addition to a fungicide yield increases were reported in a soft red winter wheat population (Kleczewski & Whaley, 2018)

The effects on spike growth through the use of TE-based plant retardant were studied on a spring wheat high biomass genotypes through the reduction of stem internode length increased grain number and yield potential.

Chapter hypotheses:

- Increase of assimilate to the spike during stem elongation in response to Moddus 250 EC application enhances floret survival hence grains per m2
- Stem internode 2 and 3 lengths are reduced by the application of plant growth retardant at GS31/32 more than other internodes.
- Spike DM per unit area is increased in response to PGR application at GS31/32 as a result of less competition with stem internode 2 and 3 during the stem-elongation stage.
- Spike growth, harvest index and grain yield showed PGR treatment x genotype interactions where Moddus 250 EC was applied during stem elongation phase.

6.2. Materials and methods

6.2.1. Plant material and experimental design

The experiment (HIBAP_PGR) was carried over one season (Y18: 2017-18) under high yield potential conditions using an alpha-lattice design with two replicates per treatment (control and PGR) at the Norman E. Borlaug experimental station near Ciudad Obregon, Sonora, Mexico (27°N, 110°W and 38 m above the sea level). Control and PGR replicates were

separated from each other by a buffer area of 7.2 m wide x 15 m long (Figure S6.1). From the HiBAP panel a subset of 12 genotypes (Table S2.1) were sown in raised beds (two beds per plot each 0.8 m wide x 5 m long) with four rows per bed (0.1 m between rows) using a seed rate of 102 kg ha^{-1}. The selection of the subset (HiBAP_PGR) was done based on representing the full range of genetic variation in stem and spike partitioning at seven days after anthesis (GS65+7d) in the HiBAP panel in 2015-16 and 2016-17 (Table S6.1).

The sowing date was 5 December 2017 and 50% plant emergence occurred on 12 December 2017. Irrigation was supplied through the whole cycle using a gravity-based system, with the first application a month after sowing and then every three to four weeks. Herbicides (one application: 02/01), for broad-leaved weeds, fungicides (two applications: 29/01 and 08/03) and insecticides (one application: 09/02) were applied to minimise the effects of weeds, diseases and pests. An application of fertiliser nitrogen (50 kg N ha^{-1}) as urea was applied during land preparation, followed by an application of triple super phosphate (50 kg P ha^{-1}) at sowing. A second and third N application (50, 150 kg N ha^{-1} respectively) as urea was applied at the same time that the experiment was irrigated (first and second irrigations).

Weather means for temperature, accumulated rainfall and solar radiation were calculated for both seasons during booting (GS41-GS49), anthesis (GS59-GS69) and grain filling (GS71-GS91) stages (Table S6.2). Meteorological data were obtained from a weather station located within 1 km of the experiment (lat: 27.4°, long: -109.9°, altitude: 38 m).

PGR application (GS31-2)

Moddus 250EC is an emulsifiable concentrate containing 250 g l^{-1} (25.5% w/w) trinexapac-ethyl per litre and was prepared following the product recommendations (Syngenta). The application of the product was done on the PGR treatment replicates over the whole bed using a knapsack sprayer according to the growth stage of each genotype (Figure S6.2).

The PGR product nearest at a concentration of 0.7 l ha^{-1} which consisted of 13.4 ml of Moddus 250EC in 1.92 l of water. The application was done according to the growth stage of the genotype, as soon as the second internode was at least one centimetre (GS31-2); the PGR was sprayed directly at canopy level. Beds adjacent to the genotype in which the application was occurring were covered with black plastic bags to avoid overexposure to the PGR treatment.

6.2.2. Crop measurements

Sampling and crop development

Samples for growth analysis were taken at four growth stages, (i) two days prior to PGR application when the second internode was extended at 1 cm (GS31-2), (ii) onset of booting (GS41), (iii) seven days after anthesis (GS65+7d) and finally at (iv) physiological maturity (PM: shoots with yellow-green peduncle, GS87) (Zadoks et al., 1974). The stages were taken as when 50% of the fertile shoots in the plot had reached the stage.

Biomass pre-PGR application at GS29

To have a comparison before and after the application of the PGR biomass sampling was done two days before application in a quadrat of 0.8 x 0.5 m avoiding edge effects (at least 50 cm from ends of plots). Stems were cut at ground level and the fresh weight (FW) of the total biomass sample was recorded in each plot. The material was then dried for 48 h at 70°C and the dry weight (DW) was recorded.

Biomass and dry-matter partitioning at GS41

At GS41 in two replicates, sampling of plant material was carried out in a quadrat of 0.8 x 0.5 m avoiding edge effects (at least 50 cm from ends of plots); shoots were cut at ground level and the fresh weight (FW) of the total sample was recorded, thereafter the material was dried for 48 h at 70°C and its dry weight (DW) recorded. From the material collected 12 fertile shoots were randomly selected from which partitioning analysis was carried out. For the plant dry-matter partitioning analysis (PI: Partitioning Index, ratio between component DM and AGDM) each fertile shoot was separated into: i) leaf lamina and ii) stem (true stem+leaf sheath). The DW for each plant component was recorded after oven drying at 70°C for 48 h.

Biomass and DM partitioning at GS65+7d

At GS65+7d in two replicates, sampling was carried out in a quadrat of 0.8 x 0.5 m as described at GS41. From the plant material, 12 fertile shoots (spike fully emerged) were randomly selected to carry out a partitioning analysis. Plant dry-matter partitioning analysis was carried out by separating the plant components: (i) spike, ii) leaf lamina and iii) stem (true stem+leaf sheath). The material for each plant component was dried for 48 h at 70°C and its weight was recorded. In addition the lengths of each stem internode: i) peduncle, ii) internode 2 (internode below peduncle) and iii) internode 3 were recorded with a ruler and the green area of the leaf lamina was measured using a planimeter (LI-3100C Area Meter: LiCOR, Lincoln).

Additionally, at this stage the stem was further separated into its phytomers, with the true-stem (TS) and the leaf sheath (LS) separated for each internode: peduncle (Ped), internode 2 (Int2), internode 3 (Int3) and internode 4 and below (Int4+). The dry weights were recorded for each component after oven drying at 70°C for 48 h. Finally, the 12 spikes sampled at GS65+7d were dissected into: i) glume, ii) lemma, iii) palea, iv) rachis and v) awn. The different spike components were bulked and weighed separately after drying at 70°C for 48 h.

Plant height, flag leaf, spike and awn length

Plant height and flag-leaf length were assessed on five randomly selected shoots per plot after the PGR application (GS41) in two replicates (ctrl: 1 & 2 and PGR: 5 & 6). At the beginning of the grain-filling period, plant height, flag-leaf, spike and awns length was recorded in two replicates on five randomly selected shoots per plot. Plant height was measured from the soil surface level (avoiding wells or irregular ground) to the tip of the spike and spike length from the spike collar to the tip of the spike (awns were excluded on both measurements) and awns from the initiation of the awn to the end of the awn.

Physiological maturity, grain yield and yield components

At physiological maturity (PM) 50 randomly selected fertile shoots were cut at ground level in two replicates and separated into the spike and stem (true stem + leaf sheath). Dry weight for each plant component was recorded after drying for 48 h at 70ºC. Spikes collected from the 50 random shoots were threshed and grains and chaff were collected. After sampling each plot for yield components, the whole experiment (two replicates) was machine-harvested in a plot area of ~3-4 m^{-2}, after harvesting grain sample was collected to determined the weight of 200 grains using the image analysis system SeedCounter (SeedCountSC5000 Image Analyser, New Jersy) and the weight recorded after drying for 48 h at 70ºC. From the data obtained spikes m^{-2} (SM2), grains m^{-2} (GN), HI, final AGDM per unit area and fruiting efficiency (FE) were calculated (Table S2.4).

6.2.3. Statistical analysis

Statistical analysis (adjusted means, ANOVA, regression analysis and heritability) of phenotypic data was carried out using the program SAS University Edition (SAS), according to the following the model (Equation 6.2):

$$Y_{gtk} = \mu + \alpha_g + n_t + \alpha_{ngt} + r(ns)_{tk} + \varepsilon_{gtk} \quad [6.2]$$

where Y_{gtk} is the trait for genotype g grown in block k and PGR treatment t, μ is the general mean, α_g is the genotype main effect, n_t is the PGR treatment main effect, α_{ngt} is the genotype × PGR treatment interaction, $r(ns)_{tk}$ is the effect of block in PGR treatment, and ε_{gtk} is the residual effect.

GenStat 17th edition (VSN International) was used for calculating the Pearson's correlation coefficients and the linear/non-linear regressions using the genotype means from the ANOVA.

6.3. Results

Significant differences, mainly at stem level and yield-related traits, were found among the control and those plots were the PGR was applied during stem elongation. Significant genetic variation was found for most traits measured during stem elongation (GS29), at booting (GS41), seven days after anthesis (GS65+7d) and physiological maturity (PM) in the control and PGR treatments (Table 6.1). The significance of the treatment (T) and G × T effects were variable for the traits measured. At GS65+7d a detailed partitioning dissection was carried at the stem internode level (Table 6.2) and within spikes (Table 6.3).

Table 6.1. Phenotypic ranges, significance (*p-values*) and broad-sense heritability (H^2) for 12 HiBAP genotypes for control and PGR treatments in Y18 (2017-18) for traits at stem elongation (GS29), booting (GS41), seven days after anthesis (GS65+7d) and physiological maturity (GS87).

Stage	Traits	Units	Control				PGR				*P(T)*	*P(G)*	*P(G×T)*
			H^2	Min	Mean	Max	H^2	Min	Mean	Max			
Stem elongation (GS29)	$AGDM_{SE}$	$g\ m^{-2}$	0.57	222	278	332	0.05	226	279	311	ns	ns	ns
	Stems	m^{-2}	0.89	489	636	859	0.57	458	631	820	ns	***	ns
Booting (GS41)	DTB	DAE	0.80	53	58	63	0.87	57	61	64	**	***	ns
	AGDM	$g\ m^{-2}$	0.45	409	490	617	0.69	408	485	554	ns	*	ns
	Stems	m^{-2}	0.85	417	552	773	0.73	450	534	655	ns	***	ns
	$AGDM_{BT}$		0.46	0.55	1.11	1.48	0.85	0.93	1.22	1.58	ns	**	ns
	DM Ste	g per $shoot^1$	0.51	0.21	0.53	0.76	0.80	0.45	0.62	0.82	*	**	*
	DM Lam		0.58	0.29	0.59	0.77	0.88	0.41	0.60	0.80	ns	***	ns
	StePI	%	0.94	0.39	0.47	0.55	0.97	0.43	0.51	0.60	ns	***	**
	LamPI		0.94	0.45	0.53	0.61	0.97	0.40	0.49	0.57	ns	***	**
	GA	$g\ cm^{-1}$	0.54	113.6	155.7	234.0	0.68	112.5	143.0	157.0	ns	**	ns
	PH	cm	0.67	46.3	52.1	60.1	0.67	26.8	31.8	39.0	***	***	ns
Anthesis + 7 days (GS65+7d)	DTA	DAE	0.98	74	83	88	0.96	83	92	96	***	***	***
	$AGDM_{A+7}$	$g\ m^{-2}$	0.09	876	1051	1151	0.38	821	1023	1597	ns	*	ns
	Stems	m^{-2}	0.81	344	492	722	0.33	418	615	755	ns	***	ns
	$DMSpk_{A+7}$	$g\ m^{-2}$	0.21	317	402	499	0.59	316	405	550	ns	***	ns
	$AGDM_{A+7}$		0.90	2.11	3.21	4.22	0.87	1.46	2.84	3.66	*	***	*
	DM Ste	g per $shoot^1$	0.90	1.01	1.68	2.24	0.92	0.64	1.32	1.74	***	***	ns
	DM Lam		0.90	0.47	0.69	1.04	0.77	0.38	0.67	0.85	ns	***	***
	DM Spk		0.84	0.56	0.83	1.18	0.79	0.48	0.85	1.21	*	***	*
	StePI		0.93	0.45	0.53	0.59	0.87	0.37	0.46	0.53	*	***	***
	LamPI		0.80	0.18	0.22	0.26	0.14	0.20	0.24	0.27	*	ns	**
	SPI		0.71	0.20	0.26	0.30	0.66	0.24	0.30	0.39	*	***	ns
	FE	grains g^{-1}	0.95	43.8	59.1	88.2	0.52	14.7	26.0	44.3	***	***	*
	GA	$cm^2\ shoot^{-1}$	0.61	99.2	144.1	183.1	0.66	98.6	125.9	158.3	*	*	ns
	SpkIspk	#	0.97	20	22	26	0.97	18	22	25	ns	***	ns
	WSCSpk		0.37	9.66	12.6	16.9	N/A	11.3	14.4	17.7	***	**	**
	WSCSte		0.55	8.25	11.9	17.3	0.83	23.7	28.6	35.2	ns	ns	ns

Stage	Traits	Units	Control				PGR				*P(T)*	*P(G)*	*P(G×T)*
			H^2	Min	Ave	Max	H^2	Min	Ave	Max			
Anthesis + 7 days (GS65+7d)	PH	cm	0.94	89.5	102.6	117.4	0.82	45.2	53.0	67.4	**	***	***
	LnPed		0.91	30.9	98.7	45.5	0.09	12.7	16.1	19.4	***	***	**
	LnInt2		0.96	17.0	19.7	23.7	0.67	6.45	9.85	13.6	***	***	*
	LnInt3		0.97	12.0	14.3	17.7	0.68	5.25	6.90	8.70	***	***	***
	LnFL		0.86	21.4	26.1	30.4	0.84	15.7	19.3	22.4	***	***	***
	LnAwn		0.70	5.87	6.87	8.07	0.79	4.41	5.25	6.34	***	***	ns
	LnSpk		0.99	8.40	11.5	13.3	0.63	7.85	11.1	14.9	ns	***	ns
Physiological maturity (GS87)	DTM	DAE	0.97	112	116	120	0.95	117	125	130	***	***	***
	$AGDM_{PM}$	g m^{-2}	0.11	1464	1984	2621	0.92	528	937	2915	**	*	**
	GY	g m^{-2}	0.88	536	648	740	0.63	213	282	403	***	***	ns
	TGW	g	0.97	32.8	41.9	47.7	0.94	28.5	37.4	44.3	***	***	**
	HI		N/A	0.26	0.35	0.43	0.53	0.14	0.36	0.43	ns	ns	ns
	GN	grains m^{-2}	0.90	12016	15644	20017	0.29	5741	7678	11982	***	*	*
	SM2	spikes m^{-2}	0.10	316	650	1348	0.67	121	292	1032	*	ns	ns
	GSP		0.40	16	32	53	N/A	13	39	54	ns	ns	ns

SE: Stem Elongation; **BT:** Booting; **A+7**: Anthesis +7 days; **PM:** Physiological Maturity; **AGDM:** Above-Ground Dry Matter; **C.T:** Canopy Temperature; **DTB:** Days from emergence to booting; **DM Ste:** Dry Matter Stem; **DM Lam**: Dry Matter Lamina; **DM Spk:** Dry Matter Spike; **StePI:** Stem Partitioning Index; **LamPI:** Lamina Partitioning Index; **$DMSpk_{A+7}$**: Green Area; **GA:** Green Area; **Spklspk:** Spikelets per spike; **PH:** Plant Height; **DTA:** Days from emergence to anthesis; **WSC:** Water-soluble carbohydrates; **FE:** Fruiting Efficiency; **LnPed**: Length Peduncle; **LnInt2:** Length Internode 2; **LInt3:** Length Internode 3; **LFL:** Length Flag Leaf; **LAwn:** Length Awns; **LSpk:** Length Spike; **DTM:** Days from emergence to maturity; **GSP:** Grains Per Spike; **GY:** Grain Yield (100% DM); **TGW:** Thousand Grain Weight; **HI:** Harvest Index; **GN:** Grain Number; **SM2:** Spikes per unit area; **GSP:** Grains per spike

***P*(T):** Significance per treatment; ***P*(G):** Significance of the genotype; ***P*(G×T):** Significance treatment × genotype; **H^2:** Broad-sense heritability (cross-year analysis)

**P<0.05, **P<0.01, ***P<0.001, ns: non-significant*

Table 6.2. Phenotypic ranges, significance (*p-values*) and broad-sense heritability (H^2) for 12 HiBAP genotypes for control and PGR treatments in Y18 (2017-18) for stem internode traits measured at GS65+7d.

	Traits			Control				PGR				*P(T)*	*P(G)*	*P(G×T)*
			Units	H^2	Min	Ave	Max	H^2	Min	Ave	Max			
Anthesis + 7days (GS65+7d)	Ped	TS	DW	g shoot^{-1}	0.87	0.25	0.39	0.54	0.91	0.12	0.21	0.32	***	***	**
			PI		0.94	0.09	0.12	0.17	0.78	0.05	0.07	0.10	**	***	ns
			SW	g cm^{-1}	0.92	0.006	0.010	0.014	0.68	0.009	0.013	0.017	*	**	ns
		LS	DW	g shoot^{-1}	0.86	0.17	0.25	0.31	0.96	0.16	0.26	0.33	ns	***	ns
			PI		0.87	0.06	0.08	0.10	0.93	0.06	0.09	0.12	ns	***	*
			SW	g cm^{-1}	0.93	0.004	0.007	0.010	0.81	0.011	0.017	0.027	***	***	**
	Int2	TS	DW	g shoot^{-1}	0.70	0.21	0.31	0.42	0.65	0.12	0.21	0.33	**	**	*
			PI		0.65	0.05	0.10	0.11	0.54	0.06	0.07	0.10	*	*	ns
			SW	g cm^{-1}	0.75	0.010	0.016	0.023	0.77	0.013	0.021	0.024	***	*	*
		LS	DW	g shoot^{-1}	0.08	0.08	0.14	0.24	0.86	0.06	0.15	0.22	ns	**	ns
			PI		0.31	0.03	0.04	0.06	0.13	0.04	0.05	0.07	*	ns	ns
			SW	g cm^{-1}	0.48	0.003	0.004	0.006	0.62	0.008	0.012	0.022	***	*	*
	Int3	TS	DW	g shoot^{-1}	N/A	0.11	0.21	0.31	0.91	0.09	0.16	0.23	*	**	ns
			PI		0.30	0.05	0.07	0.08	0.86	0.05	0.06	0.07	ns	ns	ns
			SW	g cm^{-1}	0.49	0.009	0.015	0.023	0.93	0.016	0.023	0.028	**	***	ns
		LS	DW	g shoot^{-1}	0.54	0.05	0.09	0.16	0.77	0.05	0.09	0.15	ns	***	ns
			PI		0.89	0.02	0.03	0.04	0.26	0.02	0.03	0.04	ns	ns	ns
			SW	g cm^{-1}	0.24	0.004	0.007	0.009	0.85	0.006	0.013	0.022	*	***	*
	Int4+DW			g shoot^{-1}	0.90	0.09	0.27	0.49	0.88	0.08	0.22	0.40	ns	***	ns
	Int4+PI				0.90	0.04	0.08	0.12	0.86	0.04	0.08	0.11	ns	***	*

Ped: Peduncle; **Int2**: Internode 2; **Int3**: Internode 3; **Int4+**: Internode 4+; **TS**: True-stem; **LS**: Leaf sheath; **DW**: Dry weight; **PI**: Partitioning index; **SW**: Specific weight

P(T): Significance per treatment; ***P*(G)**: Significance of the genotype; ***P*(G×T)**: Significance treatment × genotype; **H^2**: Broad-sense heritability (cross-year analysis)
**P<0.05, **P<0.01, ***P<0.001, ns: non-significant*

Table 6.3. Phenotypic ranges, significance (*p-values*) and broad-sense heritability (H^2) for 12 HiBAP genotypes for control and PGR treatments in Y18 (2017-18) for spike partitioning traits measured at GS65+7d.

	Trait		Control				PGR				*P(T)*	*P(G)*	*P(G×T)*
		Units	H^2	Min	Ave	Max	H^2	Min	Ave	Max			
Anthesis + 7days (GS65+7d)	GluDW	g spk^{-1}	0.86	0.08	0.12	0.18	0.98	0.09	0.15	0.22	***	***	*
	GluPI		0.58	0.11	0.15	0.20	0.50	0.12	0.18	0.22	ns	*	ns
	LeDW	g spk^{-1}	0.52	0.11	0.17	0.22	0.64	0.12	0.18	0.25	ns	***	ns
	LePI		0.63	0.15	0.21	0.29	0.56	0.13	0.22	0.26	ns	*	ns
	PaDW	g spk^{-1}	0.73	0.04	0.07	0.08	0.40	0.04	0.08	0.14	ns	*	ns
	PaPI		0.60	0.05	0.08	0.10	N/A	0.06	0.09	0.14	ns	ns	ns
	RaDW	g spk^{-1}	0.90	0.05	0.09	0.13	0.97	0.05	0.10	0.13	***	***	*
	RaPI		0.81	0.07	0.12	0.19	0.49	0.07	0.12	0.14	ns	**	**
	RaSW	g cm^{-1}	0.78	0.006	0.008	0.010	0.88	0.006	0.009	0.011	***	***	ns
	AwDW	g spk^{-1}	0.89	0.10	0.15	0.23	0.96	0.07	0.12	0.19	**	***	*
	AwPI		0.63	0.11	0.19	0.25	0.63	0.10	0.14	0.19	ns	**	*

Glu: Gluma; **Le:** Lemma; **Pa:** Palea; **Ra:** Rachis; **Aw:** Awns; **DW:** Dry weight; **PI:** Partitioning Index; **SW:** Specific weight

P(T): Significance per treatment; ***P*(G)**: Significance of the genotype; ***P*(G×T)**: Significance treatment × genotype; **H^2**: Broad-sense heritability (cross-year analysis)

**P<0.05, **P<0.01, ***P<0.001, ns: non-significant*

6.3.1. Crop development and canopy temperature

Crop development was delayed in the PGR treatment where treated plants reached booting from 57 to 64 days after emergence (DAE) and control plants from 53 to 63 DAE (*P<0.01*; Figure 6.2a). Similarly, PGR-treated plants reached anthesis later with genotypes ranging from 83 to 96 DAE and control plants from 74 to 88 DAE (*P<0.001*; Figure 6.2b). For physiological maturity (*P<0.001*) PGR-treated plants were later ranging from 112 to 120 DAE than control plants ranging from 117 to 130 DAE (Figure 6.2c). For GS65+7d and PM the GxT interaction was significant (*P<0.001*; Table 6.1).

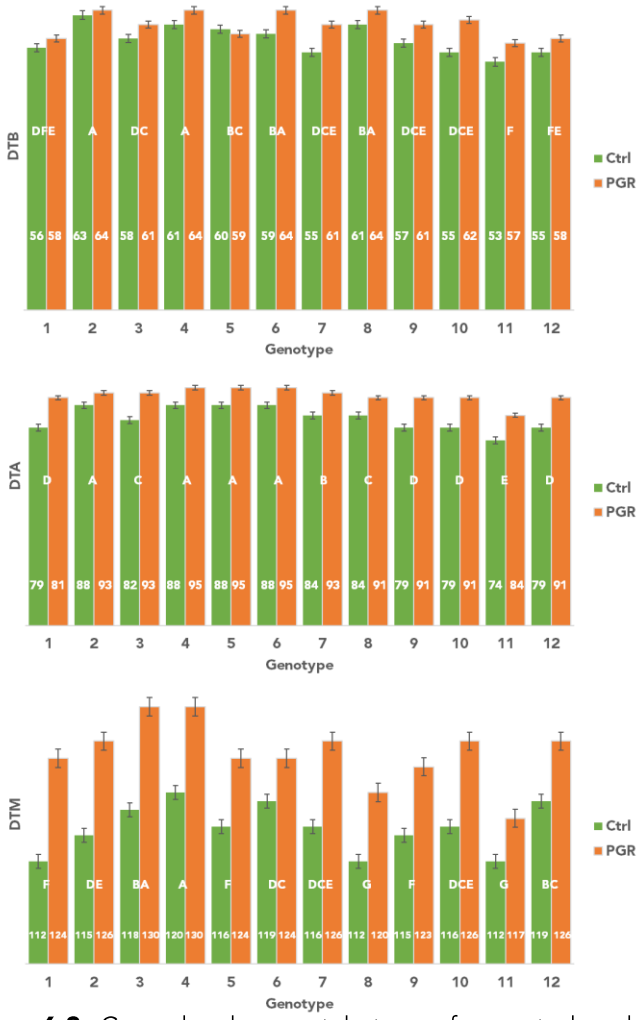


Figure 6.2. Crop developmental stages for control and PGR treatment for 12 HiBAP genotypes from emergence to a) booting (DTB:GS41), b) seven days after anthesis (DTA: GS65+7d) and c) physiological maturity (DTM: PM).
Means with a common letter are not significantly different. (*P<0.05*).

6.3.2. GS29 and GS41 biomass DM partitioning

For above-ground DM at GS29 ($AGDM_{SE}$) prior to application of PGR no significant effect was detected for treatment, genotype and GxT. For fertile shoots per m^2 no significance was found for treatment, but genotypes ranged from 458 to 820 m^{-2} in the PGR treatment and

from 489 to 859 m^{-2} in the control (*P<0.001*); the GxT interaction was not significant (Table 6.1).

Post-PGR application treatment (Figure 6.3) effects for traits measured at GS41 were not significant except for plant height which was reduced by almost 40% with PGR treatment (*P<0.001*) and stem DM $shoot^{-1}$ where higher values were recorded for the PGR treatment than the control (Figure 6.4). Genotype x treatment interaction for DM ste, stePI and lamPI was detected (*P<0.05*; Table 6.1).

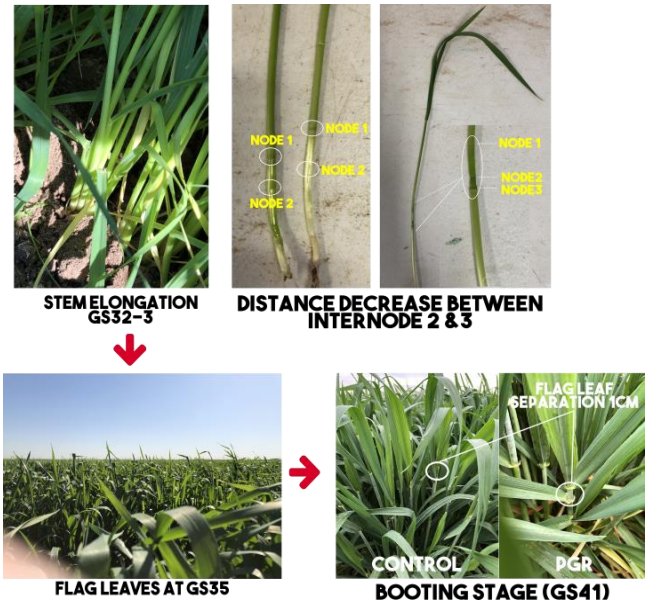


Figure 6.3. Experiment development through stem elongation and booting stage.

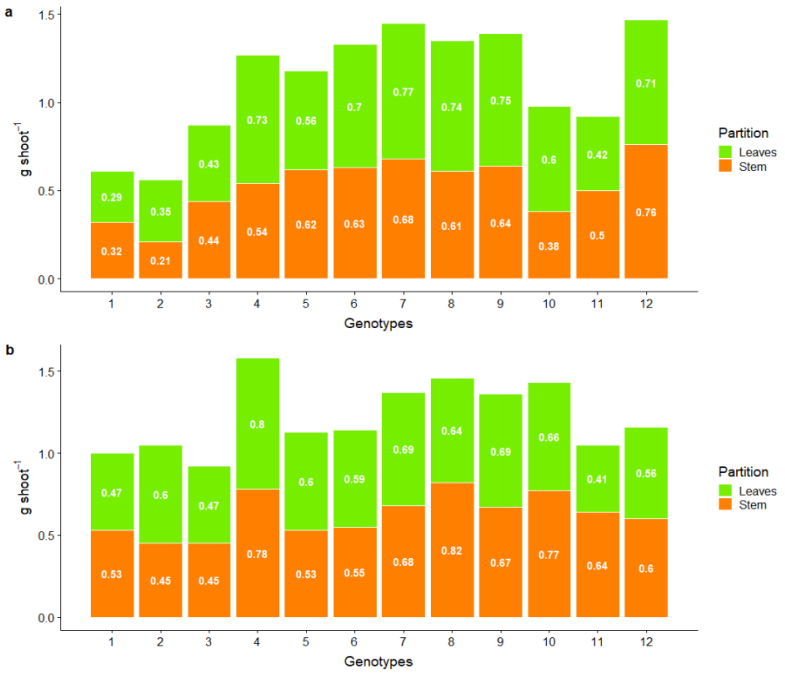


Figure 6.4. DM stem and leaf-sheath (stem) and leaf lamina (leaves) partition (g $shoot^{-1}$) among the 12 genotypes at a) control and b) PGR blocks at booting (GS41).

6.3.3. GS65+7d biomass DM partitioning and plant components lengths

At this stage no effect of PGR treatment was detected on $AGDM_{A+7}$, shoots and spikes per unit area, lamPI, true-stem water-soluble carbohydrates (WSC) and spikelets per spike (Table 6.1). PGR treatment decreased AGDM per $shoot^{-1}$, DM ste, DM spk, green area per $shoot^{-1}$ (GA) and fruiting efficiency (FE: number of grains set per unit spike dry weight at anthesis) compared to the control plants (*P<0.05*; Table 6.1). On the other hand, the amount of assimilates partitioned to the spike (SPI; Figure 6.5) and WSC on the spike increased around 15% on those plants were the PGR was applied compared to the control block (*P<0.01*; Table 6.1).

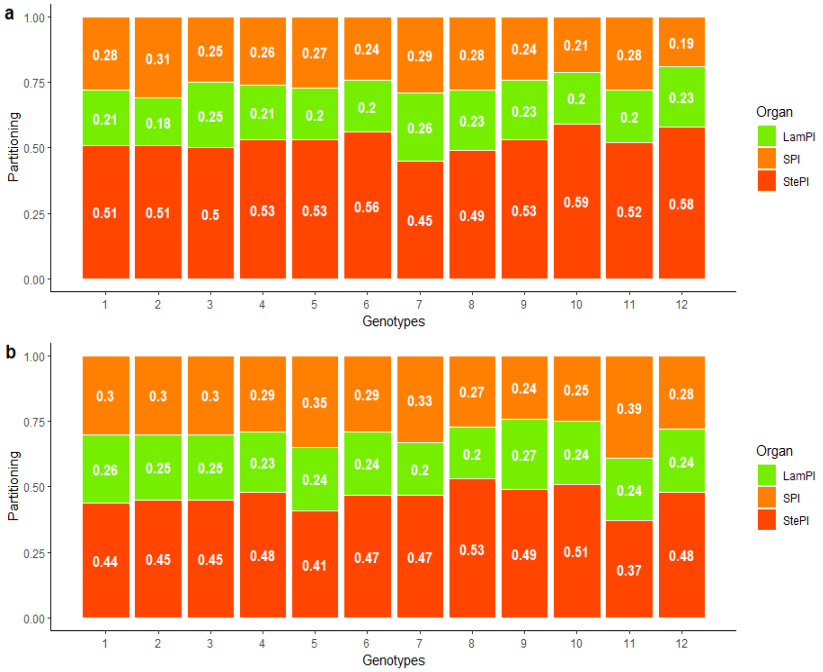


Figure 6.5. Partitioning of above-ground DM at GS65+7d among leaf lamina (LamPI), spike (SPI) and stem (StePI) on a) control and b) PGR blocks.

The only traits that showed a GxT interaction were those that scored a treatment interaction, except for DM ste, SPI and GA. At this stage most of the traits showed high heritability value (H^2>0.50) excluding $AGDM_{A+7}$, $DMSpk_{A+7}$, WSCSpk on both block and lamPI just on the PGR side (Table 6.1).

Plant height and lengths of stem internodes, spike, awns and flag leaf were measured at GS65+7d (Figure 6.6). The traits showed high heritability (h^2>0.60), except for peduncle length in PGR-treated plants (Table 6.1). Significant treatment, genotype and GxT interaction effects were detected for most of the length-related traits, except for spike length (no genotype effect and GxT interaction) and awns length (no GxT interaction) (Table 6.1, Figure 6.6). Plant height was reduced almost 50% when PGR was applied (*P<0.01*), with the peduncle the most affected internode (-80%), followed by internodes 2 and 3 (both -50%) (Table 6.1, Figure 6.6). At the

same time, awns and flag leaf length in the PGR-treated plants were reduced compared to the control plants. (Table 6.1, Figure 6.6).

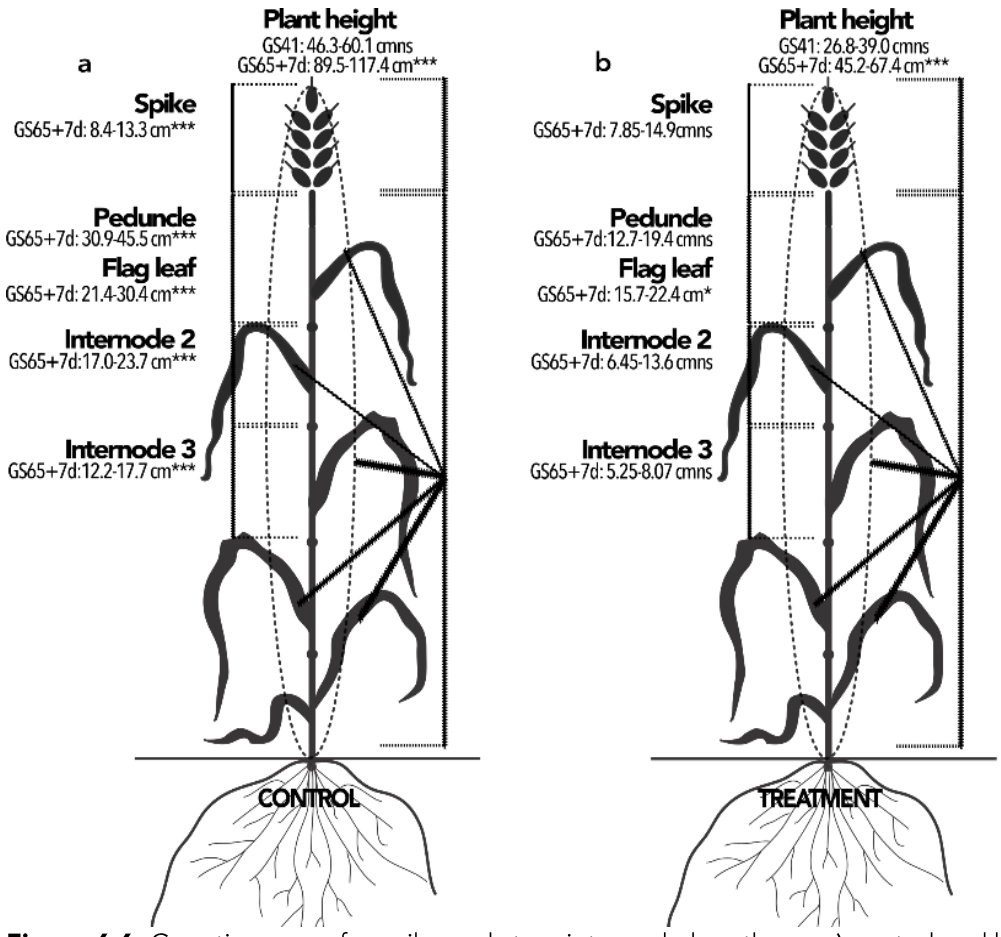


Figure 6.6. Genetic ranges for spike and stem-internode lengths on a) control and b) PGR plants.

6.3.4. Stem internode DM partitioning at GS65+7d

Overall significant effects for genotype, PGR treatment and GxT interaction were found for stem internode traits where more DM was allocated in the upper phytomers for the control plants: pedTS > int2TS > int4+ > pedLS > int3TS > int2LS > int3LS. On the other hand, for PGR-treated plants the order changed slightly: pedLS > int4+ > pedTS > int2TS > int3TS > int2LS > int3LS. For these traits high heritability (h^2>0.50) was scored, except for the control plants for internode 2 and 3 (Table 6.2).

In PGR-treated plants relatively more DM was partitioned to peduncle LS and the int2 LS, and in control plants relatively more DM was partitioned to the peduncle and internode 2 TS than other plant components (Table 6.2). The ratio of length to the amount of DM accumulated per phytomer (specific weight) was highest in the central internodes, being highest for int3 for PGR-treated plants and int2 for control plants (Table 6.2).

6.3.5. Spike morphological partitioning

Moderate heritability and significant genetic variation was found for most of the traits, but for some no significance was found for treatment and GxT interaction. The order of DM accumulation per spike component was lemma > awns > glume > rachis > palea for the control and the same order in the PGR treatment (Table 6.3). Significant PGR treatment increased glume DW (*P<0.001*), gluPI (*P<0.05*) and rachis SW (*P<0.05*) compared to control plants. Nevertheless, awn PI was decreased (*P<0.05*) in PGR-treated plants in comparison with control plants (Table 6.3).

6.3.6. Biomass, grain yield, yield components and DM partitioning at PM

Moderately high heritability values (h^2>0.50), genetic and PGR treatment variation was found for most of the traits measured at physiological maturity, but GxT interaction was only found for $AGDM_{PM}$, TGW and GN. A large decrease of around ~50%, was observed in $AGDM_{PM}$ in PGR plants treated compared to control plants which was also reflected in grain yield and GN (Figure 6.7a to c). However, there was no decrease in harvest index (HI) or fruiting efficiency (FE) (Table 6.1).

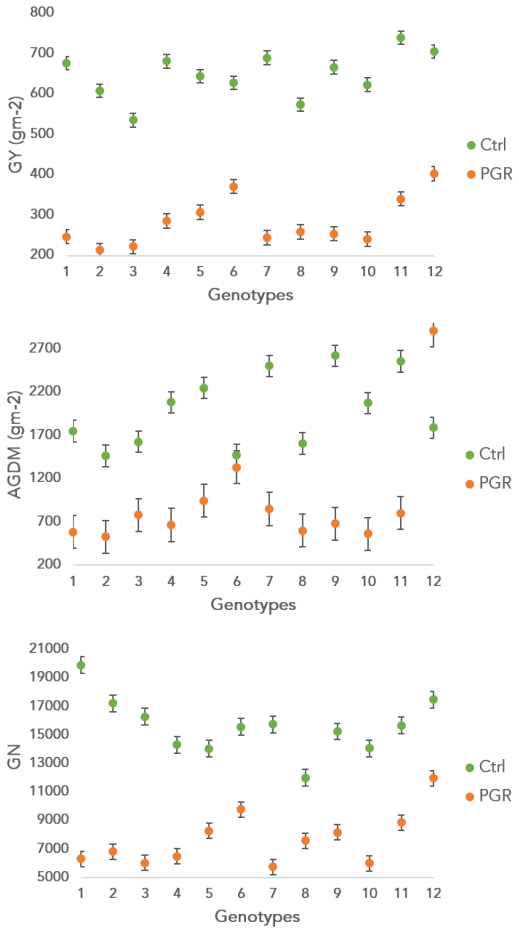


Figure 6.7. Genetic variation among 12 HiBAP genotypes at PM in the control (ctrl) and PGR-treatment in a) grain yield (GY: 100% DM), b) Above-Ground DM (AGDM) and c) grains per m^2 (GN).

6.3.7. Correlations between partitioning traits, grain number, harvest index and grain yield

Positive associations were found between grain yield (GY) and above-ground DM at physiological maturity ($AGDM_{PM}$) and spikes m^{-2} (SM2), and a significant negative association between harvest index (HI) had $AGDM_{PM}$ in both treatments. Grain number per unit area (GN) and SM2 were negatively associated with HI in the PGR treatment, whereas in the control the associations were not significant. Interestingly variation between treatments was found among GN and internode lengths, as in the PGR-treated plants peduncle, internode 2 and internode 3 were positively associated, whereas in the control plants only internode 2 and internode 3 lengths were positively associated. Grains m^{-2} was positively related with fruiting efficiency (FE) in both treatments, more strongly for the PGR treatment than in the control. A negative relation was found between FE and spike partitioning index (SPI) and length of peduncle (LPed) in the control which were not observed in the PGR-treated plants. On the other hand, FE was positively associated with $AGDM_{PM}$, GN and SM2 in PGR-treated plants but only FE and GN were also positively associated with the control (Table 6.4 and Table 6.5). The trade-off between SPI and stem partitioning index (stePI) was observed, as reported in chapters 2 and 3, in both treatments, been slightly stronger in the PGR treatment. This could be partly explained by the negative association between DM spike m^{-2} at anthesis ($DMSpkA_{+7}$) and the lengths of internodes, which were observed for peduncle length in the PGR treatment and internode 2 and internode 3 length in the control plants (Table 6.4 & Table 6.5).

Table 6.4. Pearson's phenotypic correlation coefficients between traits measured at GS65+7d and physiological maturity in the *control* among 12 HiBAP genotypes in 2017-18 (Y18).

Traits	$DMSpk_{A+7}$	StePI	LamPI	SPI	LnPed	LnInt2	LnInt3	PH	TGW	GY	HI	$AGDM_{PM}$	GN	SM2	FE
$DMSpk_{A+7}$	-														
StePI	0.18	-													
LamPI	-0.09	-0.44	-												
SPI	-0.05	**-0.85*****	-0.03	-											
LnPed	0.12	-0.31	-0.40	0.40	-										
LnInt2	**-0.58***	-0.25	0.32	0.06	-0.08	-									
LnInt3	**-0.58***	-0.14	0.46	-0.23	-0.06	**0.83*****	-								
PH	**-0.58***	0.17	-0.26	-0.18	0.37	**0.66***	**0.62***	-							
TGW	**-0.76*****	0.00	-0.11	0.04	-0.11	**0.71****	0.43	**0.68****	-						
GY	-0.38	0.14	-0.03	-0.04	**-0.64***	0.22	-0.02	-0.04	**0.51**†	-					
HI	0.32	0.18	-0.25	-0.05	0.22	-0.40	-0.17	-0.12	-0.44	-0.25	-				
$AGDM_{PM}$	-0.42	-0.16	0.19	0.10	-0.41	0.42	0.14	0.07	**0.57**†	**0.67***	**-0.87*****	-			
GN	**0.52**†	0.11	0.09	-0.06	-0.40	**-0.60***	**-0.50**†	**-0.80*****	**-0.70****	0.25	0.32	-0.11	-		
SM2	0.08	-0.09	0.36	0.11	**-0.58****	0.17	-0.21	-0.34	0.30	**0.54**†	-0.48	**0.60**†	0.10	-	
FE	0.37	**0.56**†	0.30	**-0.66****	**-0.68****	-0.29	-0.15	-0.44	-0.42	0.22	0.14	-0.08	**0.65**†	0.28	-

A+7: Anthesis + 7 days; **PM**: Physiological Maturity; **DMSpk**: Spike DM per unit area; **StePI**: Stem Partitioning Index; **LamPI**: Lamina Partitioning Index; **SPI**: Spike Partitioning Index; **LnPed**: Length Peduncle; **LnInt2**: Length Internode 2; **LnInt3**: Length Internode 3; **PH**: Plant Height; **TGW**: Thousand Grain Weight; **GY**: Grain Yield (100% DM); **HI**: Harvest Index; **AGDM**: Above-Ground DM; **GN**: Grains per m^2; **SM2**: Spike per m^2; **FE**: Fruiting Efficiency

$^{\dagger}P<0.10$; $^{*}P<0.05$; $^{**}P<0.01$; $^{***}P<0.001$

Table 6.5. Pearson's phenotypic correlation coefficients between traits measured at GS65+7d and physiological maturity in the *PGR-treatment* among 12 HiBAP genotypes in 2017-18 (Y18).

Traits	$DMSpk_{A+7}$	StePI	LamPI	SPI	LPed	LnInt2	LnInt3	PH	TGW	GY	HI	$AGDM_{PM}$	GN	SM2	FE
$DMSpk_{A+7}$	-														
StePI	-0.25	-													
LamPI	0.11	-0.27	-												
SPI	0.20	**-0.90*****	-0.19	-											
LnPed	**-0.58***	-0.15	**-0.52**†	0.39	-										
LnInt2	-0.13	-0.10	**-0.64***	0.39	**0.74****	-									
LnInt3	-0.22	-0.02	**-0.64***	0.31	**0.74****	**0.97*****	-								
PH	-0.21	0.43	**-0.81*****	-0.07	**0.58***	**0.75****	**0.76*****	-							
TGW	-0.35	-0.16	**-0.59***	0.43	**0.67***	**0.68***	**0.75****	0.49	-						
GY	-0.22	-0.23	0.01	0.23	0.42	0.16	0.21	0.16	0.29	-					
HI	0.37	-0.07	0.00	0.07	-0.28	0.13	0.10	-0.08	0.25	**-0.52**†	-				
$AGDM_{PM}$	-0.34	0.04	0.03	-0.06	0.29	-0.04	-0.01	0.20	-0.10	**0.79*****	**-0.88*****	-			
GN	-0.34	-0.13	0.20	0.04	0.46	0.13	0.16	0.16	0.11	**0.89*****	**-0.58***	**0.83*****	-		
SM2	-0.30	0.08	0.03	-0.10	0.27	-0.10	-0.06	0.17	-0.16	**0.77*****	**-0.91*****	**0.98*****	**0.80*****	-	
FE	**-0.55**†	0.25	0.33	-0.40	0.30	-0.08	-0.07	0.11	-0.20	**0.52**†	**-0.57**†	**0.72****	**0.82*****	**0.70****	-

A+7: Anthesis + 7 days; **PM:** Physiological Maturity; **DMSpk:** Spike DM per unit area**; StePI:** Stem Partitioning Index; **LamPI:** Lamina Partitioning Index; **SPI:** Spike Partitioning Index; **LnPed**: Length Peduncle; **LnInt2:** Length Internode 2; **LnInt3:** Length Internode 3; **PH:** Plant Height; **TGW:** Thousand Grain Weight; **GY:** Grain Yield (100% DM); **HI:** Harvest Index; **AGDM:** Above-Ground DM; **GN:** Grains per m^2; **SM2:** Spike per m^2; **FE:** Fruiting Efficiency

$^{\dagger}P<0.10$; $^{*}P<0.05$; $^{**}P<0.01$; $^{***}P<0.001$

6.4. Discussion

The use and development of synthetic retardant growth compounds have benefited many farming systems improving yield production by avoiding lodging in plants though the reduction of stem elongation and increase in stem strength. However, relatively little information is known about how the distribution of DM among stem internodes is affected and the associations with spike growth and grain number.

6.4.1. Enhance and effective timing for PGR

Plant growth regulators have been used in wheat to improve crop growth and development resulting in a rise in yield potential, but the efficiency of the PGR will depend on the rate, timing and environmental conditions (Matysiak, 2006). Alteration of tiller production and enhancement of root growth has been reported when Paclobutrazol was applied during seedling growth (Abraham et al., 2008), and stem shortening occurs at early stem-elongation phases (meristematic activity starts at basal nodes, as the peduncle is the final stem to expand) or at the early-booting stage (Rajala, 2004). For wheat, most of the products (TE: Trinexapac-ethyl based) are recommended to be applied between when the first node (GS31) and the fourth node is detectable (GS37) (Syngenta). Using hard red spring wheat cultivars Wiersma et al. (2011) tested several rates of Moddus applied at different developmental stages concluding that 150 g l^{-1} and when the flag leaf is visible (GS37) where the best dose/time for application, avoiding crop injury and delayed growth and maximising lodging resistance. In this experiment, following the dose recommended by the manufacturer (250 g l^{-1}) and applying the product when the second internode was 1 cm, reduction in plant height was shorter than expected. In addition, yellowish-orange spots were detected on the stem and leaves and the development overall was delayed after the stem elongation phase. The timing of the application was targeted to have a maximum effect in reducing lengths of internode 2 and 3 in the PGR treatment. However, results showed a relatively greater reduction in length of peduncle than stem internode 2 and 3, suggesting that the application stage was too late. The present reduction of internode 3 following the concentration provided by the manufacture is consistent with the results of Matysiak (2006) on winter wheat cultivars where internode 3 was reduced from 19 to 16% (depending on the TE concentration). In a greenhouse experiment using six different spring wheat varieties where different PGRs (Manipulator 620-CCC based and Palisade-TE based) were applied following recommended doses at GS31, Zhang et al. (2017) reported a plant height reduction from 6 to 33% leading to increased lodging resistance by increasing and changing the dimensions of sclerenchyma and parenchyma cells in the second basal internode.

6.4.2. Plant growth regulators on yield potential crops

Since genetic gains in modern wheat are mainly explained through grain number per m^2 (González-Navarro et al., 2016; Soriano et al., 2017; Thapa et al., 2019), increasing the amount of available assimilate during stem elongation for spike growth and floret survival is

fundamental to increasing yield. Improvements in grain number have been evident since thanks to the discovery and introduction of the semi-dwarf *Rht* (reduced height) genes asextra resources for alternatives sinks could reduce the trade-off between spike and stem DM (Rivera-Amado et al., 2019). For these 12 genotypes pleiotropic effect cannot be attributed as all lines used on this experiment carried a variation of the *Rht* gene. On the other hand, sgnificant interaction between genotype and treatments were found for plant height, length of internode 3, length of peduncle and length of stem internode 2. The reduction of internode length in the PGR treatment increased WSC in the stem rather than the spike, which could partially explain the reduction in length due to the presence of a negative association between stem partitioning index and spike partitioning index which was stronger and greater in the PGR treatment than in the control. In the present study a negative association was also found between the spike DM per unit area and the peduncle length in the PGR treatment. Increased assimilate supply could result in genetic gains in spikes per unit area associated with improved floret fertility as observed in this experiment at GS65+7d. In a greenhouse experiment using two types of PGRs (spermine and paclobutrazol) Orabi & Sadak (2015) reported increases yield components were attributed to growth rate (efficiency of solar energy conversion) and stimulating cytokinin production. In the present experiment most of the yield components declined with the largest effects on spikes m^{-2} and grains m^{-2}. There was a GxT interaction found on above-ground DM at physiological maturity as PGR treatment reduced the amount of assimilates produced (-12%). Similar findings related to absence of yield gain were observed on a spring barley experiment where Miziniak et al. (2017) reported a stem height reduction from 5.6 to 16.5% when trinexapac-ethyl was applied at GS31 resulting in no significant increase in grains per spike or yield which could have been partly due to weather conditions (air temperature and rain precipitation). However, in the present study the number of spikes per unit area at seven days after anthesis and spike partitioning index did not differ between treatments and not showed any genotype x treatment interaction.

The yield decrease in this study from seven days after anthesis to physiological maturity was associated with the reduction in green area during grain filling as the duration was similar in both treatments (~33 days). In desert yield potential conditions, using four wheat varieties (Rafi C97, Altar C84, Nacori C97, Rayon F89) and following the recommended application of TE for spring wheat (Figure S6.2), Grijalva-Contreras et al. (2012) recorded a decrease in plant height from 5-27% resulting in yield reductions of 10%; they also reported an effect of high temperatures on the wheat plants (23°C) causing phytotoxicity. PGR applications may therefore cause considerable yield reduction, especially when there is no lodging. In addition, on some occasions PGR applications at this stage may increase the floret abortion rate and consequently reduce grain number per spike (Rajala, 2004).

6.5. Conclusion

- Plant growth regulator (Moddus 250 EC) shorted plant height by 50%, impacting relatively more on the peduncle than the internode 2 and internode 3 lengths, following application of the manufacturer's rate (concentration) and timing.
- Plants treated with PGR presented phytotoxicity symptoms resulting in plants with delayed development; tiller survival was reduced influencing on above-ground DM and grain yield.
- A trade-off between stem partitioning index and spike partitioning index was recorded in the control and PGR treatment which could partially explain the negative link between harvest index and above-ground DM at physiological maturity.
- Spike partitioning index values were higher in PGR plants, associated with greater reduction of plant height, but this was not translated into yield advantages.

6.6. Supplementary material

Figure S6.1. HiBAP_PGR panel field arrangement: control replicates (blue shaded) and treatment replicates (yellow shaded) blocks.

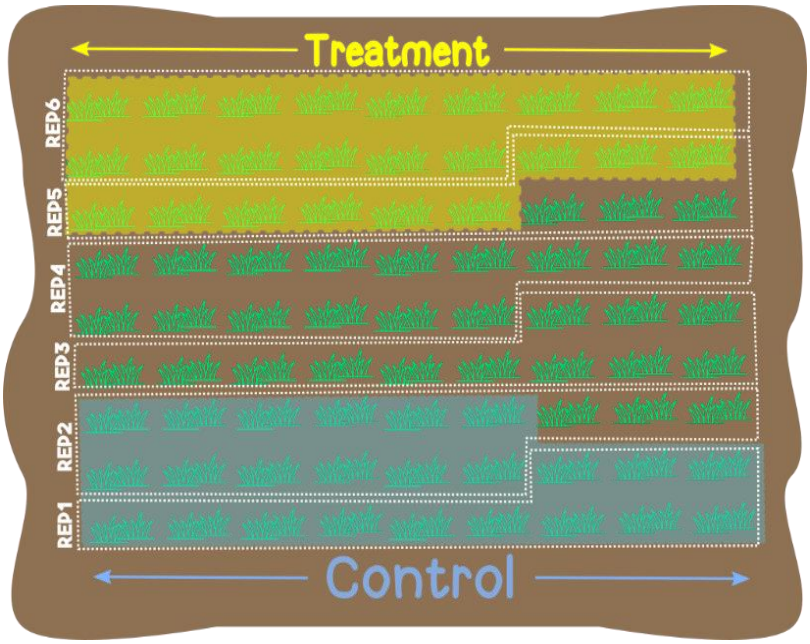


Table S6.1. Cross-year (Y16 and Y17) averaged means (BLUEs) for traits at GS65+7d and PM the 12 genotypes of the HIBAP_PGR panel and genetic ranges of the HiBAP (150 genotypes).

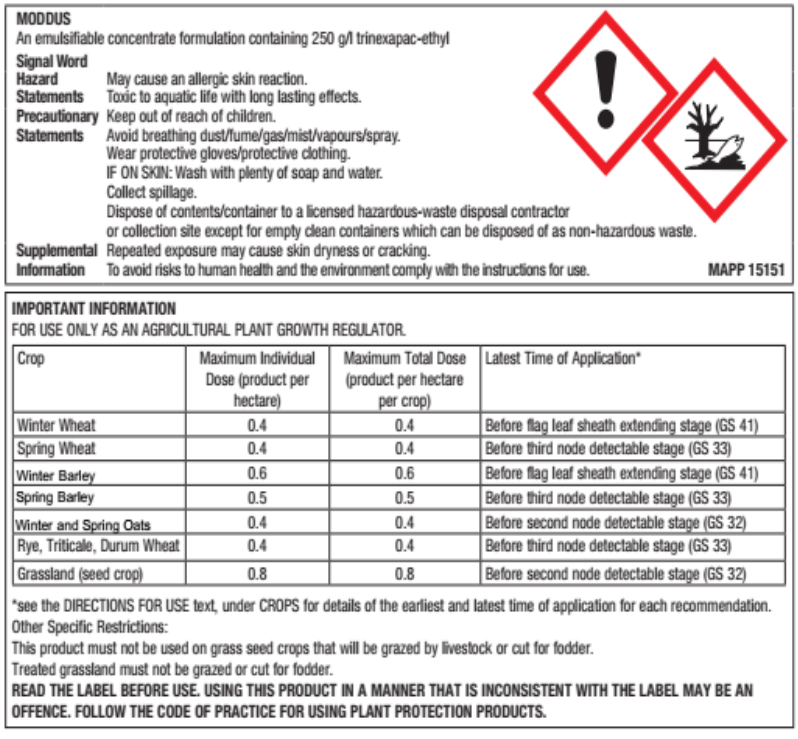
	Genotype	DTA	GY	HI	GN	FE	PH	LPed	LInt2	LInt3	DM Spk	DM Ste	SPI
1	SIETE CERROS T66	75	527	0.45	15468	69.2	92.5	35.7	17.5	13.5	0.81	1.51	0.28
2	PAVON F 76	79	504	0.44	13889	64.8	94.9	41.7	16.7	11.7	0.56	0.98	0.27
3	KRICHAUFF	74	485	0.42	14952	60.6	89.9	39.7	18.8	10.6	0.63	1.11	0.28
4	KFA/3/PFAU/WEAVER//BRAMBLING/4 /PFAU/WEAVER*2//BRAMBLING	81	553	0.41	12726	60	98.1	30.4	20.2	14	0.97	1.93	0.26
5	CHEWINK #1	79	705	0.46	15204	61.9	104.5	41.7	18.9	12.4	0.87	1.65	0.27
6	CHEN/AE.SQ//WEAVER/3/SSERI1	79	555	0.45	14211	71.2	98.7	39.5	18.2	13.5	0.72	1.45	0.26
7	CNO79//PF70354/MUS/3/PASTOR/4/B AV92*2/5/FH6-1-7	76	615	0.49	13522	52.9	97.5	36.8	20.2	14.3	1.00	1.97	0.27
8	OR791432/VEE#3.2//ATTILA/3*BCN	75	529	0.47	11392	56.2	113	41.3	22.8	16.4	0.89	2.01	0.25
9	WBLL1*2/KUKUNA	75	648	0.48	14533	66.1	103.6	36.8	20.4	14.9	0.86	1.82	0.25
10	VOROBEY	74	562	0.44	12180	70.5	102.3	41.1	19.3	13.5	0.59	1.55	0.21
11	KAUZ/PASTOR//PBW343/3/KIRITATI/4 /FRNCLN	70	658	0.52	14332	49.7	97.3	35.8	21.2	12.5	0.82	1.56	0.28
12	CMH79A.955/4/AGA/3/4*SN64/CNO6 7//INIA66/5/NAC	78	587	0.45	14698	54.1	103.1	35.3	20	14.4	0.95	1.90	0.27
	Min	70	485	0.41	11392	49.7	89.9	30.4	16.7	10.6	0.56	0.98	0.21
	Mean	76	577	0.46	13926	61.4	99.6	38.0	19.5	13.5	0.81	1.62	0.26
	Max	81	705	0.52	15468	71.2	113.0	41.7	22.8	16.4	1.00	2.01	0.28
	Genetic ranges HIBAP (150 lines)												
	Min	68	485	0.41	10382	41.5	84.6	29.0	15.1	9.90	0.56	0.98	0.17
	Mean	76	595	0.47	13676	58.7	99.5	37.5	19.4	13.7	0.83	1.61	0.21
	Max	85	705	0.53	16669	84.4	113.8	42.8	23.6	16.6	1.06	2.03	0.26

DTA: Days from emergence to anthesis (DAE); **GY**: Grain Yield (g m^{-2}); **HI**: Harvest Index; **GN**: Grain Number (grain m^{-2}); **FE**: Fruiting Efficiency (grains g^{-1}); **PH**: Plant Height (cm); **LPed**: Length Peduncle (cm); **LInt2**: Length Internode 2 (cm); **LInt3**: Length Internode 3 (cm); **DM Spk**: Dry Matter Spike at GS65+7d (g $shoot^{-1}$); **DM Ste**: Dry Matter Stem at GS65+7d (g $shoot^{-1}$); **SPI**: Spike Partitioning Index

Table S6.2. Meteorological data during booting, anthesis and grain filling (Y18: 2017-18) at NW Mexico.

		Units	*Y18: 2017-18*		
			Min	**Mean**	**Max**
Booting (GS41-GS49)	Mean Temperature	°C	9.25	17.1	27.3
	Mean Solar radiation	MJ m^{-2}		6.90	
	Mean Rainfall accumulated	Mm		0.06	
Anthesis (GS59-GS69)	Mean Temperature	°C	8.45	16.1	26.0
	Mean Solar radiation	MJ m^{-2}		8.53	
	Mean Rainfall accumulated	Mm		0.37	
Grain filling (GS71-GS91)	Mean Temperature	°C	11.0	19.8	30.3
	Mean Solar radiation	MJ m^{-2}		10.3	
	Mean Rainfall accumulated	Mm		0.01	

Figure S6.2. Moddus (Syngenta) product label.



MODDUS
An emulsifiable concentrate formulation containing 250 g/l trinexapac-ethyl

Signal Word
Hazard Statements May cause an allergic skin reaction.
Toxic to aquatic life with long lasting effects.
Precautionary Statements Keep out of reach of children.
Avoid breathing dust/fume/gas/mist/vapours/spray.
Wear protective gloves/protective clothing.
IF ON SKIN: Wash with plenty of soap and water.
Collect spillage.
Dispose of contents/container to a licensed hazardous-waste disposal contractor or collection site except for empty clean containers which can be disposed of as non-hazardous waste.
Supplemental Information Repeated exposure may cause skin dryness or cracking.
To avoid risks to human health and the environment comply with the instructions for use.

MAPP 15151

IMPORTANT INFORMATION
FOR USE ONLY AS AN AGRICULTURAL PLANT GROWTH REGULATOR.

Crop	Maximum Individual Dose (product per hectare)	Maximum Total Dose (product per hectare per crop)	Latest Time of Application*
Winter Wheat	0.4	0.4	Before flag leaf sheath extending stage (GS 41)
Spring Wheat	0.4	0.4	Before third node detectable stage (GS 33)
Winter Barley	0.6	0.6	Before flag leaf sheath extending stage (GS 41)
Spring Barley	0.5	0.5	Before third node detectable stage (GS 33)
Winter and Spring Oats	0.4	0.4	Before second node detectable stage (GS 32)
Rye, Triticale, Durum Wheat	0.4	0.4	Before third node detectable stage (GS 33)
Grassland (seed crop)	0.8	0.8	Before second node detectable stage (GS 32)

*see the DIRECTIONS FOR USE text, under CROPS for details of the earliest and latest time of application for each recommendation.
Other Specific Restrictions:
This product must not be used on grass seed crops that will be grazed by livestock or cut for fodder.
Treated grassland must not be grazed or cut for fodder.
READ THE LABEL BEFORE USE. USING THIS PRODUCT IN A MANNER THAT IS INCONSISTENT WITH THE LABEL MAY BE AN OFFENCE. FOLLOW THE CODE OF PRACTICE FOR USING PLANT PROTECTION PRODUCTS.

Table S6.3. Adjusted means (BLUEs) for traits measured at GS65+7d and PM for 12 HiBAP_PGR genotypes in the control and PGR treatment.

	HIBAP_ Y16 - Y17	HiBAP_ PGR	DTA	GY (g m^{-2})	HI	GN (g m^{-2})	FE (grains g^{-1})	PH (cm)	LPed (cm)	LInt2 (cm)	LInt3 (cm)	DM Spk (g $shoot^{-1}$)	DM Ste (g $shoot^{-1}$)	SPI
Control	3	1	79	677	0.39	19926	71.0	92.5	34.5	18.0	13.3	0.73	1.39	0.28
	4	2	88	609	0.42	17234	52.6	98.2	45.5	18.0	12.4	0.84	1.48	0.30
	12	3	82	536	0.34	16304	67.8	89.5	38.8	17.0	12.7	0.56	1.01	0.26
	16	4	88	682	0.35	14336	47.6	102.3	34.9	20.0	14.9	1.10	2.24	0.26
	26	5	88	644	0.30	14052	49.0	109.1	45.3	18.3	12.7	0.97	2.08	0.26
	28	6	88	629	0.43	15583	56.5	105.2	41.2	17.7	13.5	0.81	1.87	0.24
	88	7	84	690	0.32	15751	48.7	100.7	39.7	21.6	16.1	1.18	1.80	0.29
	92	8	84	574	0.37	12016	43.8	117.4	45.1	23.7	17.7	1.16	2.04	0.28
	109	9	79	667	0.26	15260	60.7	106.6	35.0	21.6	16.2	0.82	1.77	0.24
	117	10	79	624	0.32	14078	61.1	110.1	40.0	21.0	15.4	0.60	1.76	0.21
	143	11	74	740	0.30	15694	62.4	98.9	33.6	20.4	12.0	0.64	1.12	0.29
	147	12	79	706	0.40	17495	88.2	100.7	30.9	19.5	15.2	0.57	1.61	0.20
PGR	3	1	85	247	0.42	6324	23.8	50.7	14.0	8.3	6.1	0.77	1.12	0.30
	4	2	91	213	0.40	6819	23.7	54.6	15.0	10.2	6.8	0.67	1.03	0.31
	12	3	87	222	0.31	6030	23.8	45.2	14.5	8.0	5.4	0.48	0.64	0.30
	16	4	92	286	0.43	6499	14.7	52.9	12.7	9.8	7.0	1.05	1.74	0.29
	26	5	92	307	0.35	8291	24.2	47.1	17.3	8.5	6.1	1.09	1.28	0.35
	28	6	92	371	0.31	9794	30.1	53.6	17.5	9.9	7.1	0.79	1.20	0.29
	88	7	89	245	0.28	5741	15.7	59.3	18.6	12.1	8.5	1.08	1.57	0.33
	92	8	88	259	0.43	7600	29.6	67.4	19.4	13.6	8.7	0.89	1.74	0.27
	109	9	85	254	0.37	8183	34.1	46.1	15.7	9.1	6.8	0.71	1.47	0.24
	117	10	85	241	0.43	6007	24.4	48.8	13.1	6.5	5.3	0.67	1.35	0.25
	143	11	79	341	0.43	8871	23.6	52.0	18.5	13.0	8.4	1.21	1.17	0.39
	147	12	85	403	0.14	11982	44.3	58.1	17.5	9.7	6.9	0.84	1.50	0.28

DTA: Days from emergence to anthesis (DAE); **GY:** Grain Yield (g m^{-2}); **HI:** Harvest Index; **GN:** Grain Number (grain m^{-2}); **FE:** Fruiting Efficiency (grains g^{-1}); **PH:** Plant Height (cm); **LPed:** Length Peduncle (cm); **LInt2:** Length Internode 2 (cm); **LInt3:** Length Internode 3 (cm); **DM Spk:** Dry Matter Spike at GS65+7d (g $shoot^{-1}$); **DM Ste:** Dry Matter Stem at GS65+7d (g $shoot^{-1}$); **SPI:** Spike Partitioning Index

7. General Discussion

Wheat is one of the three principal cereals grown worldwide mainly for human consumption, and its production is fundamental for food security as this crop is characterised as a stable species which can be grown in different mega-environments. However, due to various challenges including climate change and the global population increase its current production is not meeting future demand. Consequently, new breeding strategies are required to research the traits and mechanisms that enhance dry-matter (DM) partitioning to the grain in high biomass cultivars to maximise genetic gains in yield potential.

New tools and technology are currently available, facilitating the study of grain partitioning traits and their environmental interactions. The deployment of phenotypic and genotypic data will potentially enable wheat breeders and scientists to demonstrate the genetic regulation of traits and develop molecular markers to establish grain partitioning in high biomass genotypes allowing gains to be consistently translated to grain yield, irrespective of genetic background and environment.

7.1. Genetic variation for grain partitioning traits in high biomass wheat backgrounds

The incorporation of distinctive genetic pools has enriched genotypic variation enabling the generation of plants with desirable traits whilst avoiding homogeneous breeding cycles (Voss-Fels et al., 2019; Zhang et al., 2017). In the HiBAP (High Biomass Association Panel, spring wheat), results showed how modern CIMMYT spring wheat genotypes had incorporated target characteristics from landraces and synthetics leading to higher production of above-ground DM. Not only genetic variation is required but also high trait heritability to make progress in the selection of traits in breeding crosses. Cross-year analysis, for most of the traits measured at seven days after anthesis and physiological maturity, revealed heritability values ranging from moderate to high (0.6 to 0.9) compared to the values on SxR DH (Savannah x Rialto Doubled-Haploid, winter wheat population) ranging from low to moderate (0.1 to 0.7). This difference could be partly attributed to the size of the panel/population as heritability takes into account the proportion of total variance in a population and its interaction with the environment (Khan & Naqvi, 2011; Visscher et al., 2008).

Results on the panel/population under yield potential irrigated (spring wheat) and rain-fed (winter wheat) conditions showed that genetic variation in grain yield was better explained through above-ground DM at physiological maturity than harvest index, consistent with other recent reports on the basis of genetic variation in modern wheat genotypes (Aisawi et al., 2015; Rivera-Amado et al., 2019; Shearman et al., 2005). A trade-off between above-ground DM and harvest index was identified in both types of wheat which was stronger in the spring than the winter wheat. This difference was possibly explained by effects of plant height, as spring wheat HiBAP genotypes tended to be taller genotypes than winter wheat SxR DH

genotypes. Austin (1980) estimated there is scope to increase HI values up to 0.62 (hypothetical limit) as long as the plant possesses strong reproductive sinks. Results from the present experiments over two seasons showed higher genetic range (0.40-0.53) in the spring wheat HiBAP panel than the winter wheat SxR DH population (0.36-0.46) which was an unexpected considering that the SxR had a shorter plant height and winter wheat generally has higher yield potential than spring wheat (Dai et al., 2016; Lozada et al., 2017). Environmental conditions, such as above-average rainfall during grain filling in 2015-16 and a dry grain-filling period in 2016-17 could partly explain low harvest index (HI) values for the SxR DH. Foulkes et al. (2011) suggested that it is possible to increase HI assuming stem and leaf sheath DM can be reduced by 50%, leaf-lamina DM maintained and chaff DM increased proportionally allowing to accommodate extra grain. This last statement was supported by the positive association found between fruiting efficiency (FE) and HI in both sets of germplasm in the present study.

The avenue of using high biomass genotypes as potential parental candidates to raise yield potential looks promising as long as harvest index is maintained or ideally increased; higher HI has led to higher yields linked to a better investment of assimilates in the pre-anthesis period (Calderini et al., 1999) increasing spike fertility. Fruiting efficiency, spike partitioning index and internode 2 length were positively associated with harvest index for the HiBAP experiment and in SxR DH fruiting efficiency was the only trait related with HI. The present relation between HI and FE in the HiBAP and SxR DH population reflected the positive association found between FE, grain number (GN) and FE also showed a positive association with grain yield (GY).

Optimising DM partitioning among the organs is a strategy to increase spike growth at anthesis, which can be justified by the positive associations found among GN and DM spike per unit area seven days after anthesis ($DMSpk_{A+7}$) with GN in both types of wheat. The strong association between GN and GY in both experiments suggested that genotypes were sink-limited and that assimilate supplied to the spike in the phase from booting to anthesis was limiting floret fertility and GN. Regarding the grain number model, spike partitioning index was associated with GN in both sets of germplasm, where grains per m^2 was associated with above-ground DM at GS65+7d in the SxR DH but not in the HiBAP. A different situation was presented for FE as this trait was positively associated with GN in the HiBAP which could be influenced by grains per spike (Philipp et al., 2018). Overall in the HiBAP higher values of spike partitioning index and fruiting efficiency values were obtained but with a lower amount of above-ground DM at GS65+7d compared to the SxR DH.

7.2. Partitioning traits to increase spike growth

Post-Green Revolution, grain yield was strongly boosted due to the incorporation of *Rht* (Reduced height) genes producing shorter plants with higher DM available to reproductive organs (spike) (Hedden, 2003). There was a positive association between plant height (PH), internode length and grain yield in the winter wheat but no association in the spring wheat; in both sets of germplasm plant height was positively associated with above-ground DM at physiological maturity. However, in the HIBAP there was a negative association between plant height and harvest index, whereas in the SxR DH population there was no significant association, likely related to the higher range in plant height in the HIBAP than the SxR DH population. The positive associations between internode 2 true-stem PI and grain yield in the HiBAP could be due to the positive association between plant height and above-ground DM at both stages. For the SxR DH population stem internode 2 length showed a stronger association with grain yield compared to stem internode 3 and peduncle where a positive correlation was observed with seven days after anthesis and physiological maturity biomass.

In the HiBAP and SxR DH a trade-off was found between the stem partitioning index and spike DM per unit area at GS65+7d which was stronger in SxR DH than in the HiBAP potentially limiting spike DM fertility and grain number. Similar negative associations were detected between spike and lamina partitioning index in both sets of germplasm. Increased assimilate supply to the spike during booting to anthesis is required to improve spike fertility and grain number. Different hypotheses have been proposed to increase the allocation of assimilates to the spike to increase floret survival which in turn will increase grain number. Using Argentinian cultivars released from 2000 to 2008 González et al. (2011) showed that genotypes with an increased duration of stem elongation, without altering the anthesis stage, accumulated more intercepted radiation during the rapid spike growth phase resulting in an increase of grain number. Competition for assimilates during stem elongation can also come from excessive tillering in which infertile tillers compete for assimilates with the primary fertile tillers (Berry et al., 2003; Piñera-Chavez et al., 2016).

Stem reserve accumulation and mobilisation in wheat depends on internode length, and stem specific weight (ratio between internode DM and length) (Ehdaie et al., 2008). In both sets of germplasm, the competition for assimilates between the stem internodes and the spike was stronger in middle internodes, stronger for 3 than 2. This behaviour is the outcome that lower internodes tend to store assimilates for more time compared to the peduncle, as this internode is the nearest one to the spike (Krenzer et al. 1995, Schnyder, 1993). During the floret survival phase from booting to anthesis maximum length of internode 3 will be reached while internode 2 will begin to extend, completing its growth before anthesis (Ehdaie et al., 2006; González et al., 2011). This is in agreement with results obtained from the stepwise regression for spike partitioning index where stem internode length, internode 2 for the HiBAP and internode 3 for SxR DH were important traits explaining variation found on this trait. On the

other hand, from the detailed stem internode analysis in the SxR DH population strong negative associations were found between harvest index and the amount of DM partitioned to the spike with true-stem (TS) partitioning index of each internode, values decreasing from top (spike) to bottom (ground) same scenario recorded on the leaf-sheath (LS). These findings agree with what Rivera-Amado et al. (2019) reported on CIMMYT spring wheat cultivars released from 1992 to 2009 suggesting that further genetic gains in HI could be achieved by decreasing the length of internode 2 and 3 rather than the peduncle, correlated with higher spike partitioning index.

Optimal plant height (~70 to 100 cm) may have been reached after the incorporation of *Rht* Norin-10 dwarfing genes into the genetic pool of wheat cultivars (Addisu et al., 2010; Slafer et al., 2015). However, further stem-length reductions targeted to specific internodes may be feasible, especially in CIMMYT spring wheat genotypes where plant height in presently in the range 100 to110 cm (Aisawi et al., 2015), Nevertheless, this may need to be done with caution in UK winter wheat where plant height is presently in the range 80 to 90 cm (AHDB, 2017) as suboptimal canopy architecture and light distribution could impact radiation-use efficiency resulting in decreasing biomass and/or stem water-soluble carbohydrates (Fischer, 2007; Semenov et al., 2014).

7.3. High-throughput phenotyping and application of molecular markers for grain partitioning

In wheat breeding, the introduction of economic, time effective phenotypic and genotypic platforms has allowed the generation of new data and a better understanding of mechanisms underlying yield-related traits. High-throughput phenotypic platforms characterised as non-invasive phenotypic infrastructures have extended their applications to measure traits in a precise and cost-effective way (Summerer et al., 2019). Using remote or proximal sensing and imaging technologies, such as unmanned aerial vehicles with mounted high-resolution cameras, the measurement of specific traits (plant height, vegetation indices, diseases, etc) can reduce labour-intensive work (Crain et al., 2018; Sun et al., 2019; Yang et al., 2014).

Most of the traits measured in the present experiments at seven days after anthesis and physiological maturity required sampling shoots from the field followed by destructive growth analysis. This type of methodology is feasible in experiments with moderate number of genotypes (~100 to 200). However, methods used in current experiments were laborious and time-demanding requiring trained staff. To phenotype two replicates from the HiBAP panel for 150 genotypes (considering two reps per genotype), it took around eight people over two days to measure plant morphology traits (plant height and peduncle, awns and spike lengths). For the detailed measurements recorded at the stem-internode and spike morphology level, it took around 25 days for one person to obtain the DM data for 150 genotypes in two replicates. Therefore these methodologies cannot be effectively applied in wheat breeding

programmes with many thousands of genotypes to screen. The timescale and throughput for the phenotyping of the grain partitioning traits was similar for the SxR DH population.

Marker-trait associations and/or QTL studies allow markers to be developed to facilitate the selection of the best combinations of parental alleles for target traits. Additionally, these markers open the possibility to select at early stages for grain partitioning traits when it is difficult to measure these traits representatively of field performance as spaced plants or in single rows (Robertsen et al., 2019). In the HiBAP co-locations of genetic regions for spike, stem and lamina DM (g per shoot^{1}) were identified on chromosome 1A and 6B implying that competition for DM among the organs could be regulated by the same genetic region. This was confirmed by the candidate genes found for these two chromosomes locations which related to stem elongation, stomatal opening and spikelet fertility. For the SxR DH population a co-located QTL on chromosome 3A was found for the DM assimilation among plant organs, and this genetic region was previously reported as a genetic loci for grain yield and its components (Li et al., 2019; Rustgi et al., 2013). For length-related traits, loci found on 6A and 7A associated with plant height and peduncle length, respectively, and were stable between the two sets of germplasm. Previous reports and literature showed several candidate genes for plant height on 6A (Guan et al., 2018; Sukumaran et al., 2014; Würschum et al., 2017). For the rest of the length-related traits (internode and awn lengths)presently identified, no genetic loci in wheat have previously been reported. Previous studies have reported specific chromosomal regions in wheat related to grain yield and its components (Bhatta et al., 2018; Zhang et al., 2015). In both sets of germplasm, genetic loci for grain number on 3A (grains per m^{2}) and above-ground DM at physiological maturity on 7A were identified, which were also previously reported by Molero et al. (2019).

7.4. Overall conclusions

Physiology chapter hypotheses (chapter 2, 3 and 6):

- *Incorporation of different pedigree backgrounds increases genetic variation in above-ground dry matter and grain partitioning traits.*

  In the HIBAP panel, landrace-derived and synthetic-derived pedigrees boosted above-ground DM.

- *Increases in above-ground DM amongst genotypes are negatively associated with harvest index.*

  The hypothesis was supported where the trade-off was stronger in the HiBAP panel (spring wheat) than in SxR DH population (winter wheat).

- *A positive association is recorded between grain yield and harvest index among genotypes.*

The hypothesis was supported in both sets of germplasm; therefore yield potential could be still enhanced by increasing harvest index values in modern wheat genotypes.

- *Genetic variation in grain number is determined by (i) percentage of DM partitioned to the spike and/or (ii) grains per unit spike dry matter at anthesis.*

  Spike partitioning index and fruiting efficiency showed positive associations with grain number in both sets of germplasm.

- *Strong competition is found between spike and stem DM growth during the stem-elongation period, resulting in a negative correlation between the amount of DM partitioned to the spike (SPI) and stem (StePI).*

  The hypothesis was supported in both sets of germplasm, where the negative association between SPI and StePI amongst genotypes was stronger than that with LamPI.

- *Spike partitioning index (SPI) and harvest index (HI) are linked to length and DM partitioning of internodes (peduncle, true-stem and internode 2 true-stem) near the spike rather than those close to the ground.*

  SPI and HI were negatively associated with stem-internode lengths and PIs for internode 2 and 3 but not for the peduncle, with stronger associations for SPI than for HI; however a positive association was found for internode 2 length with harvest index in the HiBAP.

- *Genetic variation in spike morphological DM partitioning is related to fruiting efficiency.*

  This hypothesis was supported as the proportion of spike DM partitioned to the lemma and rachis were positively associated with fruiting efficiency in both sets of germplasm.

- *Stem internode 2 and 3 lengths are reduced by the application of plant growth retardant at GS31/32 (Zadoks' growth scale) more than other internodes when the second node is detectable.*

  This hypothesis was not supported; the use of plant growth regulators on the HiBAP spring wheat genotypes needs further study in yield potential irrigated conditions in NE Mexico as the PGR concentration and timing resulted in some phytotoxicity symptoms, and decreased peduncle length more than internode 2 and 3 length.

- *Spike DM per unit area is increased in response to PGR application at GS31/32 as a result of less competition with stem internode 2 and 3 during the stem-elongation stage*

  This hypothesis was not supported as decreased spike DM per unit area was observed in cultivars where Moddus 250 EC was applied at the onset of the stem-elongation phase.

Genetic analysis hypotheses (chapter 4 and 5):

- *Novel MTAs, including co-locations, can be identified for harvest index, grain number and grain partitioning traits in high biomass backgrounds using sequencing data.*

  Novel MTAs, including co-locating MTAs, for DM partitioning and stem-internode length traits at seven days of anthesis were identified in both spring and winter wheat germplasm.

- *Candidate genes can be identified from SNP markers associated with MTAs.*

  Candidate genes were identified linked to the MTAs in the HiBAP for the accumulation of DM in different plant organs, fruiting efficiency, stem-internode lengths and plant organ partitioning indices. Further analysis for the QTLs identified in the SxR DH population was not feasible as specific genotyping information required for the identification of candidate genes was lacking.

7.5. Future work

The main objective of this thesis was to understand the physiological and molecular basis of grain partitioning in wheat using genotypes characterised as high biomass producers. Results on the HiBAP suggested that genetic diversity has been introduced into modern/elite cultivars with the incorporation of synthetic and landraces backgrounds, increasing the amount of dry matter (DM) in the stem and lamina. However, these biomass increases were not translated into yield gains as they were counter-acted by decreasing harvest index values. New varieties need to produce consistently high above-ground DM whilst increasing or maintaining spike partitioning to raise spike DM per unit area and the number of fertile florets boosting HI and yield through grains per unit area.

7.5.1. Optimising partitioning during stem elongation and floret development

Further testing of the hypothesis that shortening stem internodes 2 and 3 will increase assimilates for spike growth during stem elongation is required to corroborate present results which will enable increases in harvest index without significant overall changes in plant height. Additional experiments, based on pedigree information, contrasting internode lengths and different planting system, could provide more information about the interaction between spike and stem growth. Decreasing true-stem partitioning while maintaining leaf-sheath partitioning may be important in maintaining photosynthesis, particularly during the second half of grain filling, maintaining the amount of assimilates -available for grain growth. The implementation

of new breeding strategies pyramiding novel partitioning traits could allow breeders to raise spike partitioning index and fruiting efficiency simultaneously in future crosses.

Concerning the use of plant growth regulators to shorten specific internodes in spring wheat, such as gibberellic acid and/or auxins related-products, more experimentation is required to identify the appropriate concentrations and application timings on spring wheat genotypes under irrigated yield potential conditions growth to enhance spike growth, grain number, harvest index and grain yield. The effects of this hormones towards plants is the stimulus that cells will received; higher concentrations may inhibit cell elongation or division (Rademacher, 2015). Another field to consider is the quantification of genetic variation in spike hormone concentrations in specific the quantification of cytokinin and gibberellins hormones tha are associatedwith spikelet meristem activity during the reproductive stage of the plant, as the role of plant growth regulators in determining grain number is still not clear. This plant hormone analysis of the spikes could be done by ultra-performance liquid chromatography-electrospray ionization-tandem mass spectrometry.

High-throughput phenotypic techniques, such as stereoscopic sensors, could be developed for rapid and precise field-level screening of internode lengths, enabling breeders to select shorter internode 2 or 3 length genotypes but still considering the optimum height. Internode length and DM weight over 160 to 300 genotypes in two replicates were done in approximately 10 days with three to five people helping to do the measurements. The use of hyperspectral camera-imaging could potentially estimate the specific weight per stem internode and similar methodology could be used to measure rachis density. For detailed stem-internode partitioning (DM partitioned to the true-stem and leaf-sheath) and spike organ morphology due to the time-consuming trait measurements the best approach will be the generation of molecular markers.

7.5.2. Genotyping platforms available worldwide

Since wheat has a highly repetitive genome it is a challenging crop to study, especially when a critical development stage overlaps with the rapid growth of two different organs. The recent production of a new version of a whole-genome assembly in wheat has allowed a better understanding of the genetic trade-offs between spike and stem growth and how this is preventing maximising genetic gains in grain number. This could be done using molecular techniques such as the use of RNAseq transcriptomics experiments on specific plant organs at a target stage using contrasting high/low genotypes in order to locate differentially expressed RNA within identified genetic loci (MTAs/QTLs) to narrow down the number of candidate genes. Other strategies to validate candidate genes include the use of TILLING (Targeting Induced Local Lesions in Genomes) lines to compare mutant alleles for the candidate genes with their phenotypic expression (Slade et al., 2005; Jia et al., 2018). Generation of MAGIC (Multi parent Advanced Generation Intercross) population(s) could assist in map construction and the analysis of the molecular and genetic basis of target grain partitioning traits

(Stadlmeier et al., 2018; Staub et al., 1996). Results gathered on the HiBAP allowed the identification of potential candidate genes using Knetminer (Hassani-Pak et al., 2016). The list proposed in this thesis will require further validation as much of the information gathered from this database correspond to other species, which have a simpler genome such as arabidopsis, rice, barley, etc. In addition, the QTL analysis on the SxR DH population identified genomic regions which could play an essential role for developing molecular markers for the grain partitioning traits for deployment in marker-assisted selection through further fine mapping of the target QTLs using backcross-derived populations.

8. References

Abbate, P., Andrade, F. H., Culot, J. P., & Bindraban, P. S. (1997). Grain yield in wheat: Effects of radiation during spike growth period. *Field Crops Research*, *54*, 245–257. https://doi.org/10.1016/S0378-4290(97)00059-2

Abraham, S. S., Jaleel, C. A., Chang-Xing, Z., Somasundaram, R., Azooz, M. M., Manivannan, P., & Panneerselvam, R. (2008). Regulation of Growth and Metabolism by Paclobutrazol and ABA in Sesamum indicum L . Under Drought Condition. *Global Journal of Molecular Sciences*, *3*(2), 57–66.

Acreche, M. M., Briceño-Félix, G., Sánchez, J. A. M., & Slafer, G. A. (2008). Physiological bases of genetic gains in Mediterranean bread wheat yield in Spain. *European Journal of Agronomy*, *28*(3), 162–170. https://doi.org/10.1016/j.eja.2007.07.001

Addisu, M., Snape, J. W., Simmonds, J. R., & Gooding, M. J. (2010). Effects of reduced height (Rht) and photoperiod insensitivity (Ppd) alleles on yield of wheat in contrasting production systems. *Euphytica*, *172*(2), 169–181. https://doi.org/10.1007/s10681-009-0025-2

Aisawi, K. (2011). Physiological processes associated with genetic progress in yield potential of wheat (Triticum aestivum L.). *PhD Thesis, University of Nottingham School of Biosciences, Sutton Bonnington Campus, Leistershire, UK*.

Aisawi, K. A. B., Reynolds, M. P., Singh, R. P., & Foulkes, M. J. (2015). The physiological basis of the genetic progress in yield potential of CIMMYT spring wheat cultivars from 1966 to 2009. *Crop Science*, *55*(4), 1749–1764. https://doi.org/10.2135/cropsci2014.09.0601

Ali, B.; Munir, I., Iqbal; A., Ahmad; M. A., Maqsood, I.; Hafeez, M. (2018). Molecular charactarization of wheat advanced lines for leaf rust resistant genes using SSR markers. *Microbial Pathogenesis*, *123*, 348–352. https://doi.org/10.1016/j.micpath.2018.07.029

Allen, A. M., Winfield, M. O., Burridge, A. J., Downie, R. C., Benbow, H. R., Gary, L., … Edwards, K. J. (2017). Characterization of a Wheat Breeders ' Array suitable for high-throughput SNP genotyping of global accessions of hexaploid bread wheat (Triticum aestivum), 390–401. https://doi.org/10.1111/pbi.12635

Alonso, M. P., Abbate, P. E., Mirabella, N. E., Aramburu Merlos, F., Panelo, J. S., & Pontaroli, A. C. (2018). Analysis of sink/source relations in bread wheat recombinant inbred lines and commercial cultivars under a high yield potential environment. *European Journal of Agronomy*, *93*(August 2017), 82–87. https://doi.org/10.1016/j.eja.2017.11.007

Alonso, M. P., Mirabella, N. E., Panelo, J. S., Cendoya, M. G., & Pontaroli, A. C. (2018). Selection for high spike fertility index increases genetic progress in grain yield and stability in bread wheat. *Euphytica*, *214*(7), 112. https://doi.org/10.1007/s10681-018-2193-4

Alvarado, G., López, M., Vargas, M., Pacheco, Á., Rodríguez, F., Burgueño, J., & Crossa, J. (2018). META-R (Multi Environment Trail Analysis with R for Windows) Version 6.03. CIMMYT Research Data & Software Repository Network. https://doi.org/11529/10201

Ammar, K., Alfaro, C., del Moral, L. F. G., Villegas, D., Dreisigacker, S., & Royo, C. (2017). Effect of Ppd-1 photoperiod sensitivity genes on dry matter production and allocation in durum wheat. *Field Crops Research*, *221*(March 2017), 358–367. https://doi.org/10.1016/j.fcr.2017.06.005

Amram, A., Fadida-Myers, A., Golan, G., Nashef, K., Ben-David, R., & Peleg, Z. (2015). Effect of GA-sensitivity on wheat early vigor and yield components under deep sowing. *Frontiers in Plant Science*, *6*(July), 487. https://doi.org/10.3389/fpls.2015.00487

Araujo, W. L., Dias, P. C., Moraes, G. a B. K., Celin, E. F., Cunha, R. L., Barros, R. S., & DaMatta, F. M. (2008). Limitations to photosynthesis in coffee leaves from different canopy positions. *Plant Physiology and Biochemistry*, *46*(10), 884–890. https://doi.org/10.1016/j.plaphy.2008.05.005

Araus, J. L., Slafer, G. a., Royo, C., & Serret, M. D. (2008). Breeding for Yield Potential and Stress Adaptation in Cereals. *Critical Reviews in Plant Sciences*, *27*(6), 377–412. https://doi.org/10.1080/07352680802467736

Ashikari, M. (2005). Cytokinin Oxidase Regulates Rice Grain Production. *Science*, *309*(5735), 741–745. https://doi.org/10.1126/science.1113373

Asseng, S, Ewert, F., Martre, P., Rötter, R. P., Lobell, D. B., Cammarano, D., … Zhu, Y. (2015). Rising temperatures reduce global wheat production. *Nature Climate Change*, *5*(2), 143–147. https://doi.org/10.1038/nclimate2470

Asseng, Senthold, Kassie, B. T., Labra, M. H., Amador, C., & Calderini, D. F. (2017). Simulating the impact of source-sink manipulations in wheat. *Field Crops Research*, *202*, 47–56.

https://doi.org/10.1016/j.fcr.2016.04.031

Asseng, Senthold, Martre, P., Maiorano, A., Rötter, R. P., O'Leary, G. J., Fitzgerald, G. J., … Ewert, F. (2019). Climate change impact and adaptation for wheat protein. *Global Change Biology*, *25*(1), 155–173. https://doi.org/10.1111/gcb.14481

Atkinson, J. A., Wingen, L. U., Griffiths, M., Pound, M. P., Gaju, O., Foulkes, M. J., … Wells, D. M. (2015). Phenotyping pipeline reveals major seedling root growth QTL in hexaploid wheat. *Journal of Experimental Botany*, *66*(8), 2283–2292. https://doi.org/10.1093/jxb/erv006

Austin, R. B., Bingham, J., Blackwell, R. D., Evans, L. T., Ford, M. a., Morgan, C. L., & Taylor, M. (1980). Genetic improvements in winter wheat yields since 1900 and associated physiological changes. *The Journal of Agricultural Science*, *94*, 675. https://doi.org/10.1017/S0021859600028665

Austin, R. B., Ford, M. A., & Morgan, C. L. (1989). Genetic improvement in the yield of winter wheat: a further evaluation. *The Journal of Agricultural Science*, *112*(03), 295. https://doi.org/10.1017/S0021859600085749

Ayalew, H., Tsang, P. W., Chu, C., Wang, J., Liu, S., Chen, C., & Ma, X.-F. (2019). Comparison of TaqMan, KASP and rhAmp SNP genotyping platforms in hexaploid wheat. *Plos One*, *14*(5), e0217222. https://doi.org/10.1371/journal.pone.0217222

Bancal, P. (2008). Positive contribution of stem growth to grain number per spike in wheat. *Field Crops Research*, *105*(1–2), 27–39. https://doi.org/10.1016/j.fcr.2007.06.008

Bancal, P. (2009). Early development and enlargement of wheat floret primordia suggest a role of partitioning within spike to grain set. *Field Crops Research*, *110*(1), 44–53. https://doi.org/10.1016/j.fcr.2008.06.014

BBSRC. (2013). Cereal DB Database. Retrieved April 21, 2019, from http://www.cerealsdb.uk.net/cerealgenomics/CerealsDB/kasp_download.php

Bennett, D., Reynolds, M., Mullan, D., Izanloo, A., Kuchel, H., Langridge, P., & Schnurbusch, T. (2012). Detection of two major grain yield QTL in bread wheat (Triticum aestivum L.) under heat, drought and high yield potential environments. *Theoretical and Applied Genetics*, *125*, 1473–1485. https://doi.org/10.1007/s00122-012-1927-2

Berry, P. M., Spink, J. H., Foulkes, M. J., & Wade, A. (2003). Quantifying the contributions and losses of dry matter from non-surviving shoots in four cultivars of winter wheat. *Field Crops Research*, *80*(2), 111–121. https://doi.org/10.1016/S0378-4290(02)00174-0

Bhatta, M., Morgounov, A., Belamkar, V., & Baenziger, P. S. (2018). Genome-wide association study reveals novel genomic regions for grain yield and yield-related traits in drought-stressed synthetic hexaploid wheat. *International Journal of Molecular Sciences*, *19*(10). https://doi.org/10.3390/ijms19103011

Blatt, M. R. (2000). Celular signaling and volume control in stomatal movements in plants. *Cell*.

Bolger, A. M., Poorter, H., Dumschott, K., Bolger, M. E., Arend, D., Osorio, S., … Usadel, B. (2019). Computational aspects underlying genome to phenome analysis in plants. *Plant Journal*, *97*(1), 182–198. https://doi.org/10.1111/tpj.14179

Borrell, A. K., Incoll, L. D., Simpson, R. J., & Dalling, M. J. (1989). Partitioning of dry matter and the deposition and use of stem reserves in a semi-dwarf wheat crop. *Annals of Botany*, *63*(5), 527–539. Retrieved from http://www.scopus.com/scopus/inward/record.url?eid=2-s2.0-38249023427&partnerID=40&rel=R8.0.0

Borrelli, G. M., Orrù, L., De Vita, P., Barabaschi, D., Mastrangelo, A. M., & Cattivelli, L. (2015). *Crop Physiology*. *Crop Physiology* (Second Edi). Elsevier Inc. https://doi.org/10.1016/B978-0-12-417104-6.00018-2

Borrill, P., Fahy, B., Smith, A. M., & Uauy, C. (2015). Wheat grain filling is limited by grain filling capacity rather than the duration of flag leaf photosynthesis: A case study using NAM RNAi plants. *PLoS ONE*, *10*(8), 1–14. https://doi.org/10.1371/journal.pone.0134947

Bradbury, P. J., Zhang, Z., Kroon, D. E., Casstevens, T. M., Ramdoss, Y., & Buckler, E. S. (2007). TASSEL: Software for association mapping of complex traits in diverse samples. *Bioinformatics*, *23*(19), 2633–2635. https://doi.org/10.1093/bioinformatics/btm308

Breseghello, F., & Sorrells, M. E. (2006). Association analysis as a strategy for improvement of quantitative traits in plants. *Crop Science*, *46*(3), 1323–1330. https://doi.org/10.2135/cropsci2005.09-0305

Brisson, N., Gate, P., Gouache, D., Charmet, G., Oury, F. X., & Huard, F. (2010). Why are wheat yields stagnating in Europe? A comprehensive data analysis for France. *Field Crops Research*, *119*(1), 201–212. https://doi.org/10.1016/j.fcr.2010.07.012

Broman KW, Wu H, Sen Ś, C. G. (2003). R/qtl: QTL mapping in experimental crosses. Retrieved from http://www.rqtl.org/

Bustos, D. V., Hasan, A. K., Reynolds, M. P., & Calderini, D. F. (2013). Combining high grain number and weight through a DH-population to improve grain yield potential of wheat in high-yielding environments. *Field Crops Research*, *145*, 106–115. https://doi.org/10.1016/j.fcr.2013.01.015

Calderini, D. F., Reynolds, M. P., Slafer, G. A., & Satorre, E. H. (1999). Genetic gains in wheat yield and associated physiological changes during the twentieth century. *Wheat: Ecology and Physiology of Yield Determination*, *61*, 351–377; 5 pp.

Carmo-Silva, E., Scales, J. C., Madgwick, P. J., & Parry, M. A. J. (2015). Optimizing Rubisco and its regulation for greater resource use efficiency. *Plant, Cell and Environment*, *38*(9), 1817–1832. https://doi.org/10.1111/pce.12425

Chang, T.-G., & Zhu, X.-G. (2017). Source–sink interaction: a century old concept under the light of modern molecular systems biology. *Journal of Experimental Botany*. https://doi.org/10.1093/jxb/erx002

Chao, S., Dubcovsky, J., Dvorak, J., Luo, M.-C., Baenziger, S. P., Matnyazov, R., … Akhunov, E. D. (2010). Population- and genome-specific patterns of linkage disequilibrium and SNP variation in spring and winter wheat (Triticum aestivum L.). *BMC Genomics*, *11*(1), 727. https://doi.org/10.1186/1471-2164-11-727

Chen, H., Semagn, K., Iqbal, M., Moakhar, N. P., Haile, T., N'Diaye, A., … Spaner, D. (2017). Genome-wide association mapping of genomic regions associated with phenotypic traits in Canadian western spring wheat. *Molecular Breeding*, *37*(11). https://doi.org/10.1007/s11032-017-0741-6

Chen, W., Zhang, J., & Deng, X. (2019). The spike weight contribution of the photosynthetic area above the upper internode in a winter wheat under different nitrogen and mulching regimes. *Crop Journal*, *7*(1), 89–100. https://doi.org/10.1016/j.cj.2018.10.004

Chen, Z. (2013). Statistical Methods for QTL Mapping, 308. Retrieved from http://proquest.tech.safaribooksonline.de/book/statistics/9781439868317

Cooper, M., & Bänziger, M. (2017). Breeding for low input conditions and consequences for participatory plant breeding: Examples from tropical maize and wheat. *Euphytica*, *122*(June), 503–519. https://doi.org/10.1023/A

Crain, J., Mondal, S., Rutkoski, J., Singh, R. P., & Poland, J. (2018). Combining High-Throughput Phenotyping and Genomic Information to Increase Prediction and Selection Accuracy in Wheat Breeding. *The Plant Genome*, *11*(1), 0. https://doi.org/10.3835/plantgenome2017.05.0043

Cruz-Aguado, J. A., Rodes, R., Perez, I. P., & Dorado, M. (2000). Morphological characteristics and yield components associated with accumulation and loss of dry mass in the internodes of wheat. *Field Crops Research*, *66*(2), 129–139. https://doi.org/10.1016/S0378-4290(00)00070-8

Dai, J., Bean, B., Brown, B., Bruening, W., Edwards, J., Flowers, M., … Wiersma, J. (2016). Harvest index and straw yield of five classes of wheat. *Biomass and Bioenergy*, *85*, 223–227. https://doi.org/10.1016/j.biombioe.2015.12.023

Daoura, B. G., Chen, L., Du, Y., & Hu, Y. G. (2014). Genetic effects of dwarfing gene Rht-5 on agronomic traits in common wheat (Triticum aestivum L.) and QTL analysis on its linked traits. *Field Crops Research*, *156*, 22–29. https://doi.org/10.1016/j.fcr.2013.10.007

Denison, R. F. (2015). Evolutionary tradeoffs as opportunities to improve yield potential. *Field Crops Research*, *182*, 3–8. https://doi.org/10.1016/j.fcr.2015.04.004

Dodig, D., Ranc̆I, D., Vuceli Radovi, B., Zori, M., Savi, J., Kandi, V., … Peki-Quarrie, A. S. (2017). Response of wheat plants under post-anthesis stress induced by defoliation: II. Contribution of peduncle morpho-anatomical traits and carbon reserves to grain yield, (May), 475–493. https://doi.org/10.1017/S0021859616000551

Dreccer, M. F., Wockner, K. B., Palta, J. A., McIntyre, C. L., Borgognone, M. G., Bourgault, M., … Miralles, D. J. (2014). More fertile florets and grains per spike can be achieved at higher temperature in wheat lines with high spike biomass and sugar content at booting. *Functional Plant Biology*, *41*(5), 482. https://doi.org/10.1071/FP13232

Du, Y., Chen, L., Wang, Y., Yang, Z., Saeed, I., Daoura, B. G., & Hu, Y. G. (2018). The combination of dwarfing genes Rht4 and Rht8 reduced plant height, improved yield traits of rainfed bread wheat (Triticum aestivum L.). *Field Crops Research*, *215*(September 2017), 149–155. https://doi.org/10.1016/j.fcr.2017.10.015

Duan, J., Wu, Y., Zhou, Y., Ren, X., Shao, Y., Feng, W., & Zhu, Y. (2018). Grain number responses to pre- anthesis dry matter and nitrogen in improving wheat yield in the Huang-Huai Plain. *Scientific*

Reports, (April), 1–10. https://doi.org/10.1038/s41598-018-25608-0

Duveiller, G., Weiss, M., Baret, F., & Defourny, P. (2011). Retrieving wheat Green Area Index during the growing season from optical time series measurements based on neural network radiative transfer inversion. *Remote Sensing of Environment*, *115*(3), 887–896. https://doi.org/10.1016/j.rse.2010.11.016

Ehdaie, B., Alloush, G. A., Madore, M. A., & Waines, J. G. (2006). Genotypic Variation for Stem Reserves and Mobilization in Wheat: I. Postanthesis Changes in Internode Dry Matter. *Crop Sci.*, *46*(2), 735–746. https://doi.org/10.2135/cropsci2005.04-0033

Ehdaie, B., Alloush, G. a., & Waines, J. G. (2008). Genotypic variation in linear rate of grain growth and contribution of stem reserves to grain yield in wheat. *Field Crops Research*, *106*(1), 34–43. https://doi.org/10.1016/j.fcr.2007.10.012

Ehdaie, Bahman, Alloush, G., Madore, M., & Waines, J. (2006). Genotypic Variation for Stem Reserves and Mobilization in Wheat: I. Post Anthesis Changes in Internode Dry Matter. *Crop Science*, *46*(2), 735–746. https://doi.org/10.2135/cropsci2005.04-0033

Elhani, S., Martos, V., Rharrabti, Y., Royo, C., & García del Moral, L. F. (2007). Contribution of main stem and tillers to durum wheat (Triticum turgidum L. var. durum) grain yield and its components grown in Mediterranean environments. *Field Crops Research*, *103*(1), 25–35. https://doi.org/10.1016/j.fcr.2007.05.008

Elía, M., Savin, R., & Slafer, G. A. (2016). Fruiting efficiency in wheat: Physiological aspects and genetic variation among modern cultivars. *Field Crops Research*, *191*, 83–90. https://doi.org/10.1016/j.fcr.2016.02.019

Endelman, J. B., & Jannink, J.-L. (2012). Shrinkage estimation of the realized relationship matrix. *Genes|Genomes|Genetics*, *2*(11), 1405–1413. https://doi.org/10.1534/g3.112.004259

Ernesto, O., & Navarro, G. (2017). *Understanding the developmental basis of grain yield potential in bread wheat*. University of East Anglia.

Ersoz, Elhan; Yu, Jianming; Buckler, E. (2007). Application of linkage disequilibrium and association mapping in crop plants. *Genomics Approaches and Platforms*, *1*, 97–119.

Espindula, M. C., Rocha, V. S., Grossi, J. A. S., Souza, M. A., Souza, L. T., & Favarato, L. F. (2009). Use of growth retardants in wheat. *Planta Daninha*, *27*(2), 379–387. https://doi.org/10.1590/s0100-83582009000200022

Evenson, R. E. (2003). Assessing the Impact of the Green Revolution, 1960 to 2000. *Science*, *300*(5620), 758–762. https://doi.org/10.1126/science.1078710

Fan, J., McConkey, B., Janzen, H., Townley-Smith, L., & Wang, H. (2017). Harvest index-yield relationship for estimating crop residue in cold continental climates. *Field Crops Research*, *204*, 153–157. https://doi.org/10.1016/j.fcr.2017.01.014

FAO. (2009). How to Feed the World in 2050. *Insights from an Expert Meeting at FAO*, (1), 1–35. https://doi.org/10.1111/j.1728-4457.2009.00312.x

FAO. (2011). The state of the world's land and water resources for food and agriculture. Retrieved July 22, 2019, from http://www.fao.org/3/i1688e/i1688e03.pdf

FAO. (2017). World Food Situation.

FAO. (2018). Global cereal production and inventories to decline but overall supplies remain adequate.

FAO. (2019). FAO Cereal Supply and Demand Brief.

FAOSTAT. (2013). Crop production Statistics. Food and Agriculture Organization: Rome.

Fernandez-Gallego, J. A., Kefauver, S. C., Gutiérrez, N. A., Nieto-Taladriz, M. T., & Araus, J. L. (2018). Wheat ear counting in-field conditions: High throughput and low-cost approach using RGB images. *Plant Methods*, *14*(1). https://doi.org/10.1186/s13007-018-0289-4

Ferrante, A., Cartelle, J., Savin, R., & Slafer, G. A. (2017). Yield determination, interplay between major components and yield stability in a traditional and a contemporary wheat across a wide range of environments. *Field Crops Research*, *203*, 114–127. https://doi.org/10.1016/j.fcr.2016.12.028

Ferrante, A., Savin, R., & Slafer, G. a. (2012). Differences in yield physiology between modern, well adapted durum wheat cultivars grown under contrasting conditions. *Field Crops Research*, *136*, 52–64. https://doi.org/10.1016/j.fcr.2012.07.015

Ferrante, A., Savin, R., & Slafer, G. a. (2015). Relationship between fruiting efficiency and grain weight in durum wheat. *Field Crops Research*, *177*, 109–116. https://doi.org/10.1016/j.fcr.2015.03.009

Figueroa-Bustos, V., Palta, J., Chen, Y., & Siddique, K. (2018). Characterization of Root and Shoot Traits

in Wheat Cultivars with Putative Differences in Root System Size. *Agronomy*, *8*(7), 109. https://doi.org/10.3390/agronomy8070109

Fischer, R. . (1984). Symposium on Potential Productivity of Field Crops Under Different Environments (pp. 129–159).

Fischer, R. A. (2007). Paper Presented at International Workshop on Increasing Wheat Yield Potential, Cimmyt, Obregon, Mexico, 20-24 March 2006: Understanding the physiological basis of yield potential in wheat. *Journal of Agricultural Science*, *145*(2), 99–113. https://doi.org/10.1017/S0021859607006843

Fischer, R. A. (2014). Definitions and determination of crop yield, yield gaps, and of rates of change. *Field Crops Research*, *182*, 9–18. https://doi.org/10.1016/j.fcr.2014.12.006

Fischer, R. A., & Edmeades, G. O. (2010). Breeding and cereal yield progress. *Crop Science*, *50*(Supplement 1), S-85-S-98. https://doi.org/10.2135/cropsci2009.10.0564

Fischer, Ra. (2011). Wheat physiology : A review of recent developments. *Crop and Pasture Science*, *62*(2), 95–114. https://doi.org/10.1071/CP10344

Fischer, RA, & Stockman, Y. (2006). Increased Kernel Number in Norin 10-Derived Dwarf Wheat: Evaluation of the Cause. *Functional Plant Biology*, *13*(6), 767. https://doi.org/10.1071/pp9860767

Flint-Garcia, S. A., Thornsberry, J. M., S, E., & IV, B. (2003). Structure of linkage desequilibrium in plants. *Annual Review of Plant Biology*, *54*(1), 357–374. https://doi.org/10.1146/annurev.arplant.54.031902.134907

Flintham, J. E. (1997). Optimising wheat grain yield: Effects of Rht (gibberellin-insensitive dwarfing genes. *Journal of Agricultural Science*, *128*, 11–25.

Foulkes, M. J., Snape, J. W., Shearman, V. J., Reynolds, M. P., Gaju, O., & Sylvester-Bradley, R. (2007). Paper presented at international workshop on increasing wheat yield potential, CIMMYT, Obrego, Mexico, 20–24 MARCH 2006; Genetic progress in yield potential in wheat: recent advances and future prospects. *The Journal of Agricultural Science*, *145*(01), 17. https://doi.org/10.1017/S0021859607006740

Foulkes, M. John, Slafer, G. a., Davies, W. J., Berry, P. M., Sylvester-Bradley, R., Martre, P., … Reynolds, M. P. (2011). Raising yield potential of wheat. III. Optimizing partitioning to grain while maintaining lodging resistance. *Journal of Experimental Botany*, *62*(2), 469–486. https://doi.org/10.1093/jxb/erq300

Foyer, C. H. (2001). Source – Sink Relationships. *Life Sciences*, 1–11.

Friesner, J., Assmann, S. M., Bastow, R., Bailey-Serres, J., Beynon, J., Brendel, V., … Brady, S. M. (2017). The Next Generation of Training for Arabidopsis Researchers: Bioinformatics and Quantitative Biology. *Plant Physiology*, *175*(4), 1499–1509. https://doi.org/10.1104/pp.17.01490

Gaju, O., Reynolds, M. P., Sparkes, D. L., Mayes, S., Ribas-Vargas, G., Crossa, J., & Foulkes, M. J. (2014). Relationships between physiological traits, grain number and yield potential in a wheat DH population of large spike phenotype. *Field Crops Research*, *164*(1), 126–135. https://doi.org/10.1016/j.fcr.2014.05.015

Gao, L., Kathryn Turner, M., Chao, S., Kolmer, J., & Anderson, J. A. (2016). Genome wide association study of seedling and adult plant leaf rust resistance in elite spring wheat breeding lines. *PLoS ONE*, *11*(2), 1–25. https://doi.org/10.1371/journal.pone.0148671

Garcia, A. L., Savin, R., & Slafer, G. A. (2019). Fruiting efficiency differences between cereal species. *Field Crops Research*, *231*(November 2018), 68–80. https://doi.org/10.1016/j.fcr.2018.11.005

García, G. A., Serrago, R. A., Appendino, M. L., Lombardo, L. A., Vanzetti, L. S., Helguera, M., & Miralles, D. J. (2011). Variability of duration of pre-anthesis phases as a strategy for increasing wheat grain yield. *Field Crops Research*, *124*(3), 408–416. https://doi.org/10.1016/j.fcr.2011.07.006

García, G. A., Serrago, R. A., González, F. G., Slafer, G. A., Reynolds, M. P., & Miralles, D. J. (2014). Wheat grain number: Identification of favourable physiological traits in an elite doubled-haploid population. *Field Crops Research*, *168*, 126–134. https://doi.org/10.1016/j.fcr.2014.07.018

Gebbing, T. (2003). The enclosed and exposed part of the peduncle of wheat (Triticum aestivum) – spatial separation of fructan storage. *New Phytologist*, *159*, 245–252. https://doi.org/10.1046/j.0028-646x.2003.00799.x

Ghanem, M. E., Marrou, H., & Sinclair, T. R. (2015). Physiological phenotyping of plants for crop improvement. *Trends in Plant Science*, *20*(3), 139–144. https://doi.org/10.1016/j.tplants.2014.11.006

Giunta, F., Pruneddu, G., & Motzo, R. (2009). Radiation interception and biomass and nitrogen accumulation in different cereal and grain legume species. *Field Crops Research*, *110*(1), 76–84. https://doi.org/10.1016/j.fcr.2008.07.003

Golzarian, M. R., Frick, R. A., Rajendran, K., Berger, B., Roy, S., Tester, M., & Lun, D. S. (2011). Accurate inference of shoot biomass from high-throughput images of cereal plants. *Plant Methods*, *7*(1), 1–11. https://doi.org/10.1186/1746-4811-7-2

González-Navarro, O. E., Griffiths, S., Molero, G., Reynolds, M. P., & Slafer, G. a. (2016). Variation in developmental patterns among elite wheat lines and relationship with spike fertility. *Field Crop Research*, *196*, 294–304. https://doi.org/10.1016/j.fcr.2016.07.019

González-Navarro, O. E., Griffiths, S., Molero, G., Reynolds, M. P., & Slafer, G. A. (2015). Dynamics of floret development determining differences in spike fertility in an elite population of wheat. *Field Crops Research*, *172*, 21–31. https://doi.org/10.1016/j.fcr.2014.12.001

González, F. G., Terrile, I. I., & Falcón, M. O. (2011). Spike fertility and duration of stem elongation as promising traits to improve potential grain number (and yield): Variation in modern Argentinean wheats. *Crop Science*, *51*(4), 1693–1702. https://doi.org/10.2135/cropsci2010.08.0447

González, Fernanda G., Aldabe, M. L., Terrile, I. I., & Rondanini, D. P. (2014). Grain weight response to different postflowering source:Sink ratios in modern high-yielding argentinean wheats differing in spike fruiting efficiency. *Crop Science*, *54*(february), 297–309. https://doi.org/10.2135/cropsci2013.03.0157

González, Fernanda G., Miralles, D. J., & Slafer, G. a. (2011). Wheat floret survival as related to pre-anthesis spike growth. *Journal of Experimental Botany*, *62*, 4889–4901. https://doi.org/10.1093/jxb/err182

González, Fernanda G., Slafer, G. a., & Miralles, D. J. (2003). Floret development and spike growth as affected by photoperiod during stem elongation in wheat. *Field Crops Research*, *81*, 29–38. https://doi.org/10.1016/S0378-4290(02)00196-X

González, Fernanda G., Slafer, G. A., & Miralles, D. J. (2005). Floret development and survival in wheat plants exposed to contrasting photoperiod and radiation environments during stem elongation. *Functional Plant Biology*, *32*(3), 189–197. https://doi.org/10.1071/FP04104

Griffiths, S., Wingen, L., Pietragalla, J., Garcia, G., Hasan, A., Miralles, D., … Reynolds, M. (2015). Genetic Dissection of Grain Size and Grain Number Trade-Offs in CIMMYT Wheat Germplasm. *Plos One*, *10*(3), e0118847. https://doi.org/10.1371/journal.pone.0118847

Grijalva-Contreras, R. L., Macías-Duarte, R., Martínez-Díaz, G., Robles-Contreras, F., & Nuñez-Ramírez, F. (2012). Effects of Trinexapac-Ethyl on different wheat varieties under desert conditions of Mexico. *Agricultural Sciences*, *03*(05), 658–662. https://doi.org/10.4236/as.2012.35079

Groos, C., Robert, N., Bervas, E., & Charmet, G. (2003). Genetic analysis of grain protein-content, grain yield and thousand-kernel weight in bread wheat. *Theoretical and Applied Genetics.*, *106*(6), 1032–1040. https://doi.org/10.1007/s00122-002-1111-1

Guan, P., Lu, L., Jia, L., Kabir, M. R., Zhang, J., Lan, T., … Peng, H. (2018). Global QTL Analysis Identifies Genomic Regions on Chromosomes 4A and 4B Harboring Stable Loci for Yield-Related Traits Across Different Environments in Wheat (Triticum aestivum L.). *Frontiers in Plant Science*, *9*(April). https://doi.org/10.3389/fpls.2018.00529

Guo, Z., Chen, D., Röder, M. S., Ganal, M. W., & Schnurbusch, T. (2018). Genetic dissection of pre-anthesis sub-phase durations during the reproductive spike development of wheat. *The Plant Journal*, 909–918. https://doi.org/10.1111/tpj.13998

Guo, Z., & Schnurbusch, T. (2015). Variation of floret fertility in hexaploid wheat revealed by tiller removal. *Journal of Experimental Botany*, *66*(19), 5945–5958. https://doi.org/10.1093/jxb/erv303

Gustafson, P., Raskina, O., & Nevo, E. (2009). Wheat Evolution, Domestication, and Improvement. *Wheat: Science and Trade*, 1–26. https://doi.org/10.1002/9780813818832

Hassani-Pak, K., Castellote, M., Esch, M., Hindle, M., Lysenko, A., Taubert, J., & Rawlings, C. (2016). Developing integrated crop knowledge networks to advance candidate gene discovery. *Applied and Translational Genomics*, *11*, 18–26. https://doi.org/10.1016/j.atg.2016.10.003

Hedden, P. (2003). The genes of the Green Revolution. *Trends in Genetics*, *19*(1), 5–9. https://doi.org/10.1016/S0168-9525(02)00009-4

Heidari, B., Saeidi, G., Sayed Tabatabaei, B. E., & Suenaga, K. (2012). QTLs involved in plant height, peduncle length and heading date of wheat (Triticum aestivum L.). *Journal of Agricultural Science and Technology*, *14*(5), 1093–1104.

Herder, G. Den, Van Isterdael, G., Beeckman, T., & De Smet, I. (2010). The roots of a new green

revolution. *Trends in Plant Science*, *15*(11), 600–607. https://doi.org/10.1016/j.tplants.2010.08.009

Hetherington, a M. (2001). Guard cell signaling. *Cell*, *107*(6), 711–714.

Ho, L. C. (1988). Metabolism and Compartmentation of Imported Sugars in Sink Organs in Relation to Sink Strength. *Annual Review of Plant Physiology and Plant Molecular Biology*, *39*(1), 355–378. https://doi.org/10.1146/annurev.pp.39.060188.002035

Hoisington, David; Khairallah, Mireille; Reeves, Timothy; Ribaut, Jean-Marcel; Skovmand, Bent; Taba, Suketoshi; Warburton, M. (1999). Plant genetic resources: What can they contribute toward increased crop productivity? *PNAS*, *96*(May), 5937–5943.

Hospital, F. (2009). Challenges for effective marker-assisted selection in plants. *Genetica*, *136*(2), 303–310. https://doi.org/10.1007/s10709-008-9307-1

Hu, Y. shan, Ren, T. heng, Li, Z., Tang, Y. zi, Ren, Z. long, & Yan, B. ju. (2017). Molecular mapping and genetic analysis of a QTL controlling spike formation rate and tiller number in wheat. *Gene*, *634*(September), 15–21. https://doi.org/10.1016/j.gene.2017.08.039

IRRI. (1983). *Symposium on Potential Productivity of Field Crops Under Different Environments*. *Crops*.

IWGSC. (2018). Shifting the limits in wheat research and breeding through a fully annotated and anchored reference genome sequence. *Science*, *7191*. https://doi.org/10.1126/science.aar7191

IWSC. (2016). Wheat Genome Sequencing Gets Major Boost. *International Wheat Genome Sequencing Consortium*, (January).

Jaikumar, N. S., Snapp, S. S., Flore, J. A., & Loescher, W. (2014). Photosynthetic responses in annual rye, perennial wheat, and perennial rye subjected to modest source:Sink ratio changes. *Crop Science*, *54*(1), 274–283. https://doi.org/10.2135/cropsci2013.04.0280

Jaradat, A. (2011). Wheat landraces: genetic resources for sustenance and sustainability. *Usda-Ars*, 1–20. Retrieved from http://www.usmarc.usda.gov/SP2UserFiles/Place/36450000/products-wheat/AAJ-Wheat Landraces.pdf

Jia, M., Guan, J., Zhai, Z., Geng, S., Zhang, X., Mao, L., & Li, A. (2018). Wheat functional genomics in the era of next generation sequencing: An update. *Crop Journal*, *6*(1), 7–14. https://doi.org/10.1016/j.cj.2017.09.003

Jiang, X.L; Chen, G.F; Li, X.J; Li, G.; Ru, Z.G.; Tian, J. C. (2018). Genome-wide association study for flour color-related traits and polyphenol oxidase activity in common wheat. *Cereal Research Communications*, *46*(3), 388–398. https://doi.org/10.1556/0806.46.2018.027

Jonas, E., & De Koning, D. J. (2013). Does genomic selection have a future in plant breeding? *Trends in Biotechnology*, *31*(9), 497–504. https://doi.org/10.1016/j.tibtech.2013.06.003

Jones, N., Ougham, H., & Thomas, H. (1997). Markers and mapping: We are all geneticists now. *New Phytologist*, *137*(1), 165–177. https://doi.org/10.1046/j.1469-8137.1997.00826.x

Juliana, P., Singh, R. P., Singh, P. K., Poland, J. A., Bergstrom, G. C., Huerta-Espino, J., … Sorrells, M. E. (2018). Genome-wide association mapping for resistance to leaf rust, stripe rust and tan spot in wheat reveals potential candidate genes. *Theoretical and Applied Genetics*, *131*(7), 1405–1422. https://doi.org/10.1007/s00122-018-3086-6

Kato, K., Miura, H., & Sawada, S. (2000). Mapping QTLs controlling grain yield and its components on chromosome 5A of wheat. *Theoretical and Applied Genetics*, *101*(7), 1114–1121. https://doi.org/10.1007/s001220051587

Kearsey, M. J. (1998). The principles of QTL analysis (a minimal mathematics approach). *Journal of Experimental Botany*. https://doi.org/10.1093/jxb/49.327.1619

Khan, N., & Naqvi, F. N. (2011). Heritability of Morphological Traits in Bread Wheat Advanced Lines Under Irrigated and Non-Irrigated Conditions. *Asian Journal of Agricultural Sciences*, *3*(3), 215–222.

Khush, G. S. (2001). Green revolution: the way forward. *Nature Reviews Genetics*, *2*(10), 815–822. https://doi.org/10.1038/35093585\n35093585 [pii]

Kirigwi, F. M., Ginkel, M. Van, Brown-Guedira, G., Gill, B. S., Paulsen, G. M., & Fritz, A. K. (2007). Markers associated with a QTL for grain yield in wheat under drought. *Molecular Breeding*, *20*(4), 401–413. https://doi.org/10.1007/s11032-007-9100-3

Kleczewski, N. M., & Whaley, C. (2018). Assessing the utility of the growth regulator trinexapac-ethyl and fungicides in mid-Atlantic soft red winter wheat production systems. *Crop Protection*, *104*(October 2017), 60–64. https://doi.org/10.1016/j.cropro.2017.10.011

Knapp, J. S., Harms, C. L., & Volenec, J. J. (1987). Growth Regulator Effects on Wheat Culm

Nonstructural and Structural Carbohydrates and Lignin. *Crop Science*, *27*(6), 1201. https://doi.org/10.2135/cropsci1987.0011183X002700060022x

Korte, A., & Farlow, A. (2013). The advantages and limitations of trait analysis with GWAS: a review. *Plant Methods*, *9*(1), 29. https://doi.org/10.1186/1746-4811-9-29

Krenzer, G., Small, O., Extension, G., & Resources, N. (1995). Glossary for "Growth of a Wheat Plant"*. *Specialist*.

Kristensen, P. S., Jahoor, A., Andersen, J. R., Cericola, F., Orabi, J., Janss, L. L., & Jensen, J. (2018). Genome-Wide Association Studies and Comparison of Models and Cross-Validation Strategies for Genomic Prediction of Quality Traits in Advanced Winter Wheat Breeding Lines. *Frontiers in Plant Science*, *9*(February). https://doi.org/10.3389/fpls.2018.00069

Kuchel, H., Williams, K. J., Langridge, P., Eagles, H. a., & Jefferies, S. P. (2007). Genetic dissection of grain yield in bread wheat. I. QTL analysis. *Theoretical and Applied Genetics*, *115*, 1029–1041. https://doi.org/10.1007/s00122-007-0629-7

Kumar, A.; Jain, S; Elias, E.M.; Ibrahim, M.; Sharma, L. K. (2018). An overview of QTL identification and marker-assisted selection for grain protein content in wheat. In *Eco-friendly Agro-biological Techniques for Enhancing Crop Productivity* (pp. 245–274). https://doi.org/10.1007/978-981-10-6934-5_11

Kumar, N., Kiszonas, A. M., Ibba, M. I., & Morris, C. F. (2019). Identification of loci and molecular markers associated with Super Soft kernel texture in wheat. *Journal of Cereal Science*, *87*(February), 286–291. https://doi.org/10.1016/j.jcs.2019.04.014

Kusaba, M., Tanaka, A., & Tanaka, R. (2013). Stay-green plants: What do they tell us about the molecular mechanism of leaf senescence. *Photosynth Res*, *117*(1–3), 221–234. https://doi.org/10.1007/s11120-013-9862-x

Landjeva, S., Korzun, V., & Börner, A. (2007). Molecular markers: Actual and potential contributions to wheat genome characterization and breeding. *Euphytica*, *156*(3), 271–296. https://doi.org/10.1007/s10681-007-9371-0

Lázaro, L., & Abbate, P. E. (2012). Cultivar effects on relationship between grain number and photothermal quotient or spike dry weight in wheat. *The Journal of Agricultural Science*, *150*(04), 442–459. https://doi.org/10.1017/S0021859611000736

Leng, G., & Hall, J. (2019). Crop yield sensitivity of global major agricultural countries to droughts and the projected changes in the future. *Science of the Total Environment*, *654*, 811–821. https://doi.org/10.1016/j.scitotenv.2018.10.434

Leonova, I. N. (2013). Molecular markers: Implementation in crop plant breeding for identification, introgression and gene pyramiding. *Russian Journal of Genetics: Applied Research*, *3*(6), 464–473. https://doi.org/10.1134/S2079059713060051

Li, G., Xu, X., Bai, G., Carver, B. F., Hunger, R., Bonman, J. M., … Dong, H. (2016). Genome-Wide Association Mapping Reveals Novel QTL for Seedling Leaf Rust Resistance in a Worldwide Collection of Winter Wheat. *The Plant Genome*, *9*(3), 0. https://doi.org/10.3835/plantgenome2016.06.0051

Li, H., & Durbin, R. (2009). Fast and accurate short read alignment with Burrows-Wheeler transform. *Bioinformatics*, *25*(14), 1754–1760. https://doi.org/10.1093/bioinformatics/btp324

Li, J., Wan, H. S., & Yang, W. Y. (2014). Synthetic hexaploid wheat enhances variation and adaptive evolution of bread wheat in breeding processes. *Journal of Systematics and Evolution*, *52*(6), 735–742. https://doi.org/10.1111/jse.12110

Li, W. L., Nelson, J. C., Chu, C. Y., Shi, L. H., Huang, S. H., & Liu, D. J. (2002). Chromosomal locations and genetic relationships of tiller and spike characters in wheat. *Euphytica*, *125*, 357–366. https://doi.org/10.1023/A:1016069809977

Li, X., Xia, X., Xiao, Y., He, Z., Wang, D., Trethowan, R., … Chen, X. (2015). QTL mapping for plant height and yield components in common wheat under water limited and full irrigation environments. *Crop and Pasture Science*, *8*, 660–670. https://doi.org/10.1071/CP14236

Li, Y., Cui, Z., Ni, Y., Zheng, M., Yang, D., Jin, M., … Yin, Y. (2016). Plant density effect on grain number and weight of two winter wheat cultivars at different spikelet and grain positions. *PLoS ONE*, *11*(5), 1–15. https://doi.org/10.1371/journal.pone.0155351

Liu, L.; Wang, M.N; Feng, J.Y; See, D.R; Chao, S.M; Chen, X. M. (2018). Combination of all-stage and high-temperature adult-plant resistance QTL confers high-level, durable resistance to stripe rust in winter wheat cultivar Madsen. *Theoretical and Applied Genetics*, (9), 1835–1849. https://doi.org/10.1007/s00122-018-3116-4

Liu, J., Feng, B., Xu, Z., Fan, X., Jiang, F., Jin, X., … Wang, T. (2018). A genome-wide association study of wheat yield and quality-related traits in southwest China. *Molecular Breeding*, *38*(1), 1–11. https://doi.org/10.1007/s11032-017-0759-9

Liu, Y., Wang, L., Deng, M., Li, Z., Lu, Y., Wang, J., … Zheng, Y. (2015). Genome-wide association study of phosphorus-deficiency-tolerance traits in Aegilops tauschii. *Theoretical and Applied Genetics*, *128*(11), 2203–2212. https://doi.org/10.1007/s00122-015-2578-x

Lo Valvo, P. J., Miralles, D. J., & Serrago, R. A. (2018). Genetic progress in Argentine bread wheat varieties released between 1918 and 2011: Changes in physiological and numerical yield components. *Field Crops Research*, *221*(December 2016), 314–321. https://doi.org/10.1016/j.fcr.2017.08.014

Long SP, Zhu XG, Naidu SL, O. D. (2006). Can improvement in photosynthesis increase crop yields? *Plant, Cell and Environment*, *29*(3), 315–330. https://doi.org/10.1111/j.1365-3040.2005.01493.x

Lopes, M. S., Dreisigacker, S., Peña, R. J., Sukumaran, S., & Reynolds, M. P. (2015). Genetic characterization of the wheat association mapping initiative (WAMI) panel for dissection of complex traits in spring wheat. *Theoretical and Applied Genetics*, *128*(3), 453–464. https://doi.org/10.1007/s00122-014-2444-2

Lopes, M. S., Reynolds, M. P., Jalal-Kamali, M. R., Moussa, M., Feltaous, Y., Tahir, I. S. a, … Baum, M. (2012). The yield correlations of selectable physiological traits in a population of advanced spring wheat lines grown in warm and drought environments. *Field Crops Research*, *128*, 129–136. https://doi.org/10.1016/j.fcr.2011.12.017

Lopes, Marta S., & Reynolds, M. P. (2010). Partitioning of assimilates to deeper roots is associated with cooler canopies and increased yield under drought in wheat. *Functional Plant Biology*, *37*(2), 147–156. https://doi.org/10.1071/FP09121

Lopes, Marta S., & Reynolds, M. P. (2012). Stay-green in spring wheat can be determined by spectral reflectance measurements (normalized difference vegetation index) independently from phenology. *Journal of Experimental Botany*, *63*(10), 3789–3798. https://doi.org/10.1093/jxb/ers071

Lozada, D. N., Mason, R. E., Babar, M. A., Carver, B. F., Guedira, G. B., Merrill, K., … Dreisigacker, S. (2017). Association mapping reveals loci associated with multiple traits that affect grain yield and adaptation in soft winter wheat. *Euphytica*, *213*(9), 1–15. https://doi.org/10.1007/s10681-017-2005-2

Luche, H. de S., Silva, J. A. G. da, Nörnberg, R., Zimmer, C. M., Arenhardt, E. G., Caetano, V. da R., … Oliveira, A. C. de. (2015). Stay-green effects on adaptability and stabiity in wheat. *African Journal of Agricultural Research*, *10*(11), 1142–1149. https://doi.org/10.5897/AJAR2013.9308

Lupton, F. (2014). *Wheat Breeding: Its scientific basis*. Springer.

Lynch, Joseph; Doyle, Deirdre; McAuley, Shauna; McHardy, Fiona; Danneels, Quentin; Black, Lisa; White, E. S. J. (2017). The impact of variation in grain number and individual grain weight on winter wheat yield in the high yield potential environment of Ireland. *European Journal of Agronomy*, 40–49.

Lynch, J. P., & Brown, K. M. (2012). New roots for agriculture: Exploiting the root phenome. *Philosophical Transactions of the Royal Society B: Biological Sciences*, *367*(1595), 1598–1604. https://doi.org/10.1098/rstb.2011.0243

Mago, R., Zhang, P., Xia, X., Zhang, J., Hoxha, S., Lagudah, E., … Dundas, I. (2019). Transfer of stem rust resistance gene SrB from Thinopyrum ponticum into wheat and development of a closely linked PCR-based marker. *Theoretical and Applied Genetics*, *132*(2), 371–382. https://doi.org/10.1007/s00122-018-3224-1

Marcelis, L. F. (1996). Sink strength as a determinant of dry matter partitioning in the whole plant. *Journal of Experimental Botany*, *47 Spec No*(August), 1281–1291. https://doi.org/10.1093/jxb/47.Special_Issue.1281

Martino, D. L., Abbate, P. E., Cendoya, M. G., Gutheim, F., Mirabella, N. E., & Pontaroli, A. C. (2015). Wheat spike fertility: inheritance and relationship with spike yield components in early generations. *Plant Breeding*, *134*(3), 264–270. https://doi.org/10.1111/pbr.12262

Matysiak, K. (2006a). Influence of trinexapac-ethyl on growth and development of winter wheat. *Journal of Plant Protection Research*, *46*(2), 133–143. Retrieved from http://www.plantprotection.pl/PDF/46(2)/JPPR_46(2)_2_Matysiak.pdf

Matysiak, K. (2006b). Influence of Trinexapac-Ethyl on Growth and Development of Winter Wheat. *Journal of Plant Protection Research*, *46*(2), 133–143.

Maydup, M. L., Antonietta, M., Graciano, C., Guiamet, J. J., & Tambussi, E. A. (2014). The contribution of the awns of bread wheat (Triticum aestivum L.) to grain filling: Responses to water deficit and the effects of awns on ear temperature and hydraulic conductance. *Field Crops Research*, *167*, 102–111. https://doi.org/10.1016/j.fcr.2014.07.012

Maydup, M. L., Antonietta, M., Guiamet, J. J., Graciano, C., López, J. R., & Tambussi, E. a. (2010). The contribution of ear photosynthesis to grain filling in bread wheat (Triticum aestivum L.). *Field Crops Research*, *119*(1), 48–58. https://doi.org/10.1016/j.fcr.2010.06.014

Maydup, M. L., Antonietta, M., Guiamet, J. J., & Tambussi, E. a. (2012). The contribution of green parts of the ear to grain filling in old and modern cultivars of bread wheat (Triticum aestivum L.): Evidence for genetic gains over the past century. *Field Crops Research*, *134*, 208–215. https://doi.org/10.1016/j.fcr.2012.06.008

Milner, S. G., Maccaferri, M., Huang, B. E., Mantovani, P., Massi, A., Frascaroli, E., … Salvi, S. (2016). A multiparental cross population for mapping QTL for agronomic traits in durum wheat (Triticum turgidum ssp. durum). *Plant Biotechnology Journal*, *14*(2), 735–748. https://doi.org/10.1111/pbi.12424

Mir, R. R., Reynolds, M., Pinto, F., Khan, M. A., & Bhat, M. A. (2019). High-throughput phenotyping for crop improvement in the genomics era. *Plant Science*, (January), 1–13. https://doi.org/10.1016/j.plantsci.2019.01.007

Miziniak, W., Matysiak, K., & Kaczmarek, S. (2017). Studies on trinexapac-ethyl dose reduction by combined application with adjuvants in spring barley. *Journal of Plant Protection Research*, *57*(1), 36–42. https://doi.org/10.1515/jppr-2017-0005

Molero, G., Joynson, R., Pinera-Chavez, F. J., Gardiner, L., Rivera-Amado, C., Hall, A., & Reynolds, M. P. (2019). Elucidating the genetic basis of biomass accumulation and radiation use efficiency in spring wheat and its role in yield potential. *Plant Biotechnology Journal*, 1–13. https://doi.org/10.1111/pbi.13052

Motzo, R., Pruneddu, G., & Giunta, F. (2013). The role of stomatal conductance for water and radiation use efficiency of durum wheat and triticale in a mediterranean environment. *European Journal of Agronomy*, *44*, 87–97. https://doi.org/10.1016/j.eja.2012.09.002

Mu, J., Dai, M., Wang, X., Tang, X., & Huang, S. (2019). Combining genome-wide linkage mapping with extreme pool genotyping for stripe rust resistance gene identification in bread wheat. *Molecular Breeding*, *39*(82). https://doi.org/https://doi.org/10.1007/s11032-019-0991-6

Müller, T., Schierscher-Viret, B., Fossati, D., Brabant, C., Schori, A., Keller, B., & Krattinger, S. G. (2018). Unlocking the diversity of genebanks: whole-genome marker analysis of Swiss bread wheat and spelt. *Theoretical and Applied Genetics*, *131*(2), 407–416. https://doi.org/10.1007/s00122-017-3010-5

Nelson, J. C., Sorrells, M. E., Van Deynze, a. E., Yun Hai Lu, Atkinson, M., Bernard, M., … Anderson, J. a. (1995). Molecular mapping of wheat: Major genes and rearrangements in homoeologous groups 4, 5, and 7. *Genetics*, *141*(2), 721–731.

O'Rourke, J. A. (2014). Genetic and Physical Map Correlation. *ELS*, 1–7. https://doi.org/10.1002/9780470015902.a0000819.pub3

Ogbonnaya, F. C., Rasheed, A., Okechukwu, E. C., Jighly, A., Makdis, F., Wuletaw, T., … Agbo, C. U. (2017). Genome-wide association study for agronomic and physiological traits in spring wheat evaluated in a range of heat prone environments. *Theoretical and Applied Genetics*. https://doi.org/10.1007/s00122-017-2927-z

Ogihara, Yasunari; Takumi, Shigeo; Handa, H. (2015). *Advances in Wheat Genetics: From Genome to Field*. https://doi.org/10.1007/978-4-431-55675-6

Olanrewaju, S., Rajan, N., Ibrahim, A. M. H., Rudd, J. C., Liu, S., Sui, R., … Xue, Q. (2019). Using aerial imagery and digital photography to monitor growth and yield in winter wheat. *International Journal of Remote Sensing*, *40*(18), 6905–6929. https://doi.org/10.1080/01431161.2019.1597303

Orabi, S. A., & Sadak, M. S. (2015). Improvement of productivity and quality of two wheat cultivars by foliar application of spermine and paclobutrazol. *Middle East Journal of Agriculture Research*, *4*(2), 195–203.

Ozdemir, F., Ozer, E., Singh, S., El-Basyoni, I., Aktas, H., Baenziger, P. S., … Ozbek, K. (2015). Exploiting genetic diversity from landraces in wheat breeding for adaptation to climate change. *Journal of Experimental Botany*, *66*(12), 3477–3486. https://doi.org/10.1093/jxb/erv122

Parry, M. a J., Reynolds, M., Salvucci, M. E., Raines, C., Andralojc, P. J., Zhu, X. G., … Furbank, R. T. (2011). Raising yield potential of wheat. II. Increasing photosynthetic capacity and efficiency.

Journal of Experimental Botany, *62*(2), 453–467. https://doi.org/10.1093/jxb/erq304

Pasam, R. K., Sharma, R., Malosetti, M., van Eeuwijk, F. A., Haseneyer, G., Kilian, B., & Graner, A. (2012). Genome-wide association studies for agronomical traits in a world wide spring barley collection. *BMC Plant Biology*, *12*. https://doi.org/10.1186/1471-2229-12-16

Pask, A., Pietragalla, J., & Mullan, D. (2012). *Physiological Breeding II: A Field Guide to Wheat Phenotyping*. *Chemistry & …*. https://doi.org/10.1017/CBO9781107415324.004

Patel, R; Mohapatra, P. . (1992). Regulation of spikelet development in rice by hormones. *Journal of Experimental Botany*, *43*(247), 257–262.

Pedro, A., Savin, R., Parry, M. A. J., & Slafer, G. A. (2012). Selection for high grain number per unit stem length through four generations from mutants in a durum wheat population to increase yields of individual plants and crops. *Field Crops Research*, *129*, 59–70. https://doi.org/10.1016/j.fcr.2012.01.016

Peltonen-Sainio, P., Kangas, A., Salo, Y., & Jauhiainen, L. (2007). Grain number dominates grain weight in temperate cereal yield determination: Evidence based on 30 years of multi-location trials. *Field Crops Research*, *100*(2–3), 179–188. https://doi.org/10.1016/j.fcr.2006.07.002

Peña-Bautista, R. J., Hernandez-Espinosa, N., Jones, J. M., Guzmán, C., & Braun, H. J. (2017). CIMMYT Series on Carbohydrates, Wheat, Grains, and Health: Wheat-Based Foods: Their Global and Regional Importance in the Food Supply, Nutrition, and Health ·. *Cereal Foods World*, *62*(5), 231–249. https://doi.org/10.1094/CFW-62-5-0231

Perdomo, J. A., Capó-Bauçà, S., Carmo-Silva, E., & Galmés, J. (2017). Rubisco and Rubisco Activase Play an Important Role in the Biochemical Limitations of Photosynthesis in Rice, Wheat, and Maize under High Temperature and Water Deficit. *Frontiers in Plant Science*, *8*(April), 1–15. https://doi.org/10.3389/fpls.2017.00490

Philipp, N., Weichert, H., Bohra, U., Weschke, W., Schulthess, W., & Weber, H. (2018). Grain number and grain yield distribution along the spike remain stable despite breeding for high yield in winter wheat. *PLoS ONE*, *13*(10), 1–17. https://doi.org/https://doi.org/10.1371/journal.pone.0205452

Piñera-Chavez, F. J., Berry, P. M., Foulkes, M. J., Jesson, M. A., & Reynolds, M. P. (2016). Avoiding lodging in irrigated spring wheat. I. Stem and root structural requirements. *Field Crops Research*, *196*, 325–336. https://doi.org/10.1016/j.fcr.2016.06.009

Pingali, P. L. (2012). Green Revolution: Impacts, limits, and the path ahead. *Proceedings of the National Academy of Sciences*, *109*(31), 12302–12308. https://doi.org/10.1073/pnas.0912953109

Pinto, R. S., & Reynolds, M. P. (2015). Common genetic basis for canopy temperature depression under heat and drought stress associated with optimized root distribution in bread wheat. *Theoretical and Applied Genetics*, *128*(4), 575–585. https://doi.org/10.1007/s00122-015-2453-9

Pinto, R. S., Reynolds, M. P., Mathews, K. L., McIntyre, C. L., Olivares-Villegas, J. J., & Chapman, S. C. (2010). Heat and drought adaptive QTL in a wheat population designed to minimize confounding agronomic effects. *Theoretical and Applied Genetics*, *121*(6), 1001–1021. https://doi.org/10.1007/s00122-010-1351-4

Pirahmadi, L., Shekari, F., Javanmard, A., & Noori, K. (2016). Improvement of wheat (Triticum Aestivum L.) yield by application of paclobutrazol, *7*, 314–325.

Porras-Hurtado, L., Ruiz, Y., Santos, C., Phillips, C., Carracedo, ??ngel, & Lareu, M. V. (2013). An overview of STRUCTURE: Applications, parameter settings, and supporting software. *Frontiers in Genetics*, *4*(MAY), 1–13. https://doi.org/10.3389/fgene.2013.00098

Pritchard, J. K., Stephens, M., & Donnelly, P. (2000). Inference of population structure using multilocus genotype data. *Genetics Society of America*, *155*, 954–959. https://doi.org/10.1111/j.1471-8286.2007.01758.x

Qin, X., Zhang, F., Liu, C., Yu, H., Cao, B., Tian, S., … Siddique, K. H. M. (2015). Wheat yield improvements in China: Past trends and future directions. *Field Crops Research*, *177*, 117–124. https://doi.org/10.1016/j.fcr.2015.03.013

Quarrie, S. A., Steed, A., Calestani, C., Semikhodskii, A., Lebreton, C., Chinoy, C., … Dodig, D. (2005). A high-density genetic map of hexaploid wheat (Triticum aestivum L.) from the cross Chinese Spring × SQ1 and its use to compare QTLs for grain yield across a range of environments. *Theoretical and Applied Genetics*, *110*(5), 865–880. https://doi.org/10.1007/s00122-004-1902-7

Quintero, A., Molero, G., Reynolds, M. P., & Calderini, D. F. (2018). Trade-off between grain weight and grain number in wheat depends on GxE interaction: A case study of an elite CIMMYT panel (CIMCOG). *European Journal of Agronomy*, *92*(January), 17–29.

https://doi.org/10.1016/j.eja.2017.09.007

Rademacher, W. (2000). Growth retardants: Effects on Gibberellin. *Annual Review of Plant Physiology & Plant Molecular Biology*, *51*, 501–531.

Rajala, A. (2004). Plant growth regulators to manipulate oat stands. *Agricultural and Food Science*, *13*(1–2), 186–197. https://doi.org/10.2137/1239099041838058

Rajala, A., Hakala, K., Mäkelä, P., Muurinen, S., & Peltonen-Sainio, P. (2009). Spring wheat response to timing of water deficit through sink and grain filling capacity. *Field Crops Research*, *114*(2), 263–271. https://doi.org/10.1016/j.fcr.2009.08.007

Rasheed, A., Wen, W., Gao, F., Zhai, S., Jin, H., Liu, J., … He, Z. (2016). Development and validation of KASP assays for genes underpinning key economic traits in bread wheat. *Theoretical and Applied Genetics*, *129*(10), 1843–1860. https://doi.org/10.1007/s00122-016-2743-x

Rasheed, A., & Xia, X. (2019). From markers to genome-based breeding in wheat. *Theoretical and Applied Genetics*, (i). https://doi.org/10.1007/s00122-019-03286-4

Ray, D. K., Ramankutty, N., Mueller, N. D., West, P. C., & Foley, J. A. (2012). Recent patterns of crop yield growth and stagnation. *Nature Communications*, *3*, 1293. https://doi.org/10.1038/ncomms2296

Rebetzke, G. J., Ellis, M. H., Bonnett, D. G., Mickelson, B., Condon, a. G., & Richards, R. a. (2012). Height reduction and agronomic performance for selected gibberellin-responsive dwarfing genes in bread wheat (Triticum aestivum L.). *Field Crops Research*, *126*, 87–96. https://doi.org/10.1016/j.fcr.2011.09.022

Rebetzke, G. J., Jimenez-Berni, J., Fischer, R. A., Deery, D. M., & Smith, D. J. (2018). Review: High-throughput phenotyping to enhance the use of crop genetic resources. *Plant Science*, (April), 1–9. https://doi.org/10.1016/j.plantsci.2018.06.017

Rebetzke, G. J., Richards, R. A., & Holland, J. B. (2017). Population extremes for assessing trait value and correlated response of genetically complex traits. *Field Crops Research*, *201*, 122–132. https://doi.org/10.1016/j.fcr.2016.10.019

Reed, E., Nunez, S., Kulp, D., Qian, J., Reilly, M. P., & Foulkes, A. S. (2015). A guide to genome-wide association analysis and post-analytic interrogation. *Statistics in Medicine*, *34*(28), 3769–3792. https://doi.org/10.1002/sim.6605

Reynolds, M., Foulkes, M. J., Slafer, G. a., Berry, P., Parry, M. a. J., Snape, J. W., & Angus, W. J. (2009). Raising yield potential in wheat. *Journal of Experimental Botany*, *60*(7), 1899–1918. https://doi.org/10.1093/jxb/erp016

Reynolds, M., Manes, Y., Izanloo, a., & Langridge, P. (2009). Phenotyping approaches for physiological breeding and gene discovery in wheat. *Annals of Applied Biology*, *155*(3), 309–320. https://doi.org/10.1111/j.1744-7348.2009.00351.x

Reynolds, M P, Pellegrineschi, a, & Skovmand, B. (2005). Sink-limitation to yield and biomass: a summary of some investigations in spring wheat. *Annals of Applied Biology*, *146*(1), 39–49. https://doi.org/10.1111/j.1744-7348.2005.03100.x

Reynolds, Matthew, Foulkes, J., Furbank, R., Griffiths, S., King, J., Murchie, E., … Slafer, G. (2012). Achieving yield gains in wheat. *Plant, Cell & Environment*, *35*(10), 1799–1823. https://doi.org/10.1111/j.1365-3040.2012.02588.x

Reynolds, Matthew P., Pask, A. J. D., Hoppitt, W. J. E., Sonder, K., Sukumaran, S., Molero, G., … Joshi, A. K. (2017). Strategic crossing of biomass and harvest index—source and sink—achieves genetic gains in wheat. *Euphytica*, *213*(11). https://doi.org/10.1007/s10681-017-2040-z

Rhizopoulou, S, Meletiou-Christou, MS, Diamantoglou, S. (1991). Water relations for sn and shade leaves of four Mediterranean evergreen schlerophylls. *Journal of Experimental Botany*, *42*(238), 627–635.

Rivera-Amado, Carolina; Trujillo-Negrellos, Eliseo; Reynolds, Matthew, Molero, Gemma; Foulkes, J. (2019). Optimizing dry-matter partitioning for increased spike growth, grain number and harvest index in spring wheat. *Field Crop Research*, (8). https://doi.org/10.1016/j.indcrop.2018.12.082

Robertsen, C., Hjortshøj, R., & Janss, L. (2019). Genomic Selection in Cereal Breeding. *Agronomy*, *9*(2), 95. https://doi.org/10.3390/agronomy9020095

Rose, T., Nagler, S., & Kage, H. (2017). Yield formation of Central-European winter wheat cultivars on a large scale perspective. *European Journal of Agronomy*, *86*, 93–102. https://doi.org/10.1016/j.eja.2017.03.003

Roselló, M., Villegas, D., Álvaro, F., Soriano, J. M., Lopes, M. S., Nazco, R., & Royo, C. (2019).

Unravelling the relationship between adaptation pattern and yield formation strategies in Mediterranean durum wheat landraces. *European Journal of Agronomy*, *107*(February), 43–52. https://doi.org/10.1016/j.eja.2019.04.003

Rustgi, S., Shafqat, M. N., Kumar, N., Baenziger, P. S., Ali, M. L., Dweikat, I., … Gill, K. S. (2013). Genetic Dissection of Yield and Its Component Traits Using High-Density Composite Map of Wheat Chromosome 3A: Bridging Gaps between QTLs and Underlying Genes. *PLoS ONE*, *8*(7), e70526. https://doi.org/10.1371/journal.pone.0070526

Sa, A. (2009). Review Article QTL Mapping : A Few Key points. *International Journal of Applied Research in Natural Products*, *2*(July), 1–3.

Sadras, V. O., & Rebetzke, G. J. (2013). Plasticity of wheat grain yield is associated with plasticity of ear number. *Crop and Pasture Science*, *64*(3), 234–243. https://doi.org/10.1071/CP13117

Sadras, Victor O., & Denison, R. F. (2009). Do plant parts compete for resources? An evolutionary viewpoint. *New Phytologist*, *183*(3), 565–574. https://doi.org/10.1111/j.1469-8137.2009.02848.x

Sanchez-Garcia, M., Royo, C., Aparicio, N., Martín-Sánchez, J. a., & Álvaro, F. (2012). Genetic improvement of bread wheat yield and associated traits in Spain during the 20th century. *The Journal of Agricultural Science*, *1*, 1–14. https://doi.org/10.1017/S0021859612000330

SAS. SAS University Edition.

Satorre, E H ; Slafer, G. A. (1999). *Wheat: Ecology and Physiology of Yield Determination*. CRC Press.

Schork, A. J., Thompson, W. K., Pham, P., Torkamani, A., Roddey, J. C., Sullivan, P. F., … Levy, D. (2013). All SNPs are not created equal: Genome-wide association studies reveal a consistent pattern of enrichment among functionally annotated SNPs. *PLoS Genetics*, *9*(4). https://doi.org/10.1371/journal.pgen.1003449

Scofield, G. N., Ruuska, S. a., Aoki, N., Lewis, D. C., Tabe, L. M., & Jenkins, C. L. D. (2009). Starch storage in the stems of wheat plants: Localization and temporal changes. *Annals of Botany*, *103*(6), 859–868. https://doi.org/10.1093/aob/mcp010

Semenov, M.A., Stratonovitch, P., Alghabari, F., & Gooding, M. J. (2014). Adapting wheat in Europe for climate change. *Journal of Cereal Science*, *59*(3), 245–256. https://doi.org/10.1016/j.jcs.2014.01.006

Semenov, Mikhail A., & Halford, N. G. (2009). Identifying target traits and molecular mechanisms for wheat breeding under a changing climate. *Journal of Experimental Botany*, *60*(10), 2791–2804. https://doi.org/10.1093/jxb/erp164

Senapati, N., Brown, H. E., & Semenov, M. A. (2019). Raising genetic yield potential in high productive countries: Designing wheat ideotypes under climate change. *Agricultural and Forest Meteorology*, *271*(February), 33–45. https://doi.org/10.1016/j.agrformet.2019.02.025

Sezer, İ., Unan, R., Sahin, M., & Way, M. O. (2016). The effect of trinexapac-ethyl and seeding rate on rice milling yields. *Turkish Journal of Agriculture and Forestry*, *40*(January), 53–61. https://doi.org/10.3906/tar-1406-143

Sharma-Natu, P., & Ghildiyal, M. C. (2005). Potential targets for improving photosynthesis and crop yield. *Current Science*, *88*(12), 1918–1928.

Shearman, V. J., Scott, R. K., & Foulkes, M. J. (2005). Crop Physiology and Metabolism. Physiological Processes Associated with Wheat Yield Progress in the UK. *Crop Science*, *185*, 175–185. https://doi.org/10.2135/cropsci2005.0175

Shewry, P. R. (2009). Wheat. *Journal of Experimental Botany*, *60*(6), 1537–1553. https://doi.org/10.1093/jxb/erp058

Siddique, K. H. M., Liao, Y., Qin, X., Wen, X., & Feng, F. (2018). Historical genetic responses of yield and root traits in winter wheat in the yellow-Huai-Hai River valley region of China due to modern breeding (1948–2012). *Plant and Soil*, 7–18. https://doi.org/10.1007/s11104-018-3832-1

Singh, B. D., & Singh, A. K. (2015). *Marker-assisted plant breeding: Principles and practices*. *Marker-Assisted Plant Breeding: Principles and Practices*. https://doi.org/10.1007/978-81-322-2316-0

Slack, S., York, L. M., Roghazai, Y., Lynch, J., Bennett, M., & Foulkes, J. (2018). Wheat shovelomics II: Revealing relationships between root crown traits and crop growth. *BioRxiv*, *44*(March), 280917. https://doi.org/10.1101/280917

Slade, A. J., Fuerstenberg, S. I., Loeffler, D., Steine, M. N., & Facciotti, D. (2005). A reverse genetic, nontransgenic approach to wheat crop improvement by TILLING. *Nature Biotechnology*, *23*(1), 75–81. https://doi.org/10.1038/nbt1043

Slafer, G. a., Elia, M., Savin, R., García, G. a., Terrile, I. I., Ferrante, A., … González, F. G. (2015).

Fruiting efficiency: an alternative trait to further rise wheat yield. *Food and Energy Security*, *4*(2), 92–109. https://doi.org/10.1002/fes3.59

Slafer, G. A., & Savin, R. (1994). Source—sink relationships and grain mass at different positions within the spike in wheat. *Field Crops Res.*, *37*(1), 39–49. https://doi.org/10.1016/0378-4290(94)90080-9

Slewinski, T. L. (2012). Non-structural carbohydrate partitioning in grass stems: A target to increase yield stability, stress tolerance, and biofuel production. *Journal of Experimental Botany*, *63*(13), 4647–4670. https://doi.org/10.1093/jxb/ers124

Sonder, K., Sukumaran, S., Molero, G., Saint, C., Payne, T., Singh, R. P., … Hussain, M. (2017). Strategic crossing of biomass and harvest index — source and sink — achieves genetic gains in wheat. https://doi.org/10.1007/s10681-017-2040-z

Soriano, J. M., Malosetti, M., Rosello, M., Sorrells, M. E., & Royo, C. (2017). Dissecting the old Mediterranean durum wheat genetic architecture for phenology, biomass and yield formation by association mapping and QTL meta-analysis. *PLoS One*, *12*(5), 1–19. https://doi.org/10.1371/journal.pone.0178290

Sorrells, M. E., & Yu, J. (2009). *Linkage Disequilibrium and Association Mapping in the Triticeae*. https://doi.org/10.1007/978-0-387-77489-3

Spielmeyer, W., & Richards, R. a. (2004). Comparative mapping of wheat chromosome 1AS which contains the tiller inhibition gene (tin) with rice chromosome 5S. *TAG. Theoretical and Applied Genetics. Theoretische Und Angewandte Genetik*, *109*(6), 1303–1310. https://doi.org/10.1007/s00122-004-1745-2

Sreenivasulu, N., & Schnurbusch, T. (2012). A genetic playground for enhancing grain number in cereals. *Trends in Plant Science*, *17*(2), 91–101. https://doi.org/10.1016/j.tplants.2011.11.003

Staub, J. E., Serquen, F. C., & Gupta, M. (1996). Genetic markers, map construction, and their application in plant breeding. *HortScience*, *31*(5), 729–740.

Sukumaran, S., Dreisigacker, S., Lopes, M., Chavez, P., & Reynolds, M. P. (2014). Genome-wide association study for grain yield and related traits in an elite spring wheat population grown in temperate irrigated environments. *Theoretical and Applied Genetics*, *128*(2), 353–363. https://doi.org/10.1007/s00122-014-2435-3

Sukumaran, S., Lopes, M., Dreisigacker, S., & Reynolds, M. (2017). Genetic analysis of multi-environmental spring wheat trials identifies genomic regions for locus-specific trade-offs for grain weight and grain number. *Theoretical and Applied Genetics*. https://doi.org/10.1007/s00122-017-3037-7

Summerer, S., Povero, G., Cellini, F., Petrozza, A., De Paola, D., Briglia, N., … Danzi, D. (2019). Can High Throughput Phenotyping Help Food Security in the Mediterranean Area? *Frontiers in Plant Science*, *10*(January), 1–13. https://doi.org/10.3389/fpls.2019.00015

Sun, C., Zhang, F., Yan, X., Zhang, X., Dong, Z., Cui, D., & Chen, F. (2017). Genome-wide association study for 13 agronomic traits reveals distribution of superior alleles in bread wheat from the Yellow and Huai Valley of China. *Plant Biotechnology Journal*, *15*(8), 953–969. https://doi.org/10.1111/pbi.12690

Sun, J., Poland, J. A., Mondal, S., Crossa, J., Juliana, P., Singh, R. P., … Sorrells, M. E. (2019). High-throughput phenotyping platforms enhance genomic selection for wheat grain yield across populations and cycles in early stage. *Theoretical and Applied Genetics*. https://doi.org/10.1007/s00122-019-03309-0

Sun, T. (2008). Gibberellin Metabolism, Perception and Signaling Pathways in Arabidopsis. *The Arabidopsis Book*, *6*, e0103. https://doi.org/10.1199/tab.0103

Sylvester-Bradley, R., Riffkin, P., & OLeary, G. (2012). Designing resource-efficient ideotypes for new cropping conditions: Wheat (Triticum aestivum L.) in the high rainfall zone of southern Australia. *Field Crops Research*, *125*, 69–82. https://doi.org/10.1016/j.fcr.2011.07.015

Tadesse, W., Ogbonnaya, F. C., Jighly, A., Sanchez-Garcia, M., Sohail, Q., Rajaram, S., & Baum, M. (2015). Genome-wide association mapping of yield and grain quality traits in winter wheat genotypes. *PLoS ONE*, *10*(10), 1–18. https://doi.org/10.1371/journal.pone.0141339

Tanksley, S. D. (1997). Seed Banks and Molecular Maps: Unlocking Genetic Potential from the Wild. *Science*, *277*(5329), 1063–1066. https://doi.org/10.1126/science.277.5329.1063

Terrile, I. I., Miralles, D. J., & Gonz??lez, F. G. (2017). Fruiting efficiency in wheat (Triticum aestivum L): Trait response to different growing conditions and its relation to spike dry weight at anthesis and grain weight at harvest. *Field Crops Research*, *201*, 86–96. https://doi.org/10.1016/j.fcr.2016.09.026

Thapa, S., Xue, Q., Jessup, K. E., Rudd, J. C., Liu, S., Marek, T. H., … Baker, S. (2019). Yield determination in winter wheat under different water regimes. *Field Crops Research*, *233*(January), 80–87. https://doi.org/10.1016/j.fcr.2018.12.018

Thomas, H., & Ougham, H. (2014). The stay-green trait. *Journal of Experimental Botany*, *65*(14), 3889–3900. https://doi.org/10.1093/jxb/eru037

Thomas, H, & Howarth, C. J. (2000). Five ways to stay green. *Journal of Experimental Botany*, *51 Spec No*(February), 329–337. https://doi.org/10.1093/jexbot/51.suppl_1.329

Thomas, Howard, Ougham, H., Canter, P., & Donnison, I. (2002). What stay-green mutants tell us about nitrogen remobilization in leaf senescence. *Journal of Experimental Botany*, *53*(370), 801–808. https://doi.org/10.1093/jexbot/53.370.801

Tian, Z., Jing, Q., Dai, T., Jiang, D., & Cao, W. (2011). Effects of genetic improvements on grain yield and agronomic traits of winter wheat in the Yangtze River Basin of China. *Field Crops Research*, *124*(3), 417–425. https://doi.org/10.1016/j.fcr.2011.07.012

Tripathi, A. M., Pohanková, E., Fischer, M., Orság, M., Trnka, M., Klem, K., & Marek, M. V. (2018). The evaluation of radiation use efficiency and leaf area index development for the estimation of biomass accumulation in short rotation poplar and annual field crops. *Forests*, *9*(4). https://doi.org/10.3390/f9040168

Turuspekov, Y., Baibulatova, A., Yermekbayev, K., Tokhetova, L., Chudinov, V., Sereda, G., … Abugalieva, S. (2017). GWAS for plant growth stages and yield components in spring wheat (Triticum aestivum L.) harvested in three regions of Kazakhstan. *BMC Plant Biology*, *17*. https://doi.org/10.1186/s12870-017-1131-2

USDA. (2019). European Union (EU-27) Wheat Production by Year.

Valluru, R., Reynolds, M. P., Davies, W. J., & Sukumaran, S. (2017). Phenotypic and genome-wide association analysis of spike ethylene in diverse wheat genotypes under heat stress. *New Phytologist*, *214*(1), 271–283. https://doi.org/10.1111/nph.14367

Verlag, F., Lu, Q., Lu, C., Zhang, J., & Kuang, T. (2002). Photosynthesis and chlorophyll a fluorescence during flag leaf senescence of field-grown wheat plants. *Journal of Plant Physiology*, *159*, 1173–1178. https://doi.org/10.1078/0176-1617-00727

Visscher, P. M., Hill, W. G., & Wray, N. R. (2008). Heritability in the genomics era - Concepts and misconceptions. *Nature Reviews Genetics*, *9*(4), 255–266. https://doi.org/10.1038/nrg2322

Voss-Fels, K., Herzog, E., Dreisigacker, S., Sukumaran, S., Watson, A., Frisch, M., … Hickey, L. T. (2019). "SpeedGS" to Accelerate Genetic Gain in Spring Wheat. *Applications of Genetics and Genomics Research in Cereals*, 303–327. https://doi.org/10.1016/B978-0-08-102163-7.00014-4

VSN International. GenStat for Windows 17th Edition. VSN International, Hemel Hempstead, UK.

Walter, J., Edwards, J., McDonald, G., & Kuchel, H. (2018). Photogrammetry for the estimation of wheat biomass and harvest index. *Field Crops Research*, *216*(November 2017), 165–174. https://doi.org/10.1016/j.fcr.2017.11.024

Wang, Zhaolong; Cao, Weixing; Dai, T. Z. Q. (2001). Effects of exogenous hormones on floret development and grain set in wheat. *Plant Growth Regulation*, *35*, 225–231. https://doi.org/10.1023/A

Wang, D., Sun, Y., Stang, P., Berlin, J. A., Wilcox, M. A., & Li, Q. (2009). Comparison of methods for correcting population stratification in a genome-wide association study of rheumatoid arthritis: principal-component analysis versus multidimensional scaling. *BMC Proceedings*, *3*(Suppl 7), S109. https://doi.org/10.1186/1753-6561-3-s7-s109

Wang, F., Cheng, F., & Zhang, G. (2006). The relationship between grain filling and hormone content as affected by genotype and source-sink relation. *Plant Growth Regulation*, *49*(1), 1–8. https://doi.org/10.1007/s10725-006-0017-3

Wang, M., Wang, S., & Xia, G. (2015). From genome to gene: a new epoch for wheat research? *Trends in Plant Science*, *20*(6), 380–387. https://doi.org/http://dx.doi.org/10.1016/j.tplants.2015.03.010

Wang, R., Liu, Y., Isham, K., Zhao, W., Wheeler, J., Klassen, N., … Chen, J. (2018). QTL identification and KASP marker development for productive tiller and fertile spikelet numbers in two high-yielding hard white spring wheat cultivars. *Molecular Breeding*, *38*(11). https://doi.org/10.1007/s11032-018-0894-y

Wang, Shuguang, Dong, F., Sun, D., Chen, Y., Yan, X., & Jing, R. (2018). QTL analysis for stomatal density and size in wheat spike organ. *Emirates Journal of Food and Agriculture*, *30*(3), 173–179. https://doi.org/10.9755/ejfa.2018.v30.i3.1636

Wang, Shusen, Yang, Y., Trishchenko, A. P., Barr, A. G., Black, T. a., & McCaughey, H. (2009). Modeling the Response of Canopy Stomatal Conductance to Humidity. *Journal of Hydrometeorology*, *10*(1977), 521–532. https://doi.org/10.1175/2008JHM1050.1

Wang, X., Zhang, R., Han, L., Yang, H., Song, W., Liu, X., … Engineering, G. (2018). Dynamic plant height QTL revealed in maize through remote sensing phenotyping using a high-throughput unmanned aerial vehicle (UAV). *Scientific Reports*, (January), 1–10. https://doi.org/10.1038/s41598-019-39448-z

Wang, Z., Cao, W., Dai, T., & Zhou, Q. (2001). Effects of exogenous hormones on floret development and grain set in wheat. *Plant Growth Regulation*, *35*(3), 225–231. https://doi.org/10.1023/A:1014442006862

Warburton, M. L., Crossa, J., Franco, J., Kazi, M., Trethowan, R., Rajaram, S., … Ginkel, M. Van. (2006). Bringing wild relatives back into the family: recovering genetic diversity in CIMMYT improved wheat germplasm. *Euphytica*, *149*(3), 289–301. https://doi.org/10.1007/s10681-005-9077-0

Ward, B. P., Brown-Guedira, G., Kolb, F. L., Sanford, D. A. Van, Tyagi, P., Sneller, C. H., & Griffey, C. A. (2019). Genome-wide association studies for yield-related traits in soft red winter wheat grown in Virginia. *PLoS ONE*, *1*, 1–28.

Wardlaw, I. F., & Willenbrink, J. (1994). Carbohydrate Storage and Mobilisation by the Culm of Wheat between Heading and Grain Maturity : the Relation to Sucrose Synthase and Sucrose-phosphate Synthase. *Australian Journal of Plant Physiology*, *21*, 255–271. https://doi.org/http://dx.doi.org/10.1071/PP9940255

Wiersma, J. J., Dai, J., & Durgan, B. R. (2011). Optimum timing and rate of trinexapac-ethyl to reduce lodging in spring wheat. *Agronomy Journal*, *103*(3), 864–870. https://doi.org/10.2134/agronj2010.0398

Wilkinson, P.A., Winfield, M.O., Barker, G.L.A., Allen, A.M., Burridge, A, Coghill, J.A., Burridge, A. and Edwards, K. J. (2012). CerealsDB 2.0: an integrated resource for plant breeders and scientists. Retrieved from http://www.cerealsdb.uk.net/cerealgenomics/CerealsDB/table_crop_club_varieties.php

Wu, B.-J., Chow, W. S., Liu, Y.-J., Shi, L., & Jiang, C.-D. (2014). Effects of stomatal development on stomatal conductance and on stomatal limitation of photosynthesis in Syringa oblata and Euonymus japonicus Thunb. *Plant Science*, *229*, 23–31. https://doi.org/10.1016/j.plantsci.2014.08.009

Wu, X., Chang, X., & Jing, R. (2012). Genetic insight into yield-associated traits of wheat grown in multiple rain-fed environments. *PLoS ONE*, *7*(2). https://doi.org/10.1371/journal.pone.0031249

Würschum, T., Langer, S. M., Longin, C. F. H., Tucker, M. R., & Leiser, W. L. (2017). A modern Green Revolution gene for reduced height in wheat. *Plant Journal*, *92*(5), 892–903. https://doi.org/10.1111/tpj.13726

Würschum, T., Leiser, W. L., Langer, S. M., Tucker, M. R., & Longin, C. F. H. (2018). Phenotypic and genetic analysis of spike and kernel characteristics in wheat reveals long-term genetic trends of grain yield components. *Theoretical and Applied Genetics*, *131*(10), 2071–2084. https://doi.org/10.1007/s00122-018-3133-3

Xiao, Y. G., Qian, Z. G., Wu, K., Liu, J. J., Xia, X. C., Ji, W. Q., & He, Z. H. (2012). Genetic gains in grain yield and physiological traits of winter wheat in Shandong province, China, from 1969 to 2006. *Crop Science*, *52*(1), 44–56. https://doi.org/10.2135/cropsci2011.05.0246

Xie, Q., Fernando, K. M. C., Mayes, S., & Sparkes, D. L. (2017). Identifying seedling root architectural traits associated with yield and yield components in wheat. *Annals of Botany*, *119*(7), 1115–1129. https://doi.org/10.1093/aob/mcx001

Xie, Q., Mayes, S., & Sparkes, D. L. (2016). Optimizing tiller production and survival for grain yield improvement in a bread wheat × spelt mapping population. *Annals of Botany*, *117*(1), 51–66. https://doi.org/10.1093/aob/mcv147

Xu, Y., Li, P., Zou, C., Lu, Y., Xie, C., Zhang, X., … Olsen, M. S. (2017). Enhancing genetic gain in the era of molecular breeding. *Journal of Experimental Botany*, *68*(11), 2641–2666. https://doi.org/10.1093/jxb/erx135

Yang, W., Guo, Z., Huang, C., Duan, L., Chen, G., Jiang, N., … Xiong, L. (2014). Combining high-throughput phenotyping and genome-wide association studies to reveal natural genetic variation in rice. *Nature Communications*, *5*, 5087. https://doi.org/10.1038/ncomms6087

Yang, X., Chen, X., Ge, Q., Li, B., Tong, Y., Li, Z., … Lu, C. (2007). Characterization of photosynthesis of flag leaves in a wheat hybrid and its parents grown under field conditions. *Journal of Plant*

Physiology, *164*(3), 318–326. https://doi.org/10.1016/j.jplph.2006.01.007

Yu, J., Pressoir, G., Briggs, W. H., Vroh Bi, I., Yamasaki, M., Doebley, J. F., … Buckler, E. S. (2006). A unified mixed-model method for association mapping that accounts for multiple levels of relatedness. *Nature Genetics*, *38*(2), 203–208. https://doi.org/10.1038/ng1702

Yue, J., Yang, G., Li, C., Li, Z., Wang, Y., Feng, H., & Xu, B. (2017). Estimation of winter wheat above-ground biomass using unmanned aerial vehicle-based snapshot hyperspectral sensor and crop height improved models. *Remote Sensing*, *9*(7). https://doi.org/10.3390/rs9070708

Zadoks, J., Chang, T., & Konzak, C. (1974). A decimal growth code for the growth stages of cereals. *Weed Research*, *14*(14), 415–421.

Zhai, H., Feng, Z., Du, X., Song, Y., Liu, X., Qi, Z., … Ni, Z. (2018). A novel allele of TaGW2-A1 is located in a finely mapped QTL that increases grain weight but decreases grain number in wheat (Triticum aestivum L.). *Theoretical and Applied Genetics*, *131*(3), 539–553. https://doi.org/10.1007/s00122-017-3017-y

Zhang, C. J., Chen, G. X., Gao, X. X., & Chu, C. J. (2006). Photosynthetic decline in flag leaves of two field-grown spring wheat cultivars with different senescence properties. *South African Journal of Botany*, *72*(1), 15–23. https://doi.org/10.1016/j.sajb.2005.03.002

Zhang, D., Bai, G., Zhu, C., Yu, J., & Carver, B. F. (2010). Genetic Diversity, Population Structure, and Linkage Disequilibrium in U.S. Elite Winter Wheat. *The Plant Genome Journal*, *3*(2), 117. https://doi.org/10.3835/plantgenome2010.03.0004

Zhang, G., Wang, Y., Guo, Y., Zhao, Y., Kong, F., & Li, S. (2015). Characterization and mapping of QTLs on chromosome 2D for grain size and yield traits using a mutant line induced by EMS in wheat. *The Crop Journal*, *3*(2), 135–144. https://doi.org/http://dx.doi.org/10.1016/j.cj.2014.11.002

Zhang, Hengyou, Mittal, N., Leamy, L. J., Barazani, O., & Song, B. H. (2017). Back into the wild—Apply untapped genetic diversity of wild relatives for crop improvement. *Evolutionary Applications*, *10*(1), 5–24. https://doi.org/10.1111/eva.12434

Zhang, Heping, Turner, N. C., & Poole, M. L. (2012). Increasing the harvest index of wheat in the high rainfall zones of southern Australia. *Field Crops Research*, *129*, 111–123. https://doi.org/10.1016/j.fcr.2012.02.002

Zhang, L. Y., Liu, D. C., Guo, X. L., Yang, W. L., Sun, J. Z., Wang, D. W., … Engineering, C. (2010). Distribution in genome of Quantitative trait loci (QTL) for yield and yield-related traits in common wheat (Triticum aestivum L.). *Journal of Integrative Plant Biology*, *52*(11), 996–1007.

Zhang, Y., Su, S., Tabori, M., Yu, J., Chabot, D., Baninasab, B., … Khanizadeh, S. (2017). Effect of Selected Plant Growth Regulators on Yield and Stem Height of Spring Wheat in Ontario. *Journal of Agricultural Science*, *9*(12), 30. https://doi.org/10.5539/jas.v9n12p30

Zhang, Z., Ersoz, E., Lai, C. Q., Todhunter, R. J., Tiwari, H. K., Gore, M. A., … Buckler, E. S. (2010). Mixed linear model approach adapted for genome-wide association studies. *Nature Genetics*, *42*(4), 355–360. https://doi.org/10.1038/ng.546

Zhou, Y., He, Z. H., Sui, X. X., Xia, X. C., Zhang, X. K., & Zhang, G. S. (2007). Genetic improvement of grain yield and associated traits in the Northern China Winter Wheat Region from 1960 to 2000. *Crop Science*, *47*, 245–253. https://doi.org/10.2135/cropsci2006.03.0175

Zhu, C., Gore, M., Buckler, E. S., & Yu, J. (2008). Status and Prospects of Association Mapping in Plants. *The Plant Genome Journal*, *1*(1), 5. https://doi.org/10.3835/plantgenome2008.02.0089

Zikhali, M., Leverington-Waite, M., Fish, L., Simmonds, J., Orford, S., Wingen, L. U., … Griffiths, S. (2014). Validation of a 1DL earliness per se (eps) flowering QTL in bread wheat (Triticum aestivum). *Molecular Breeding*, *34*(3), 1023–1033. https://doi.org/10.1007/s11032-014-0094-3